Technische Universität München

Department Chemie

Lehrstuhl für Biotechnologie

TUMOR CELL-SELECTIVE MEMBRANE HSP70 TARGETING OF MALIGNANT LESIONS

Stefan Stangl

Vollständiger Abdruck der von der Fakultät für Chemie der Technischen Universität München zur Erlangung des akademischen Grades eines Doktors der Naturwissenschaften genehmigten Dissertation.

Vorsitzender: Univ.-Prof. Dr. Stephan Sieber

Prüfer der Dissertation 1. Univ.-Prof. Dr. Johannes Buchner

2. Univ.-Prof. Dr. Gabriele Multhoff

Die Dissertation wurde am 15.09.2015 bei der Technischen Universität München eingereicht und durch die Fakultät für Chemie am 20.10.2015 angenommen.

“Today we fight. Tomorrow we fight. The day after, we fight. And if this disease plans on whipping us, it better bring a lunch, 'cause it's gonna have a long day doing it.”

— Jim Beaver, Life's That Way: A Memoir

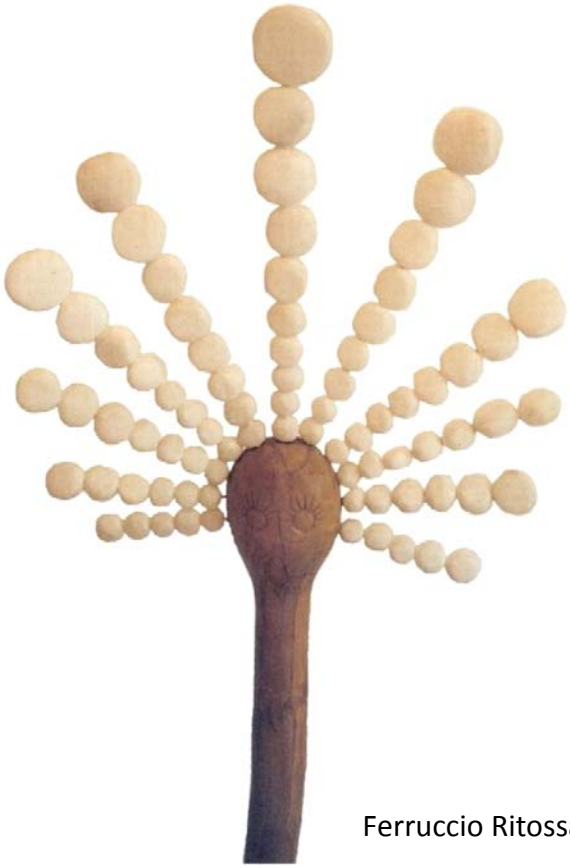

Ferruccio Ritossa,

“Regina di Muffe”

INDEX

SUMMARY OF THE WORK

Heat Shock Proteins (HSPs), also termed stress proteins, provide a powerful network of highly conserved stress response molecules which are induced following a wide variety of physiological and environmental stress insults. A major function of the stress protein system is to prevent the denaturation of proteins, transport and refold them. As a consequence, this stress response network protects and restores the protein homeostasis of the cell.

In cancer cells of a wide range of entities, however, HSPs are constitutively over-expressed to fulfill numerous functions such as mediating tumor growth, survival and metastasation. Furthermore, development of resistance against therapies is strongly associated with an upregulation of the HSP expression. In 1992, the major stress-inducible member of the HSP70 family, termed Heat shock protein 70 (Hsp70), was firstly found to be presented on the plasma membrane of cancer cells of various entities by the group of Gabriele Multhoff. In contrast to tumor cells, Hsp70 is only found in the intracellular compartment, but not on the plasma membrane of corresponding normal cells.

In my PhD thesis, novel strategies have been developed and assessed that aim to target this tumor-specific membrane form of Hsp70 both, *in vitro* and *in vivo*. For tumor detection, three different near infrared fluorescently labeled targeting compounds were used that differing in their molecular size and biodistribution characteristics. The molecular weight of these compounds ranged from 1.5 kDa for the 14mer Tumor cell Penetrating Peptide (TPP), which provides Hsp70 specificity by mimicking the oligomerization domain of Hsp70, to 150 kDa for the full length murine IgG1 monoclonal antibody (mAb) cmHsp70.1. An intermediate sized compound, the cmHsp70.1 derived F_{ab} fragment (cmHsp70.1 F_{ab}) covers a molecular weight of 35.5 kDa. Whereas *in vivo* imaging by the use of cmHsp70.1 was mainly used to investigate its biodistribution characteristics and tumor specificity to evaluate its quality as a therapeutic compound, TPP and cmHsp70.1 F_{ab} have been generated for a tumor-selective *in vivo* imaging which, due to the low immunogenicity of these compounds, could be potentially applied in human patients. In addition, small molecules such as peptides or antibody F_{ab} fragments represent a promising class of tumor-targeting tools due to their advantageous biodistribution with a fast body clearance and their capacity to effectively and rapidly penetrate viable tumor cells. In *in vitro* studies, I could show that targeting of membrane-Hsp70 with TPP and cmHsp70.1F_{ab} proved to be advantageous for tumor detection due to a tumor cell specific binding and rapid intracellular uptake. In *in vivo* studies, I could demonstrate efficient and specific uptake in tumors of various entities as well as lung metastases of primary mammary carcinomas, but not in normal tissues. These results were comparable to those obtained following administration of the cmHsp70.1F_{ab} fragment in a murine model of a syngeneic colon carcinoma. Binding studies on single cell suspensions, derived from *in vivo* grown tumors,

revealed membrane-staining of TPP on tumor cells, which was similar to that achieved with the full length mAb cmHsp70.1. Interestingly, cells of the tumor microenvironment, such as tumor-associated macrophages and fibroblasts, did not show significant binding of the Hsp70-specific tools (cmHsp70.1 mAb, TPP, Hsp70 F_{ab} fragment).

Monoclonal antibody-based treatment of cancer is well-accepted as one of the most successful therapeutic strategies. Taking advantage of the tumor-selective expression of membrane-bound Hsp70, I tested the therapeutic capacity of the murine IgG1 monoclonal antibody cmHsp70.1 in a syngeneic, immune competent tumor mouse model. In a preclinical setup, I could demonstrate significant induction of antibody dependent cellular cytotoxicity (ADCC) following administration of full length cmHsp70.1 mAb in a membrane $Hsp70^+$ colon carcinoma (CT26) tumor model. An intravenous injection of cmHsp70.1 mAb not only delayed the growth of subcutaneous and intraperitoneal CT26 tumors, but also significantly prolonged the overall survival of mice bearing these $Hsp70^+$ tumors. In line with these findings, I could show an enhanced intra-tumoral accumulation of innate immune cells such as NK cells, macrophages, and granulocytes. As control, an isotype-mached IgG1 control antibody or the F_{ab} fragment, which lacks the ADCC mediating Fc part of the antibody, were used. As expected, none of these control reagents induced immunological effects such as ADCC. Functional *ex vivo* assays further demonstrated that tumor cell killing is mediated via ADCC. The Hsp70-specificity of this approach is supported by the finding that cmHsp70.1 mAb had no effect on tumor growth or the survival of mice bearing membrane $Hsp70^-$ A20 B-cell lymphomas.

In summary, targeting the membrane-associated form of Hsp70 on tumor cells provides a promising new approach for a tumor-selective imaging and for future therapeutic intervention.

ZUSAMMENFASSUNG DER ARBEIT

Mitglieder der Familien der Hitze Schock Proteine (HSPs) kommen zytoplasmatisch in nahezu allen Zellen (Prokaryoten und Eukaryoten) vor. Verschiedenste Stressfaktoren können die Expression dieser HSPs in einer Stressantwort Reaktion verstärken, um Zellen vor den letalen Schäden einer Stresseinwirkung, beispielsweise die Denaturierung von Proteinen, zu schützen und um die Protein-Homöostase durch Wiederherstellung der 3D-Struktur entfalteter Proteine wiederherzustellen.

In einer Vielzahl von Tumortypen unterschiedlichster Herkunft sind HSP konstitutiv verstärkt exprimiert. HSPs unterstützen eine Vielzahl onkologischer Prozesse, wie z.B. das ungebremste Zellwachstum, den Schutz vor Apoptose, und die Fähigkeit zur Metastasierung. Weiterhin können HSP die Resistenz von Tumoren gegenüber therapeutischen Maßnahmen, wie z.B. einer Radiochemotherapie, verstärken. Im Jahre 1992 konnte von der Gruppe um Gabriele Multhoff erstmals eine außergewöhnliche Lokalisation des Haupt-stressinduzierbaren Mitglieds der HSP70 Familie, Hsp70 (neue Nomenklatur: HSPA1A), auf der Zellmembran von Tumorzellen verschiedener Entitäten, nachgewiesen werden. Im Gegensatz dazu kommt Hsp70 bei Normalzellen nur im Zytosol vor. Deshalb eignet sich Membran-gebundenes Hsp70 als eine ideale Tumor-spezifische Erkennungsstruktur.

Meine Doktorarbeit beschäftigt sich mit neuen Ansätzen zur zielgerichteten Erkennung und Behandlung von Tumoren, die auf der Tumor-spezifischen Membranlokalisation von Hsp70 beruhen. Zur Hsp70-basierten Tumordetektion wurden von mir drei Werkzeuge mit unterschiedlichen Molekulargewichten entwickelt, die mit Fluoreszenz-markierten Farbstoffen, die Licht im nahen Infrarot Bereich emittieren, markiert wurden. Die Molekulargewichte dieser Werkzeuge reichen von 1,5 kDa für das „Tumor Penetrating Peptide“ TPP, über ein dem cmHsp70.1 entstammenden F_{ab} Fragment (cmHsp70.1F_{ab}; 35.5 kDa) bis hin zu 150 kDa für den monoklonalen Maus-IgG1 Antikörper (mAb) cmHsp70.1. Der cmHsp70.1 mAb diente in erster Linie für den Nachweis einer spezifischen Anreicherung im Tumor und der Analyse der Biodistributionseigenschaften im Modellorganismus Maus. Zusätzlich dazu wurde der Antikörper hinsichtlich seiner Eignung, eine Antikörper vermittelte, zellulären Zytotoxizität (ADCC) spezifisch in Hsp70 membran-positiven Tumorzellen auszulösen, untersucht. Die Werkzeuge TPP und cmHsp70.1 F_{ab} Fragment wurden zur Tumor-selektiven Bildgebung generiert, da kleine Präparate wie Peptide oder F_{ab} Fragmente aufgrund ihrer vorteilhaften Biodistribution und schnelleren Auswaschung aus Normalgewebe, ihrer geringen Immunogenität, sowie ihrer Eigenschaft, in vitale Tumorzellen leichter eindringen zu können, eine vielversprechende Klasse von Molekülen für Bildgebungsverfahren darstellen. Zusätzlich dazu handelt es sich bei TPP um ein natürlich vorkommendes Peptid, das aufgrund seiner guten Verträglichkeit und Biokompatibilität relativ rasch in klinischen Studien eingesetzt werden könnte. *In vitro* Studien mit TPP und cmHsp70.1F_{ab}

zeigten vergleichbar gute Bindungseigenschaften an Zellmembran-assoziiertes Hsp70 auf Tumorzellen sowie ähnliche Kinetiken hinsichtlich ihrer Internalisierung. Diese für die Bildgebung nützlichen Eigenschaften zeigten sich auch in *in vivo* Studien an tumortragenden Mäusen. In einer Reihe von Tumormausmodellen (syngen, spontan, xenograft) mit Maus- und humanen Tumoren unterschiedlichster Entitäten konnte ich zeigen, dass die von mir generierten Hsp70 Werkzeuge nach intravenöser Injektion in die Schwanzvene der Maus effektiv und selektiv in Hsp70 Membran-positiven Primärtumoren und Metastasen angereichert werden, nicht aber in gesunden Geweben. Durchflusszytometrische Untersuchungen an Einzelzellsuspensionen von Tumoren und Tumor-assoziierten Geweben zeigten eine deutliche Bindung der Hsp70 Werkzeuge in der Tumorzellfraktion, nicht aber in Zellen des Tumor Mikromilieus wie Tumor assoziierte Makrophagen oder Fibroblasten.

Auf monoklonale Antikörper basierende Tumortherapieverfahren sind in der klinischen Routine derzeit bereits gut etabliert. Die Tumor-selektive Lokalisation von Membran-assoziiertem Hsp70 nutzte ich, um den cmHsp70.1 mAb hinsichtlich seiner Eignung als Therapeutikum zur Induktion einer Antikörper-vermittelten zellulären Zytotoxizität von Tumorzellen zu untersuchen. Nachdem die Tests zur spezifischen Anreicherug im Tumor mittels Fluoreszenz-basierten Bildgebungsverfahren abgeschlossen waren, fokussierte ich mich auf die therapeutischen Eigenschaften des cmHsp70.1 mAb in präklinischen Mausmodellen mit Kolonkarzinomen, die eine Hsp70 Expression auf ihrer Zellmembran aufwiesen. Nach intravenöser Injektion des cmHsp70.1 mAb konnte ich eine spezifische Lyse der CT26 Kolon Karzinome in der Maus beobachten. Dieses tumorspezifische Killing wurde nach Gabe eines Isotypen-Kontrollantikörpers oder des cmHsp70.1F_{ab} Fragments nicht beobachtet. Funktionelle *ex vivo* Experimente bestätigten, dass die zytotoxischen Reaktionen auf eine „Antikörper vermittelte zelluläre Zytotoxiozität“ (ADCC) zurückzuführen ist. Infolgedessen beobachtete ich nach intravenöser Gabe des cmHsp70.1 mAb nicht nur eine Verzögerung des Tumorwachstums, sondern auch ein signifikant verlängertes Gesamtüberleben der Mäuse. Im Einklang mit diesen Ergebnissen konnte ich auch eine intra-tumorale Akkumulation von Immun-effektorzellen der angeborenen Immunantwort, wie z.B. NK-Zellen, Makrophagen oder Granulozyten, im Tumor nachweisen. Die Hsp70-Spezifität der cmHsp70.1 basierten Immuntherapie konnte zusätzlich in einem A20 Lymphom Tumormausmodell bestätigt werden. Die Hsp70 Membran-negativen Lymphom-Zelllinie konnte mit Hilfe des cmHsp70.1 mAb nicht abgetötet werden.

Zusammenfassend konnte ich in meiner Promotionsarbeit innovative Werkzeuge entwickeln, die Hsp70 auf der Zellmembran von Tumoren selektiv adressieren. Diese Werkzeuge besitzen nicht nur das Potential, Tumore *in vivo* zu detektieren und Therapieansprechen zu überwachen, sondern könnten zukünftig auch für therapeutische Zwecke im Menschen eingesetzt werden.

PART A – INTRODUCTION AND DISCUSSION

I. INTRODUCTION INTO HSP70 BASED TUMOR TARGETING

I-1 A brief history of tumor targeting

"Cancer was an all-consuming presence in our lives. It invaded our imaginations; it occupied our memories; it infiltrated every conversation, every thought." In his Purlitzer prize rewarded work "The Emperor of All Maladies: A Biography of Cancer", Prof. Dr. Siddhartha Mukherjee, Physician and Oncologist at the Columbia University New York City, describes the pervasive influence of this disease on patients as well as on their attending physicians. However, the circle of people for which this statement comes true can be widened to include the large number of scientists working in various disciplines, who have dedicated their life on the obliteration of cancer. The effort in basic research and its translational implementation into effective therapies has grown exponentially during the last decades. Although far-reaching progress could be achieved, cancers is still among the leading causes of morbidity and mortality worldwide, with approximately 14 million new cases and 8.2 million cancer related deaths in 2012 (World cancer report, WHO, International Agency for Research on Cancer, 2014).

Although being an omnipresent topic in the present world, cancer accompanies the whole history of mankind. Earliest reports of this disease reach back to as early as 2500 BC, when Imhotep, chancellor and physician of king Djoser of Egypt, describes in one of the earliest medical texts of history, the so-called "Edin Smith Papyrus", swollen masses of the female breast appearing like rolled up wrappers.

2000 years later, Herodotus describes in his work "History" the ordeal of Atossa (550 to 475 BC), queen of the ancient Persian Empire. Atossa suffered from a developing bleeding lumb in her breast. Atossas reaction to the arising awareness of a severe disease reflects many case histories of cancer patients till modern days. In a first destitute attempt of disregard she wrapped herself in cloths, followed by concealing in a self-imposed quarantine. Her medical history ultimately resulted in the excision of her breast done by her Greek slave. Herodotus´ report ends here, leaving Atossas destiny in the dark of history.

The first insight into the nature of cancer could be achieved another 2500 years later, in 1845. That year, Dr. John Bennett (1812 – 1875), a Scottish surgeon, and the German pathologist Dr. Rudolph Virchow (1821 – 1902), independently of each other described patients with severe alterations in the peripheral blood as well as hypertrophy of spleens and lymph nodes. In his publication, entitled "Weisses Blut" (Virchow 1845), Virchow was the first who termed the

disease: “leukemia”. That was in November 1845, 6 weeks after Bennett's paper (Bennett 1845) has been published. Impressed from the severe case history of the patient, Virchow postulated a fundamental truth of cancer, “omnis cellula e cellula” – all living cells origin from other living cells. This postulation contributed to a new understanding of cancer as pathologic hyperplasia based on uncontrolled cell division processes. Despite the big step forward in the understanding of cancer biology and pathology, at the time of Bennet and Virchow patients were usually treated with bloodletting and enema, therapies originating from the medieval doctrine of the humors and ineffective in treatment of cancerous diseases.

Nevertheless, these times signed the start of a rapid increase in oncologic research, leading to first systemic treatment trials. A tragic accident in 1943 marked the beginning of chemotherapeutic treatment of cancer: The bombing of the Italian harbor city Bari during World War II caused a disastrous explosion of the cargo ship “John Harvey”, loaded with 100s of tons of nitrogen mustard bombs. The gas spread over the city and killed thousands of men. Paradoxically, the investigations following this severe tragedy have led to the beginning of the chemotherapeutic treatment strategy. After the bombing, biopsies taken of the survivors showed severe alterations in the blood: nearly all white blood cells were missing, caused by a strong lymphoid and myeloid suppression following nitrogen mustard exposure. Dr. Steward Alexander, who performed these examinations, hypothesized in his report that since mustard gas ceased the division of certain somatic cell types whose nature was to divide fast, it could also be used to suppress the division of cancerous cells (Li 2006).

After this first evidence that individual tissue types can be affected by certain compounds, the intellectual input of Dr. Paul Ehrlich (1854 – 1915) was to translate this basic principle into his famous concept of the “magic bullet”, a theory of the existence of individual agents for the treatment each disease. In his habilitation, the physician and passionate scientist himself proved the concept by implementing his experience in histological staining of various specimens into intravital applications (Ehrlich 1885). Chemotherapeutic treatment, the first cornerstone of the magic bullet of cancer, was introduced by the pioneering work of Dr. Sidney Farber (1903 – 1973), a pediatric pathologist at the Harvard Medical School in Boston, Massachusetts. Faber discovered the proliferative effect of folic acid (Vitamin B_9) on leukemic blasts, a finding that he, in the reverse, utilized to treat patients with folate antagonists. His anti-folates, in particular aminopterine, achieved remission in leukemic diseases already in its first clinical application (Farber and Diamond 1948). This major success – the first clinically relevant treatment study with a chemotherapeutic agent - was, to his disappointment, impaired by relapse already a few months later. Nevertheless, his work was the beginning of a new concept of cancer therapies, the targeting of essential oncologic processes. More than 60 years later, the most promising novel treatment strategies of cancerous diseases comprise of the use of highly specific targeted

inhibitors and next generation antibodies, engineered for high tumor-specificity with simultaneous maximum efficacy.

A major mode of action of full length antibody therapeutics is thereby the cancer-specific redirection and activation of the components of the immune system, representing the wide field of therapeutic immune modulating strategies, the second main branch of targeted cancer therapy. The basis of immunotherapeutic cancer treatments was founded more than a century ago, when William B Coley (1862 – 1936), an American bone surgeon and oncologist, hit upon an extraordinary case study while searching for a treatment strategy for osteosarcoma patients. The case study which sparked his attention reported on the spontaneous remission of sarcoma in a patient suffering from a severe Streptococcus infection. This allowed the idea of taking advantage of the immune system to treat cancer. After several years of experience, he was successful with treating patients using a crude mixture of disintegrated bacteria, which led to a systemic boost of immune reactions (Coley 1910). This marked the beginning of the new branch of immunotherapy of cancer, a field which developed to become one of the most important in cancer therapy until today. Since the times of Coley, increasing knowledge on the principles of immune responses led to more specific and selective possibilities of immune modulation strategies to treat cancer. Thereby, the various adoptive immune cell therapies play a key role, as does the rapidly growing field of cancer-specific antibodies.

I-2 Targeted cancer therapies

I-2.1 Overview of targeted therapies

With a global budget of 14,030 million Euros in 2004/2005 (Eckhouse et al. 2008), and a strong consolidation of research area towards a translational interface from the 1990s onwards (Cambrosio et al. 2006), the fast progressing knowledge on tumor biology and effective translational implementation strategies led to nearly 5.000 preclinically tested tumor-targeting drug candidates between 2003 and 2010, of which about 9% received FDA-approval (Thomas 2011). In all systemically applied cancer-therapeutic approaches, one main tendency becomes apparent – the shift from unspecific, but nonetheless highly effective attack on any proliferative cell, to highly specific tumor targeting drugs, mainly comprising of antibody-based therapeutics or small molecule inhibitors of modern age (Gerber 2008). This area of tumor drug development can be divided into three “epochs” that emerged sequentially (Dobbelstein and Moll 2014). From epoch to epoch, the decrease in adverse side-effects of therapeutics was paralleled by an increase in the tumor cell specificity of the newly developed compounds.

According to Dobbenstein and Moll, the first “wave” drugs mainly blocked DNA replication and cell division and thus were affecting all dividing cells of the body. Although, these drugs were

highly effective in eliminating cancer cells, severe side effects, such as fatigue, mucositis, diarrhea, nausea, anemia and leucopenia and others, represent a huge disadvantage of this treatment option. Therefore, one primary goal of today's research is to enhance the targeting precision of anti-cancer agents, and, by targeting selective cellular components and mechanisms, to achieve a reduction in the systemic side effects.

Subsequently, second-wave compounds, which were aiming to inhibit tumor-related signaling pathways, mostly important for tumor growth and survival, were developed. These drugs, although theoretically more advantageous than cytotoxic chemotherapeutic agents, soon showed drawbacks, reflected by the development of resistance and disease relapse due to developing escape mechanisms by redundant signaling pathways. Although there are limitations in their capacity to cure cancer, these compounds cause relatively mild side-effects, owing to their increased tumor-specificity. The subsequent search for a more effective therapeutic approach resulted in the development of drugs targeting cellular machineries which are essential for tumor-cell growth, with omission of sensitive cellular mechanisms such as DNA replication or cell division. Instead, these third-wave cancer therapeutics target epigenetic and chromatin modifiers (Bhalla 2005), the proteasome network (Adams 2004), the chaperone machinery (Wilson and Hay 2011), (Powers and Workman 2007), (Multhoff 2007), or the spliceosome (Bonnal et al. 2012). The common principle behind these recent drugs is the selective mode of action on cellular machineries which are predominantly essential only for chronically stress-exposed tumor cells. The main cornerstones in the development of tumor-targeted therapeutics are summarized in Figure 1.

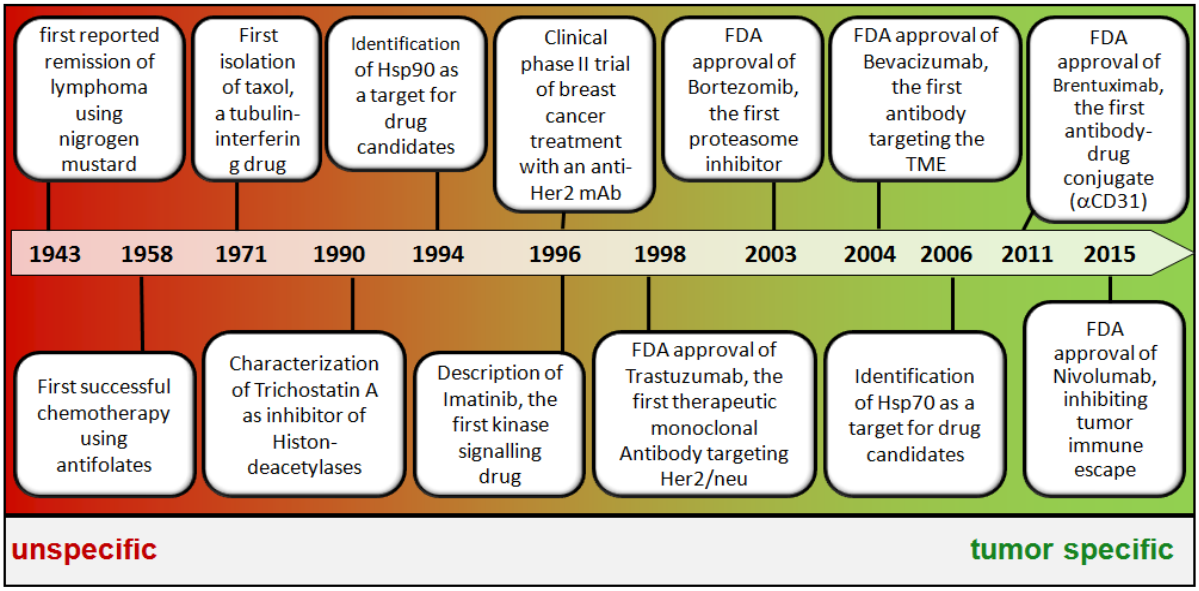

Figure 1: **Chronological listing of key discoveries in targeted anticancer therapy**. Adapted from (Dobbelstein and Moll 2014).

As most of these approaches are highly selective, their applicability is strictly linked to the presence of their respective target structures, such as tumor specific antigens, hyperactive signaling pathways or some other cellular mechanisms that are important for tumor cell survival. However, due to high grade interpersonal heterogeneity appropriate diagnostic test must be performed in order to determine the best treatment options. These extensive diagnostic examinations also demonstrate, how big efforts are being necessary for this kind of personalized therapy.

In addition to exclusive targeting of the tumor cells, some approaches focus on the complex interactions of the malignant tumor cells with their tumor supportive microenvironment, such as tumor vasculature (e.g. by anti-VEGF/VEGFR therapies, (Sitohy et al. 2012)) cancer associated inflammation (e.g. tumor associated macrophages, (Loberg et al. 2007)), communication between tumor cells and the extracellular matrix (Onishi et al. 2010), as well as intertumoral hypoxia (Xia et al. 2012; Schilling et al. 2013). However, in following years, clinical trials revealed severe side effects of some representatives of this class of cancer targeting drugs. This may be due to toxicity-induced alteration of cellular homeostasis in normal tissues, a consequence of drug-induced on-target toxicity, which occurs due to interaction of the drug with normal tissue cells that are expressing the target epitope. These effects typically occur following treatment with a non tumor cell-exclusive targeted compound (Guengerich 2011). In some cases, side effects were so severe that the trials had to be stopped (Fang and Declerck 2013).

Despite the initial drawbacks in therapeutic targeting of the tumor microenvironment, a more precise knowledge about its supporting role in tumor development and survival may lead to the development of comprehensive therapeutic approaches dealing with both, the neoplastic cells as well as the tumor-promoting features of their microenvironment.

I-2.2 Tumor targeted immune modulation

One main strategy of targeted cancer treatment is to modulate the host´s immune system towards the cancer cells in order to (re-)direct its sensitivity and cytotoxic capacity. The major advantage of this approach is the quantitative eradication of all malignant cells and, moreover, a potential to sustain anti-cancer immunity. Already in the 1940s cancer-protective immunity was demonstrated (Klein 2001). In the following, reports accumulated discussing a correlation between the regression of cancers and immune-stimulatory infections occurring in the patients. An early hype was created around “Coley´s toxin”, a crude mixture of inactivated bacteria which caused systemic inflammation and triggered a significant antitumor immune response (McCarthy 2006). Since then, reasonable efforts have been made to not only cure cancer by directed activation of the immune system, but also to avoid its development by the means of vaccination. Different immune modulating approaches, taking advantage of the various facets of the immune

system, have been investigated for cancer therapy. According to Li and Rubinstein (Li et al. 2013b), these include (i) allogenic hematopoietic stem cell transplantation (Kolb 2008), (ii) T cell checkpoint blockage against inhibitory pathways (Wolchok et al. 2013), (Topalian et al. 2012) and (iii) the transfer of clonally expanded and genetically engineered T cells (Porter et al. 2011; Brentjens et al. 2013; Grupp et al. 2013).

A different, yet similar important cell-based approach utilizes *ex vivo* activated, autologous or allogenic natural killer (NK) cells (Jiang et al. 2013), whose intrinsic, evolutionary task is, besides elimination of virus-infected cells, the detection and elimination of potentially malignant neoplastic cells. Development of tumor specific immunotherapy, utilizing Heat-shock protein 70 (Hsp70)- stimulated NK cells, is one main research area of Gabriele Multhoff´s laboratory. With the activation and tumor-specific redirection of NK cells with low-dose interleukin-2 (IL-2) and the Hsp70 derived peptide TKD, a therapeutic approach was developed that was successfully implemented into the clinics. The scientific bases for this study were *in vitro* experiments (Multhoff et al. 1999; Gastpar et al. 2005), and preclinical murine xenograft tumor models (Stangl et al. 2006), evolving through a pilot phase trial (Milani et al. 2009), and resulting in clinical phase I (Krause et al. 2004) and clinical phase II (Specht et al. 2015) trials.

Last but not least, the prevailing part of recent immune modulating approach utilizes monoclonal antibodies directed against tumor-associated antigens (TAA). The applied antibodies can be utilized in different melodies. “Naked” antibodies provide direct functional effects on the targeted cells or trigger immune-responses, and modulated antibody-conjugates possess tailored cytotoxic effects mediated by coupled toxins or radionuclides. Here, we focus on therapeutic possibilities provided by the immune stimulatory capacity of “naked” antibodies for antibody depenedent cellular cytotoxicity (ADCC).

For strictly tumor-selective therapeutic effects, the most important feature of the target structure which is addressed is the tumor exclusivity. This is either ensured by targeting a tumor-associated mutated membrane protein which is only expressed by tumor cells, or by targeting intracellular proteins in its *de novo* membrane-associated location in cancer cells. Nevertheless, a significant proportion of antibody-based tumor targeting approaches target over-expressed membrane-receptors, which are also expressed at lower densities on their non-malignant counterparts. Antibody-binding to these normal tissues may result in characteristic adverse side-effects that are related to the respective target antigen (Hansel et al. 2010; Liu and Li 2014). As a prominent example, Cetuximab, a broadly used therapeutic monoclonal antibody against Epidermal Growth Factor Receptor (EGFR), which is also expressed in normal skin cells, has been reported to trigger serious rushes of the skin in several cases.

Despite these drawbacks, antibody-based cancer treatment feature several beneficial therapeutic effects, of which the most important are (i) the alteration of signaling receptor functions on tumor cells, such as the inhibition of proliferative signaling pathways, as the above

mentioned anti EGFR antibody Cetuximab (Ming Lim et al. 2013) or activation of death receptors like the tumor necrosis factor receptors (TNFR) (Kaplan-Lefko et al. 2010), (ii) neutralizing trophic signals of tumor-stroma components or malignant cells like the Vascular Epithelial Growth Factor (VEGF) (Ferrara et al. 2004), and (iii) by obsonizing cancer cells with subsequent induction of the host´s anti-tumor Immune response (Galluzzi et al. 2014). Among others, the major antibody-guided immune-responses consist of two main components: the induction of antibody dependent cellular cytotoxicity (ADCC), predominantly mediated by NK cells, neutrophiles and macrophages (Hubert and Amigorena 2012) or by direct recruitment of the complement cascade (Zipfel and Skerka 2009). Scott, Wolchok and Old (Scott et al. 2012) summarized all main mechanisms of action of the different antibody modifications used for cancer treatment. This overview is given in Figure 2.

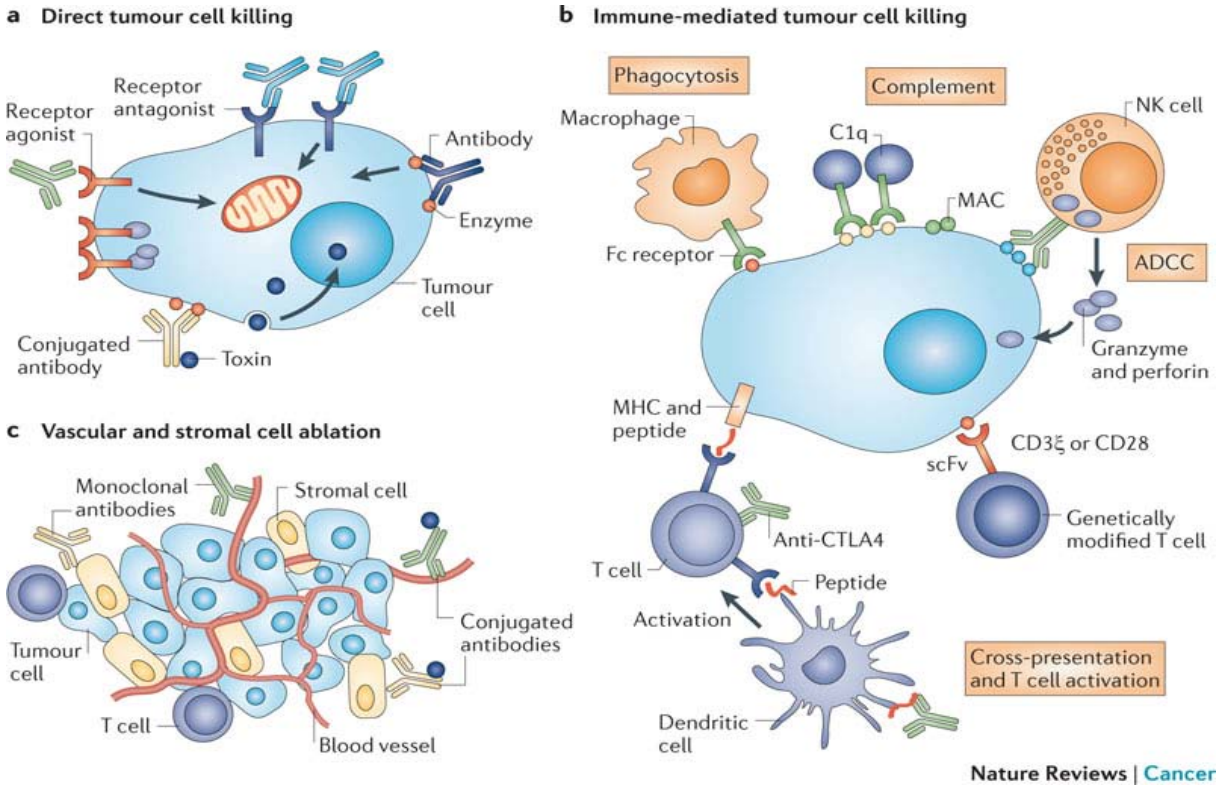

Figure 2. **Mechanisms of tumour cell killing by antibodies**. **a.** Direct tumour cell killing can be elicited by receptor agonist activity, such as an antibody binding to a tumour cell surface receptor and activating it, leading to apoptosis (represented by the mitochondrion). It can also be mediated by receptor antagonist activity, such as an antibody binding to a cell surface receptor and blocking dimerization, kinase activation and downstream signalling, leading to reduced proliferation and apoptosis. An antibody binding to an enzyme can lead to neutralization, signalling abrogation and cell death, and conjugated antibodies can be used to deliver a payload (such as a drug, toxin, small interfering RNA or radioisotope) to a tumour cell. b. Immune-mediated tumour cell killing can be carried out by the induction of phagocytosis; complement activation; antibody-dependent cellular cytotoxicity (ADCC); genetically modified T cells being targeted to the tumour by single-chain variable fragment (scFv); T cells being activated by antibody-mediated cross-presentation of antigen to dendritic cells; and inhibition of T cell inhibitory receptors, such as cytotoxic T lymphocyte-associated antigen 4 (CTLA4). c. Vascular and stromal cell ablation can be induced by vasculature receptor antagonism or ligand trapping (not shown); stromal cell inhibition; delivery of a toxin to stromal cells;

and delivery of a toxin to the vasculature. MAC, membrane attack complex; MHC, major histocompatibility complex; NK, natural killer. From (Scott et al. 2012).

The first, in 1997 FDA-approved, cancer-therapeutic antibody was Rituximab, a chimeric monoclonal antibody directed against the B-lymphocyte antigen CD20, and thus this antibody was applied to treat B-cell lymphoma. In rapid follow-up, several newly developed therapeutic Antibodies followed, such as Trastuzumab, targeting ErbB2 on breast cancer cells. Nowadays, more than 30 therapeutic antibody drugs have been approved by the FDA (Liauw W, 2013), and a rapidly growing number with many more in the research pipelines. An overview of anticancer immunotherapeutics is given in the supplemented Table 1, appendix 1.

The laboratory of Gabriele Multhoff developed a monoclonal antibody-triggered, ADCC mediated cancer immunotherapy in a preclinical setting, taking advantage of the membrane-associated form of the molecular chaperone Hsp70 (HspA1A, #3303, see chapter I-3.2). As this targeted molecule is predominantly expressed on the plasma membrane of tumor cells, the risk of antibody-induced on-target side effects is low. In line with this prognosis, our preclinical studies on tumor bearing mice did not reveal any adverse side effects. Yet, after intravenous administration, the antibody was capable to induce ADCC, resulting in significant reduction of the tumor burden and hence, prolonged overall survival. The report on these studies is implemented into this work (see Chapter IV: Short Summaries of the included publications, publication B).

I-2.3. Tumor Targeting to Detect and Diagnose – early diagnoses saves lives

Early tumor detection and diagnosis is crucial for a positive outcome of the therapy. Those patients that are diagnosed at early stages of tumor development have dramatically improved prognosis and survival rates. For instance, more than 90% of women, diagnosed with breast cancer in the earliest stage, reach the 5-year survival time, compared to as less as 15% when diagnosed with metastatic disease (Cancer Research UK. Breast cancer survival statistics. 2015). Similar statistics are found for ovarian cancer, with only 5% of the late diagnosed patients reaching the 5-years survival (Cancer Research UK. Ovarian cancer survival statistics. 2015). These numbers indicate that, apart from tumor prevention, early diagnosis is the most important for the improvement of survival rates. In general, tumor detection can be achieved in two ways, screening for tumor biomarkers in the peripheral blood or using intra-vital *in vivo* imaging. This chapter will discuss tumor targeting contrast agent guided *in vivo* imaging for tumor detection.

In recent years, the technology to detect and diagnose cancer has dramatically improved. New advances in clinical imaging tools, such as the development of highly sensitive sensors and image processing algorithms, took their sensitivity to new frontiers. Some of the techniques are capable to detect – or are even dependent on - signals originating from distinct reporter

particles, including Positron Emission Tomography (PET), Single Photon Emission Computed Tomography (SPECT), Magnetic Resonance Imaging and many more, helping the physicians to diagnose and detect cancer. After therapeutic intervention, the outcome can be accurately screened and evaluated using these non-invasive imaging techniques (Conway et al. 2014). For surgical interventions, intra-operative imaging techniques are used, to perform real time image-guided surgery to accurately delineate tumor margins (van Dam et al. 2011). To extract more information and enhance the precision of these imaging technologies, a new class of tumor-targeted contrast agents has been employed to direct the respective reporter particles to the cancer side. Molecular imaging, based on these contrast agents, is considered to be the future of medical imaging, as it provides multiple layers of information additional to diagnostic and predictive appliance, such as spatiotemporal distribution of molecular or cellular processes for biochemical and biological investigations (Kobayashi et al. 2010).

An applicative compound for *in vivo* imaging of malignancies needs to fulfill certain conditional aspects, most important its tumor specificity and sensitivity to ensure sufficient detection of primary tumors and metastases, including early stage lesions at sub-mm sizes. Prevention of false-positive signals at normal tissues requires utilization of strictly tumor-selective target epitopes as well as the usage of non-immunogenic compounds to avoid side-specific enrichment to immune organs.

For favorable pharmacokinetics and biodistribution of a tumor targeting compound, the molecular weight is of vast importance. Size and shape determine not only half-life in the circulation or immune recognition dependent biodistribution features but also efficient perfusion, penetration and retention in the targeted tissue. Antibodies are large molecules exceeding the threshold of renal clearance, which is at about 70 kDa, and thus are excreted following the hepatic pathway. They feature the inherent property of long serum half-lives of up to three weeks, for the most part mediated by their accessibility towards recognition by various cell types. Their Fc portion can interact with the neonatal Fc receptor (FcR) expressed at the surface of several cell types like macrophages, monocytes, vascular endothelium cells or intestinal epithelial cells. Binding to several other Fc Receptors which are present at the surface of most immune cells, such as Fcε, Fcγ and Fcα receptors, significantly increases their retention in the circulation (Chames et al. 2009; Milla et al. 2012). In contrast to antibodies, small, oligopeptidie-sized molecules, undergo mainly renal clearance and do not inherit features prolonging their half-life in the circulation or accumulation in distinct immune organs. Additional, an accelerated intracellular enrichment of small compounds targeting rapidly internalizing epitopes provides efficient signal quantities and prevention of accessibility to body clearance. Taken together, small molecules are more beneficial for *in vivo* detection due to their lower enrichment in normal tissues, compared to immunoglobulin-like molecules.

The second main part of this work comprises of the preclinical evaluation of three different membrane-bound Hsp70 compounds for *in vivo* tumor targeting. These compounds differ in their molecular sizes, ranging from the 1.5 kDa Tumor cell Penetrating Peptide (TPP) to the full length murine IgG1 monoclonal antibody cmHsp70.1, and covering, as an intermediate sized compound, a cmHsp70.1 derived F_{ab} fragment (cmHsp70.1Fab) of 35.5 kDa, synthesized in collaboration with the laboratory of Arne Skerra (Friedrich et al. 2010). Whereas the *in vivo* imaging of cmHsp70.1 was mainly used to investigate its biodistribution characteristics and specific enrichment at the tumor side to evaluate the qualification as a therapeutic compound (see chapter previous), cmHsp70.1F_{ab} and TPP have been optimized for tumor-selective *in vivo* imaging. Small molecules such as peptides or antibody F_{ab} Fragments represent a promising new class of tumor-targeting tools due to their advantageous bio-distribution with fast body clearance, no accumulation in the liver and their capacity to effectively penetrate viable tumor cells. Taking advantage of the membrane location pattern of Hsp70 in tumor cells, we successfully developed these two compounds for diagnostic *in vivo* targeting.

Given the central role of Hsp70 in the tumor targeting approaches described in this work, the multiple roles of this molecular chaperone in health and cancerous diseases will be described in the following.

I-3 Hsp70 and the heat shock response machinery

I-3.1 Hsp70 physiology

Through the entire evolution, life continuously had to face hazardous threats and perilous, rapid changes of environmental conditions such as temperature and pH shifts, oxidative stress, heavy metals, radiation and other proteotoxic insults. In strictly organized organisms with subtle optima in physical and chemical conditions, stress, induced by rapid alterations in the environmental conditions, also elevated stress, can result in various damages, mainly denaturation of proteins with subsequent unspecific aggregation. Besides protein-denaturation, stress induced changes affect the organization of the whole cell on transcriptional level, like alteration of RNA splicing (Vogel et al. 1995), as well as the cellular morphology, including formation of stress-induced cytosolic granules containing RNA-protein complexes for regulation of translatory processes. Other effect can include changes in other cellular components as the cytoskeleton, the microtubule network and the cellular membrane (Welch and Suhan 1985). In combination, these effects can lead to cell cycle arrest with reduced growth and proliferation (Lindquist 1986).

In reaction to these various challenges with the potential to irreversibly damage essential cellular structures, early organisms developed a complex system of stress response molecules,

also known as HSPs. The main task of this system is to prevent the denaturation of proteins, refold them and, so, to protect and restore the essential protein homeostasis. As one of the first in the field, in the 1950s Ritossa discovered in Drosophila the occurrence of chromosomic puffs as local sites of enhanced transcription, marking the initial step of the heat shock response (Ritossa 1962). Similar phenomena could subsequently be observed not only in eukaryotic cells but also in prokaryotes (Peterson et al. 1979), indicating the maintenance of the heat shock response system through evolution. This was a major hint for the great importance and, consequently, universality of this system (Richter et al. 2010). However, HSPs as molecular chaperones, are not exclusively induced following stress, yet there is a constant need of chaperones during post-transcriptional modification of proteins, as well as in stabilizing the existing proteomic homeostasis (Mayer 2010). Yet, following stress, cellular heat shock response is rapidly and transiently induced.

The transcription of HSP messenger RNAs is mediated by a family of transcription factors, called Heat Shock Factors (HSF), with HSF1 as the mayor player for the fast response. The rapid, yet transient, activation of HSF1 is a subject of reversible transformation from an inactive, monomeric form to the active, trimeric, transcription factor with DNA binding capacity. Under physiological conditions, HSF1 is stabilized in its inert, inactive monomeric configuration by complexation with basal levels of Hsp70, Hsp90 and co-chaperones. Upon stress, several mechanisms of HSF1 activation are described. The most prominent pathway, however, is triggered by elevated levels of cytoplasmatic, hydrophobic HSP substrate proteins, that cause the release of the chaperone complex from HSF1, leading to subsequent trimerization. The trimeric pre-form of HSF1 is then transported into the nucleus where it, activated upon phosphorylation, binds to the heat shock element (HSE) sequences on the DNA, which is present on the promoter-regions of heat shock protein genes, and leading to their elevated transcription. (Shamovsky and Nudler 2008). In a concentration dependent manner, HSF1-regulated transcription products like Hsp70 and other Hsps, recurrently stabilize the inactive HSF1 monomer. Thus, the activity of HSF1 is controlled by a negative feedback loop mechanism with attenuation by HSPs binding to its transactivation domain (Shi et al. 1998; Voellmy and Boellmann 2007). Altogether, the protein profiling after exposure to cell stress exhibits, species-dependent, of a number of up to 200 significantly induced genes which are involved in nearly all essential cellular functions, such as cellular function and maintenance, post-transcriptional modification, protein folding, cell morphology, cell cycle, and cellular development.

According to Richter, Haslbeck and Buchner (Richter et al. 2010), the stress response molecules can be devided in 7 functional classes: The firstly discovered and best-known class is represented by the HSPs or stress proteins, accompanied by a group of proteolytic proteins, which clear misfolded or irreversibly aggregated proteins. The 3rd group of stress response molecule is composed of the class of nucleic acid modifying enzymes, which is involved in the repair of non-

physiological DNA and RNA modifications. The 4th class, metabolic enzymes, regulates and stabilizes the energy supply during cell stress. This may help to enable the elevated synthesis and operational capacities of regulatory proteins, as transcription factors and kinases, comprising the 5th class of stress response molecules. The 6th group consists of proteins which sustain cellular structures, like the cytoskeleton. Finally, to accomplish the adaptation of the cell to the changed conditions following cell stress, are transport-, detoxifying, and membrane-modulating enzymes, needed to prevent toxification and maintain membrane integrity. The synthesis and action of the various stress response molecules hereby follows an organized kinetic meshing in space and time to keep cell integrity, covering stabilization of integral cellular components, disposal and detoxification of irreversibly denaturated proteins, repair of proteins and nucleic acids, and finally recovery of the cells which do not undergo apoptosis.

I-3.2 The inducible Hsp70

The predominant class of stress response molecules – the molecular chaperones - is composed of five main HSP families, HSPH (Hsp100), HSPC (Hsp90), HSPA (Hsp70), HSPD/E and CCT (chaperonins, Hsp60) and HSPB (small Hsp), which lack ATPase activity. Each family is composed of constitutively expressed and inducible members (Kampinga et al. 2009). In general, chaperones do not contribute any conformational information to the folding of proteins; rather they increase the efficacy by preventing competing reactions, such as aggregation. The most conserved proteins of the HSPs, with about 60% similarities in sequence between the prokaryotic version (referred to as DnaK) and the eukaryotic version, is HSP70, a family consisting of at least 13 members in *homo* sapiens (Tang et al. 2005; Kampinga et al. 2009). HSP70s can be found in the lumen of the endoplasmatic reticulum (HSPA5 / GRP78) or mitochondria (HSPA9 / GRP75), whereas the other 6 HSP members are distributed in the cytosol and nucleus (Hartl and Hayer-Hartl 2002; Daugaard et al. 2007). Hsp70 consist of two structurally independent domains, an N-terminal, nucleotide binding domain with ATPase activity, and the C-terminal substrate binding domain, composed of an α-helical lid segment and a β-sandwich domain, including an HSP oligomerization domain (Aprile et al. 2013). The activity of Hsp70 chaperones is ATP-dependent and regulated by cofactors like Hsp40/J-protein containing proteins and various nucleotide exchange factors (NEFs) (Kampinga and Craig 2010; Hartl et al. 2011). During the reaction cycle, unfolded or partially folded client proteins are delivered to ATP-activated Hsp70 and accommodated into the binding pocket by the cofactors (Kampinga and Craig 2010). Hsp40 subsequently stimulates ATP hydrolysis by Hsp70, thus stabilizing the Hsp70-substrate complexes by the α- helical lid domain, which then induces the conformational changes in the bound substrate (Hartl et al. 2011; Marcinowski et al. 2011; Schlecht et al. 2011). NEF binding catalyzes ADP dissociation and subsequent binding of ATP through Bag (Bcl2-

associated athanogene, functioning as a cofactor for Hsp70) results in opening of the helical lid and substrate release (Sondermann et al. 2001), thereby completing the reaction cycle. Proteins which remain unfold may be transferred subsequently to downstream chaperone systems like HSP90 or chaperonins (Langer et al. 1992). Irreversibly misfolded proteins are furthermore targeted to the proteasome through interaction of Hsp70 with CHIP (Carboxyl-terminus of Hsc70 interacting Protein) and subsequent polyubiquitination, linking the protein processing of the chaperone machinery to protein degradation (Petrucelli et al. 2004; Arndt et al. 2010).

Two different forms of HSP70 molecules exist in the cytosol of higher eukaryotes: constitutively expressed Hsp70s, termed Hsc70, and the inducible Hsp70s, with the main representatives Hsp70A1A and A1B (Chang et al. 2007). They are encoded by closely related, intron-less genes which reside in the major histocompatibility complex (MHC) III cluster on chromosome 6p, being more than 99% homologous (Milner and Campbell 1990). Under physiological conditions, Hsp70 proteins are expressed in a cell type and cell cycle dependent manner, slightly up-regulated in G1- and S-phase (Taira et al. 1997). Thus, promoters for inducible Hsp70 also contain several binding sites for basal transcription factors (TATA factors, CCAAT-box-binding transcription factor and SP1) (Greene et al. 1987).

Besides *de novo* folding of proteins and its protein-stabilizing, transport- and anti-proteotoxic function, it has been shown that inducible Hsp70 plays substantive roles in the regulation of proliferation and apoptosis as well as immunomodulation. In view of the fact that Hsp70 is significantly upregulated in tumor cells of various entities, and can be found at the cell membranes as well as in the extracellular space, Hsp70 has shifted into focus of cancer research in the last decades.

I-3.3: Hsp70 in tumor malignancies – the role in the hallmarks of cancer

Imbalances in the regulation of cell proliferation, differentiation, homeostasis, cell death as well as the ability of tumor cells to tissue invasion and metastasis reflect fundamental hallmarks of cancer, underlined in Hanahan and Weinbergs “Hallmarks of cancer: the next generation” (Hanahan and Weinberg 2011). A growing body of evidence suggests, that among other members of the HSP families like Hsp27, Hsp90 and Hsp110 (Hwang et al. 2003), Hsp70 plays an important role in many aspects of tumor biology (Calderwood and Ciocca 2008; Zorzi and Bonvini 2011). Constitutive over-expression of Hsp70 in human tumor cells was firstly reported as early as 1986 (Ferrarini et al. 1992). The crucial role of inducible Hsp70 in tumor cell survival and growth has been discovered soon after (Nylandsted et al. 2000; Gabai et al. 2005).

This chapter will give an overview over the involvement of Hsp70 in tumor-biology and sum up recent approaches to target the stress response machinery in cancer therapy. Furthermore, the involvement of Hsp70 in the “hallmarks of cancer 2011”, as described from Hanahan and

Wineberg, will be outlined. In their review, the authors discuss key traits of cancer biology, including (i) sustaining proliferative signaling, (ii) resisting cell death, (iii) enabling replicative immortality, (iv) activating invasion and metastases and (v) evading immune destruction (Hanahan and Weinberg 2011). To date, little is known about the participation of Hsp70 in the further hallmarks of cancer. Yet, the particular role of Hsp70 in the induction of angiogenesis, the genome instability and mutations, and the reprogramming of the energy metabolism is a matter of ongoing investigation.

An overview over the incidences of Hsp70 in tumors including potential intervention strategies is given in Figure 3.

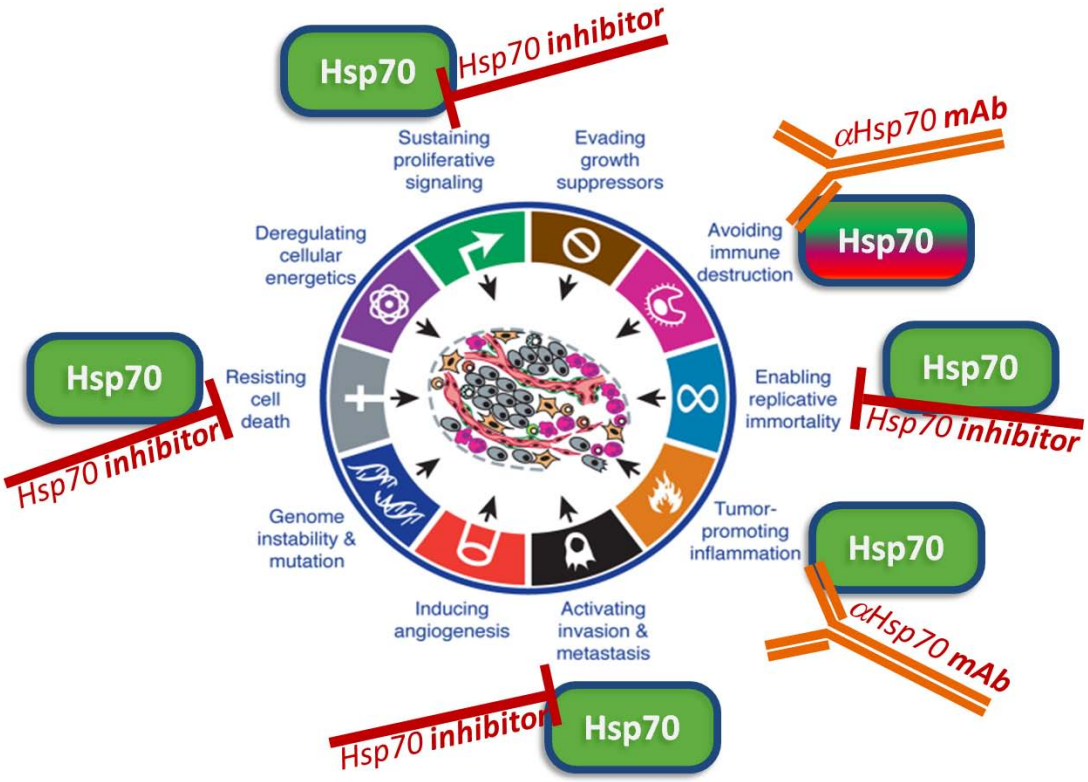

Figure 3: **Involvement of Hsp70 in the hallmarks of cancer and potential intervention strategies using Hsp70 targeted compounds**. Red, tumor-inhibiting Hsp70; green, tumor-supportive Hsp70. Adapted from (Hanahan and Weinberg 2011).

I-3.3.1 Induction of elevated Hsp70 expression patterns

At present, the mechanisms of the HSP induction in cancer still are a matter of investigation. Several activation mechanisms are under discussion, including irregular HSF1- expression and activation due to malignant cell signal transduction pathways, translational miss-control or epigenetic alterations of the regulation of HSPs.

In post-translational modifications of the HSF1, its hyper-phosphorylation is an essential trigger in the Hsp-transcription (Sarge et al. 1993; Chu et al. 1996). Carcinoma cells, moreover, display

an alternated phosphorylation pattern of HSF1 through the receptor-tyrosine-kinases HER2 and HER3, the cytoplasmatic serine kinase phosphatidyl-inositol 3 kinase (PI3K) and protein kinase A (PKA) (Ciocca and Calderwood 2005; Khaleque et al. 2008; Murshid et al. 2010). Additive to enhanced HSF1 activation, its level in carcinoma cells is also increased (Santagata et al. 2011). Translation of the tumor proteome, including HSPs, is furthermore altered due to changes in microRNA (miRNA) accompanying malignant transformation (Spizzo et al. 2009; Visone and Croce 2009).

In general, basic features of tumor cells like genomic polyploidy, elevated protein load as well as elevated levels of mutated proteins require enhanced chaperoning, and thus enhanced levels of molecular chaperones. This phenomenon is summed up in the "addiction to chaperones" hypothesis (Fishel et al. 1994; Dai et al. 2007).

Consequently, the elevated HSF1 mediated transcription results in constitutive upregulation of Hsp70 protein biosynthesis.

I-3.3.2 Hsp70 in the cell cycle regulation - sustaining proliferative signalling

Several mammalian cells show an increase in both, Hsp70 mRNA and protein, in the S-phase of cell cycle when Hsp70 translocates to the nucleus, indicating that Hsp70 has critical functions in cell division control (Milarski and Morimoto 1986; Spector et al. 1992; Rensing et al. 1999; Calderwood et al. 2006). Indications for a role of Hsp70 in the cell cycle regulation and proliferation in tumor cells have been obtained from Hsp70 knockdown experiments. Absence of Hsp70 results in the arrest of the cell-cycle at G1 and S-phase in human tumor cells (Wei et al. 1995). Furthermore, overexpression of Hsp70 in tumor cells stimulated growth and increased the number of cells in the S-phase.

Exposure of human tumor cell lines to stress, results in alteration of the cell cycle-dependent appearance pattern of Hsp70 suggesting the involvement of Hsp70 in DNA synthesis (Hang et al. 1995). Cancer cells depleted for either Hsp70A1A or Hsp70A1B also displayed cell cycle arrest predominantly in G2/M or G1 phase, respectively (Daugaard et al. 2005).

Furthermore, Hsp70 and its co-chaperones are found to be associated with proteins of the mitotic machinery. The co-chaperones regulate the association of the client proteins to Hsp70. Nucleotide exchange factors such as the BAG-domain proteins Bag1 and Bag3 are found to interfere with proteosomal degradation of the oncogenic IKKγ and subsequently increase proliferative cell growth through escalation of the NFκB pathway (Ammirante et al. 2010).

Additionally, chaperones, including Hsp70, interact with mitogenic signaling cascade proteins such as Src kinase, tyrosine kinases, and with Raf and the MAP-kinase activating kinase (MEK) by helping the folding and translocation of these proteins (Helmbrecht et al. 2000).

These data strengthen the role of Hsp70 not only in the proteome-homeostasis, but also in stabilization of the genome in proliferative processes.

I-3.3.3 Hsp70 is anti-apoptotic in tumor cells

A strong correlation between Hsp70 expression and therapy resistance has been observed (Gehrmann et al. 2008b). Rapidly growing tumors have to face multiple threats like hypoxia and nutrient deprivation due to chaotic vascularization, or impeding interventions of the immune system. It has been suggested that the cytoprotective properties of the stress response system are not only due their essential role in protein homeostasis, but additional effects might play a role. These events appear to interfere at key points of apoptosis control resulting in downregulation of pro-apoptotic pathway protein activity, or by stabilization and activation of survival pathway regulators (Igney and Krammer 2002). Resistance of tumor cells to apoptosis also renders them resistant to host defense mechanisms as well as to various forms of therapeutic interventions (Jaattela 1999; Sreedhar and Csermely 2004).

Hence, overexpression of Hsp70 is found to protect cells from stress-induced apoptosis, both upstream and downstream of the caspase cascade activation (Rerole et al. 2011) as well as at extrinsic apoptotic pathways mediated through FAS and TNF (Jaattela et al. 1998; Van Molle et al. 2002). Elevated levels suppress the release of cytochrome c from mitochondria and the activation of caspases via inhibition of upstream components of the apoptotic signal cascade, like JNK, p38 or ASK1 (Gabai et al. 2005). Inhibition of the interaction between procaspase-9 and Apaf-1 and subsequent apoptosome formation was also observed (Beere et al. 2000). On the other hand, the pro-survival capacity of Hsp70 by activation of major cellular survival pathways through MAP kinase and NF-kB signaling is well described (Wang et al. 1999; Volloch et al. 2000; Orlowski and Baldwin 2002; Kucharczak et al. 2003).

Further studies also describe an additional pro-survival effect of Hsp70 in ER-stress induced pro-apoptotic branch of the unfolded protein response (UPR) pathway. Hsp70 binds to- and enhances the RNase activity of IRE1α, a stress-sensitive ER membrane protein, resulting in stabilized expression pattern and anti-apoptotic downstream signaling (Gupta et al. 2010).

I-3.3.4 Hsp70 promotes replicative immortality

As a cell ages, it can undergo senescence typically after exceeding the limited number of replications. Senescence as a result of telomeres shortening, is complemented by findings which indicate the triggering of senescence by DNA damage and subsequent accumulation of the cell cycle inhibitors p16 and p21 and involving activation of p53 (Roninson 2002; Roninson 2003; Ben-Porath and Weinberg 2005). However, senescent – non-dividing – fibroblasts become

resistant to programmed cell death and are unable to undergo p53-dependent apoptosis (Wang 1995; Seluanov et al. 2001), features which typically also can be found in tumors. Recent data identified Hsp70 as an additional important regulator of senescence pathways in tumor cells, providing proliferative immortality. It has been shown that depletion of Hsp70 leads to p53 activation, induction of p21 and cell cycle arrest (Yaglom et al. 2007; Gabai et al. 2009; Sherman 2010).

I-3.3.5 Hsp70 activates invasion and metastases

One key hallmark of cancer and the major cause of cancer-related death is metastatic dissemination of cancer cells. In order to metastasize cells have to undergo epithelial–to–mesenchymal transition (EMT), alteration of cell adhesion, gain motility, invade and intravasate into blood- or lymphatic vessels, survive in circulation, extravasate at the site of metastases, adapt to a new environment, reacquire an epithelial phenotype and start to proliferate. During the multistep process of metastasis tumor cells have to face numerous threats such as mechanical stress, lack of survival signals, nutrient deprivation and hypoxia. Therefore, cell-autonomus pro-survival pathways and intrinsic cytoprotective properties must be enhanced for successful metastasization. Here, just as in the case of the primary tumor, stress response mechanisms play a major role. In a comparative analysis of primary tumors and distant metastases, it has been shown that the cellular Hsp70 levels are significantly higher in the metastases compared to the primary lesions (Farkas et al. 2003). Furthermore, Hsp70 has been reported to be involved in metastasatic processes like migration and invasion (Nakajima et al. 2002; Garg et al. 2010; Chiu et al. 2011).

An early step in the metastatic cascade is the alteration of cell adhesion to the extracellular matrix (Felding-Habermann 2003). Activity of signaling molecules as focal adhesion kinase, Met or Akt, drivers of cell death pathways following detaching from the ECM and regulators of invasive growth (Juhasz et al. 2013), is described to be triggered by elevated Hsp70 levels (Mao et al. 2003; Jang et al. 2011), demonstrating the metastasis-promoting role of Hsp70. In addition to protection of invasive cells from anoikis, activation and secretion of Matrix Metalloproteases (MMPs), enzymes involved in ECM remodeling, is reported to be triggered by Hsp70 (Lee et al. 2006; Sims et al. 2011).

In order to metastasize, tumor cells have to acquire a more mesenchymal-like phenotype by hijacking the embryonic developmental program EMT (Sims et al. 2011). During this process, invading tumor cells gain enhanced motility and reduced adhesion, thus enabling migration and invasion. Met, a key factor in triggering EMT, is highly influenced by the carboxyl-terminus of Hsp70 Interacting protein (CHIP) by switching cytosolic Hsp70 chaperone activity to proteasomal targeting (Jang et al. 2011). Furthermore, in hepatocellular carcinoma, extracellular Hsp70

promoted the expression of the mesenchymal cell marker α-smooth muscle actin protein (α-SMA), while the expression of the epithelial marker E-cadherin was down-regulated (Li et al. 2013a). Overall, Hsp70 plays a pleiotropic role in the regulation of metastatic processes.

Stem cell like cancer cells (SCLCS) are described to be the (small portion of) cancer cells which possess the capacity of comprising tumors due to their ability to self-renew and generate heterogeneous lineages of cancer cells. However, according to this SCLCS hypothesis, they are the active source of metastastic spread (Wicha 2006). The cell surface molecule CD44, which is upregulated in SCLCS, is involved in the regulation of proliferation, differentiation and migration of cells and is described to play a major role in metastasis (Martin et al. 2003) Recent studies observed elevated Hsp70 levels in tumor-initiating and highly metastatic, CD44/Sca1 positive, mammary carcinoma cells and loss of tumorigenicity following Hsp70, inactivation, indicating the requirement of Hsp70 for the generation and survival of CD44/Sca1+ cells (Calderwood 2013). Supporting evidence comes from a study showing co-expression of Hsp70 and CD44 in colorectal cancer (Wang et al. 2008b). Furthermore, binding of Hsp70 to Bag-1 and Bag-3 co-chaperones might couple Hsp70 properties to the cancer / stem cell signaling pathways involved in proliferation (Calderwood 2013). The BCL-associated athanogenes Bag-1 and Bag-3 act as co-chaperones in the regulation of Hsp70 (Song et al. 2001; Pagliuca et al. 2003), and, as such, are promoting cell-survival (Townsend et al. 2005). Importantly, BAG-1 and -3 are reported to be strongly associated with malignancy and capacity of metastazation in a variety of cancer incidences (Sharp et al. 2004; Ammirante et al. 2010).

I-3.4 Membrane-bound and secreted Hsp70 – aberrant localizations of Hsp70 in cancer

Additional to their common functions in mammalian cells, several members of the Hsp70 family perform distinct, non-overlapping tasks, depending on their location in the cytosol, nucleus, endoplasmatic reticulum or mitochondria (Daugaard et al. 2007). In neoplastic cells, besides having an essential role in cell growth and survival, it has been shown that - among other Hsps like Hsp27, Hsp60 Hsc70 and Hsp90 - Hsp70, notably the inducible Hsp70A1A, can be found at additional localizations. Several work groups detected a membrane-bound form of Hsp70 (mHsp70) (Multhoff et al. 1995), accompanied by a secreted form of Hsp70 (Ferrarini et al. 1992). These non-canonical locations were soon proved to be of major importance in the relationship of the tumor cells with the cells of the tumor microenvironment, suggesting a role for Hsp70 in intercellular communication. Indeed, evidence accumulates that membrane-bound and extracellular secreted Hsp70 not only contributes to tumor growth and progression, but also has a strong immunogenic activity (Schmitt et al. 2007).

As Hsp70 lacks both, a classical transmembrane domain (Gallucci and Matzinger 2001) and a consensus signal for ER / Golgi secretion (Hightower and Guidon 1989), it was believed that

Hsp70 is released secondary to necrotic cell death (Basu et al. 2000). However, soon it has been shown that Hsp70 is actively secreted by viable tumor cells with a intact plasma-membrane (Ferrarini et al. 1992; Multhoff et al. 1995). In the following years, the membrane-associated form of Hsp70 was found to be present on tumor cells of a wide variety of tumor types. Indeed it is reported in a wide variety of human tumors such as melanoma (Farkas et al. 2003), adenocarcinoma of the lung (Pfister et al. 2007), leukemia (Hantschel et al. 2000), carcinomas of the head and neck (Kaur et al. 1998; Kleinjung et al. 2003; Gehrmann et al. 2014b), tumors of the gastrointestinal tract, as colorectal carcinoma, (Gehrmann et al. 2008a; Stangl et al. 2011a) pancreatic carcinoma (Bayer et al. 2014), esophageal carcinoma (Fujita et al. 2008), lung carcinomas (Ferrarini et al. 1992; Botzler et al. 1996) and hepatocellular carcinoma (Gehrmann et al. 2014a). Moreover, the secreted form of Hsp70, among other HSP family members, is found to be present in the blood circulation of numerous tumor entities (Azuma et al. 2003; Faure et al. 2004).

Interaction of Hsp70 with lipid membranes was detected at electron microscopic level (Kurucz et al. 1999) as well as after profiling the tumor cell surface proteome (Shin et al. 2003). Hsp70 was found to be associated with cholesterol rich microdomains, containing, amongst others, the phospholipid membrane component globoyltriaosylceramide (Arispe et al. 2004; Gehrmann et al. 2008a), adding further evidence to the existence of a membrane-anchored form of Hsp70 in tumor cells. Subsequent studies on the function of the plasma membrane-associated Hsp70 revealed its upregulation and a cell protective and anti-apoptotic effect following γ-irradiation (Gehrmann et al. 2005).

For extracellular Hsp70 different modes of secretion have been suggested, including the lysis of the cell of origin, release in vesicles by a “blebbing” followed by subsequent lysis of the vesicles, secretion through the endolysosomal pathway (Mambula et al. 2007) as well as in a membrane-associated form (Clayton et al. 2005; Gastpar et al. 2005; Lancaster and Febbraio 2005).

Reports describe Hsp70 to be present on the lipid membrane surface of exosomes, which are released by the fusion of multivesicular bodies with the plasma membrane.

I-3.5 Immunmodulatory features of extracellular and membrane-bound Hsp70 – a double edged sword

Tumor immunosurveillance has been shown to be an essential protection mechanism against carcinogenesis. Comparative studies in immuno-competent and immune-deficient mouse models have confirmed the involvement of innate and adaptive immune cells in elimination of aberrant neoplastic cells (Dunn et al. 2002). Since Hsp70 is a highly conserved molecule with multiple intracellular functions, it is not surprising that the extracellular and membrane-bound Hsp70 forms can function as tumor antigens, and thus contribute to immune surveillance.

After discovery, almost instantly diverse functions of extracellular and plasma membrane-bound Hsp70 were explored, mostly pointing in the direction of serving as a danger signal for the immune system (Matzinger 2002; De Maio and Vazquez 2013). Particularly, extracellular Hsp70 has been associated with both, immunostimulatory and immunosuppressive, activities (Pockley et al. 2008). However, the mechanisms involved in the modulation of the response of cells of the immune system are still not clear.

One major responder to extracellular Hsp70, such as Hsp70-protein and -peptide complexes, was found to be the group of antigen presenting cells (APC), in particular macrophages. The group of Robert Binder investigated tumor-antigen specific priming of cytotoxic T-lymphocytes by APC following cross-presentation of tumor-derived HSP/tumor peptide complexes. This finding altered the classical understanding of antigen cross-presentation. HSPs, molecules which are present in the circulation at very low densities, and additionally are of self-origin, in general lack classical pathogen-associated molecular patterns recognized by corresponding pattern recognition receptors. Yet, tumor derived HSP/peptide complexes, in particular for Hsp70, appear to be recognized by their common receptor on APC, the alpha2-macroglobulin receptor CD91. Binding subsequently initiates cross-presentation of the chaperoned tumor-antigens and downstream signaling cascades activating CD4 and CD8 T-cells through MHC presentation (Basu et al. 2001; Pawaria and Binder 2011; Zhou et al. 2014). In addition, scavenger receptors including LOX-1 were also found to play pivotal roles in the uptake of Hsp70 / peptide complexes by dentritic cells and cross-presentation of tumor-derived peptides (Delneste et al. 2002). Of importance, also in the absence of immunogenic, tumor-derived peptides, Hsp70 can provide danger signals to APC. The group of De Maio found an induction of TNF-α release by APC, in particular macrophages, following Hsp70 exposure. This activation appeared to be ~260-fold more potent using a membrane-associated form of Hsp70, compared to the single recombinant protein, indicating the importance of actively released Hsp70 containing exosomes in tumor immunology. These findings may be explained as a result of the interaction of peptide-free Hsp70 with the pattern recognition receptor CD14 and Toll-Like Receptors 2 / 4 on APC and subsequent release of pro-inflammatory cytokines (including TNF-α, IL-1β, IL-12, IL-6 and GM-CSF), leading to general activation of the innate immune system (Vega et al. 2008).

A second major class of effector cells of the innate immune system, and in the first line of defense in tumor-immunosurveillance, is the natural killer (NK) cell linage of lymphocytes. The lytic activity of NK cells is controlled by a fine balanced system of inhibitory and stimulatory receptors and their respective binding pattern to antigens. According to the “missing self” hypothesis (Ljunggren and Karre 1990), tumor cells with an altered or missing MHC expression pattern are prone to NK cell mediated cytolysis. 40-90% of human tumors and metastases are reported to have a low or deficient MHC class I expression (Garcia-Lora et al. 2003), representing a main mechanism of tumor immune escape from T-cell mediated immune response. Due to the

“missing self” activation, NK cells contribute to immune response of these tumors and thus are involved in the maintenance of immune reaction.

Furthermore, NK cells are also directly capable to specifically recognize tumor cell antigens. Soluble Hsp70 was identified as triggering factor for NK cells expressing the C-type lectin receptor CD94 (Gross et al. 2003a). Incubation of NK cells with cytokines plus Hsp70 containing exosomes, soluble HSP70 protein, or the Hsp70 substrate binding domain- derived peptide increases the cell surface density of activatory NK cell receptors, including CD94, resulting in enhanced migration and cytolytic activity of primed NK cells towards Hsp70 membrane-positive tumor cells (Gross et al. 2003b; Gastpar et al. 2005).

We have seen the potent stimulatory modulation of the innate immune system by extracellular Hsp70 via direct signaling or cross-presentaton. However, this molecular chaperone also has the opposite, immunosuppressive, effect. Immuneregulatory T (T_{reg}) cell activation triggered by Hsp70 has been shown to be mediated by increased IL-10 and TGF-beta secretion, suppression of IFN-gamma and TNF-alpha release, and inhibition of CD4+ T cell proliferation (Todryk et al. 2003; Wieten et al. 2007; Pockley et al. 2008).

In summary, membrane-bound, exosome-derived and soluble Hsp70 strongly contribute to the modulation of tumor immune responses, mainly by the initiation of an anti-tumor reaction, yet, it also might contribute to T_{reg} mediated tumor escape mechanisms.

II. AIM OF THE PROJECT

Although *in vivo* targeting of tumors has greatly gained in importance over the last decades, most of the clinically applied reagents lack tumor cell specificity. Hsp70 can be found, despite of its intercellular constitutively upregulated form in cancerous malignancies, additionally in a membrane-associated manner, presented to the extracellular environment. Consequently, membrane-associated Hsp70 provides a possible cancer cell-selective target structure for *in vivo* tumor targeting of multiple tumor entities under exclusion of on-target toxicity. One of the most critical issues in cancer detection using tumor-targeting probes is selectivity and specificity, as many of the applied compounds also bind to epitope-positive cells of the tumor-associated stroma and normal tissue cells. Despite many reports on tumor markers in oncology the number of clinically useful, tumor-specific markers with prognostic relevance remains low (Hosotani et al. 2002; Schilsky and Taube 2002; Cardoso et al. 2008; Altman et al. 2012). Taking advantage of the presence of Hsp70 on tumor cells of a wide variety of murine and human tumor entities, and its prognostic values, we developed *in vivo* targeting approaches of Hsp70 membrane-positive cancer malignancies.

This thesis is based on the preclinical evaluation of three different *in vivo* targeting compounds – a full length IgG1-antibody, a F_{ab} fragment derived thereof, and a 14mer polypeptide - for cancer detection and therapy. Immunization of mice with a polypeptide vaccine comprising amino acids 450–461 (aa 450–461) in the C terminus of inducible Hsp70, resulted in the generation of an IgG1 mouse mAb cmHsp70.1. The tumor-specific binding of the mAb cmHsp70.1 was verified in a near infrared fluorescence imaging (nIR) approach ((Stangl et al. 2011a), see included publication "A"). Subsequently the therapeutic, ADCC inducing potential of cmHsp70.1 mAb was evaluated in tumor bearing mice ((Stangl et al. 2011b), see included publication "B"). Furthermore, small molecules like a F_{ab} fragment, derived of cmHsp70.1 ((Friedrich et al. 2010; Stangl et al. 2011c), see included publication "C"), as well as a 14mer peptide structure, named "Tumor cell Penetrating Peptide" (TPP) (Gehrmann et al. 2014c; Stangl et al. 2014), see included publications "D" and "E"), have been developed for diagnostic *in vivo* imaging of solid tumors, taking advantage of their more favorable biodistribution characteristics, compared to full length antibodies. The therapeutic and the diagnostic targeting of murine and human tumors taking advantage of the membrane-associated localization of the Hsp70 chaperone as target structure, will be discussed in the publications implemented in this thesis.

III. SHORT SUMMARY OF THE MAIN METHODOLOGY

The majority of the scientific work implemented in this thesis has been performed in the laboratories of the Department of Radiation Oncology, Klinikum rechts der Isar, Technische Universität München, as well as the animal facilities of the ZPF (Zentrum für Präklinische Forschung). It implements studies to evaluate the specific binding capacities and intracellular uptake of the different Hsp70 targeting compounds to be examined *in vitro* as well as their *in vivo* biodistribution, the tumor-specific enrichment and characterization of immune modulations. The utilized murine tumor models comprise of various syngeneic, xenografted, endogenous and chemically induced tumors. A short description of my own methodological tasks is given below.

Cell lines. The cell lines used in this work represent both, Hsp70 membrane-negative as well as Hsp70 membrane-positive wild type cell lines of multiple tumor entities. A Hsp70 knock out ($Hsp70^{-/-}$) murine mammary carcinoma cell line, generated in collaboration with the work group of Prof. R. Rad, Medical Clinic II, Klinikum rechts der Isar, Munich, Germany, was used as a control. Cell lines include human colon (CX2, HCT114), breast (MCF-7, MDA-MB436, T-47D), lung (A549, H-1339, EPLC-272H), pancreas (Panc-1, MiaPaCa-2, COLO357), head and neck (FaDu, Cal-33) carcinomas, as well as melanoma cell lines (Malme, Mel Ei, Mel Ho, Parl, A375 and Sk Mel29). For syngenic tumor mouse models, the following murine cell lines were used: colon (CT26), breast (4T1wt and 4T1 $Hsp70^{-/-}$) and pancreas (1048) carcinoma cell lines, melanoma cell lines (B16F0, low malignant and B16F10, high malignant), as well as the B-cell lymphoma cell line A20. Cell lines were purchased from Leibniz-Institute DSMZ – German Collection of Microoranisms and Cell Cultures, Braunschweig, Germany, the Tumorbank of Deutsches Krebsforschungszentrum, Heidelberg, Germany, and American Type Culture Collection ATCC/LGC Standards, Wesel, Germany. Further cell lines were kindly provided by Prof. J. Johnson, Institute of Immunology, Ludwig-Maximilians-Universität Munich, Germany,Prof. E. Kremmer, HelmholtzZentrum München, Munich, Germany,and Prof. J. Siveke, Medical Clinic II, Klinikum rechts der Isar, Munich, Germany.

Flow cytometric phenotyping. The membrane-Hsp70 phenotype of *in vitro* cultured tumor cell lines as well as of tumors grown *in vivo* was determined by flow cytometric analysis. Single cell suspensions of tumors were generated following 30 min collagenase /dispase digestion at 37°C and 5% CO_2. Cell suspensions were incubated for 30min at 4°C with fluorescein isothiocyanate (FITC)-conjugated cmHsp70.1 mAb (IgG1, multimmune GmbH, Munich) or carboxyfluorescein-conjugated TPP (TPP[CF]). After washing, viable (7-AAD negative) cells were analyzed using a FACSCalibur™ flow cytometer (BD Biosciences, San Jose, CA, USA). Gating was applied to distinguish the $CD45^-/CD140b^-$ tumor cell population from the fibrotic cells of the tumor

microenvironment ($CD45^-/CD140b^+$ fibroblasts, $CD45^+/F4/80^+$ macrophages, and the proportion of lymphocyte subpopulations, monocytes and granulocytes, using FITC/PE-labeled mAb directed against CD4, CD8, CD205, CD11c, Ly6G/Ly6C (Gr-1), B220, CD11b, CD49b, CD56 and CD25 (all BD Biosciences, San Jose, CA, USA). The proportion of positively stained cells was defined as the difference of the number of cells stained with the relevant antibody minus the number of cells stained with the appropriate isotype-matched control immunoglobulin. To assess antigen-specificity of the anti-Hsp70 antibody, blocking experiments were performed following co-incubation of viable tumor cells with cmHsp70.1-FITC mAb and an excess of TKD or scrambled NGL peptide.

Microscopic immunofluorescence studies were performed on tumor cells cultured in 8-well chamber slides (Nunc, Rochester, NY, USA) following incubation with cmHsp70.1-FITC for 30min, either at 4°C for surface staining or at 37°C for internalization analysis (both on viable, adherent cells). For analysis of the internalization pathways, after fixation and permeabilization, the cells were incubated with antibodies directed against the endosomal markers Rab4, Rab5a, Rab7, Rab9, Rab11 (all from Santa Cruz Biotechnology, Heidelberg, Germany), lysosomal associated membrane proteins (LAMP)1, LAMP2 (kindly provided by Prof. Stefan Höning, University of Cologne, Germany) for one hour, followed by the appropriate Cy3-conjugated secondary antibodies (anti-rabbit-Cy3 and anti-goat-Cy3, Jackson ImmunoResearch, West Grove, PA, USA) for 30 min. After counterstaining of the nuclei with 4,6-Diamidine-2-phenylindole (DAPI, Vector Laboratories, Burlingame, CA, USA) the slides were analyzed on a Zeiss Axioscop 2 plus scanning microscope (Zeiss, Jena, Germany) equipped with a 100x oil-immersion objective and standard filters.

A*DCC Assays.* Antibody-dependent cellular toxicity was measured using a standard 4 h ^{51}Cr release assay (Nishioka et al. 1997). Briefly, viable tumor cells were labelled with 0.1 µCi of $Na^{51}CrO_4$ at 37°C and incubated with cmHsp70.1 mAb (0, 0.7, 1, 1.4 µg/ml). Freshly isolated or pre-stimulated with 100 IU/ml IL-2 (Thermo Fischer, Waltham, USA) plus 2 µg/ml TKD peptide (Bachem, Bubendorf, Swizerland) wild type mouse spleen cells were added at various effector to target cell ratios (E:T). After a 4 hr co-incubation period, the levels of radioactive ^{51}Cr in the supernatant were determined using a gamma counter (Coulter-Counter, Billerica, MA, USA). Percentage of ADCC was calculated using the formula: %specific lysis = (experimental release – spontaneous release) / (maximum release – spontaneous release) x 100.

In vivo *studies*. All animal experiments were approved by the District Government of Upper Bavaria and performed in accordance with the German Animal Welfare and Ethical Guidelines of the Klinikum rechts der Isar, Technische Universität München, Munich, Germany.

T*umor models.* Immunocompetent BALB/c and FvB, as well as immunodeficient SCID/bg and SHO-*Prkdc*^{scid}*Hr*^{Hr} (CHO) mice were obtained from an animal breeding colony (Charles River, Borchen, Germany) and were maintained in pathogen-free, individually ventilated cages (Tecniplast, Hohenpeißenberg, Germany). Cell suspensions were inoculated intraperitoneal (CT26, syngeneic), subcutaneously (all cell lines, syngeneic and xenograft), or orthotopically into the mammary fad pad of female mice (mammary carcinoma cell lines, syngeneic or xenograft) using a 22 gauge needle.

The endogeneous pancreatic ductal adenocarcinoma (PDAC) model (Ptf1a$^{+/Cre}$; Kras$^{+/LSL\text{-}G12D}$; p53$^{LoxP/LoxP}$, CKP, described in (Ardito et al. 2012)) was used to more realistically mimic histology and morphology of human tumors. This model was kindly provided by Prof. J. Siveke, Medical Clinic II, Klinikum rechts der Isar, Munich, Germany.

Spontaneous colonic tumors were induced by i.p. injection of a single dose of azoxymethane (AOM; Sigma-Aldrich, Steinheim, Germany) at 10 mg/kg body weight. Following AOM treatment, the mice were subjected to three cycles of dextran sulfate sodium salt (MP Biomedicals, Santa Ana, CA, USA) administration in their drinking water. After 15 to 18 weeks of tumor development, the mice were sacrificed and the colon was resected for experiments. The presence of colorectal tumors was confirmed using standard histologic techniques.

Near *infrared fluorescence* in vivo *imaging*. Intraoperative epifluorescence imaging experiments were performed 30 min, 2, 4 and 8, 12, 24, 48 and 72 hrs after intravenous injection of the near infrared labeled compounds (cmHsp70.1 mAb, IgG1 isotype matched control mAb, TPP and CP; 100 µg each, as well as IntegriSense™ 750 (IS[750], Perkin Elmer, Waltham, MA, USA) at the recommended dose of 2 nmol) into the tail vain of tumor-bearing mice. After sacrificing the animals, fluorescence imaging of the exposed tumors and its surrounding normal tissue was configured to simulate an intraoperative imaging situation. Signal specificity was determined by calculating the ratio of the mean signal intensity in the exposed tumor tissue and that of the surrounding normal tissue (tumor-to-background ratio, TBR) (Themelis et al. 2011). For fluorescence measurements, a back illuminated EM-charge-coupled device (CCD) camera (iXon DV888, Andor, Belfast, Northern Ireland) was used. Light from the tissue was collected using a variable zoom objective lens (NT58–240, Edmund Optics, Barrington, NJ, USA) and filtered using 710/10 nm and 800/10 nm band pass filters. 670 nm and 740 nm diode lasers (B&W Tek, Newark, DE, USA) were used for the excitation.

The data acquired by intraoperative imaging were verified by transcutaneous epifluorescence imaging performed at the ExploreOptix system (Advanced Research Technologies, Montreal, Canada). The output of the system consists of maps of intensity and lifetime of the fluorescence distribution. Lifetime analysis describes the mean residence time of the fluorophore in an excited state and provides a characteristic parameter for the proportion of the antigen-bound

probe, and thus the *in vivo* specificity. The fluorescence intensity was determined in anaesthetized, viable mice.

Biodistribution studies. For biodistribution, tumor-bearing mice were sacrificed 12, 24 or 48 hr after i.v. injection of TPP[Cy5.5]. Fluorescent signal intensities of 0.25 cm^3 tissue cubes, taken from the tumor, spleen, pancreas, liver, lung, duodenum, kidney, heart, and 0.25 ml of peripheral blood were measured as described for intraoperative imaging. Agarose gel cubes, supplemented with standardized concentrations of the respective dyes, were used to calculate the probe concentrations in the investigated tissue samples using linear regression.

Microscopic in situ *fluorescence analysis.* To evaluate the microscopic distribution of the targeted compounds in tumor and normal tissue, microscopic in situ fluorescence analysis were performed. CF-labeled TPP, FITC-labeled cmHsp70.1mAb and mouse IgG1 (100 µg each), and the recommended dose of IntegriSense™ 750 (IS[750]) were injected i.v. into tumor bearing mice and allowed to circulate for 24 h. Tissues (tumor, liver, lung, kidney, heart and spleen) were collected and 8 µm cryosections, counterstained with DAPI (DAKO, Hamburg, Germany), were examined microscopically using a Zeiss Observer Z1 (Carl Zeiss, Oberkochen, Germany), equipped with standard filters for GFP and Cy7.

*Toxicity testing***.** Potential toxic effects of TPP were investigated by injecting healthy BALB/c mice intravenously (i.v.) with 500 and 1050 µg of TPP. The health status and the general behavior of mice were inspected. Animals were sacrificed on day 5 and the heart, liver, spleen, lung and kidneys examined for pathological changes using standard histological techniques.

Histology, immunohistochemistry (IHC) and fluorescence microscopy. Morphology of tissues was observed on 5µm paraformaldehyde-fixed, paraffin-embedded (FFPE) tissue sections following standard hematoxylin and eosin (H&E) staining. For IHC, endogenous peroxidase activity was blocked using 1% H_2O_2 containing 0.1% NaN_3. Following antigen retrieval in citrate buffer, effector cells were stained using antibodies directed against murine NK cells (α-CD49b, (BioLegend, San Diego, CA, USA) and α-CD56 (BD Biosciences, Heidelberg, Germany)), T cells (α-CD3 (Biolegend, San Diego, CA, USA)), macrophages (anti EGF-like module-containing mucin-like hormone receptor-like 1 (α-F4/80), ACRIS Antibodies, Herford; Germany), granulocytes/macrophages (α-Ly6C/Ly6G, Biolegend San Diego, CA, USA) mAbs or the appropriate isotype-matched control reagent overnight at 4 °C. For Hsp70-specific IHC using cmHsp70.1 mAb, an additional blocking step of unspecific mouse-on-mouse reactions was performed, using M.O.M. kit (Vector Labs, Burlingame, CA). Sections were counter stained with 1% Mayer's Hematoxylin (Dako) and analyzed on an Axio Image Z1 microscope (Zeiss, Jena, Germany).

IV. SUMMARIES OF THE INCLUDED PUBLICATIONS

A) *In vivo* imaging of CT26 mouse tumors by using cmHsp70.1 monoclonal antibody

J Cell. Mol. Med. 2011; vol.15, No. 4, pp.874-887

Stefan Stangl[a], Mathias Gehrmann[a], Ralf Dressel[b], Frauke Alves[c], Christian Dullin[d], George Themelis[e], Vasilis Ntziachristos[e], Eva Staeblein[a], Axel Walch[f], Isabel Winkelmann[f], Gabriele Multhoff[a]

[a]Department of Radiation Oncology, Klinikum rechts der Isar, Technische Universität München, and Clinical Cooperation Group (CCG) 'Innate Immunity in Tumor Biology', Helmholtz Zentrum München, German Research Center for Environmental Health (HMGU), Munich, Germany. [b]Department of Cellular and Molecular Immunology, University Medical Center Göttingen, Göttingen, Germany [c]Department of Hematology and Oncology, University Medical Center Göttingen, Göttingen, Germany [d]Department of Diagnostic Radiology, University Medical Center Göttingen, Göttingen, Germany [e]Department of Nuclear Medicine, Klinikum rechts der Isar, Technische Universität München, and CCG 'Institute of Biological and Medical Imaging', HMGU, Munich, Germany [f]Institute of Pathology, HMGU, German Research Center for Environmental Health, Munich, Germany

Background / Purpose. Herein, the binding characteristics and tumor homing abilities of the mouse monoclonal antibody (mAb) cmHsp70.1 were evaluated both, *in vitro* and *in vivo*.

Principal Findings. In flow cytometric analyses following incubation of the murine colon carcinoma cell line CT26 with the fluorescein isothiocyanate labelled cmHsp70.1 mAb at 4°C, the membrane presence of Hsp70 was determined to be more than 50%. After a temperature shift to 37°C, the cmHsp70.1 is internalized into the cells via translocation into early endosomes and lysosomes as revealed by immune fluorescence microscopy following co-staining of cmHsp70.1 fluorescein isothiocyanate with red fluorescence-labelled markers for early endosomes, late endosomes and lysosomes. Intraoperative, near-infrared fluorescence imaging revealed an enrichment of Cy5.5-conjugated mAb cmHsp70.1, but not an identically labeled IgG1 isotype-matched control Antibody, in i.p. and s.c. located CT26 tumors, as soon as 30 min after i.v. injection into the tail vein. Due to the rapid turn-over rate of membrane-bound Hsp70, the fluorescence-labeled cmHsp70.1 mAb became endocytosed and accumulated in the tumor, reaching a maximum after 24 hrs and remained detectable at least up to 96 hrs after a single i.v. injection of 100 µg of the compound.

Conclusions / Significance. The tumor-selective internalization of cmHsp70.1 mAb at the physiological temperature of 37°C might enable a targeted uptake of toxins or radionuclides, coupled to cmHsp70.1 mAb, into Hsp70 membrane-positive tumors. The anti-tumoral activity of the cmHsp70.1 mAb is further supported by its capacity to mediate antibody-dependent cytotoxicity.

The potential of Hsp70.1 induced ADCC is evaluated in publication B) "Targeting membrane heat-shock protein 70 (Hsp70) on tumors by cmHsp70.1 antibody".

B) Targeting membrane heat-shock protein 70 (Hsp70) on tumors by cmHsp70.1 antibody

PNAS 2011; vol. 108, No. 2, pp. 733-738

Stefan Stangl[a,1], Mathias Gehrmann[a,1], Julia Riegger[a], Kristin Kuhs[a], Isabelle Riederer[a], Wolfgang Sievert[a], Kathrin Hube[a], Ralph Mocikat[b], Ralf Dressel[c], Elisabeth Kremmer[b], Alan G. Pockley[d], Lars Friedrich[e], Laszlo Vigh[f], Arne Skerra[e], and Gabriele Multhoff[a,2]

[a]Department of Radiation Oncology, Klinikum rechts der Isar, Technische Universität München, and Clinical Cooperation Group "Innate Immunity in Tumor Biology," [b]Institute of Molecular Immunology, Helmholtz-Zentrum München, Deutsches Forschungszentrum für Gesundheit und Umwelt, 81675 Munich, Germany; [c]Department of Cellular and Molecular Immunology, University of Göttingen, 37073 Göttingen, Germany; [d]Department of Oncology, The Medical School, University of Sheffield, Sheffield S10 2RX, United Kingdom; [e]Lehrstuhl für Biologische Chemie, Technische Universität München, 85354 Freising-Weihenstephan, Germany; and [f]Biological Research Centre, Institute of Biochemistry, Hungarian Academy of Sciences, 6701 Szeged, Hungary.
1these authors contributed equally to the work.

Background / Purpose. Membrane-associated Hsp70 was proven to be present on a wide variety of tumor entitites while being absent in normal corresponding tissues. Hence, this tumor exclusive localization of membrane Hsp70 might represent a tumor selective target structure. Therapeutic targeting of membrane Hsp70 positive tumors with systemically applied compounds might consequently lead to tumor restrictive therapeutic effects with reduced adverse on-target toxicity on normal tissue. In this publication, the ADCC mediated therapeutic potential of an Hsp70 specific monoclonal Antibody in a preclinical setting is evaluated.

Principal Findings. Immunization of mice with a 14mer peptide TKDNNLLGRFELSG, termed "TKD," comprising amino acids 450–461 (aa450–461) in the C terminus of inducible Hsp70, resulted in the generation of an IgG1 mouse mAb cmHsp70.1. The epitope recognized by cmHsp70.1 mAb, which has been confirmed to be located in the TKD sequence by SPOT analysis, is frequently detectable on the cell surface of human and mouse tumors, but not on isogenic cells and normal tissues, and membrane Hsp70 might thus serve as a tumor-specific target structure. Herein, it is shown that the cmHsp70.1 mAb can selectively induce antibody-dependent cellular cytotoxicity (ADCC) of membrane Hsp70$^+$ mouse tumor cells *in vitro* and *in vivo*, mediated by unstimulated mouse spleen cells. Tumor killing could be further enhanced by activating the effector cells with TKD and IL-2. Three consecutive injections of the cmHsp70.1 mAb into mice bearing CT26 tumors significantly inhibited tumor growth and enhanced the overall survival. These effects were associated with infiltrations of NK cells, macrophages, and granulocytes. The Hsp70 specificity of the ADCC response was confirmed by inhibition of the antitumor response in tumor-bearing mice by co-injecting the cognate TKD peptide with the cmHsp70.1 mAb, and by blocking the binding of cmHsp70.1 mAb to CT26 tumor cells using either Hsp70 peptide or the C-terminal substrate-binding domain of Hsp70.

Conclusions / Significance. The tumor specific targeting potential of the Hsp70 specific monoclonal antibody cmHsp70.1 and subsequent induction of tumor-directed immune response was proven in a preclinical mouse tumor model. In this proof-of principle study, the therapeutic capacity of membrane Hsp70 targeting of malignant lesions could be demonstrated. Given the high proportion of membrane Hsp70 positive tumor entities might enable to establish a novel, tumor selective therapeutic targeting strategy with reduced adverse on-target side effects.

The utilization of membrane-bound Hsp70 on a variety of tumor entities for diagnostic targeting of solid tumors is described in the publications C: “Detection of irradiation-induced, membrane heat shock protein 70 (Hsp70) in mouse tumors using Hsp70 F_{ab} fragment”, D: “Tumor Imaging and Targeting Potential of an Hsp70 Derived 14-Mer Peptide” and E: ”Selective *In Vivo* Imaging of Syngeneic, Spontaneous, and Xenograft Tumors Using a Novel Tumor Cell-Specific Hsp70 Peptide-Based Probe”. Therefore non-immunogeneic, small Hsp70 targeted molecules with improved biodistribution characteristics were used.

C) Detection of irradiation-induced, membrane heat shock protein 70 (Hsp70) in mouse tumors using Hsp70 F_{ab} fragment

Radiotherapy and Oncology 2011; vol. 99, pp.313–316

Stefan Stangl[a], George Themelis[b], Lars Friedrich[c], Vasilis Ntziachristos[b], Athanasios Sarantopoulos[b], Michael Molls[a], Arne Skerra[c], Gabriele Multhoff[a],

[a]Dept. of Radiation Oncology, TU München and Helmholtz Zentrum München (HMGU), CCG-Innate Immunity in Tumor Biology, Germany; [b]HMGU, Institute of Biological and Medical Imaging, Munich, Germany; [c]Munich Center for Integrated Protein Science, Technische Universität München, Freising-Weihenstephan, Germany

*Background / Purpos*e: The major stress-inducible heat shock protein 70 (Hsp70) is frequently overexpressed in highly aggressive tumors, and elevated intracellular Hsp70 levels mediate protection against apoptosis. Following therapeutic intervention, such as ionizing irradiation, translocation of cytosolic Hsp70 to the plasma membrane is selectively increased in tumor cells and therefore, membrane Hsp70 might serve as a therapy-inducible, tumor-specific target structure.

Principal Findings: Based on the IgG1 mouse monoclonal antibody (mAb) cmHsp70.1, the Hsp70-specific recombinant F_{ab} fragment (Hsp70 F_{ab}) was generated as an imaging tool for the detection of membrane Hsp70 positive tumor cells *in vitro* and *in vivo*. The binding characteristics of Hsp70 Fab towards mouse colon (CT26) and pancreatic (1048) carcinoma cells at 4°C were comparable to that of cmHsp70.1 mAb, as determined by flow cytometry. Following a temperature shift to 37°C, Hsp70 F_{ab} rapidly translocates into subcellular vesicles of mouse tumor cells. Furthermore, accumulation of the Cy5.5-conjugated Hsp70 F_{ab}, but not of the unrelated IN-1 control F_{ab} fragment (IN-1 ctrl F_{ab}) in tumor-bearing mice between 12 and 55 hrs after i.v. injection was shown, whereas peaking of the specific enrichment of Hsp70 F_{ab} occured 24 hrs after i.v. injection.

Conclusions / Significance: F_{ab} fragments, derived of the murine monoclonal IgG1 antibody cmHsp70.1 provide an innovative, low immunogenic tool for imaging of membrane Hsp70 positive tumors, *in vivo* with improved biodistribution and reduced interference with the immune system, compared to the full length antibody.

D) Tumor imaging and targeting potential of an Hsp70-derived 14mer peptide

PLoS ONE 2014; 9(8): e105344.

Mathias Gehrmann[1§], Stefan Stangl[1§], Gemma A. Foulds[2], Rupert Oellinger[3], Stephanie Breuninger[1], Roland Rad[3], Alan G. Pockley[2], Gabriele Multhoff[1,4]

[1]Department of Radiation Oncology, Klinikum rechts der Isar, Technische Universität München, Munich, Germany, [2]John van Geest Cancer Research Centre, Nottingham Trent University, Nottingham, United Kingdom, [3]Medical Department II, Translational Gastroenterological Oncology, Klinikum rechts der Isar, Technische Universität München, Munich, Germany, [4]Clinical Cooperation Group (CCG) ''Innate Immunity in Tumor Biology'', Helmholtz Zentrum München, Deutsches Forschungszentrum für Gesundheit und Umwelt, Munich, Germany.
[§]these authors contributed equally to the work.

Background / Purpose: We have previously used a unique mouse monoclonal antibody cmHsp70.1 to demonstrate the selective presence of a membrane-bound form of Hsp70 (memHsp70) on a variety of leukemia cells and on single cell suspensions derived from solid tumors of different entities, but not on non-transformed cells or cells from corresponding 'healthy' tissue. This antibody can be used to image tumors *in vivo* and target them for antibody-dependent cellular cytotoxicity. Tumor specific expression of memHsp70 therefore has the potential to be exploited for theranostic purposes. Given the advantages of peptides as imaging and targeting agents, this study assessed whether a 14mer tumor penetrating peptide (TPP; TKDNNLLGRFELSG), the sequence of which is derived from the oligomerization domain of Hsp70 which is expressed on the cell surface of tumor cells, can also be used for targeting membrane Hsp70 positive ($Hsp70^+$) tumor cells, *in vitro*.

Principal Findings: The specificity of carboxy-fluorescein (CF-) labeled TPP (TPP) to Hsp70 was proven in an Hsp70 knock out mammary tumor cell system. TPP specifically binds to different membrane $Hsp70^+$ mouse and human tumor cell lines and is rapidly taken up via endosomes. Two to four-fold higher levels of CF-labeled TPP were detected in MCF7 (82% membrane $Hsp70^+$) and MDA-MB-231 (75% membrane $Hsp70^+$) cells compared to T47D cells (29% membrane $Hsp70^+$) that exhibit a lower membrane Hsp70 positivity. After 90 min incubation, TPP co-localized with mitochondrial membranes in memHsp70+ tumors. Although there was no evidence that any given vesicle population was specifically localized, fluorophore-labeled cmHsp70.1 antibody and TPP preferentially accumulated in the proximity of the adherent surface of cultured cells. These findings suggest a potential association between membrane Hsp70 expression and cytoskeletal elements that are involved in adherence, the establishment of intercellular synapses and / or membrane reorganization.

Conclusions / Significance: This study demonstrates the specific binding and rapid internalization of TPP by tumor cells with a membrane $Hsp70^{+}$ phenotype. TPP might therefore have potential for targeting and imaging the large proportion of tumors (50%) that express memHsp70.

E) Selective *in vivo* imaging of syngeneic, spontaneous, and xenograft tumors using a novel tumor cell-specific Hsp70 peptide-based probe

CancerRes 2014; 74(23); pp.6903–6912

Stefan Stangl[a], Julia Varga[b], Bianca Freysoldt[a], Marija Trajkovic-Arsic[c], Jens T. Siveke[c], Florian R. Greten[b], Vasilis Ntziachristos[e], and Gabriele Multhoff[a]

[a]Department of Radiation Oncology, Klinikum rechts der Isar, TU München and CCG -"Innate Immunity in Tumor Biology", Helmholtz Zentrum München (HMGU), Munich, Germany, [b]Institute for Tumor Biology and Experimental Therapy, Georg-Speyer-Haus, Frankfurt/Main, Germany, [c]Department of Medicine II, Klinikum rechts der Isar, TU München, Munich, Germany, [d]Institute of Pathology, Helmholtz Zentrum München (HMGU), Munich, Germany, [e]Institute of Biological and Medical Imaging, Helmholtz Zentrum München (HMGU), Munich, Germany

Background / Purpose: Although *in vivo* targeting of tumors using fluorescently-labeled probes has greatly gained in importance over the last few years, most of the clinically applied reagents lack tumor cell specificity. Our novel tumor cell-penetrating peptide-based probe (TPP) recognizes an epitope of Hsp70 that is exclusively present on the cell surface of a broad variety of human and mouse tumors and metastases, but not on normal tissues.

Principal Findings: Due to the rapid turn-over rate of membrane-Hsp70, fluorescently-labeled TPP is continuously internalized into syngeneic, spontaneous, chemically/genetically induced and xenograft tumors following intravenous administration, thereby enabling site-specific labeling of primary tumors and metastases in subcutaneously and orthotopic implanted, chemically induced and endogenous murine tumor models. In contrast to the commercially available non-peptide small molecule αvβ3-integrin antagonist IntegriSense™, TPP exhibits a significantly higher tumor-to-background contrast and stronger tumor-specific signal intensity in all tested tumor models. Moreover, in contrast to IntegriSense™, TPP reliably differentiates between tumor cells and cells of the tumor microenvironment, such as tumor-associated macrophages and fibroblasts which were found to be membrane- Hsp70 negative.

*Conclusions / Significanc*e: TPP provides a useful tool for multimodal imaging of tumors and metastases that might help to improve our understanding of tumorigenesis and allow the establishment of improved diagnostic procedures and more accurate therapeutic monitoring. TPP might also be a promising platform for tumor-specific drug delivery and other Hsp70- based targeted therapies.

V. DISCUSSION

The era of innovative personalized tumor treatment strategies is rapidly evolving. Personalization in oncology, based on genetic and biomarker aided approaches, enables the definition of individual tumor-associated target epitopes and thus determines most efficient treatment strategies for targeted cancer therapies. Being tailored to tumor-individual characteristics, these therapies provide beneficial effects in effective tumor treatment with a simultaneous reduction of adverse side effects which are caused by traditional, systemic applied chemotherapeutics. After about 3 decades of research and development, more than 40 different cancer- targeting and immune modulating drug compounds, including 18 monoclonal antibodies, have been approved by the regulatory authorities and have entered the clinical routine. To date, most clinically applied targeted therapies address cancer cells or tumor-supportive compartments of its microenvironment by (1) functional manipulation (blocking or hyper-activating) of the targets, utilizing small molecule inhibitors (predominantly tyrosine kinase inhibitors) or antibodies, or (2) priming the host´s individual immune response. The affected cellular mechanisms are, among others, agonistic triggering of the Toll-like receptor induced immune activation, blockage of immunological checkpoints, inhibition of growth factor- and hormone receptors of neoplastic or tumor-supportive cells, opsonization or redirecting of the immune system towards the target cells (Galluzzi et al. 2014).

Although significant therapeutic success has been achieved using these novel therapeutic strategies, cancer still remains a leading cause of death in the modern world, making further substantial research effort on improved intervention regimes and novel therapeutic access indispensable. Modern targeted therapies are often less toxic and better tolerated than traditional chemotherapy due to the substantially reduced adverse side effects on fast dividing normal tissue cells, and thus well improved the patients' quality of live. Still, studies on targeted therapies, especially after mono-therapeutic application, soon displayed limitations. Adverse side effects appeared to occur, dependent on the functionality of the target as well as potential cytotoxic labeling of the compound. Most targeted cancer therapeutics interfere with cell surface targets that are involved in tumor growth and progression. Such targets include growth factor receptors (Mendelsohn and Baselga 2006), signaling molecules (Downward 2003), cell-cycle proteins (Parmar et al. 2015), modulators of apoptosis (Ghobrial et al. 2005; von Schwarzenberg and Vollmar 2013), and pro-angiogenic molecules (Ferrara and Kerbel 2005). Targeted therapies take advantage of the fact that these molecules are over-expressed on tumor cells and are important for tumor growth. As these receptors are mostly involved in physiological development and homeostasis of normal tissue cells, the cytotoxic, inhibitory or immune (re-) directing effects of the targeted therapeutics also may affect normal tissues. Indeed, clinical

treatments disclosed typical on-target side effects, such as diarrhea and abnormalities of the liver (such as hepatitis or elevated liver enzymes), high blood pressure, insufficiency in wound healing and blood clotting mechanisms, and (more rarely) gastrointestinal perforation (National Cancer Institute, 2014, web source).

To prevent these complications, latest research on cancer-targeting drugs concentrated on the discovery and utilization of cancer-related mutations in the proteins of interest (Tenedini et al. 2014), as mutation-specific targeting may exclude affection of normal tissue.

A key challenge has been to identify antigens that are suitable for antibody-based therapeutics as well as tumor-selective diagnostic and prognostic imaging. Alternatively to targeting **cancer-related mutations**, cancer-selectivity can be also achieved by targeting **cancer-related alterations of the epitope localization**, such as *de novo* membrane-association and extracellular presentation of intracellular protein structures. In 1992, Gabriele Multhoff discovered such a situation in the case of the 72kDa molecular chaperone Hsp70 (Botzler et al. 1998). With membrane-localized Hsp70, we provide a promising targeting structure for therapeutic and diagnostic *in vivo* tumor targeting, which is exclusively presented at the plasma membrane of a broad variety of tumor entities, but not on corresponding normal tissues.

V-1 Immunotherapeutic targeting of membrane-associated Hsp70

Monoclonal antibody-based treatment of cancer is well-accepted as one of the most successful therapeutic strategies. The fundament of antibody-based therapy is laid by the observation that tumor cells express certain antigens on their cell surface (Rettig and Old 1989). The definition of cell surface antigens that are expressed by human cancers has revealed a broad array of targets that are overexpressed, mutated or selectively expressed, making them sufficiently distinguishable from normal tissues. Taking advantage of the extracellulary exposed localization of membrane-associated Hsp70 we developed a murine monoclonal IgG1 antibody (cmHsp70.1), which is capable of recognizing this membrane-bound form of Hsp70. In order to evaluate the tumor-specific enrichment capabilities of cmHsp70.1, we characterized the mHsp70 binding specificity and internalization characteristics of cmHsp70.1 *in vitro,* followed by *in vivo* imaging experiments in tumor-bearing mice utilizing near-infrared fluorescence labeling of the antibody.

After proving the tumor-specific enrichment of cmHsp70.1 in *in vivo* fluorescence imaging approaches, we focused on its immune therapeutic capabilities in a preclinical set-up utilizing a syngeneic murine tumor model with CT26 colon carcinoma cells. Despite the relatively low density of Hsp70 molecules that are presented on the cell surface of CT26 mouse tumor cells (≈10,000 per cell), and that IgG1 has a low capacity to induce ADCC (Steplewski et al. 1983) in mice, the cmHsp70.1mAb mediates specific killing in membrane Hsp70^{+} CT26 tumors. In

contrast, other IgG1 control antibodies directed against theta, or the F_{ab} fragment of cmHsp70.1 mAb had no such effect.

Functional *ex vivo* assays demonstrated the induction of antibody dependent cellular cytotoxicity (ADCC), mediated by syngeneic peripheral blood mononuclear cells, but did not reveal recruitment of the complement system. Intravenous injection of cmHsp70.1 mAb not only delayed the growth of subcutaneous and intraperitoneal CT26 tumors, but also significantly prolonged the survival of the mice. In line with these findings, we could observe an enhanced intra-tumoral accumulation of innate immune cells (NK cells, macrophages, granulocytes).The Hsp70-specificity of this approach is supported by the finding that cmHsp70.1 mAb had no effect on tumor growth or the survival of mice bearing membrane $Hsp70^{-}$ A20 B-cell lymphomas.

We have previously demonstrated that the incubation of lymphocytes with Hsp70 peptide TKD in the presence of low-dose IL-2 enhances the cytolytic and migratory capacity of NK cells toward membrane Hsp70+ tumor cells *in vitro* and *in vivo* (Multhoff et al. 2001; Stangl et al. 2006). The cytolytic effects of TKD/IL-2–activated NK cells against membrane $Hsp70^{+}$ mouse tumors were clearly detectable, as has previously been described for human tumors (Krause et al. 2004; Milani et al. 2009). Thus, additional administration of low dose IL-2 plus the Hsp70 peptide TKD further improved the anti-tumoral effect of cmHsp70.1 mediated immune therapy.

Of interest, no direct or immune-mediated systemic adverse side effects could be observed following treatment with cmHsp70.1. Furthermore, binding of cmHsp70.1 mAb to membrane $Hsp70^{+}$ tumors did not enhance the intracellular Hsp70 levels and thus a cmHsp70.1 mAb-based therapy is not likely to enhance protection of tumors against Hsp70-mediated apoptosis.

As radiochemotherapy has been shown to enhance the cell surface density of Hsp70 on tumors (Gehrmann et al. 2008b; Multhoff et al. 2015), a combined approach consisting of an Hsp70 mAb-based immunotherapy, similarly to Her2-targeted ADCC (Carson et al. 2001), might provide a novel strategy to improve the clinical outcome of patients undergoing standard radio-chemotherapy. This proposition is in line with the observation that a metastasis-free survival rate of patients can be associated with an enhanced NK cell activity (Kondo et al. 2003). The clinical relevance of our data is further supported by published observations on the ADCC activity of trastuzumab in metastatic breast cancer patients (Beano et al. 2008). In this study, the *in vitro* ADCC activity toward Her2 overexpressing tumor cells, which was quantitatively comparable to that which was seen against membrane $Hsp70^{+}$ tumor cells in the current study, could be correlated to the short-term antitumor responses in trastuzumab-treated breast cancer patients.

V-2 Diagnostic targeting of membrane-associated Hsp70

For diagnostic tumor targeting approaches, antibodies like cmHsp70.1 have several size-dependent limitations. To overcome these limitations, we generated Hsp70 specific small molecules, cmHsp70.1 F_{ab} and TPP. Additional to specificity, an important property of diagnostic compounds is the exclusive interaction with the target cell, as interference with the immune system may trigger immune reactions or lead to unspecific enrichment effects. As a naturally occurring polypeptide following necrotic cell death, the likeliness of strong anti-TPP immune reactions is limited. Although enrichment of TPP in tumor-associated macrophages occurred in the preclinical studies, none of the mice showed signs of auto-immune reactions, nor acute inflammation or signs of toxicity following administration of TPP. In dose-escalation studies, up to 50µg/g body weight of TPP has been administered intraveneously. After a circulation time of 5 days, the mice did not show toxic reactions, as assessed by gross monitoring. In addition, histological examination of the heart, liver, spleen, lung and kidney, evaluated by a veterinarian, did not reveal pathological changes (Stangl et al. 2014).

The favorable biodistribution of small tumor-targeting molecules *in vivo* can be explained by the distinct clearance pathways. In patients, small polypeptide structures with molecular weights of about 1kDa display rapid clearance with short blood half-life between a few minutes and 1.5 hours and subsequent renal excretion (Werle and Bernkop-Schnurch 2006); whereas larger immunglobulines like IgG1 antibodies have, dependend of the initial concentration, a plasma half-life of 8 – 25 days (Wang et al. 2008a) and are mainly metabolized in the liver. 24h after i.v. administration of 100µg of fluorescently labeled TPP, the compound showed accumulation at the tumor site (10.4±2.2 µg/cm^3), with less enrichment in the kidneys (5.4±3.2 µg/cm^3). The other investigated tissues, including liver and blood, showed minor background accumulation below 2.5µg/cm^3 tissue (Stangl et al. 2014). After comparable circulation time, ^{89}Zr labeled cmHsp70.1 mAb displayed an enrichment of 15.9±3.7% ID/g tumor tissue, 9.0±1.3% ID/g in the kidneys and 21.5±4.3% ID/g in the liver (unpublished data).

Apart from the tumor-selectivity of the Hsp70 targeting compounds, the tumor-related biology of membrane-bound Hsp70 is also beneficial for targeting approaches. After an incubation time of 30 minutes, a temperature shift from 4°C to 37°C resulted in an relative increase of the uptake of fluorescently labeled cmHsp70.1, cmHsp70.1F_{ab}, as well as TPP, by the factors of 1.6x, 4.1x, and 5.5x, respectively, representing the rapid turnover rate of membrane-bound Hsp70 at physiological temperatures and the inverse correlation of uptake of the different sizes of targeting compounds (Stangl et al. 2011c; Gehrmann et al. 2014c). The time-dependent accumulation of cmHsp70.1-FITC mAb in early endosomes and lysosomes supported the hypothesis of Hsp70 trafficking through the recycling pathway. As expected, part of the intracellularly located Hsp70 becomes degraded in lysosomes (Stenmark 2009). As a result of the

rapid turnover rates of mHsp70 and the subsequent accumulation of Hsp70 targeting compounds within the tumor cells, detection of Hsp70 targeting compounds can be performed after circulation times as long as 24h, due to the effective clearance of the compounds from normal tissues. According to the tumor-specific enrichment with simultaneous reduction in the background accumulation of normal tissues, *in vivo* imaging with TPP provided favorable tumor delineation, resulting in tumor to background ratios (TBR) of up to 7.1±1.7 in xenograft, subcutaneous pancreatic carcinoma model, 24 hrs after i.v. injection. In contrast to this, the maximum TBR yield of the commercially available small molecule antagonist of the $\alpha_v\beta_3$-integrin after comparable circulation times was 4.0±0.6 (Stangl et al. 2014). Using alternative tumor targeting compounds which target less quantitatively internalized membrane-epitopes, imaging of preclinical tumor models usually is performed within the first hours after i.v. application, due to fast body clearance of small molecules. At this early time points, organs like liver, kidney or spleen display several times higher accumulation of the compounds and obviously less contrast of tumor versus normal tissue (Zhang et al. 2013). The rapid internalization rate of membrane-associated Hsp70 is not only beneficial for tumor-selective *in vivo* imaging, it is also beneficial for the enrichment of therapeutic compounds, such as toxins or alpha-particle emitting nuclides, in the tumor cells. Therefore, highly selective Hsp70 targeting tools may also provide a potent drug delivery tool or, in combination with reporter molecules, may serve for theranostic applications.

Recent studies proved the capability of mHsp70 to be internalized into tumor cells even when coupled with gold-nanoparticels (Gehrmann et al. 2015). Particles of a size of up to 50nm could be shown to be effectively internalized into the cytoplasm of 4T1 mouse mammary tumor cells *in vitro*. This findings open up new opportunities for tumor-selective theranostic targeting approaches of mHsp70 positive tumor cells utilizing toxin-loaded nanoparticles equipped with reporter molecules for sensitive detection. Ongoing research addresses construction of advanced nanoparticles with distinct release of the toxins only after entering the endosomal-lysosomal pathway (Zhang et al. 2014) as well as providing useful reporter functions (Kircher et al. 2012). Due to the tumor-selectiveness and fast internalization of mHsp70, targeting mHsp70 with such next-generation theranostic compounds may provide a promising new approach for therapy with simultaneous diagnostic capabilities.

V-3 Furter approaches targeting the heat shock machinery

After global efforts and more than 40 years of work in the fight against cancer, the "magic bullet" has not yet been found. Being essential for cancer cells survival and sustaining their proliferative capacity, molecular chaperones represent further promising target candidates for

cancer therapies. During the past decades, therapeutic cancer targeting approaches inhibiting the heat shock machinery have evolved from concepts to robust clinical reality.

Inhibition of Hsp90 has been shown to result in degradation of multiple oncologic client proteins, including HER2, EGFR, AKT, mutant p53, MMP2 and many others, as well as in blockage of numerous oncogenic pathways (Workman 2004). Consequently, Hsp90 targeting drugs like the geldanamycin analogue 17-AAG as the most prominent example, exhibit broad-spectrum anti-tumour activity. However, as a secondary effect they activate HSF1 and subsequently induce the synthesis of other Heat Shock Proteins, like Hsp70. As a consequence, combinatorial treatment strategies targeting Hsp90 paralleled by inhibitors of other key factors of the heat shock response machinery were successfully developed. These include the inhibition of FSF1 (Schilling et al. 2015) or Hsc70 and Hsp70 proteins (Powers et al. 2008).

Currently, inhibitory treatment of other Heat Shock Proteins, like Hsp27, additionally shift into the focus of research (Schultz et al. 2012).

V-4 General conclusion – future aspects of targeted cancer therapies

In the last decades, “third-wave” cancer treatment compounds, comprising of selective, mechanism-based therapeutics and immune modulating strategies, accompany and complete the classical therapeutic inventions as the surgical dissection of malign lesions, radiotherapy or chemotherapies. Integrative approaches include screening of individual cases to design most effective treatment strategies for personalized therapies. The overall aim is thereby to quantitatively eradicate residual cancer cells following surgery and radiochemotherapy, including the tumor-initiating stem cell like cancer cells, to prevent relapse of the disease. For sufficient effects, systemic approaches have to take over, capable to target residual lesions and distant metastases down to sub-mm sizes. Most important, the cancer-specific redirection of the immune system, paralleled with selective, mechanism-based therapeutics, shifted in the focus of interest. Best results have been achieved following combinatory treatment together with mechanism-based treatment (Vanneman and Dranoff 2012). However, immune escape mechanisms and development of resistance still remains a critical issue in clinical treatment reality. As the stress response machinery comprise strongly cancer-supportive mediators of tumor growth, survival, metastasis as well as resistance against therapies, including the main players of this network may contribute to enhanced therapeutic outcome. Moreover, the tumor-restricted localization of Hsp70, the main inducible Heat shock response protein, provides a novel target epitope for targeted therapeutic approaches including the redirection of the immune system.

VI. REFERENCES

Adams J. 2004. The proteasome: a suitable antineoplastic target. *Nature reviews Cancer* **4**: 349-360.

Altman DG, McShane LM, Sauerbrei W, Taube SE. 2012. Reporting Recommendations for Tumor Marker Prognostic Studies (REMARK): explanation and elaboration. *PLoS medicine* **9**: e1001216.

Ammirante M, Rosati A, Arra C, Basile A, Falco A, Festa M, Pascale M, d'Avenia M, Marzullo L, Belisario MA et al. 2010. IKK{gamma} protein is a target of BAG3 regulatory activity in human tumor growth. *Proceedings of the National Academy of Sciences of the United States of America* **107**: 7497-7502.

Aprile FA, Dhulesia A, Stengel F, Roodveldt C, Benesch JL, Tortora P, Robinson CV, Salvatella X, Dobson CM, Cremades N. 2013. Hsp70 oligomerization is mediated by an interaction between the interdomain linker and the substrate-binding domain. *PloS one* **8**: e67961.

Ardito CM, Gruner BM, Takeuchi KK, Lubeseder-Martellato C, Teichmann N, Mazur PK, Delgiorno KE, Carpenter ES, Halbrook CJ, Hall JC et al. 2012. EGF receptor is required for KRAS-induced pancreatic tumorigenesis. *Cancer cell* **22**: 304-317.

Arispe N, Doh M, Simakova O, Kurganov B, De Maio A. 2004. Hsc70 and Hsp70 interact with phosphatidylserine on the surface of PC12 cells resulting in a decrease of viability. *FASEB journal : official publication of the Federation of American Societies for Experimental Biology* **18**: 1636-1645.

Arndt V, Dick N, Tawo R, Dreiseidler M, Wenzel D, Hesse M, Furst DO, Saftig P, Saint R, Fleischmann BK et al. 2010. Chaperone-assisted selective autophagy is essential for muscle maintenance. *Current biology : CB* **20**: 143-148.

Azuma K, Shichijo S, Takedatsu H, Komatsu N, Sawamizu H, Itoh K. 2003. Heat shock cognate protein 70 encodes antigenic epitopes recognised by HLA-B4601-restricted cytotoxic T lymphocytes from cancer patients. *British journal of cancer* **89**: 1079-1085.

Basu S, Binder RJ, Ramalingam T, Srivastava PK. 2001. CD91 is a common receptor for heat shock proteins gp96, hsp90, hsp70, and calreticulin. *Immunity* **14**: 303-313.

Basu S, Binder RJ, Suto R, Anderson KM, Srivastava PK. 2000. Necrotic but not apoptotic cell death releases heat shock proteins, which deliver a partial maturation signal to dendritic cells and activate the NF-kappa B pathway. *International immunology* **12**: 1539-1546.

Bayer C, Liebhardt ME, Schmid TE, Trajkovic-Arsic M, Hube K, Specht HM, Schilling D, Gehrmann M, Stangl S, Siveke JT et al. 2014. Validation of heat shock protein 70 as a tumor-specific biomarker for monitoring the outcome of radiation therapy in tumor mouse models. *International journal of radiation oncology, biology, physics* **88**: 694-700.

Beano A, Signorino E, Evangelista A, Brusa D, Mistrangelo M, Polimeni MA, Spadi R, Donadio M, Ciuffreda L, Matera L. 2008. Correlation between NK function and response to trastuzumab in metastatic breast cancer patients. *Journal of translational medicine* **6**: 25.

Beere HM, Wolf BB, Cain K, Mosser DD, Mahboubi A, Kuwana T, Tailor P, Morimoto RI, Cohen GM, Green DR. 2000. Heat-shock protein 70 inhibits apoptosis by preventing recruitment of procaspase-9 to the Apaf-1 apoptosome. *Nature cell biology* **2**: 469-475.

Ben-Porath I, Weinberg RA. 2005. The signals and pathways activating cellular senescence. *The international journal of biochemistry & cell biology* **37**: 961-976.

Bhalla KN. 2005. Epigenetic and chromatin modifiers as targeted therapy of hematologic malignancies. *Journal of clinical oncology : official journal of the American Society of Clinical Oncology* **23**: 3971-3993.

Bonnal S, Vigevani L, Valcarcel J. 2012. The spliceosome as a target of novel antitumour drugs. *Nature reviews Drug discovery* **11**: 847-859.

Botzler C, Issels R, Multhoff G. 1996. Heat-shock protein 72 cell-surface expression on human lung carcinoma cells in associated with an increased sensitivity to lysis mediated by adherent natural killer cells. *Cancer immunology, immunotherapy : CII* **43**: 226-230.

Botzler C, Schmidt J, Luz A, Jennen L, Issels R, Multhoff G. 1998. Differential Hsp70 plasma-membrane expression on primary human tumors and metastases in mice with severe combined immunodeficiency. *International journal of cancer Journal international du cancer* **77**: 942-948.

Brentjens RJ, Davila ML, Riviere I, Park J, Wang X, Cowell LG, Bartido S, Stefanski J, Taylor C, Olszewska M et al. 2013. CD19-targeted T cells rapidly induce molecular remissions in adults with chemotherapy-refractory acute lymphoblastic leukemia. *Science translational medicine* **5**: 177ra138.

Calderwood SK. 2013. Molecular cochaperones: tumor growth and cancer treatment. *Scientifica* **2013**: 217513.

Calderwood SK, Ciocca DR. 2008. Heat shock proteins: stress proteins with Janus-like properties in cancer. *International journal of hyperthermia : the official journal of European Society for Hyperthermic Oncology, North American Hyperthermia Group* **24**: 31-39.

Calderwood SK, Khaleque MA, Sawyer DB, Ciocca DR. 2006. Heat shock proteins in cancer: chaperones of tumorigenesis. *Trends in biochemical sciences* **31**: 164-172.

Cambrosio A, Keating P, Mercier S, Lewison G, Mogoutov A. 2006. Mapping the emergence and development of translational cancer research. *European journal of cancer* **42**: 3140-3148.

Cardoso F, Saghatchian M, Thompson A, Rutgers E, Committee TCS. 2008. Inconsistent criteria used in American Society of Clinical Oncology 2007 update of recommendations for the use of tumor markers in breast cancer. *Journal of clinical oncology : official journal of the American Society of Clinical Oncology* **26**: 2058-2059; author reply 2060-2051.

Carson WE, Parihar R, Lindemann MJ, Personeni N, Dierksheide J, Meropol NJ, Baselga J, Caligiuri MA. 2001. Interleukin-2 enhances the natural killer cell response to Herceptin-coated Her2/neu-positive breast cancer cells. *European journal of immunology* **31**: 3016-3025.

Chames P, Van Regenmortel M, Weiss E, Baty D. 2009. Therapeutic antibodies: successes, limitations and hopes for the future. *British journal of pharmacology* **157**: 220-233.

Chang HC, Tang YC, Hayer-Hartl M, Hartl FU. 2007. SnapShot: molecular chaperones, Part I. *Cell* **128**: 212.

Chiu CC, Lin CY, Lee LY, Chen YJ, Lu YC, Wang HM, Liao CT, Chang JT, Cheng AJ. 2011. Molecular chaperones as a common set of proteins that regulate the invasion phenotype of head and neck cancer. *Clinical cancer research : an official journal of the American Association for Cancer Research* **17**: 4629-4641.

Chu B, Soncin F, Price BD, Stevenson MA, Calderwood SK. 1996. Sequential phosphorylation by mitogen-activated protein kinase and glycogen synthase kinase 3 represses transcriptional activation by heat shock factor-1. *The Journal of biological chemistry* **271**: 30847-30857.

Ciocca DR, Calderwood SK. 2005. Heat shock proteins in cancer: diagnostic, prognostic, predictive, and treatment implications. *Cell stress & chaperones* **10**: 86-103.

Clayton A, Turkes A, Navabi H, Mason MD, Tabi Z. 2005. Induction of heat shock proteins in B-cell exosomes. *Journal of cell science* **118**: 3631-3638.

Coley WB. 1910. The Treatment of Inoperable Sarcoma by Bacterial Toxins (the Mixed Toxins of the Streptococcus erysipelas and the Bacillus prodigiosus). *Proceedings of the Royal Society of Medicine* **3**: 1-48.

Conway JR, Carragher NO, Timpson P. 2014. Developments in preclinical cancer imaging: innovating the discovery of therapeutics. *Nature reviews Cancer* **14**: 314-328.

Dai C, Whitesell L, Rogers AB, Lindquist S. 2007. Heat shock factor 1 is a powerful multifaceted modifier of carcinogenesis. *Cell* **130**: 1005-1018.

Daugaard M, Jaattela M, Rohde M. 2005. Hsp70-2 is required for tumor cell growth and survival. *Cell cycle* **4**: 877-880.

Daugaard M, Rohde M, Jaattela M. 2007. The heat shock protein 70 family: Highly homologous proteins with overlapping and distinct functions. *FEBS letters* **581**: 3702-3710.

De Maio A, Vazquez D. 2013. Extracellular heat shock proteins: a new location, a new function. *Shock* **40**: 239-246.

Delneste Y, Magistrelli G, Gauchat J, Haeuw J, Aubry J, Nakamura K, Kawakami-Honda N, Goetsch L, Sawamura T, Bonnefoy J et al. 2002. Involvement of LOX-1 in dendritic cell-mediated antigen cross-presentation. *Immunity* **17**: 353-362.

Dobbelstein M, Moll U. 2014. Targeting tumour-supportive cellular machineries in anticancer drug development. *Nature reviews Drug discovery* **13**: 179-196.

Downward J. 2003. Targeting RAS signalling pathways in cancer therapy. *Nature reviews Cancer* **3**: 11-22.

Dunn GP, Bruce AT, Ikeda H, Old LJ, Schreiber RD. 2002. Cancer immunoediting: from immunosurveillance to tumor escape. *Nature immunology* **3**: 991-998.

Eckhouse S, Lewison G, Sullivan R. 2008. Trends in the global funding and activity of cancer research. *Molecular oncology* **2**: 20-32.

Ehrlich P. 1885. Das Sauerstoffbedürfnis des Organismus: eine farbenanalytische Studie. Berlin: Hirschwald. Habilitation treatise.

Fang H, Declerck YA. 2013. Targeting the tumor microenvironment: from understanding pathways to effective clinical trials. *Cancer research* **73**: 4965-4977.

Farber S, Diamond LK. 1948. Temporary remissions in acute leukemia in children produced by folic acid antagonist, 4-aminopteroyl-glutamic acid. *The New England journal of medicine* **238**: 787-793.

Farkas B, Hantschel M, Magyarlaki M, Becker B, Scherer K, Landthaler M, Pfister K, Gehrmann M, Gross C, Mackensen A et al. 2003. Heat shock protein 70 membrane expression and melanoma-associated marker phenotype in primary and metastatic melanoma. *Melanoma research* **13**: 147-152.

Faure O, Graff-Dubois S, Bretaudeau L, Derre L, Gross DA, Alves PM, Cornet S, Duffour MT, Chouaib S, Miconnet I et al. 2004. Inducible Hsp70 as target of anticancer immunotherapy: Identification of HLA-A*0201-restricted epitopes. *International journal of cancer Journal international du cancer* **108**: 863-870.

Felding-Habermann B. 2003. Integrin adhesion receptors in tumor metastasis. *Clinical & experimental metastasis* **20**: 203-213.

Ferrara N, Hillan KJ, Gerber HP, Novotny W. 2004. Discovery and development of bevacizumab, an anti-VEGF antibody for treating cancer. *Nature reviews Drug discovery* **3**: 391-400.

Ferrara N, Kerbel RS. 2005. Angiogenesis as a therapeutic target. *Nature* **438**: 967-974.

Ferrarini M, Heltai S, Zocchi MR, Rugarli C. 1992. Unusual expression and localization of heat-shock proteins in human tumor cells. *International journal of cancer Journal international du cancer* **51**: 613-619.

Fishel R, Lescoe MK, Rao MR, Copeland NG, Jenkins NA, Garber J, Kane M, Kolodner R. 1994. The human mutator gene homolog MSH2 and its association with hereditary nonpolyposis colon cancer. *Cell* **77**: 1 p following 166.

Friedrich L, Stangl S, Hahne H, Kuster B, Kohler P, Multhoff G, Skerra A. 2010. Bacterial production and functional characterization of the Fab fragment of the murine IgG1/lambda monoclonal antibody cmHsp70.1, a reagent for tumour diagnostics. *Protein engineering, design & selection : PEDS* **23**: 161-168.

Fujita Y, Nakanishi T, Miyamoto Y, Hiramatsu M, Mabuchi H, Miyamoto A, Shimizu A, Takubo T, Tanigawa N. 2008. Proteomics-based identification of autoantibody against heat shock protein 70 as a diagnostic marker in esophageal squamous cell carcinoma. *Cancer letters* **263**: 280-290.

Gabai VL, Budagova KR, Sherman MY. 2005. Increased expression of the major heat shock protein Hsp72 in human prostate carcinoma cells is dispensable for their viability but confers resistance to a variety of anticancer agents. *Oncogene* **24**: 3328-3338.

Gabai VL, Yaglom JA, Waldman T, Sherman MY. 2009. Heat shock protein Hsp72 controls oncogene-induced senescence pathways in cancer cells. *Molecular and cellular biology* **29**: 559-569.

Gallucci S, Matzinger P. 2001. Danger signals: SOS to the immune system. *Current opinion in immunology* **13**: 114-119.

Galluzzi L, Vacchelli E, Bravo-San Pedro JM, Buque A, Senovilla L, Baracco EE, Bloy N, Castoldi F, Abastado JP, Agostinis P et al. 2014. Classification of current anticancer immunotherapies. *Oncotarget* **5**: 12472-12508.

Garcia-Lora A, Algarra I, Garrido F. 2003. MHC class I antigens, immune surveillance, and tumor immune escape. *Journal of cellular physiology* **195**: 346-355.

Garg M, Kanojia D, Saini S, Suri S, Gupta A, Surolia A, Suri A. 2010. Germ cell-specific heat shock protein 70-2 is expressed in cervical carcinoma and is involved in the growth, migration, and invasion of cervical cells. *Cancer* **116**: 3785-3796.

Gastpar R, Gehrmann M, Bausero MA, Asea A, Gross C, Schroeder JA, Multhoff G. 2005. Heat shock protein 70 surface-positive tumor exosomes stimulate migratory and cytolytic activity of natural killer cells. *Cancer research* **65**: 5238-5247.

Gehrmann M, Cervello M, Montalto G, Cappello F, Gulino A, Knape C, Specht HM, Multhoff G. 2014a. Heat shock protein 70 serum levels differ significantly in patients with chronic hepatitis, liver cirrhosis, and hepatocellular carcinoma. *Front Immunol* **5**: 307.

Gehrmann M, Liebisch G, Schmitz G, Anderson R, Steinem C, De Maio A, Pockley G, Multhoff G. 2008a. Tumor-specific Hsp70 plasma membrane localization is enabled by the glycosphingolipid Gb3. *PloS one* **3**: e1925.

Gehrmann M, Marienhagen J, Eichholtz-Wirth H, Fritz E, Ellwart J, Jaattela M, Zilch T, Multhoff G. 2005. Dual function of membrane-bound heat shock protein 70 (Hsp70), Bag-4, and Hsp40: protection against radiation-induced effects and target structure for natural killer cells. *Cell death and differentiation* **12**: 38-51.

Gehrmann M, Radons J, Molls M, Multhoff G. 2008b. The therapeutic implications of clinically applied modifiers of heat shock protein 70 (Hsp70) expression by tumor cells. *Cell stress & chaperones* **13**: 1-10.

Gehrmann M, Specht HM, Bayer C, Brandstetter M, Chizzali B, Duma M, Breuninger S, Hube K, Lehnerer S, van Phi V et al. 2014b. Hsp70--a biomarker for tumor detection and monitoring of outcome of radiation therapy in patients with squamous cell carcinoma of the head and neck. *Radiation oncology* **9**: 131.

Gehrmann M, Stangl S, Foulds GA, Oellinger R, Breuninger S, Rad R, Pockley AG, Multhoff G. 2014c. Tumor imaging and targeting potential of an Hsp70-derived 14-mer peptide. *PloS one* **9**: e105344.

Gerber DE. 2008. Targeted therapies: a new generation of cancer treatments. *American family physician* **77**: 311-319.

Ghobrial IM, Witzig TE, Adjei AA. 2005. Targeting apoptosis pathways in cancer therapy. *CA: a cancer journal for clinicians* **55**: 178-194.

Greene JM, Larin Z, Taylor IC, Prentice H, Gwinn KA, Kingston RE. 1987. Multiple basal elements of a human hsp70 promoter function differently in human and rodent cell lines. *Molecular and cellular biology* **7**: 3646-3655.

Gross C, Hansch D, Gastpar R, Multhoff G. 2003a. Interaction of heat shock protein 70 peptide with NK cells involves the NK receptor CD94. *Biological chemistry* **384**: 267-279.

Gross C, Schmidt-Wolf IG, Nagaraj S, Gastpar R, Ellwart J, Kunz-Schughart LA, Multhoff G. 2003b. Heat shock protein 70-reactivity is associated with increased cell surface density of CD94/CD56 on primary natural killer cells. *Cell stress & chaperones* **8**: 348-360.

Grupp SA, Kalos M, Barrett D, Aplenc R, Porter DL, Rheingold SR, Teachey DT, Chew A, Hauck B, Wright JF et al. 2013. Chimeric antigen receptor-modified T cells for acute lymphoid leukemia. *The New England journal of medicine* **368**: 1509-1518.

Guengerich FP. 2011. Mechanisms of drug toxicity and relevance to pharmaceutical development. *Drug metabolism and pharmacokinetics* **26**: 3-14.

Gupta S, Deepti A, Deegan S, Lisbona F, Hetz C, Samali A. 2010. HSP72 protects cells from ER stress-induced apoptosis via enhancement of IRE1alpha-XBP1 signaling through a physical interaction. *PLoS biology* **8**: e1000410.

Hanahan D, Weinberg RA. 2011. Hallmarks of cancer: the next generation. *Cell* **144**: 646-674.

Hang H, He L, Fox MH. 1995. Cell cycle variation of Hsp70 levels in HeLa cells at 37 degrees C and after a heat shock. *Journal of cellular physiology* **165**: 367-375.

Hansel TT, Kropshofer H, Singer T, Mitchell JA, George AJ. 2010. The safety and side effects of monoclonal antibodies. *Nature reviews Drug discovery* **9**: 325-338.

Hantschel M, Pfister K, Jordan A, Scholz R, Andreesen R, Schmitz G, Schmetzer H, Hiddemann W, Multhoff G. 2000. Hsp70 plasma membrane expression on primary tumor biopsy material and bone marrow of leukemic patients. *Cell stress & chaperones* **5**: 438-442.

Hartl FU, Bracher A, Hayer-Hartl M. 2011. Molecular chaperones in protein folding and proteostasis. *Nature* **475**: 324-332.

Hartl FU, Hayer-Hartl M. 2002. Molecular chaperones in the cytosol: from nascent chain to folded protein. *Science* **295**: 1852-1858.

Helmbrecht K, Zeise E, Rensing L. 2000. Chaperones in cell cycle regulation and mitogenic signal transduction: a review. *Cell proliferation* **33**: 341-365.

Hightower LE, Guidon PT, Jr. 1989. Selective release from cultured mammalian cells of heat-shock (stress) proteins that resemble glia-axon transfer proteins. *Journal of cellular physiology* **138**: 257-266.

Hosotani R, Kawaguchi M, Masui T, Koshiba T, Ida J, Fujimoto K, Wada M, Doi R, Imamura M. 2002. Expression of integrin alphaVbeta3 in pancreatic carcinoma: relation to MMP-2 activation and lymph node metastasis. *Pancreas* **25**: e30-35.

Hubert P, Amigorena S. 2012. Antibody-dependent cell cytotoxicity in monoclonal antibody-mediated tumor immunotherapy. *Oncoimmunology* **1**: 103-105.

Hwang TS, Han HS, Choi HK, Lee YJ, Kim YJ, Han MY, Park YM. 2003. Differential, stage-dependent expression of Hsp70, Hsp110 and Bcl-2 in colorectal cancer. *Journal of gastroenterology and hepatology* **18**: 690-700.

Igney FH, Krammer PH. 2002. Death and anti-death: tumour resistance to apoptosis. *Nature reviews Cancer* **2**: 277-288.

Jaattela M. 1999. Escaping cell death: survival proteins in cancer. *Experimental cell research* **248**: 30-43.

Jaattela M, Wissing D, Kokholm K, Kallunki T, Egeblad M. 1998. Hsp70 exerts its anti-apoptotic function downstream of caspase-3-like proteases. *The EMBO journal* **17**: 6124-6134.

Jang KW, Lee JE, Kim SY, Kang MW, Na MH, Lee CS, Song KS, Lim SP. 2011. The C-terminus of Hsp70-interacting protein promotes Met receptor degradation. *Journal of thoracic oncology : official publication of the International Association for the Study of Lung Cancer* **6**: 679-687.

Jiang J, Wu C, Lu B. 2013. Cytokine-induced killer cells promote antitumor immunity. *Journal of translational medicine* **11**: 83.

Juhasz K, Lipp AM, Nimmervoll B, Sonnleitner A, Hesse J, Haselgruebler T, Balogi Z. 2013. The complex function of hsp70 in metastatic cancer. *Cancers* **6**: 42-66.

Kampinga HH, Craig EA. 2010. The HSP70 chaperone machinery: J proteins as drivers of functional specificity. *Nature reviews Molecular cell biology* **11**: 579-592.

Kampinga HH, Hageman J, Vos MJ, Kubota H, Tanguay RM, Bruford EA, Cheetham ME, Chen B, Hightower LE. 2009. Guidelines for the nomenclature of the human heat shock proteins. *Cell stress & chaperones* **14**: 105-111.

Kaplan-Lefko PJ, Graves JD, Zoog SJ, Pan Y, Wall J, Branstetter DG, Moriguchi J, Coxon A, Huard JN, Xu R et al. 2010. Conatumumab, a fully human agonist antibody to death receptor 5, induces apoptosis via caspase activation in multiple tumor types. *Cancer biology & therapy* **9**: 618-631.

Kaur J, Das SN, Srivastava A, Ralhan R. 1998. Cell surface expression of 70 kDa heat shock protein in human oral dysplasia and squamous cell carcinoma: correlation with clinicopathological features. *Oral oncology* **34**: 93-98.

Khaleque MA, Bharti A, Gong J, Gray PJ, Sachdev V, Ciocca DR, Stati A, Fanelli M, Calderwood SK. 2008. Heat shock factor 1 represses estrogen-dependent transcription through association with MTA1. *Oncogene* **27**: 1886-1893.

Kircher MF, de la Zerda A, Jokerst JV, Zavaleta CL, Kempen PJ, Mittra E, Pitter K, Huang R, Campos C, Habte F et al. 2012. A brain tumor molecular imaging strategy using a new triple-modality MRI-photoacoustic-Raman nanoparticle. *Nature medicine* **18**: 829-834.

Klein G. 2001. The strange road to the tumor-specific transplantation antigens (TSTAs). *Cancer immunity* **1**: 6.

Kleinjung T, Arndt O, Feldmann HJ, Bockmuhl U, Gehrmann M, Zilch T, Pfister K, Schonberger J, Marienhagen J, Eilles C et al. 2003. Heat shock protein 70 (Hsp70) membrane expression on head-and-neck cancer biopsy-a target for natural killer (NK) cells. *International journal of radiation oncology, biology, physics* **57**: 820-826.

Kobayashi H, Ogawa M, Alford R, Choyke PL, Urano Y. 2010. New strategies for fluorescent probe design in medical diagnostic imaging. *Chemical reviews* **110**: 2620-2640.

Kolb HJ. 2008. Graft-versus-leukemia effects of transplantation and donor lymphocytes. *Blood* **112**: 4371-4383.

Kondo E, Koda K, Takiguchi N, Oda K, Seike K, Ishizuka M, Miyazaki M. 2003. Preoperative natural killer cell activity as a prognostic factor for distant metastasis following surgery for colon cancer. *Digestive surgery* **20**: 445-451.

Krause SW, Gastpar R, Andreesen R, Gross C, Ullrich H, Thonigs G, Pfister K, Multhoff G. 2004. Treatment of colon and lung cancer patients with ex vivo heat shock protein 70-peptide-activated, autologous natural killer cells: a clinical phase i trial. *Clinical cancer research : an official journal of the American Association for Cancer Research* **10**: 3699-3707.

Kucharczak J, Simmons MJ, Fan Y, Gelinas C. 2003. To be, or not to be: NF-kappaB is the answer--role of Rel/NF-kappaB in the regulation of apoptosis. *Oncogene* **22**: 8961-8982.

Kurucz I, Tombor B, Prechl J, Erdo F, Hegedus E, Nagy Z, Vitai M, Koranyi L, Laszlo L. 1999. Ultrastructural localization of Hsp-72 examined with a new polyclonal antibody raised against the truncated variable domain of the heat shock protein. *Cell stress & chaperones* **4**: 139-152.

Lancaster GI, Febbraio MA. 2005. Exosome-dependent trafficking of HSP70: a novel secretory pathway for cellular stress proteins. *The Journal of biological chemistry* **280**: 23349-23355.

Langer T, Lu C, Echols H, Flanagan J, Hayer MK, Hartl FU. 1992. Successive action of DnaK, DnaJ and GroEL along the pathway of chaperone-mediated protein folding. *Nature* **356**: 683-689.

Lee KJ, Kim YM, Kim DY, Jeoung D, Han K, Lee ST, Lee YS, Park KH, Park JH, Kim DJ et al. 2006. Release of heat shock protein 70 (Hsp70) and the effects of extracellular Hsp70 on matric metalloproteinase-9 expression in human monocytic U937 cells. *Experimental & molecular medicine* **38**: 364-374.

Li H, Li Y, Liu D, Sun H, Su D, Yang F, Liu J. 2013a. Extracellular HSP70/HSP70-PCs promote epithelial-mesenchymal transition of hepatocarcinoma cells. *PloS one* **8**: e84759.

Liauw W. 2013. Molecular mechanisms and clinical use of targeted anticancer drugs. *Aust Prescr* **36**:126-131.

Li Z, Chen L, Rubinstein MP. 2013b. Cancer immunotherapy: are we there yet? *Experimental hematology & oncology* **2**: 33.

Lindquist S. 1986. The heat-shock response. *Annual review of biochemistry* **55**: 1151-1191.

Liu L, Li Y. 2014. The unexpected side effects and safety of therapeutic monoclonal antibodies. *Drugs of today* **50**: 33-50.

Ljunggren HG, Karre K. 1990. In search of the 'missing self': MHC molecules and NK cell recognition. *Immunology today* **11**: 237-244.

Loberg RD, Ying C, Craig M, Day LL, Sargent E, Neeley C, Wojno K, Snyder LA, Yan L, Pienta KJ. 2007. Targeting CCL2 with systemic delivery of neutralizing antibodies induces prostate cancer tumor regression in vivo. *Cancer research* **67**: 9417-9424.

Mambula SS, Stevenson MA, Ogawa K, Calderwood SK. 2007. Mechanisms for Hsp70 secretion: crossing membranes without a leader. *Methods* **43**: 168-175.

Mao H, Li F, Ruchalski K, Mosser DD, Schwartz JH, Wang Y, Borkan SC. 2003. hsp72 inhibits focal adhesion kinase degradation in ATP-depleted renal epithelial cells. *The Journal of biological chemistry* **278**: 18214-18220.

Marcinowski M, Holler M, Feige MJ, Baerend D, Lamb DC, Buchner J. 2011. Substrate discrimination of the chaperone BiP by autonomous and cochaperone-regulated conformational transitions. *Nature structural & molecular biology* **18**: 150-158.

Martin TA, Harrison G, Mansel RE, Jiang WG. 2003. The role of the CD44/ezrin complex in cancer metastasis. *Critical reviews in oncology/hematology* **46**: 165-186.

Matzinger P. 2002. The danger model: a renewed sense of self. *Science* **296**: 301-305.

Mayer MP. 2010. Gymnastics of molecular chaperones. *Molecular cell* **39**: 321-331.

McCarthy EF. 2006. The toxins of William B. Coley and the treatment of bone and soft-tissue sarcomas. *The Iowa orthopaedic journal* **26**: 154-158.

Mendelsohn J, Baselga J. 2006. Epidermal growth factor receptor targeting in cancer. *Seminars in oncology* **33**: 369-385.

Milani V, Stangl S, Issels R, Gehrmann M, Wagner B, Hube K, Mayr D, Hiddemann W, Molls M, Multhoff G. 2009. Anti-tumor activity of patient-derived NK cells after cell-based immunotherapy--a case report. *Journal of translational medicine* **7**: 50.

Milarski KL, Morimoto RI. 1986. Expression of human HSP70 during the synthetic phase of the cell cycle. *Proceedings of the National Academy of Sciences of the United States of America* **83**: 9517-9521.

Milla P, Dosio F, Cattel L. 2012. PEGylation of proteins and liposomes: a powerful and flexible strategy to improve the drug delivery. *Current drug metabolism* **13**: 105-119.

Milner CM, Campbell RD. 1990. Structure and expression of the three MHC-linked HSP70 genes. *Immunogenetics* **32**: 242-251.

Ming Lim C, Stephenson R, Salazar AM, Ferris RL. 2013. TLR3 agonists improve the immunostimulatory potential of cetuximab against EGFR head and neck cancer cells. *Oncoimmunology* **2**: e24677.

Multhoff G. 2007. Heat shock protein 70 (Hsp70): membrane location, export and immunological relevance. *Methods* **43**: 229-237.

Multhoff G, Botzler C, Wiesnet M, Muller E, Meier T, Wilmanns W, Issels RD. 1995. A stress-inducible 72-kDa heat-shock protein (HSP72) is expressed on the surface of human tumor cells, but not on normal cells. *International journal of cancer Journal international du cancer* **61**: 272-279.

Multhoff G, Mizzen L, Winchester CC, Milner CM, Wenk S, Eissner G, Kampinga HH, Laumbacher B, Johnson J. 1999. Heat shock protein 70 (Hsp70) stimulates proliferation and cytolytic activity of natural killer cells. *Experimental hematology* **27**: 1627-1636.

Multhoff G, Pfister K, Gehrmann M, Hantschel M, Gross C, Hafner M, Hiddemann W. 2001. A 14-mer Hsp70 peptide stimulates natural killer (NK) cell activity. *Cell stress & chaperones* **6**: 337-344.

Multhoff G, Pockley AG, Schmid TE, Schilling D. 2015. The role of heat shock protein 70 (Hsp70) in radiation-induced immunomodulation. *Cancer letters*.

Murshid A, Chou SD, Prince T, Zhang Y, Bharti A, Calderwood SK. 2010. Protein kinase A binds and activates heat shock factor 1. *PloS one* **5**: e13830.

Nakajima M, Kuwano H, Miyazaki T, Masuda N, Kato H. 2002. Significant correlation between expression of heat shock proteins 27, 70 and lymphocyte infiltration in esophageal squamous cell carcinoma. *Cancer letters* **178**: 99-106.

Nishioka Y, Yano S, Fujiki F, Mukaida N, Matsushima K, Tsuruo T, Sone S. 1997. Combined therapy of multidrug-resistant human lung cancer with anti-P-glycoprotein antibody and monocyte chemoattractant protein-1 gene transduction: the possibility of immunological overcoming of multidrug resistance. *International journal of cancer Journal international du cancer* **71**: 170-177.

Nylandsted J, Brand K, Jaattela M. 2000. Heat shock protein 70 is required for the survival of cancer cells. *Annals of the New York Academy of Sciences* **926**: 122-125.

Onishi T, Hayashi N, Theriault RL, Hortobagyi GN, Ueno NT. 2010. Future directions of bone-targeted therapy for metastatic breast cancer. *Nature reviews Clinical oncology* **7**: 641-651.

Orlowski RZ, Baldwin AS, Jr. 2002. NF-kappaB as a therapeutic target in cancer. *Trends in molecular medicine* **8**: 385-389.

Pagliuca MG, Lerose R, Cigliano S, Leone A. 2003. Regulation by heavy metals and temperature of the human BAG-3 gene, a modulator of Hsp70 activity. *FEBS letters* **541**: 11-15.

Parmar MB, Aliabadi HM, Mahdipoor P, Kucharski C, Maranchuk R, Hugh JC, Uludag H. 2015. Targeting Cell Cycle Proteins in Breast Cancer Cells with siRNA by Using Lipid-Substituted Polyethylenimines. *Frontiers in bioengineering and biotechnology* **3**: 14.

Pawaria S, Binder RJ. 2011. CD91-dependent programming of T-helper cell responses following heat shock protein immunization. *Nature communications* **2**: 521.

Peterson NS, Moller G, Mitchell HK. 1979. Genetic mapping of the coding regions for three heat-shock proteins in Drosophila melanogaster. *Genetics* **92**: 891-902.

Petrucelli L, Dickson D, Kehoe K, Taylor J, Snyder H, Grover A, De Lucia M, McGowan E, Lewis J, Prihar G et al. 2004. CHIP and Hsp70 regulate tau ubiquitination, degradation and aggregation. *Human molecular genetics* **13**: 703-714.

Pfister K, Radons J, Busch R, Tidball JG, Pfeifer M, Freitag L, Feldmann HJ, Milani V, Issels R, Multhoff G. 2007. Patient survival by Hsp70 membrane phenotype: association with different routes of metastasis. *Cancer* **110**: 926-935.

Pockley AG, Muthana M, Calderwood SK. 2008. The dual immunoregulatory roles of stress proteins. *Trends in biochemical sciences* **33**: 71-79.

Porter DL, Levine BL, Kalos M, Bagg A, June CH. 2011. Chimeric antigen receptor-modified T cells in chronic lymphoid leukemia. *The New England journal of medicine* **365**: 725-733.

Powers MV, Clarke PA, Workman P. 2008. Dual targeting of HSC70 and HSP72 inhibits HSP90 function and induces tumor-specific apoptosis. *Cancer cell* **14**: 250-262.

Powers MV, Workman P. 2007. Inhibitors of the heat shock response: biology and pharmacology. *FEBS letters* **581**: 3758-3769.

Rensing H, Bauer I, Datene V, Patau C, Pannen BH, Bauer M. 1999. Differential expression pattern of heme oxygenase-1/heat shock protein 32 and nitric oxide synthase-II and their impact on liver injury in a rat model of hemorrhage and resuscitation. *Critical care medicine* **27**: 2766-2775.

Rerole AL, Jego G, Garrido C. 2011. Hsp70: anti-apoptotic and tumorigenic protein. *Methods in molecular biology* **787**: 205-230.

Rettig WJ, Old LJ. 1989. Immunogenetics of human cell surface differentiation. *Annual review of immunology* **7**: 481-511.

Richter K, Haslbeck M, Buchner J. 2010. The heat shock response: life on the verge of death. *Molecular cell* **40**: 253-266.

Ritossa F. 1962. A new puffing pattern induced by temperature shock and DNP in Drosophila. *Experientia 13.XII.* **18**: 571-573

Roninson IB. 2002. Oncogenic functions of tumour suppressor p21(Waf1/Cip1/Sdi1): association with cell senescence and tumour-promoting activities of stromal fibroblasts. *Cancer letters* **179**: 1-14.

Roninson IB. 2003. Tumor cell senescence in cancer treatment. *Cancer research* **63**: 2705-2715.

Santagata S, Hu R, Lin NU, Mendillo ML, Collins LC, Hankinson SE, Schnitt SJ, Whitesell L, Tamimi RM, Lindquist S et al. 2011. High levels of nuclear heat-shock factor 1 (HSF1) are associated with poor prognosis in breast cancer. *Proceedings of the National Academy of Sciences of the United States of America* **108**: 18378-18383.

Sarge KD, Murphy SP, Morimoto RI. 1993. Activation of heat shock gene transcription by heat shock factor 1 involves oligomerization, acquisition of DNA-binding activity, and nuclear localization and can occur in the absence of stress. *Molecular and cellular biology* **13**: 1392-1407.

Schilling D, Duwel M, Molls M, Multhoff G. 2013. Radiosensitization of wildtype p53 cancer cells by the MDM2-inhibitor PXN727 is associated with altered heat shock protein 70 (Hsp70) levels. *Cell stress & chaperones* **18**: 183-191.

Schilling D, Kuhnel A, Konrad S, Tetzlaff F, Bayer C, Yaglom J, Multhoff G. 2015. Sensitizing tumor cells to radiation by targeting the heat shock response. *Cancer letters* **360**: 294-301.

Schilsky RL, Taube SE. 2002. Tumor markers as clinical cancer tests--are we there yet? *Seminars in oncology* **29**: 211-212.

Schlecht R, Erbse AH, Bukau B, Mayer MP. 2011. Mechanics of Hsp70 chaperones enables differential interaction with client proteins. *Nature structural & molecular biology* **18**: 345-351.

Schmitt E, Gehrmann M, Brunet M, Multhoff G, Garrido C. 2007. Intracellular and extracellular functions of heat shock proteins: repercussions in cancer therapy. *Journal of leukocyte biology* **81**: 15-27.

Schultz CR, Golembieski WA, King DA, Brown SL, Brodie C, Rempel SA. 2012. Inhibition of HSP27 alone or in combination with pAKT inhibition as therapeutic approaches to target SPARC-induced glioma cell survival. *Molecular cancer* **11**: 20.

Scott AM, Wolchok JD, Old LJ. 2012. Antibody therapy of cancer. *Nature reviews Cancer* **12**: 278-287.

Seluanov A, Gorbunova V, Falcovitz A, Sigal A, Milyavsky M, Zurer I, Shohat G, Goldfinger N, Rotter V. 2001. Change of the death pathway in senescent human fibroblasts in response to DNA damage is caused by an inability to stabilize p53. *Molecular and cellular biology* **21**: 1552-1564.

Shamovsky I, Nudler E. 2008. New insights into the mechanism of heat shock response activation. *Cellular and molecular life sciences : CMLS* **65**: 855-861.

Sharp A, Crabb SJ, Townsend PA, Cutress RI, Brimmell M, Wang XH, Packham G. 2004. BAG-1 in carcinogenesis. *Expert reviews in molecular medicine* **6**: 1-15.

Sherman M. 2010. Major heat shock protein Hsp72 controls oncogene-induced senescence. *Annals of the New York Academy of Sciences* **1197**: 152-157.

Shi Y, Mosser DD, Morimoto RI. 1998. Molecular chaperones as HSF1-specific transcriptional repressors. *Genes & development* **12**: 654-666.

Shin BK, Wang H, Yim AM, Le Naour F, Brichory F, Jang JH, Zhao R, Puravs E, Tra J, Michael CW et al. 2003. Global profiling of the cell surface proteome of cancer cells uncovers an abundance of proteins with chaperone function. *The Journal of biological chemistry* **278**: 7607-7616.

Sims JD, McCready J, Jay DG. 2011. Extracellular heat shock protein (Hsp)70 and Hsp90alpha assist in matrix metalloproteinase-2 activation and breast cancer cell migration and invasion. *PloS one* **6**: e18848.

Sitohy B, Nagy JA, Dvorak HF. 2012. Anti-VEGF/VEGFR therapy for cancer: reassessing the target. *Cancer research* **72**: 1909-1914.

Sondermann H, Scheufler C, Schneider C, Hohfeld J, Hartl FU, Moarefi I. 2001. Structure of a Bag/Hsc70 complex: convergent functional evolution of Hsp70 nucleotide exchange factors. *Science* **291**: 1553-1557.

Song J, Takeda M, Morimoto RI. 2001. Bag1-Hsp70 mediates a physiological stress signalling pathway that regulates Raf-1/ERK and cell growth. *Nature cell biology* **3**: 276-282.

Specht HM, Ahrens N, Blankenstein C, Duell T, Fietkau R, Gaipl US, Gunther C, Gunther S, Habl G, Hautmann H et al. 2015. Heat shock protein 70 (Hsp70) peptide activated Natural Killer (NK) cells for the treatment of patients with non-small cell lung cancer (NSCLC) after radiochemotherapy (RCTx) - from preclinical studies to a clinical phase II trial. *Front Immunol* **6**.

Spector NL, Samson W, Ryan C, Gribben J, Urba W, Welch WJ, Nadler LM. 1992. Growth arrest of human B lymphocytes is accompanied by induction of the low molecular weight mammalian heat shock protein (Hsp28). *Journal of immunology* **148**: 1668-1673.

Spizzo R, Nicoloso MS, Croce CM, Calin GA. 2009. SnapShot: MicroRNAs in Cancer. *Cell* **137**: 586-586 e581.

Sreedhar AS, Csermely P. 2004. Heat shock proteins in the regulation of apoptosis: new strategies in tumor therapy: a comprehensive review. *Pharmacology & therapeutics* **101**: 227-257.

Stangl S, Gehrmann M, Dressel R, Alves F, Dullin C, Themelis G, Ntziachristos V, Staeblein E, Walch A, Winkelmann I et al. 2011a. In vivo imaging of CT26 mouse tumours by using cmHsp70.1 monoclonal antibody. *Journal of cellular and molecular medicine* **15**: 874-887.

Stangl S, Gehrmann M, Riegger J, Kuhs K, Riederer I, Sievert W, Hube K, Mocikat R, Dressel R, Kremmer E et al. 2011b. Targeting membrane heat-shock protein 70 (Hsp70) on tumors by cmHsp70.1 antibody. *Proceedings of the National Academy of Sciences of the United States of America* **108**: 733-738.

Stangl S, Themelis G, Friedrich L, Ntziachristos V, Sarantopoulos A, Molls M, Skerra A, Multhoff G. 2011c. Detection of irradiation-induced, membrane heat shock protein 70 (Hsp70) in mouse tumors using Hsp70 Fab fragment. *Radiotherapy and oncology : journal of the European Society for Therapeutic Radiology and Oncology* **99**: 313-316.

Stangl S, Varga J, Freysoldt B, Trajkovic-Arsic M, Siveke JT, Greten FR, Ntziachristos V, Multhoff G. 2014. Selective in vivo imaging of syngeneic, spontaneous, and xenograft tumors using a novel tumor cell-specific hsp70 peptide-based probe. *Cancer research* **74**: 6903-6912.

Stangl S, Wortmann A, Guertler U, Multhoff G. 2006. Control of metastasized pancreatic carcinomas in SCID/beige mice with human IL-2/TKD-activated NK cells. *Journal of immunology* **176**: 6270-6276.

Stenmark H. 2009. Rab GTPases as coordinators of vesicle traffic. *Nature reviews Molecular cell biology* **10**: 513-525.

Steplewski Z, Lubeck MD, Koprowski H. 1983. Human macrophages armed with murine immunoglobulin G2a antibodies to tumors destroy human cancer cells. *Science* **221**: 865-867.

Taira T, Narita T, Iguchi-Ariga SM, Ariga H. 1997. A novel G1-specific enhancer identified in the human heat shock protein 70 gene. *Nucleic acids research* **25**: 1975-1983.

Tang D, Khaleque MA, Jones EL, Theriault JR, Li C, Wong WH, Stevenson MA, Calderwood SK. 2005. Expression of heat shock proteins and heat shock protein messenger ribonucleic acid in human prostate carcinoma in vitro and in tumors in vivo. *Cell stress & chaperones* **10**: 46-58.

Tenedini E, Bernardis I, Artusi V, Artuso L, Roncaglia E, Guglielmelli P, Pieri L, Bogani C, Biamonte F, Rotunno G et al. 2014. Targeted cancer exome sequencing reveals recurrent mutations in myeloproliferative neoplasms. *Leukemia* **28**: 1052-1059.

Themelis G, Harlaar NJ, Kelder W, Bart J, Sarantopoulos A, van Dam GM, Ntziachristos V. 2011. Enhancing Surgical Vision by Using Real-Time Imaging of alpha(v)beta(3)-Integrin Targeted Near-Infrared Fluorescent Agent. *Annals of surgical oncology* **18**: 3506-3513.

Thomas D. 2011. Release of BIO/Biomedtracker Drug Approval Rates Study. *BiotechNow, Washington DC, USA* [pressRelease].

Todryk SM, Gough MJ, Pockley AG. 2003. Facets of heat shock protein 70 show immunotherapeutic potential. *Immunology* **110**: 1-9.

Topalian SL, Hodi FS, Brahmer JR, Gettinger SN, Smith DC, McDermott DF, Powderly JD, Carvajal RD, Sosman JA, Atkins MB et al. 2012. Safety, activity, and immune correlates of anti-PD-1 antibody in cancer. *The New England journal of medicine* **366**: 2443-2454.

Townsend PA, Stephanou A, Packham G, Latchman DS. 2005. BAG-1: a multi-functional pro-survival molecule. *The international journal of biochemistry & cell biology* **37**: 251-259.

van Dam GM, Themelis G, Crane LM, Harlaar NJ, Pleijhuis RG, Kelder W, Sarantopoulos A, de Jong JS, Arts HJ, van der Zee AG et al. 2011. Intraoperative tumor-specific fluorescence imaging in ovarian cancer by folate receptor-alpha targeting: first in-human results. *Nature medicine* **17**: 1315-1319.

Van Molle W, Wielockx B, Mahieu T, Takada M, Taniguchi T, Sekikawa K, Libert C. 2002. HSP70 protects against TNF-induced lethal inflammatory shock. *Immunity* **16**: 685-695.

Vanneman M, Dranoff G. 2012. Combining immunotherapy and targeted therapies in cancer treatment. *Nature reviews Cancer* **12**: 237-251.

Vega VL, Rodriguez-Silva M, Frey T, Gehrmann M, Diaz JC, Steinem C, Multhoff G, Arispe N, De Maio A. 2008. Hsp70 translocates into the plasma membrane after stress and is released into the extracellular environment in a membrane-associated form that activates macrophages. *Journal of immunology* **180**: 4299-4307.

Virchow R. 1845. Weisses Blut. *Froriep´s Notizen* **36**: 151-156.

Visone R, Croce CM. 2009. MiRNAs and cancer. *The American journal of pathology* **174**: 1131-1138.

Voellmy R, Boellmann F. 2007. Chaperone regulation of the heat shock protein response. *Advances in experimental medicine and biology* **594**: 89-99.

Vogel JL, Parsell DA, Lindquist S. 1995. Heat-shock proteins Hsp104 and Hsp70 reactivate mRNA splicing after heat inactivation. *Current biology : CB* **5**: 306-317.

Volloch V, Gabai VL, Rits S, Force T, Sherman MY. 2000. HSP72 can protect cells from heat-induced apoptosis by accelerating the inactivation of stress kinase JNK. *Cell stress & chaperones* **5**: 139-147.

von Schwarzenberg K, Vollmar AM. 2013. Targeting apoptosis pathways by natural compounds in cancer: marine compounds as lead structures and chemical tools for cancer therapy. *Cancer letters* **332**: 295-303.

Wang E. 1995. Senescent human fibroblasts resist programmed cell death, and failure to suppress bcl2 is involved. *Cancer research* **55**: 2284-2292.

Wang F, Zhao F, Guo J. 1999. [Preheating decrease the sensitivity of K562 cell to chemotherapeutic drugs]. *Wei sheng yan jiu = Journal of hygiene research* **28**: 81-83.

Wang W, Wang EQ, Balthasar JP. 2008a. Monoclonal antibody pharmacokinetics and pharmacodynamics. *Clinical pharmacology and therapeutics* **84**: 548-558.

Wang X, Chen W, Li X, Lin H, Wang Q. 2008b. Heat shock protein 72 associated with CD44v6 in human colonic adenocarcinoma. *Cell biology international* **32**: 860-864.

Wei YQ, Zhao X, Kariya Y, Teshigawara K, Uchida A. 1995. Inhibition of proliferation and induction of apoptosis by abrogation of heat-shock protein (HSP) 70 expression in tumor cells. *Cancer immunology, immunotherapy : CII* **40**: 73-78.

Welch WJ, Suhan JP. 1985. Morphological study of the mammalian stress response: characterization of changes in cytoplasmic organelles, cytoskeleton, and nucleoli, and appearance of intranuclear actin filaments in rat fibroblasts after heat-shock treatment. *The Journal of cell biology* **101**: 1198-1211.

Werle M, Bernkop-Schnurch A. 2006. Strategies to improve plasma half life time of peptide and protein drugs. *Amino acids* **30**: 351-367.

Wicha MS. 2006. Cancer stem cells and metastasis: lethal seeds. *Clinical cancer research : an official journal of the American Association for Cancer Research* **12**: 5606-5607.

Wieten L, Broere F, van der Zee R, Koerkamp EK, Wagenaar J, van Eden W. 2007. Cell stress induced HSP are targets of regulatory T cells: a role for HSP inducing compounds as anti-inflammatory immuno-modulators? *FEBS letters* **581**: 3716-3722.

Wilson WR, Hay MP. 2011. Targeting hypoxia in cancer therapy. *Nature reviews Cancer* **11**: 393-410.

Wolchok JD, Kluger H, Callahan MK, Postow MA, Rizvi NA, Lesokhin AM, Segal NH, Ariyan CE, Gordon RA, Reed K et al. 2013. Nivolumab plus ipilimumab in advanced melanoma. *The New England journal of medicine* **369**: 122-133.

Workman P. 2004. Combinatorial attack on multistep oncogenesis by inhibiting the Hsp90 molecular chaperone. *Cancer letters* **206**: 149-157.

World Cancer Report, WHO, International Agency for Research on Cancer, 2014.

Xia Y, Choi HK, Lee K. 2012. Recent advances in hypoxia-inducible factor (HIF)-1 inhibitors. *European journal of medicinal chemistry* **49**: 24-40.

Yaglom JA, Gabai VL, Sherman MY. 2007. High levels of heat shock protein Hsp72 in cancer cells suppress default senescence pathways. *Cancer research* **67**: 2373-2381.

Zhang X, Li F, Guo S, Chen X, Wang X, Li J, Gan Y. 2014. Biofunctionalized polymer-lipid supported mesoporous silica nanoparticles for release of chemotherapeutics in multidrug resistant cancer cells. *Biomaterials* **35**: 3650-3665.

Zhang XX, Sun Z, Guo J, Wang Z, Wu C, Niu G, Ma Y, Kiesewetter DO, Chen X. 2013. Comparison of (18)F-labeled CXCR4 antagonist peptides for PET imaging of CXCR4 expression. *Molecular imaging and biology : MIB : the official publication of the Academy of Molecular Imaging* **15**: 758-767.

Zhou YJ, Messmer MN, Binder RJ. 2014. Establishment of tumor-associated immunity requires interaction of heat shock proteins with CD91. *Cancer immunology research* **2**: 217-228.

Zipfel PF, Skerka C. 2009. Complement regulators and inhibitory proteins. *Nature reviews Immunology* **9**: 729-740.

Zorzi E, Bonvini P. 2011. Inducible hsp70 in the regulation of cancer cell survival: analysis of chaperone induction, expression and activity. *Cancers* **3**: 3921-3956.

VII. APPENDIX

VII-1: Table 1

Tumor-associated antigens and targeted anticancer immunotherapeutics including status of FDA aproval (2014) .

Antigen category	targeted antigens	antigen positive tumor types	therapeutic mAbs	FDA approved tumor entities
haematopoietic differentiation antigens	CD20	Non-Hodgkin´s Lymphoma	Rituximab	B cell NHL, CLL
			Ibritumomab	B cell NHL
			Tositumomab	NHL
			Ofatumumab	CLL
			Obinutuzumab	B cell NHL, CLL
	CD30	Hodgkin´s Lymphoma	Brentuximab v.	Hodgkin´s Lymphoma
	CD33	Acute Myelogenous Leukaemia (AML)	Gemtuzumab ozogamicin	AML
	CD52	Chronic lymphatic leukaemia	Alemtuzumab	B cell CLL
	CD194 (CCR4)	T-/NK cell lymphoma	mogamulizumab	- -
Glycoproteins	EpCAM	Epithelial tumors	IGN101,	- -
			Adecatumumab	- -
	EpCAM / CD3	malignant ascites of $EpCAM^+$ tumors	Catumaxomab (hybrid)	- -
	CEA	Breast, colon and lung tumors	Labetuzumab	- -
	gpA33	Colorectal carcinoma	huA33	- -
	Mucins	Breast, colon, lung and ovarian tumors	Pemtumomab,	- -
			Oregovomab	- -
	TAG-72	Breast, colon and lung tumors	Minretumomab	- -
	CAIX	Renal cell carcinoma	cG250	- -
	PSMA	Prostate carcinoma	J591	- -
	Folate-binding protein	Ovarian tumors	MOv18, Farletuzumab	- -
				- -
Glycolipids	Gangliosides	Neuroectodermal tumors, epithelial tumors	3F8	- -
			KW-2871	- -
			Dinutuximab	Neuroblastoma
Carbohydrates	Le^y	Breast, colon, lung, ovarian tumors	hu3s193	- -
			IgN311	- -
growth and differentiation signalling	EGFR	Glioma, lung, breast, colon, head & neck tumors (SCCHN)	Cetuximab,	SCCHN, colorectal carcinoma
			Panitumumab,	colorectal carcinoma
			Nimotuzumab	- -
	ERBB2	Breast, colon, lung, ovarian	Trastuzumab,	breast , gastric cance
		prostate tumors	Pertuzumab	breast cancer
	ERBB3	Breast, colon, lung, ovarian,prostate tumors	MM-121	- -

Table 1 (continued)

growth and differentiation signalling	MET	Breast, ovary, lung tumors	AMG 102	- -
			MetMab	- -
			Ficlatuzumab	- -
			ARCX 111	- -
	IGF1R	Glioma, lung, breast, head & neck	AVE1642	- -
		prostate, thyroid tumors	IMC-A12	- -
			MK-0646	- -
			R1507	- -
			CP 751871	- -
	EPHA3	Lung, kidney, colon tumors, melanoma	KB004,	- -
		glioma, haematological malignancies	IIIA4	- -
	TRAILR1	Colon, Lung, pancreas tumors,	Mapatumumab	- -
	TRAILR2	haematological malignancies	HGS-ETR2,	- -
			CS-1008	- -
	RANKL	Prostate cancer and bone metastases	Denosumab	- -
Targets of antiangiogenic mAbs	VEGF	Tumor vasculature	Bevacizumab	NCCLC, glioma, colon-& kidney cancer
	VEGFR-1 / VEGFR-2	Tumor vasculature	aflibercept (hybrid)	Ovarian, colorectal cancers
	integrin a_vb_3	Tumor vasculature	Etaracizumab	- -
	integrin a_vb_1	Tumor vasculature	Volociximab	- -
	VEGFR-1	Epithelal tumors	IM-2C6	- -
			CDP791	- -
	VEGFR-2		Ramucirumab	gastric carcinoma
Stroma and extracellular matrix antigens	FAB	Colon, breast, lung, pancreas, head & neck tumors	Sibrotuzumab	- -
			F19	- -
	Tenascin	Glioma, breast, prostate tumors	81C6	- -
Immune checkpoint antigens	CTLA4	Melanoma	Ipilimumab	Melanoma
	PD-1	Melanoma, NSCLC, renal cell carcinoma Melanoma, NSCLC	Nivolumab	Melanoma, NSCLC, Renal cell carcinoma
			pembrolizumab	Melanoma
cytokines	Interleukin-6	NHL, multiple myeloma, renal cell carcinoma, prostate cancer	Siltuximab	angiofollicular lymph node hyperplasia

CAIX, carbonic anhydrase IX; CEA, carcinoembryonic antigen; EGFR, epidermal growth factor receptor; EpCAM, epithelial cell adhesion molecule; EPHA3, ephrin receptor A3; FAP, fibroblast activation protein; gpA33, glycoprotein A33; IGF1R, insulin-like growth factor 1 receptor; Le^y, Lewis Y antigen; mAbs, monoclonal antibodies; PSMA, prostate-specific membrane antigen; RANKL, receptor activator of nuclear factor-κB ligand; TAG-72, tumour-associated glycoprotein 72; TRAILR, tumour necrosis factor-related apoptosis-inducing ligand receptor; VEGF, vascular endothelial growth factor; VEGFR, VEGF receptor

Table A1. **Current anticancer immunotherapeutics**. Adapted from (Scott et al. 2012)

VII-2: Own contributions to the publications

Publication #	Conception / study design	Performance / data analysis	Manuscript
A	70	80	60
B	70	60	30
C	70	80	60
D	30	50	40
E	95	95	95

in %, approximated

VII-3: Reprint permissions

A) Reprint permission: Journal of Cellular and Molecular Medicine

All articles accepted from 12 September 2012 are published under the terms of the Creative Commons Attribution License. Articles accepted before this date were published under the agreement as stated in the final article.

Copyright by the authors (© 2011 The Authors), as stated in the published article.

Creative Commons Attribution License:

You are free to:

- Share — copy and redistribute the material in any medium or format
- Adapt — remix, transform, and build upon the material for any purpose, even commercially.

  The licensor cannot revoke these freedoms as long as you follow the license terms.

  (http://creativecommons.org/licenses/by/4.0/, web source)

B) Reprint permission: Proceedings of the National Academy of Sciences of the USA

Thank you for your message. Authors do not need to obtain permission for the following uses of material they have published in PNAS: (1) to use their original figures or tables in their future works; (2) to make copies of their papers for their own personal use, including classroom use, or for the personal use of colleagues, provided those copies are not for sale and are not distributed in a systematic way; (3) to include their papers as part of their dissertations; or (4) to use all or part of their articles in printed compilations of their own works.

Please cite the original PNAS article in full when re-using the material. Because this material published after 2008, a copyright note is not needed. Feel free to contact us with any additional questions you might have.

Best regards,
Kay McLaughlin for
Diane Sullenberger
Executive Editor
PNAS

C) Reprint permission: Radiotherapy and Oncology

Thank you for your e-mail.

As an Elsevier journal author, you retain various rights including Inclusion of the article in a thesis or dissertation (provided that this is not to be published commercially) wheather in part or in toto; see http://www.elsevier.com/about/company-information/policies/copyright#Author%20rights [1] for more information. As this is a retained right, no written permission is necessary provided that proper acknowledgement is given. This extends to the online version of your dissertation and would include any version of the article including the final published version provided that is not available as an individual download but only embedded within the dissertation itself.

If the article would be available as an individual donload, only the reprint [2] or (subject to the journal-specific embargo date) accepted manuscript version [3], but not the final published version, may be made available; see http://www.elsevier.com/journal-authors/sharing-your-article [4] for more information. Information regarding embargo dates can be found here http://www.elsevier.com/__data/assets/pdf_file/0018/121293/external-embargo-list.pdf [5].

If you need any additional assistance, please let us know.

Best Wishes,
Laura

LAURA STINGELIN
PERMISSIONS HELPDESK ASSOCIATE
Elsevier
1600 John F. Kennedy Boulevard
Suite 1800
Philadelphia, PA 19103-2899
T: (215) 239-3867
F: (215) 239-3805

D) Reprint permission: PlosOne

Thank you for your message. PLOS ONE publishes all of the content in the articles under an open access license called "CC-BY." This license allows you to download, reuse, reprint, modify, distribute, and/or copy articles or images in PLOS journals, so long as the original creators are credited (e.g., including the article's citation and/or the image credit). Additional permissions are not required. You can read about our open access license here: http://www.plos.org/about/open-access/.

There are many ways to access our content, including HTML, XML, and PDF versions of each article. Higher resolution versions of figures can be downloaded directly from the article.

Thank you for your interest in PLOS ONE and for your continued support of the Open Access model. Please do not hesitate to be in touch with any additional questions.

Kind Regards,
Sue Laborda
Staff EO
PLOS ONE
Case Number: 04053473
ref:_00DU0Ifis._500U0LXxgM:ref

E) Reprint permission: Cancer Research

Authors of articles published in AACR journals are permitted to use their article or parts of their article in the following ways **without** requesting permission from the AACR. All such uses must include **appropriate attribution** to the original AACR publication. Authors may do the following as applicable:

1. Reproduce parts of their article, including figures and tables, in books, reviews, or subsequent research articles they write;
2. Use parts of their article in presentations, including figures downloaded into PowerPoint, which can be done directly from the journal's website;
3. Post the accepted version of their article (after revisions resulting from peer review, but before editing and formatting) on their institutional website, if this is required by their institution. The version on the institutional repository must contain a link to the final,

published version of the article on the AACR journal website. The posted version may be released publicly (made open to anyone) 12 months after its publication in the journal;

4. Submit a copy of the article to a doctoral candidate's university in support of a doctoral thesis or dissertation.

(http://www.aacrjournals.org/site/misc/permissions.xhtml; web source)

VII-5: Own research publications

Evaluation of c-ErbB-2 overexpression and Her2/neu gene copy number heterogeneity in Barett´s adenocarcinoma

Walch A, Bink K, Gais P, **Stangl S**, Hutzler P, Aubele M, Mueller J, Höfler H, Werner M.

Anal Cell Pathol 2000, 20 (1) 25-32.

Nucleofection of non-B cells with mini-Epstein-Barr virus DNA.

Radons J, Gross C, **Stangl S**, Multhoff G.

J Immunol Methods. 2005; 303(1-2):135-41.

Control of metastasized pancreatic carcinomas in SCID/beige mice with human IL-2/TKD-activated NK cells.

Stangl S*, Wortmann A*, Guertler U, Multhoff G.

J Immunol. 2006;176(10):6270-6.

An Hsp70 peptide initiates NK cell killing of leukemic blasts after stem cell transplantation.

Gross C, Holler E, **Stangl S**, Dickinson A, Pockley AG, Asea AA, Mallappa N, Multhoff G.

Leuk Res. 2008;32(4):527-34.

Influence of Hsp70 and HLA-E on the killing of leukemic blasts by cytokine/Hsp70 peptide-activated human natural killer (NK) cells.

Stangl S, Gross C, Pockley AG, Asea A, Multhoff G.

Cell Stress Chaperones. 2008;13(2):221-30.

Anti-tumor activity of patient-derived NK cells after cell-based immunotherapy – a case report

Milani V, **Stangl S**, Issels R, Gehrmann M, Wagner B, Hube K, Mayr D, Hiddemann W, Molls M, Multhoff G.

Journal of Translational Medicine. 2009 23;7:50

Bacterial production and functional characterization of the Fab fragment of the murine IgG1/λ monoclonal antibody cmHsp70.1, a reagent for tumour diagnostics.

Friedrich L, **Stangl S**, Hahne H, Küster B, Köhler P, Multhoff G, Skerra A.

Protein Eng Des Sel. *2010* Apr;23(4):161-8.

In vivo imaging of CT26 mouse tumors by using cmHsp70.1 monoclonal antibody

Stangl S, Gehrmann M, Dressel R, Alves F, Dullin C, Themelis G, Ntziachristos V, Staeblein E, Walch A, Winkelmann I, Multhoff G.

***J Cell Mol Med*.** 2010 Apr;15(4):874-87.

Targeting membrane heat-shock protein 70 (Hsp70) on tumors by cmHsp70.1 antibody.

Stangl S*, Gehrmann M*, Riegger J, Kuhs K, Riederer I, Sievert W, Hube K, Mocikat R, Dressel R, Kremmer E, Pockley A, Friedrich L, Vigh L, Skerra A, Multhoff G.

Proc Natl Acad Sci U S A. 2011 Jan 11;108(2):733-8.

Detection of irradiation-induced, membrane heat shock protein 70 (Hsp70) in mouse tumors using Hsp70 Fab fragment.

Stangl S, Themelis G, Friedrich L, Ntziachristos V, Sarantopoulos A, Molls M, Skerra A, Multhoff G.

Radiother Oncol. 2011 Jun;99(3):313-6.

Immunotherapeutic targeting of membrane Hsp70-expressing tumors using recombinant human granzyme B.

Gehrmann M*, **Stangl S*,** Kirschner A, Foulds G, Sievert W, Doss T, Walch A, Pockley AG, Multhoff G.

PLoS One. 2012;7(7).

Three-dimensional imaging of whole mouse models: comparing nondestructive X-ray phase-contrast micro-CT with cryotome-based planar epi-illumination imaging.

Tapfer A, Bech M, Zanette I, Symvoulidis P**, Stangl S**, Multhoff G, Molls M, Ntziachristos V, Pfeiffer F.

J Microsc*. 2014 Jan*;253(1):24-30.

Validation of heat shock protein 70 as a tumor-specific biomarker for monitoring the outcome of radiation therapy in tumor mouse models.

Bayer C, Liebhardt ME, Schmid TE, Trajkovic-Arsic M, Hube K, Specht HM, Schilling D, Gehrmann M, **Stangl S**, Siveke JT, Wilkens JJ, Multhoff G.

Int J Radiat Oncol Biol Phys*. 2014 Mar* 1;88(3).

Multimodal molecular imaging of integrin αvβ3 for in vivo *detection of pancreatic cancer.*
Trajkovic-Arsic M, Mohajerani P, Sarantopoulos A, Kalideris E, Steiger K, Esposito I, Ma X, Themelis G, Burton N, Michalski CW, Kleeff J, **Stangl S**, Beer AJ, Pohle K, Wester HJ, Schmid RM, Braren R, Ntziachristos V, Siveke JT.

J Nucl Med. 2014 Mar;55(3):446-51.

Hsp70 - a biomarker for tumor detection and monitoring of outcome of radiation therapy in patients with squamous cell carcinoma of the head and neck.
Gehrmann M, Specht H, Bayer C, Brandstetter M, Chizzali B, Duma M, Breuninger S, Hube K, Lehnerer S, v Phi V, Sage E, Schmid TE, Sedelmayr M, Schilling D, Sievert W, **Stangl S**, Multhoff G.

Radiat Oncol. 2014 Jun 9;9:131.

Tumor imaging and targeting potential of an hsp70-derived 14-mer Peptide.
Gehrmann M*, **Stangl S***,Foulds G*, Oellinger R, Breuninger S, Rad R, Pockley A, Multhoff G.

PLoS One. 2014 Aug 28, 9(8).

Selective in vivo imaging of syngeneic, spontaneous and xenograft tumors using a novel tumor cell-specific Hsp70 peptide-based probe
Stangl S, Varga J, Freysoldt B, Trajkovic-Arsic M, Siveke J, Greten F, Ntziachristos V, Multhoff G.

Cancer Res., 2014 Dec 1;74(23):6903-12.

Leveraging random forests for interactive exploration of large histological images.
Peter L, Mateus D, Chatelain P, Schworm N, **Stangl S**, Multhoff G, Navab N.

Med Image Comput Assist Interv. 2014;17(1):1-8

Role of membrane Hsp70 in radiation sensitivity
Murakami N, Schmid TE, Ilicic K, **Stangl S**, Schilling D, Gehrmann M, Walsh D, Molls M, Itami J, Multhoff G.

Rad Oncol. *(*2015) 10:149

Imaging of Hsp70-positive tumors with antibody-coated gold nanoparticles
Gehrmann G, Kimm M, **Stangl S**, Noël P, Rummeny EJ, Multhoff G.

Int J nanomedicine 2015;10: 1-14.

CD8+ tumour-infiltrating lymphocytes in relation to HPV status and clinical outcome in patients with head and neck cancer after postoperative chemoradiotherapy: A multicentre study of the German Cancer Consortium Radiation Oncology Group (DKTK-ROG)

Balermpas P*, Rodel F*, Roedel C, Krause M, Linge A, Lohaus F, Baumann M, Tinhofer I, Budach V, Gkika E, Stuschke M, Avlar M, Grosu A, Abdollahi A, Debus J, Bayer C, **Stangl S**, Belka C, Pigorsch S, Multhoff G, Combs S, Monnich D,Zips D, Fokas E for the DKTK-ROG

Int J Cancer 2015 Jul 14 [Epub ahead of print]

Depth-independent quantitative imaging of blood oxygenation of tissue and tumors using Multispectral Optoacoustic Tomography.

Tzoumas S*, Nunes A*, Olefir I, **Stangl S**, Symvoulidis P, Nasonova E, Glasl S, Bayer C, Multhoff G, Ntziachristos V.

Nat Med*.,* under revision

* these authors contributed equally

Erklärung

Hiermit erkläre ich, dass die vorliegende Arbeit selbstständig verfasst wurde und keine anderen als die hier angegebenen Quellen und Hilfsmittel verwendet wurden. Die Arbeit wurde noch keiner Prüfungskommission vorgelegt.

München, im September 2015 _____

Stefan Stangl

VIII. ACKNOWLEDGEMENTS

First of all, I owe my deepest gratitude to Prof. Gabriele Multhoff for providing me with this very interesting and fascinating topic for my thesis. Gaby´s enthusiastic discussions and constructive supports let me deep into science itself and beyond. I would like to thank her for encouraging me, for pushing me to my limits, for financial freedom of my scientific work, and for giving me the opportunity to publish my work.

Second, I am thankful to Prof. Johannes Buchner for his support, comments, and constructive suggestions.

Moreover, I would like to thank Prof. Michael Molls and Prof. Stephanie Combs for giving me the opportunity to work in the facilities of the Department of Radiotherapy of the Clinic and Policlinic for Radiotherapy and Radiooncology at the University Hospital rechts der Isar of the Munich Technical University.

Then of course I would like to thank the former and present members of Gabys group for providing a stimulating research environment, for the constructive discussions, especially during the lab meetings, and an always helping hand. Special thanks goes to Wolfgang, Christine, Steffi, Andi, Michael, Eva, Brigitte, Janina, Jessi, Dany, and Mathias; we spent uncountable hours together with scientific and non-scientific discussions inside and outside the laboratory, during coffe and lunch breaks, clubbing evenings, skiing and mountain hut trips, making this years an unforgettable time.

I wish to thank Prof. Graham Pockley and Gemma of Nottingham Trent University, for the interesting conversations and profitable suggestions during and beyond the time they joined our group.

I would like to deeply thank all my collaboration partners inside and outside the SFB824:

I am very grateful to Prof. Axel Walch from the Institute of Analytical Pathology at the Helmholtz Center, Munich, for intense, fruitful and greatly educationally excursions into pathology.

Marija of the group of Prof. Jens Siveke, medical department II, rechts der Isar, and the group of Prof. Florian Greten, Georg-Speyer-Haus Frankfurt a. M., for providing spontaneous and endogenous mouse models, George and Thanos of Prof. Vasilis Ntziachristos´ group (IBMI, HelmholtzZentrum Munich) for imaging with me at cutting-edge imaging platforms and their excellent technical advice, and Calogero of the department of the Nuclear Medicine, rechts der Isar, for PET and CT imaging. With all of them I had many exciting hours of *in vivo* imaging, good discussions, overall, marvelous collaborations.

Last but not least, I want to thank Juli for having a great time.

My family always supported me through the ups and downs during all these years, they always stood by my side. I am deeply thankful for their belief in me and for their support during my studies.

PART B: INCLUDED PUBLICATIONS

J. Cell. Mol. Med. Vol 15, No 4, 2011 pp. 874-887

In vivo imaging of CT26 mouse tumours by using cmHsp70.1 monoclonal antibody

Stefan Stangl [a], Mathias Gehrmann [a], Ralf Dressel [b], Frauke Alves [c], Christian Dullin [d], George Themelis [e], Vasilis Ntziachristos [e], Eva Staeblein [a], Axel Walch [f], Isabel Winkelmann [f], Gabriele Multhoff [a, *]

[a] *Department of Radiation Oncology, Klinikum rechts der Isar, Technische Universität München, and Clinical Cooperation Group (CCG) 'Innate Immunity in Tumor Biology', Helmholtz Zentrum München, German Research Center for Environmental Health (HMGU), Munich, Germany*
[b] *Department of Cellular and Molecular Immunology, University Medical Center Göttingen, Göttingen, Germany*
[c] *Department of Hematology and Oncology, University Medical Center Göttingen, Göttingen, Germany*
[d] *Department of Diagnostic Radiology, University Medical Center Göttingen, Göttingen, Germany*
[e] *Department of Nuclear Medicine, Klinikum rechts der Isar, Technische Universität München, and CCG 'Institute of Biological and Medical Imaging', HMGU, Munich, Germany*
[f] *Institute of Pathology, HMGU, German Research Center for Environmental Health, Munich, Germany*

Received: December 30, 2009; Accepted: March 11, 2010

Abstract

The major stress-inducible heat shock protein 70 (Hsp70) is frequently present on the cell surface of human tumours, but not on normal cells. Herein, the binding characteristics of the cmHsp70.1 mouse monoclonal antibody (mAb) were evaluated *in vitro* and in a syngeneic tumour mouse model. More than 50% of the CT26 mouse colon carcinoma cells express Hsp70 on their cell surface at 4°C. After a temperature shift to 37°C, the cmHsp70.1-fluorescein isothiocyanate mAb translocates into early endosomes and lysosomes. Intraoperative and near-infrared fluorescence imaging revealed an enrichment of Cy5.5-conjugated mAb cmHsp70.1, but not an identically labelled IgG1 isotype-matched control, in i.p. and s.c. located CT26 tumours, as soon as 30 min. after i.v. injection into the tail vein. Due to the rapid turnover rate of membrane-bound Hsp70, the fluorescence-labelled cmHsp70.1 mAb became endocytosed and accumulated in the tumour, reaching a maximum after 24 hrs and remained detectable at least up to 96 hrs after a single i.v. injection. The tumour-selective internalization of mAb cmHsp70.1 at the physiological temperature of 37°C might enable a targeted uptake of toxins or radionuclides into Hsp70 membrane-positive tumours. The anti-tumoral activity of the cmHsp70.1 mAb is further supported by its capacity to mediate antibody-dependent cytotoxicity.

Keywords: membrane-bound Hsp70 • Hsp70 antibody • tumour mouse model • flat panel volume CT • near-infrared fluorescence imaging

Introduction

Our search for innovative tumour-specific target structures for tumour therapy revealed heat shock protein 70 (Hsp70–1, HspA1A #3303) [1], the major stress-inducible member of the 70 kD heat shock proteins, as one such target. Both, Hsp70 and gp96, an endoplasmic reticulum resident member of the 90 kD heat shock protein group (gp96, HspC3 #7184), have been found on the plasma membrane of a variety of different human tumours [2–4]. During these studies we generated and characterized a mouse monoclonal antibody (mAb), termed cmHsp70.1, which specifically detects the cell surface localized Hsp70 on viable tumour cells with intact plasma membrane. The amino acid sequence of the Hsp70 molecule, which is exposed to the extracellular milieu of these tumours has been identified as being part of the 14-mer peptide TKDNNLLGRFELSG (TKD) [5, 6].

*Correspondence to: Dr. Gabriele MULTHOFF,
Department of Radiation Oncology,
Klinikum rechts der Isar, TU München,
Ismaningerstr. 22, 81675 Munich, Germany.
Tel.: +49-89-4140-4514
Fax: +49-89-4140-4299
E-mail: gabriele.multhoff@lrz.tu-muenchen.de

doi:10.1111/j.1582-4934.2010.01067.x

Screening of tumour biopsies and the corresponding normal tissues has indicated that primary diagnosed carcinoma samples, but none of the tested normal tissues, frequently exhibit an Hsp70 membrane-positive phenotype [7–9]. Moreover, an Hsp70 membrane-positive tumour phenotype has been associated with a significantly decreased overall survival in patients with lung cancer and lower rectal carcinomas suggesting that Hsp70 membrane-positivity might serve as a negative prognostic marker [10]. It has also been shown that the density of membrane Hsp70 on tumour cells can be further enhanced following therapeutic intervention such as radiotherapy or chemotherapy [11].

The anchorage of Hsp70 protein in the plasma membrane of non-stressed tumours is enabled by the glycosphingolipid globoyltriaoslyceramide (Gb3) [12, 13], which is frequently overexpressed in colorectal and gastric tumours and rarely found in the plasma membrane of normal cells. Following stress, elevated levels of Hsp70 are co-located with phosphatidylserine on the cell surface of tumour cells [14–16]. Moreover, an Hsp70 membrane-positive phenotype is associated with a higher resistance towards radiochemotherapy and membrane Hsp70 expression might therefore predict an unfavourable therapeutic outcome in lung and lower rectal tumours [17]. Taken together, these findings indicate the importance of determining the Hsp70 membrane status of tumours.

Within the last few years, non-invasive devices for the imaging of tumours in small animals have been developed [18]. Intraoperative and near-infrared fluorescence (NIRF) analyses are innovative approaches for tracking fluorophor-labelled probes, such as antibodies, in mice. Herein, we used a syngeneic tumour mouse model to study the distribution and binding characteristics of the cmHsp70.1 mAb *in vivo*. Screening of several mouse tumour cell lines revealed an Hsp70 membrane-positive phenotype on CT26 (mouse colon carcinoma cell line) colon carcinoma, ADJ (mouse plasmocytoma cell line) plasmocytoma, B16/F10 melanoma and MOS162 (mouse osteosarcoma cell line) mouse osteosarcoma cells at 4°C. Following a temperature shift to 37°C, the cmHsp70.1 mAb was rapidly taken up into early endosomes and lysosomes of CT26 tumour cells *in vitro*. Following i.v. injection of fluorescence-conjugated cmHsp70.1 mAb into the tail vein of CT26 tumour-bearing mice, the cmHsp70.1 mAb selectively and rapidly accumulates in endo-lysosomal compartments *in vivo*. In addition to its tumour imaging capacity, the cmHsp70.1 mAb can mediate cellular cytotoxicity (antibody-dependent cytotoxicity [ADCC]).

Materials and methods

Mouse tumour cell lines

The tumorigenic CT26 mouse colon adenocarcinoma (CT26.WT; ADCC CRL-2638) [19], 1048 mouse pancreatic carcinoma (kindly provided by Dieter Saur, Department of Medicine II, Technische Universität München, A20 B cell lymphoma [20], ADJ plasmocytoma cell lines, all derived from BALB/c mouse strains, the B16/F10 malignant mouse melanoma cells (C57/Bl6 mouse strain), and the MOS162 osteosarcoma cell line (C3H mouse strain; kindly provided by Dr. Michael Rosemann, HMGU Munich, Germany) were maintained in Roswell Park Memorial Institute (RPMI) 1640 medium supplemented with 10% v/v heat-inactivated foetal calf serum, 2 mM L-glutamine, 1 mM sodium-pyruvate and antibiotics (100 IU/ml penicillin, 100 μg/ml streptomycin), at 37°C in 5% CO_2. Cell lines were maintained in the exponential growth phase by regular cell passages twice a week and sub-cultivation at a ratio of 1:5 (seeding of 1×10^6 cells in 5 ml fresh culture medium). Doubling time of the cell lines was approximately 20 hrs. Single cell suspensions were derived by short-term (less than 1 min.) 0.25% (w/v) Trypsin 0.53 mM ethylenediaminetetraacetic acid treatment. All cell culture reagents were purchased from Life Technologies (Rockville, CA, USA).

Flow cytometry

The Hsp70 membrane phenotype in mouse tumour cell lines was determined by flow cytometry using the fluorescein isothiocyanate (FITC)-conjugated cmHsp70.1 mAb (IgG1; multimmune, Munich, Germany). For the CT26 mouse colon carcinoma cells, the Hsp70 status was routinely determined before their injection into the mice, and on single cell suspensions of random tumour samples after explanation on day 14. Briefly, after incubation of viable cells (0.2×10^6 cells) with the appropriate antibody for 30 min. at 4°C and following two washing steps, 7-AAD$^-$, viable cells were analysed on a FACSCalibur flow cytometer (Becton Dickinson, Heidelberg, Germany). An IgG1 isotype-matched control antibody was used to determine non-specific staining of the cell lines. The proportion of positively stained cells was defined as the difference of the number of cells stained with the relevant antibody minus the number of cells stained with the appropriate isotype-matched control immunoglobulin.

Fluorescence microscopy and kinetics of uptake of mAb cmHsp70.1-FITC

Microscopic immunofluorescence studies were performed with CT26 tumour cells which were cultured in 8-well chamber slides (Nunc, Rochester, NY, USA) at a cell density of 20,000 cells/well. After two washing steps in phosphate-buffered saline (PBS), viable cells were incubated for 30 min. with cmHsp70.1-FITC mAb either at 4°C or at 37°C. After fixation and permeabilization the cells were incubated with antibodies directed against Rab4, Rab5a, Rab7, Rab9, Rab11 (all obtained from Santa Cruz Biotechnology, Heidelberg, Germany), lysosomal associated membrane proteins (LAMP)1, LAMP2 (kindly provided by Prof. Stefan Höning, University of Cologne, Germany) for 1 hr and with the appropriate Cy3-conjugated secondary antibodies (anti-rabbit-Cy3 and anti-goat-Cy3, Jackson ImmunoResearch, West Grove, PA, USA) for 30 min. Cells were then washed twice in PBS and mounted in Vectashield containing 4,6-Diamidine-2-phenylindole (DAPI) solution (Vector Laboratories, Burlingame, CA, USA). The slides were analysed on a Zeiss Axioscop 2 plus scanning microscope (Zeiss, Jena, Germany) equipped with a ×100 oil-immersion objective and standard filters. Photographs of representative cells are shown; the localization and co-localization of Hsp70 and early (Rab4, Rab5a), late (Rab7, Rab11), trans golgi network, recycling endosomal (Rab11) and lysosomal (LAMP1, LAMP2) markers were visualized in green (FITC), red (Cy3) and yellow (merge) spectra.

The uptake of cmHsp70.1-FITC mAb and the identically labelled IgG1-FITC control antibody into tumour cells was measured by flow cytometry. For this, the tumour cells were incubated with the mAb for 2, 5, 10, 15, 30 and 60 min. either at 4°C or at 37°C. After two washing steps, viable cells were gated and analysed, as described above.

Biacore analysis

Kinetic measurements were performed with a Biacore X instrument (Biacore AB, Uppsala, Sweden) at 25°C with a CM5 chip (GE) and 25 mM HEPES, 150 mM KCl, 5 mM $MgCl_2$ pH 7.6 as running buffer and at a flow rate of 10 μl/min.

For this assay, 70 μg/ml cmHsp70.1 mAb diluted in 20 mM acetate (pH 4.8) was covalently coupled to a CM5 chip surface with primary amine groups using a standard amine coupling method, which yielded in about 1700 RU. The second channel subjected to the same activation and deactivation treatments, but without the antibody was used as control. Solutions of human Hsp70 (0.78 – 50 nM) were prepared in running buffer and tested for binding.

To determine the binding constants, association (K_{on}) and dissociation (K_{off}) phase data from each concentration were globally fitted to a simple 1:1 interaction model (A + B = AB) using the BIAevalution software 4.1.

Animals

Female and male BALB/c mice were obtained from an animal breeding colony (Harlan Winkelmann, Borchen, Germany) and maintained in pathogen-free, individually ventilated cages (Tecniplast, Hohenpeissenberg, Germany). Animals were fed with sterilized, laboratory rodent diet (Meika, Großaitingen, Germany) and were used for experiments between 6 and 12 weeks of age. All animal experiments were approved by the 'Regierung von Oberbayern' (55.2–1-54–2531-30–07; 55.2–1-54–2531-52–07) and were performed in accordance with institutional guidelines.

Intraperitoneal (i.p.) and subcutaneous (s.c.) injection of tumour cells

CT26 tumour cells were thawed from a common frozen stock and cultured *in vitro* for 2 to 3 days before use. BALB/c mice were injected into the peritoneum (i.p.) or s.c. with 100 μl of the CT26 stock solution containing 2.5×10^4 cells, using a 1000 μl plastic syringe with a 22-gauge needle. Injection was visually controlled using a 7× Stereomicroscope (Zeiss, Göttingen, Germany) and tumour weights of single tumours were determined on days 4, 6, 8, 10, 12, 14, 19 and 21 after injection. From day 23 onwards, mice died from progressive tumour growth.

Injection of the antibodies

For intraoperative and NIRF imaging 100 μg cmHsp70.1 mAb or IgG1 isotype-matched control antibody [clone electron microscopy (EM)21, directed against O6-ethly-2-deoxyguanosine] conjugated to Cy5.5-NHS (Squarix GmbH, Marl, Germany) at dye to molar ratios of 0.74 and 1.02, respectively, were injected i.v. into tumour-bearing mice on day 14. As an alternative, both antibodies were labelled with FITC at identical fluorescence intensities, as determined on the multilabel Reader Victor X4 (Perkin Elmer, Rodgau-Jügesheim, Germany).

Intraoperative fluorescence imaging

For intraoperative imaging, mice were killed 30 min., 2, 4 and 8 hrs after i.v. injection of either cmHsp70.1 mAb or control IgG1 (100 μg per injection) labelled with Cy5.5. The fluorescence imaging measurements used a back illuminated EM-charge-coupled device (CCD) camera (iXon DV887, Andor, Belfast, Northern Ireland). Light from the tissue was collected using a variable zoom objective lens (NT58–240, Edmund Optics, Barrington, NJ, USA). Light collected by the objective was filtered using a 710/10 nm band pass filter. A 670 nm CW diode laser (B&W Tek, Newark, DE, USA) with maximum power 300 mW was used for the excitation. The laser light beam was guided through a multimode fibre (200 μm core/ 0.22 NA) to a collimator and a diffuser (F260SMA-b, ED1-S20, Thorlabs, Newton, NJ, USA) for beam expansion and uniform illumination. A 24-bit colour CCD camera (PCO AG, Donaupark, Kelheim, Germany) coupled with the same objective lens was used to obtain colour images of the measured tissue. A 250 W halogen lamp (KL-2500 LCD, Edmund Optics) was used for white light illumination.

Immunofluorescence studies of tissue sections

On day 14, CT26 tumour-bearing mice were injected i.v. either with Cy5.5- or FITC-labelled cmHsp70.1 mAb or with identically labelled IgG1 control immunoglobulin (100 μg) into the tail vein. Mice were killed 3, 8, 24 and 72 hrs after injection of the antibodies and tumours and organs such as liver, lung, kidney, heart and spleen of the mice were collected, cut in four equal pieces and cryo-conserved. Consecutive sections of the tumours and organs (5–10 μm) were prepared using a Leica Cryostat (Leica CM1950, Leica Microsystems GmbH, Wetzlar, Germany) from the ventral margin of each piece for a distance of 250 μm. After fixation in formalin (10%) and counterstaining with Hoechst 33342, to visualize the nuclei, the sections were mounted with an antifade solution (Vectashield mounting media H-1000, Vector Laboratories). Sections were analysed on an upright epifluorescence microscope (Zeiss Axio Imager.Z1, Carl Zeiss MicroImaging GmbH, Jena, Germany) equipped with a C-Apochromat 40×/1.2 W Korr UV-VIS-IR objective and an AxioCam MRm camera. The visualization of the distribution of the fluorescence signals was performed with the AxioVision software (AxioVS40 V 4.8.1.9, Zeiss). Nuclei were visualized in blue (DAPI) and Hsp70 was visualized either in green (FITC) or in red (Cy5.5).

Flat-panel volume CT (VCT)

A flat-panel VCT (Fig. 4A), a non-clinical CT prototype equipped with two flat-panel detectors (GE Global Research, Niskayuna, NY, USA) [21] was used for the CT analyses. Briefly, anaesthetized mice were placed on a multimodality bed throughout the imaging session and injected i.v. with 150 μl of iodine-containing contrast agent Isovist 300 approximately 30 sec. before starting of the scan. All data sets were acquired with a step-and-shoot technique, using 1000 views per 1 full rotation, 8 sec. of rotation time per step, 360 used detector rows, 80 kVp, and 100 mA. For high-resolution image reconstructions a modified Feldkamp algorithm implemented on a simultaneous computer with eight nodes was used.

Near-infrared fluorescence imaging

The Optix system (Advanced Research Technologies, Montreal, Canada) is a 2D imaging system that works in a reflection scheme. The output of the system consists of maps of intensity and lifetime of the fluorescence distribution, in relation to a previously acquired camera image of the animal. Lifetime analysis describes the mean residence time of the fluorophor in an excited state and provides a characteristic parameter for the

fluorescent probe. The mean transit time of an emitted photon following an excitation pulse can be used to calculate the depth and concentration of the fluorescence intensity by time-resolved measurements [18]. The fluorescence intensity was determined in anaesthetized, viable mice that developed s.c. tumours before (0 hr), as well as 24, 48, 72 and 96 hrs after i.v. injection of the Cy5.5-labelled antibodies into the tail vein.

Antibody dependent cellular cytotoxicity assay

ADCC was measured using a standard 4-hr ^{51}Cr-release assay. Briefly, viable CT26 mouse colon carcinoma cells were labelled with 0.1 μCi of $Na^{51}CrO_4$ at 37°C for 1 hr. After two washes with RPMI 1640 medium, ^{51}Cr-labelled target cells (1×10^4) were transferred into triplicate wells of a 96-well plate and the cmHsp70.1 (IgG1) mAb was added (0.7, 1, 1.4 μg/ml). Freshly isolated mouse (BALB/c) spleen cells were added at various effector to target cell ratios (E:T). After a 4-hr co-incubation period supernatants (100 μl) were harvested and the levels of radioactive ^{51}Cr was counted using a gamma counter (Coulter-Counter, Billerica, MA, USA). Percentage of ADCC was calculated using the formula: %specific lysis = (experimental release – spontaneous release) / (maximum release – spontaneous release) × 100. The spontaneous release in each target cell ranged between 10% and 15%.

Statistics

Comparative analysis of the *in vitro* data was undertaken using the t-test for the analysis of two paired and unpaired samples. A significance level of $\alpha = 0.05$ was used.

Table 1 Proportion of Hsp70 membrane positive cells in different malignant mouse tumour cell lines. Hsp70 membrane positivity on mouse tumour cell lines was determined by flow cytometry using the cmHsp70.1-FITC mAb at 4°C. In line with previous reports [6–8] a sample was considered as Hsp70 membrane positive when more than 15% of the cells were positively stained with the cmHsp70.1-FITC mAb. The data represent the mean of at least six independent experiments ± S.E.

Mouse tumour cells (mouse strain)	Origin	Hsp70 membrane-positive cells (%)
CT26 (BALB/c)	Colon	44 ± 5.2
1048 (BALB/c)	Pancreas	12 ± 10.3
A20 (BALB/c)	B cell	5 ± 4.3
ADJ (BALB/c)	Plasmocytoma	45 ± 5.4
B16/F10 (C57/Bl6)	Melanoma	97 ± 6.2
MOS162 (C3H)	Osteosarcoma	70 ± 3.6

Results

Binding of mAb cmHsp70.1 mAb to cell surface-bound Hsp70 on mouse tumour cell lines *in vitro*

Screening of different mouse tumour cell lines with the IgG1 anti-human Hsp70-specific mAb cmHsp70.1, which detects the cell surface localized form of Hsp70 on human tumours, revealed that this antibody also recognizes membrane Hsp70 on mouse tumour cell lines [22]. An Hsp70 membrane-positive phenotype was determined in mouse colon carcinoma (CT26), plasmocytoma (ADJ), malignant melanoma (B16/F10) and MOS162 osteosarcoma cells (C3H) derived from different mouse strains (Table 1). In contrast, the mouse pancreatic carcinoma (1048) and the A20 B cell lymphoma cell line are considered as being membrane Hsp70$^-$ (Table 1). A representative flow cytometric image of the mouse CT26 colon carcinoma cell line is illustrated in Figure 1A. Cytosolic Hsp70 staining was excluded, as the entire staining procedure was performed at 4°C, and only 7-AAD$^-$, viable tumour cells with intact plasma cell membranes were analysed. Figure 1B illustrates the different binding patterns of the cmHsp70.1-FITC mAb to CT26 tumour cells at 4°C (left panel) and at 37°C (right panel). At 4°C, the binding of cmHsp70.1-FITC mAb to CT26 tumour cells reveals a typical ring-shaped cell surface staining pattern (Fig. 1B, left panel). The dotted staining pattern reflects the localization of membrane-bound Hsp70 in lipid rafts [23, 24]. Measurements, using fluorescence-conjugated marker beads revealed that approximately 10,000 Hsp70 molecules are present on the plasma membrane of the mouse tumour cell line CT26 at 4°C (data not shown).

A shift to 37°C resulted in a strong intracellular staining pattern, which likely results from the translocation of the FITC-conjugated antibody cmHsp70.1-FITC into the cytosol (Fig. 1B, right panel). Kinetic studies show a significant increase in the proportion of Hsp70 membrane-positive cells at 37°C between 2 and 15 min. after incubation with cmHsp70.1-FITC mAb, but not with an isotype-matched control antibody (Fig. 1C, upper right panel). In contrast, at 4°C the proportion of Hsp70 membrane-positive tumour cells remained nearly unchanged up to 60 min. (Fig. 1C, upper left panel). Furthermore, the mean fluorescence intensity (mfi) of Hsp70 per cell significantly increased after incubation with antibody at 37°C from 2 to 60 min. (Fig. 1C, lower right panel), but remained stably low at 4°C (Fig. 1C, lower left panel). These data indicate that the cmHsp70.1-FITC staining accumulates in Hsp70 membrane-positive tumour cells at the physiological temperature of 37°C, but not at 4°C. The reason for the antibody uptake is due to a rapid turnover rate of membrane-bound Hsp70. We could show that membrane Hsp70 expression is completely restored already after 15 min. after its removal by enzymatic digestion (data not shown). As expected, tumour cells with an initially low Hsp70 membrane expression level, such as 1048 pancreatic carcinoma cells and A20 B cell lymphoma cells, showed little cell surface staining at 4°C, nor did they internalize the cmHsp70.1-FITC mAb at 37°C (data not shown). In order to identify the endo-lysosomal compartment in which Hsp70 accumulates following endocytosis at 37°C a co-staining of Hsp70 (cmHsp70.1-FITC) with Cy3

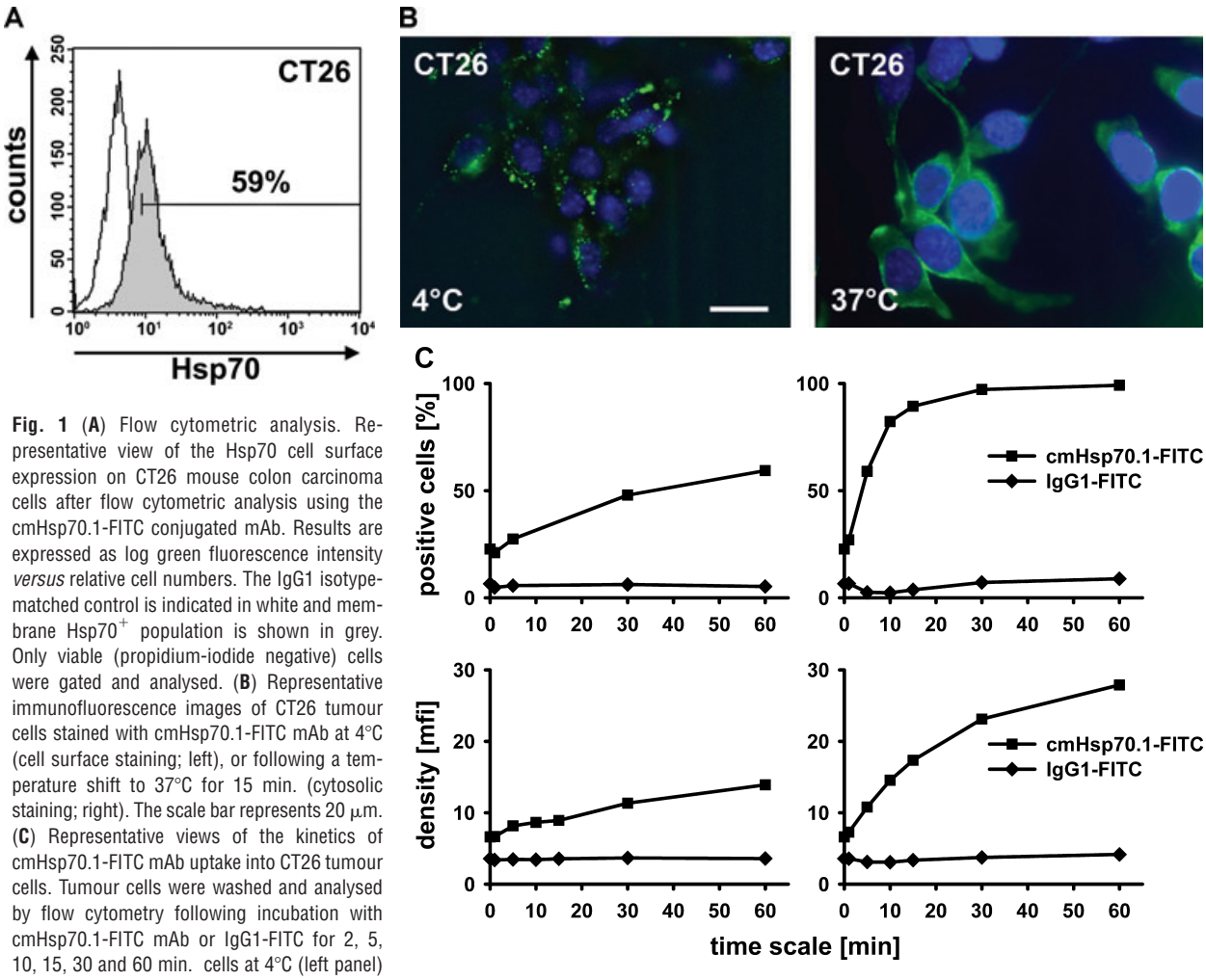

Fig. 1 (**A**) Flow cytometric analysis. Representative view of the Hsp70 cell surface expression on CT26 mouse colon carcinoma cells after flow cytometric analysis using the cmHsp70.1-FITC conjugated mAb. Results are expressed as log green fluorescence intensity *versus* relative cell numbers. The IgG1 isotype-matched control is indicated in white and membrane Hsp70^{+} population is shown in grey. Only viable (propidium-iodide negative) cells were gated and analysed. (**B**) Representative immunofluorescence images of CT26 tumour cells stained with cmHsp70.1-FITC mAb at 4°C (cell surface staining; left), or following a temperature shift to 37°C for 15 min. (cytosolic staining; right). The scale bar represents 20 μm. (**C**) Representative views of the kinetics of cmHsp70.1-FITC mAb uptake into CT26 tumour cells. Tumour cells were washed and analysed by flow cytometry following incubation with cmHsp70.1-FITC mAb or IgG1-FITC for 2, 5, 10, 15, 30 and 60 min. cells at 4°C (left panel) and 37°C (right panel). The upper graphs indicate the percentage of positively stained cells the lower graphs indicate the antigen densities at the indicated time-points, expressed as the mfi. The increase in the proportion of membrane Hsp70^{+} cells and in the mfi was significant ($P < 0.05$) at 37°C but not at 4°C. (**D**) Representative immunofluorescence images of CT26 tumour cells either stained with cmHsp70.1-FITC (green, first row) or with Cy3-secondary antibody labelled (red, second row) Rab4 (early endosome), Rab5a (early endosome), Rab7 (late endosome), Rab9 (late endosome), Rab11 (trans golgi network, recycling endosome), LAMP1 (CD107, lysosome), LAMP2 (lysosome) antibodies at 4°C (left three rows) and after an incubation of 30 min. at 37°C (right three rows). A co-localization of the FITC (green) and Cy3 (red) fluorescence, as indicated in a yellow spectrum (third row), is marked with '+' in the merged fluorescence staining pattern. Isotype-matched control antibodies did not show any staining (data not shown). Similar results were obtained in three independent experiments. The scale bar represents 20 μm.

secondary antibody labelled early (Rab4; Rab5a), late (Rab7, Rab9), recycling (Rab11) endosomal and lysosomal (LAMP1, LAMP2) markers was performed. As visualized in Figure 1D, co-localization of Hsp70 was predominantly found with Rab4, Rab5a, LAMP1 and LAMP2 at 4°C and at 37°C (yellow dots in the merged photographs, marked with a '+'). In summary, the data derived from three independent experiments (data not shown) indicate that Hsp70 predominantly accumulates in the early endosomal compartment and becomes degraded in lysosomes.

The concentration-dependent affinity of the full length cmHsp70.1 mAb to immobilized human Hsp70 was determined using a Biacore X system. The sensogram profiles of Figure 2 were globally fitted to a 1:1 binding model with the BIAevaluation software. The calculated K_{on} value was 6.99×10^{4}/M/s and the K_{off} value was 3.79×10^{-4}/s with a dissociation equilibrium constant K_D of 5.4 nM for Hsp70 with a χ^2 of 59.4.

In vivo tumour growth of intraperitoneal and subcutaneous transplanted CT26 cells

An i.p. injection of 2.5×10^{4} CT26 mouse colon adenocarcinoma cells suspended in 100 μl PBS resulted in rapidly growing

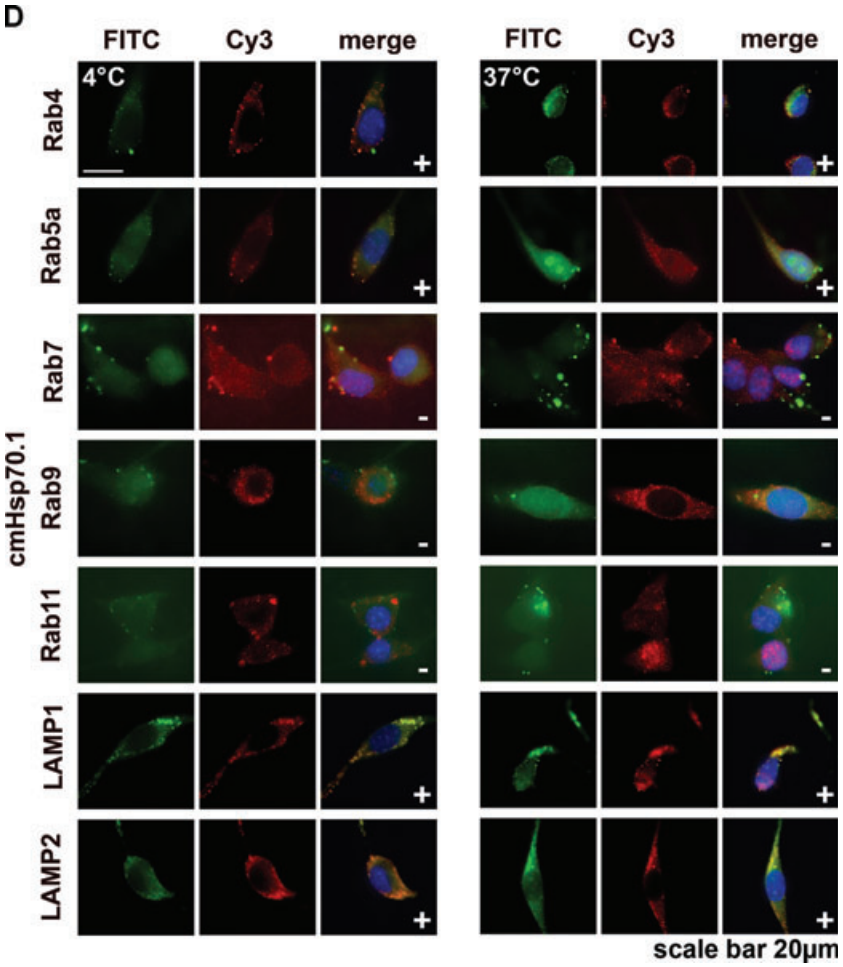

Fig. 1 Continued

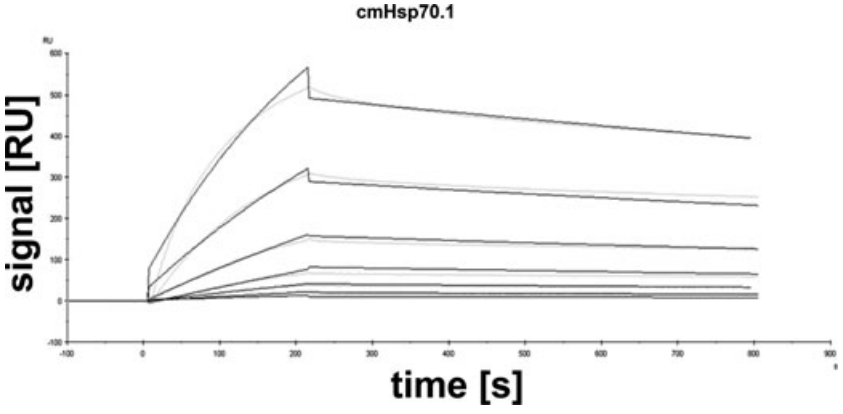

Fig. 2 Global kinetic analysis of cmHsp70.1 mAb binding human Hsp70 using a Biacore. Purified human Hsp70 protein was diluted to final concentrations of 0.78, 1.6, 3.1, 6.3, 12.5, 25, 50 nM and injected onto a cmHsp70.1 mAb-coated gold surface. Relative response units were analysed using BIAevaluation software 4.1. Kinetic constants were $K_{on} = 6.99 \times 10^4$/M/s, $K_{off} = 3.79 \times 10^{-4}$/s and a $K_D = 5.4$ nM with a $\chi^2 = 59.4$, respectively. Grey coloured lines contrast the measured data from the simulated fits (black).

tumours (Fig. 3, black bars). The average weight of an individual tumour was 2.6 g ± 1.3 ($n = 17$) on day 19 and most animals became moribund shortly thereafter due to the large tumour weight in the abdomen. Tumour take at any tested time-point was always 100%. A comparative phenotyping of CT26 cells from tissue culture and from single cell suspensions derived from tumour-bearing mice on day 14 revealed that the amount of Hsp70 membrane-positive cells was found to be significantly elevated from 56.2 ± 9% ($n = 6$) up to 79.8 ± 14% ($n = 7$) in mouse-derived tumours (data not shown). Tumour growth was similar

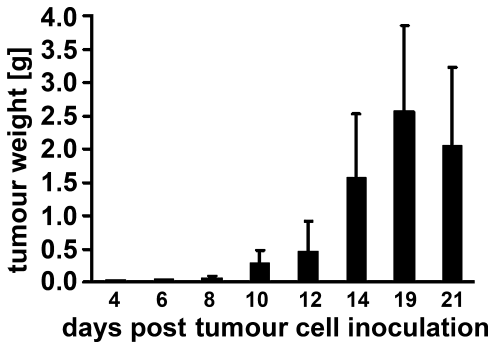

Fig. 3 Tumour growth curve for CT26 colon adenocarcinoma cells in BALB/c mice. Following i.p. injection of tumour cells (2.5×10^4) mice were killed on days 4 (0.03 ± 0.11 g; $n = 3$), 6 (0.05 ± 0.2 g; $n = 3$), 8 (0.05 ± 0.03 g; $n = 5$), 10 (0.29 ± 0.2 g; $n = 7$), 12 (0.47 ± 0.44 g; $n = 7$), 14 (1.55 ± 0.9 g; $n = 35$), 19 (2.6 ± 1.3 g; $n = 17$), 21 (2.05 ± 1.18 g; $n = 10$) and tumour weights were determined.

following s.c. injection of the same number of CT26 cells into the neck, although mice did not die until day 26 (data not shown).

Intraoperative *in vivo* imaging of Hsp70 in tumour-bearing mice

Fluorescence-labelled cmHsp70.1-Cy5.5 mAb or IgG1-Cy5.5 (100 μg each) were injected i.v. into the tail vein of tumour-bearing mice on day 14 after i.p. injection of CT26 cells (2.5×10^4), at which time the average tumour weight of 1.55 g ± 0.9 ($n = 35$, Fig. 3). In order to obtain a more detailed overview of the binding characteristics of the cmHsp70.1 mAb *in vivo,* an intraoperative technique was used for *in vivo* imaging. The upper part of Figure 4A illustrates true colour autopsy images of the CT26 tumours in mice injected either with the IgG1 isotype-matched control or the cmHsp70.1 mAb, both of which were conjugated with Cy5.5. The regions of the tumours are marked with a white dotted line. The fluorescence images of the IgG1-Cy5.5 control antibody and that of the identically labelled mAb cmHsp70.1-Cy5.5 are indicated below in false multispectral views. As indicated on the left panel, an orange spectrum represents a region of high antibody intensity, whereas a blue and green spectrum represents low antibody staining intensities. Localization of the cmHsp70.1-Cy5.5 (Fig. 4A, lower right panel), but not the IgG1-Cy5.5 isotype-matched control antibody (Fig. 4A, lower left panel), in the tumour is detectable at relatively high amounts, as early as 30 min. following i.v. injection of the antibodies in the tail vein. Kinetic studies indicated a progressive accumulation of the cmHsp70.1-Cy5.5 mAb (Fig. 4B, lower panel), but not the IgG1 isotype-matched control (Fig. 4C, lower panel), within the tumour between 2 and 8 hrs. In Figure 4B and C the Cy5.5 staining of both, cmHsp70.1-Cy5.5 mAb and isotype control is indicated in red and the antibody-free mouse tissues are represented in light blue colour spectra. It appeared that the cmHsp70.1 mAb, but not the IgG1 isotype matched control is

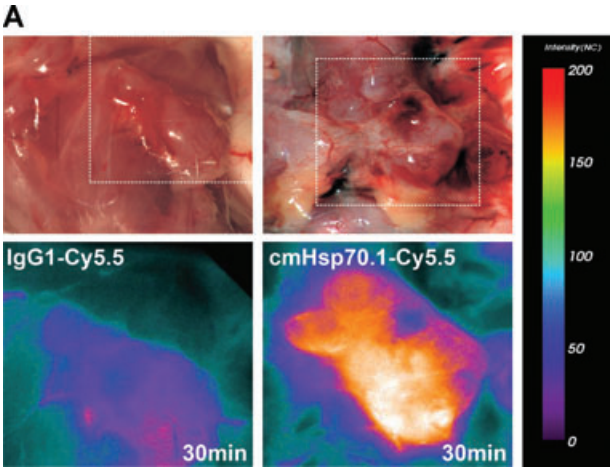

Fig. 4 (**A**) Optical imaging. Intraoperative detection of cmHsp70.1-Cy5.5 mAb in tumour-bearing BALB/c mice. 100 μg of cmHsp70.1-Cy5.5 mAb as well as the IgG1-Cy5.5 control were injected i.v. into the tail vein of CT26 tumour-bearing mice on day 14. Representative views of the Cy5.5 fluorescence and autopsy images of the dorsal part of the mice were taken 30 min. after i.v. injection of the antibodies. Upper panel, autopsy image of the dorsal located mouse tumour in true colours. Lower panel, false colour images of the Cy5.5 staining within the tumour. The massive fluorescence signal corresponds to the anatomic position of the CT26 tumour which is stained with cmHsp70.1-Cy5.5 mAb. Almost no staining with an equivalently labelled IgG1 isotype-matched control is detectable. (**B**) Kinetics of the intraoperative detection of cmHsp70.1-Cy5.5 mAb in CT26 tumour-bearing mice on day 14. Representative views of the Cy5.5 fluorescence images of the dorsal part of the mice were taken 2, 4 and 8 hrs after i.v. injection of the antibody. Upper panel, autopsy images of the dorsal located mouse tumour in true colours. Lower panel, false colour images of the Cy5.5 staining within the tumour indicated in red. (**C**) Kinetics of the intraoperative detection of IgG1-Cy5.5 control immunoglobulin in CT26 tumour-bearing mice on day 14. Representative views of the Cy5.5 fluorescence images of the ventral part of the mice were taken 4 and 8 hrs after i.v. injection of the antibody. Upper panel, autopsy images of the ventral located mouse tumour in true colours. Lower panel, false colour images of the Cy5.5 staining indicated in red. No staining was detectable within the tumour following the administration of the IgG1-Cy5.5 isotype-matched control. (**D**) Immunofluorescence studies of tumour and normal tissue (lung) sections (10 μm) derived from the same animals, 8 hrs after i.v. injection of IgG1-Cy5.5 (upper panel) or cmHsp70.1-Cy5.5 mAb (lower panel). The nuclei are visualized in blue (DAPI) and the localization of Hsp70 is visualized in red (Cy5.5). The scale bar represents 50 μm.

predominantly located within the tumour. An overall inspection of different mouse organs and the tumour revealed that apart from the CT26 tumours no other mouse tissues were positively stained for the Cy5.5-labelled mAb cmHsp70.1 (data not shown). These data are confirmed by immunofluorescence studies of sections (10 μm) of the tumours (Fig. 4D, left panel) and normal tissues (lung; Fig. 4D, right panel) of the identical animals. An endo-lysosomal Cy5.5 staining pattern, as already shown for *in vitro* cultured CT26 tumour cells (Fig. 1D), is detectable only in the tumour

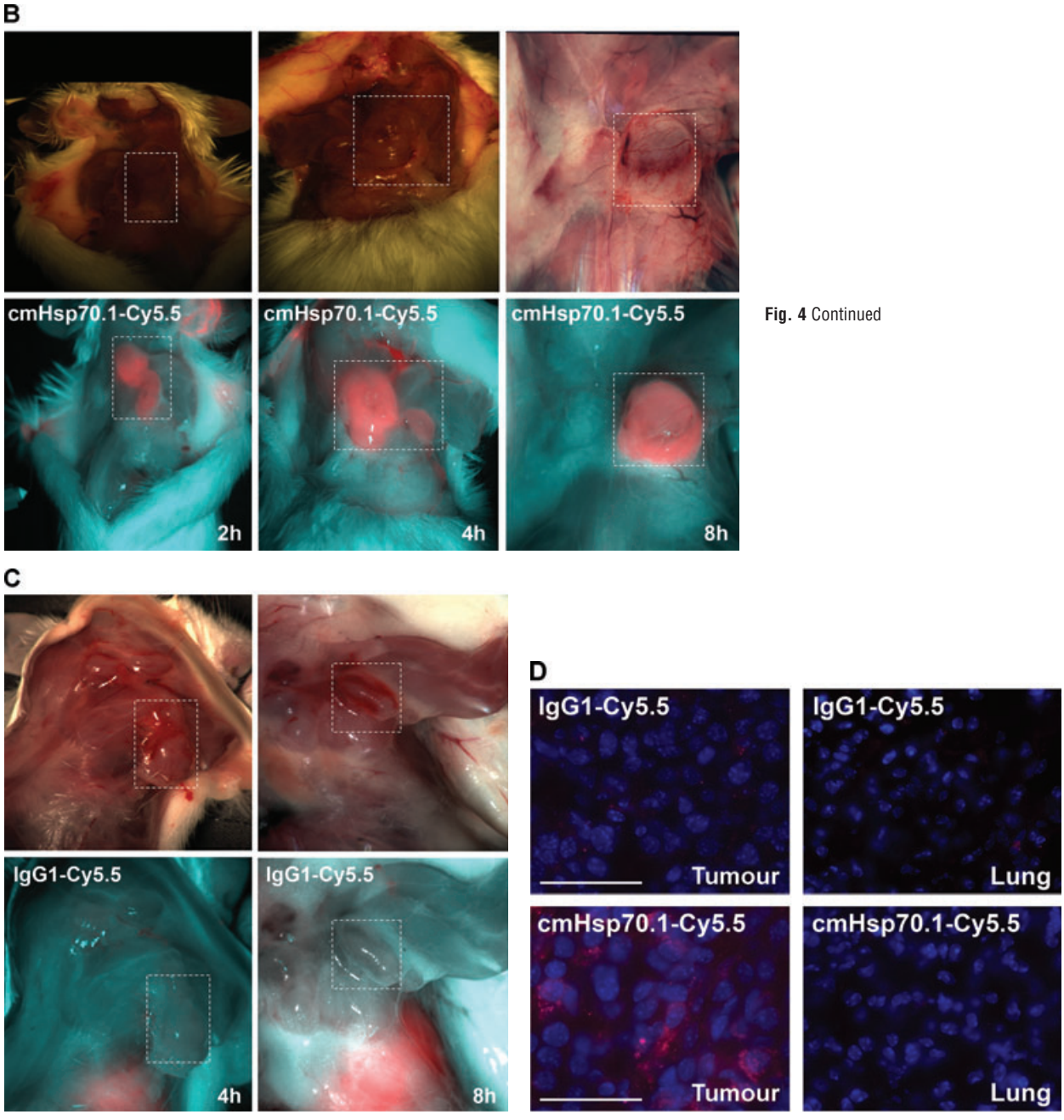

Fig. 4 Continued

sections by using the cmHsp70.1 mAb, but not in normal tissues (Fig. 4D, lower panel). The IgG1 control antibody did neither stain tumour nor normal tissues including liver, lung and heart. The lung is shown as a representative example for the normal tissue in the upper panel of Figure 4D. The cmHsp70.1-Cy5.5 mean intensity of cell area is 3.7-fold higher in the tumour compared to that in the lung tissue. In line with these findings are the results from immunofluorescence studies of sections (5 μm) derived from tumour-bearing mice that had received FITC-labelled cmHsp70.1 mAb or IgG1 immunoglobulin *via* the tail vein, the fluorescent intensities of which were identical, as determined by multicolour luminescence reader (data not shown). Representative images of sections of tumours (day 14 after i.p. injection of CT26 tumour cells, Fig. 5A) and normal tissues, such as the liver (Fig. 5B), lung (Fig. 5C) and kidney (Fig. 5D) of tumour-bearing mice, which had been injected either with cmHsp70.1-FITC or with IgG1-FITC,

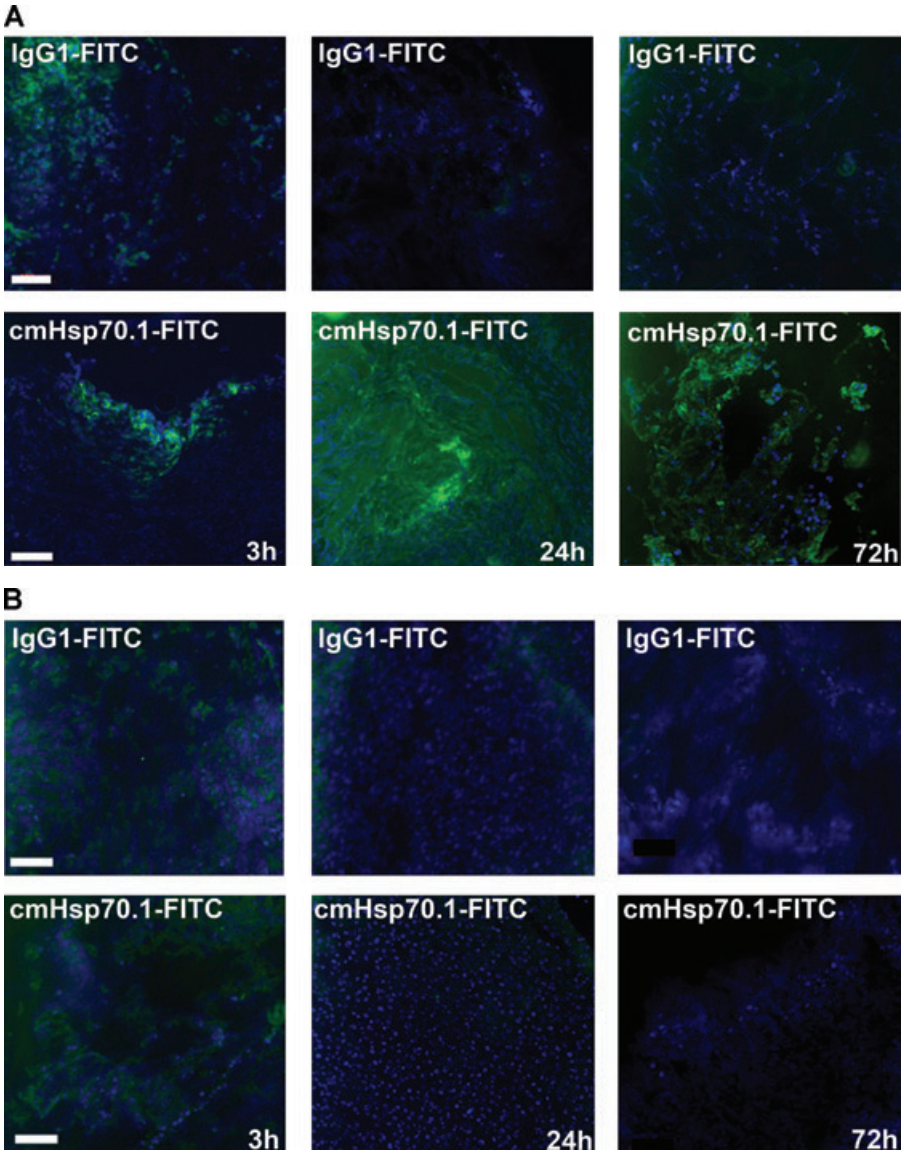

Fig. 5 Immunofluorescence analysis of tumour and normal tissue sections. cmHsp70.1-FITC mAb (lower panel) or the identically labelled IgG1 control (upper panel, 100 μg each) was injected into the tail veins of tumour-bearing mice on day 14 after i.p. tumour cell (CT26) injection. Animals were killed 3, 24 and 72 hrs thereafter and the tumour (**A**), liver (**B**), lung (**C**) and kidney (**D**) were cryo-conserved. Representative views of sections (5 μm) of the tumours and organs were taken at the indicated time-points after the injection of the IgG1-FITC (upper panel) and cmHsp70.1-FITC mAb (lower panel). The nuclei are stained in blue (DAPI) and the localization of Hsp70 is visualized in green (FITC). The scale bar represents 100 μm.

clearly demonstrate a time-dependent (from 3 to 72 hrs) and specific up-take of the Hsp70-specific antibody into the tumours. In contrast, the identically-labelled IgG1 isotype-matched control antibody was only found in the liver 3 hrs after i.v. injection. A weak staining of the liver was also detectable 3 hrs after i.v. injection of the cmHsp70.1 mAb, but this had completely disappeared after 24 hrs. Other normal tissues of the same mice, such as lung (Fig. 5C), kidney (Fig. 5D), heart (data not shown) and spleen (data not shown) did not show any fluorescence staining at the indicated time-points. In summary these data show that irrespectively of the fluorescence label (Cy5.5, Fig.4; FITC, Fig. 5; Alexa, data not shown), the cmHsp70.1 mAb binds to Hsp70 membrane-positive tumours *in vivo* in a highly selective manner. Due to the time-dependent concentration of the cmHsp70.1 mAb within the tumours of the mice, we suggest that in accordance with our *in vitro* findings (Fig. 1C) the Hsp70 mAb becomes rapidly internalized into the endo-lysosomal compartment also *in vivo*. A non-specific uptake of the fluorescence dye is unlikely since identical results have been obtained using Cy5.5 (Fig. 4), FITC (Fig. 5) and Alexa (data not shown) conjugated reagents.

Near-infrared fluorescence *in vivo* imaging of Hsp70 in tumour-bearing mice

The Optix system was used for the long-term analysis and for quantification of the fluorescence intensities in mice bearing s.c. tumours. Lifetime and fluorescence intensities were determined

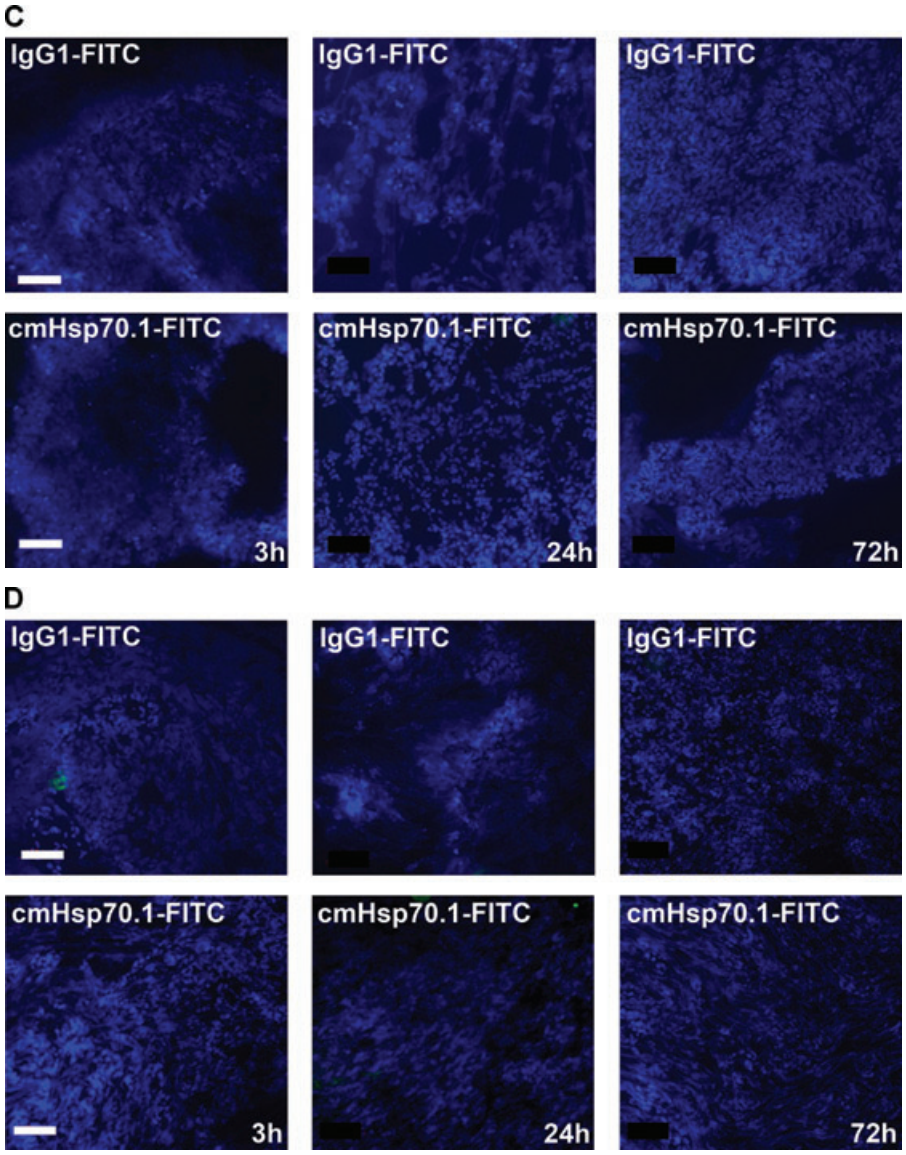

Fig. 5 Continued

0, 24, 48, 72 and 96 hrs after i.v. injection of the Cy5.5-conjugated antibodies into anaesthetized mice. The fluorescence probes were scanned by Optix *in vitro* in order to determine their specific fluorescent lifetimes prior to the *in vivo* experiments. Based on a single exponential fit to the decay of the curve, a fluorescent lifetime of 1.7 nsec. was calculated for the cmHsp70.1-Cy5.5 and the IgG1-Cy5.5.

The dye to antibody molar ratio was 0.74 for the cmHsp70.1 mAb and 1.02 for the IgG1 control. The upper panel of Figure 6A depicts fluorescence lifetimes of the scanned region in a tumour-bearing animal injected with cmHsp70.1-Cy5.5 mAb, and the lower graph in a tumour-bearing animal injected with IgG1-Cy5.5 at the indicated time-points, as determined by NIRF imaging. Lifetime images serve as specificity controls of the Cy5.5 staining and enable specific fluorescence to be distinguished from autofluorescence. The estimated fluorescence lifetime for all scanned points in both mice was approximately 1.7 nsec. This value is comparable to that of the Cy5.5 labelled antibodies measured *in vitro*.

Flat-panel VCT images, which were taken 24 hrs after i.v. injection of the antibodies, revealed comparable volumes of both tumours. The tumour volume of the mouse which had been injected with cmHsp70.1 mAb was 0.227 cm^3 and 0.211 cm^3 for the IgG1 mAb-injected mouse. Furthermore, anatomical imaging by high-resolution 3D flat-panel VCT imaging demonstrates the localization of the tumours (Fig. 6A, right panel) in correlation to the Cy5.5 fluorescence signals (Fig. 6B).

Figure 6B represents a follow-up of the fluorescence intensity of the Cy5.5-labelled cmHsp70.1 mAb (upper panel) and IgG1

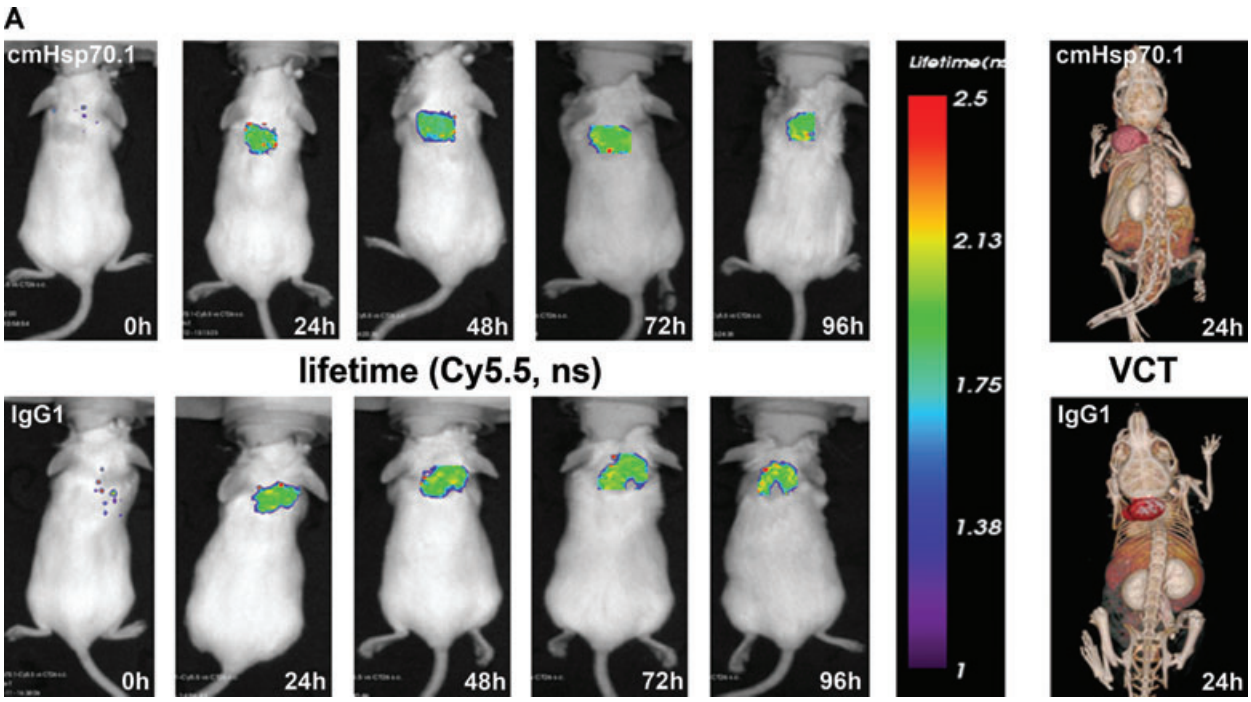

Fig. 6 (**A**) Lifetime images and flat-panel VCT scans. Representative lifetime images were obtained using the Optix system. Representative fluorescence signals over the s.c. located CT26 tumour regions show lifetimes of 1.7 nsec., which are characteristic for Cy5.5-conjugated cmHsp70.1 mAb (upper panel) and the IgG1 (lower panel) isotype-matched control. Images were taken 0, 24, 48, 72 and 96 hrs after i.v. injection into the tail vein. The peak emission of Cy5.5 is at 694 nm in the bright green area. Localization of the CT26 colon adenocarcinoma in the dorsal neck region of the mice is depicted in the volume rendered flat-panel VCT scans which were taken 24 hrs after the injection of the cmHsp70.1 mAb and isotype-matched control on days 14, 15, 16 and 17 after the tumour cell injection. On day 14, the tumour size which was determined by flat-panel VCT, was 0.227 cm^3 in mice injected with cmHsp70.1 mAb, and 0.211 cm^3, in mice injected with the IgG1 control antibody. (**B**) Representative fluorescence intensity images obtained by the Optix system. Fluorescence intensity is displayed in normalized counts and is presented from two CT26 tumour-bearing mice 0, 24, 48, 72 and 96 hrs after i.v. injection of the cmHsp70.1-Cy5.5 mAb (upper panel) and an identically labelled IgG1 isotype-matched control (lower panel). Strong fluorescence signals (red outline) over the tumour of the mouse that had received the cmHsp70.1-Cy5.5 mAb, but not over the tumour in the animal that had been injected with the IgG1-Cy5.5 control were visible between 24 and 96 hrs. Whole body scans of the identical mice 72 hrs after injection of the mAb and isotype control are shown on the outer right part of the graph. Fluorescence signals were only apparent over the tumour region. (**C**) Quantitative analysis of the fluorescence intensity images of the tumours of mice that received either cmHsp70.1-Cy5.5 mAb (black bars) or IgG1-Cy5.5 (white bars). Average intensities of fluorescence signals in the s.c. tumour regions of the two mice shown in (**B**) at the indicated time-points 0, 24, 48, 72 and 96 hrs after i.v. injection of the antibodies are displayed. The data were corrected for their labelling intensities. (**D**) Kinetics of average fluorescence intensity of cmHsp70.1-Cy5.5 mAb (black dots) and IgG1-Cy5.5 control (white dots) in tumour-bearing mice. The data represent a summary of the average fluorescence intensity over tumour regions in mice at 24, 48, 72 and 96 hrs after i.v. injection of the antibodies. Data represent mean values of five animals; * marks values $P < 0.05$; ** marks values $P < 0.001$.

isotype-matched control (lower panel) 0, 24, 48, 72 and 96 hrs after i.v. injection of the probe. The whole body fluorescence intensity scans, which are taken 72 hrs after i.v. injection, demonstrate a selective binding of the Cy5.5 labelled cmHsp70.1 mAb to the tumour tissues (Fig. 6B, right panel). A quantitative analysis of the average fluorescence intensities in these two mice at the indicated time-points is summarized in Figure 6C. It appears that the average intensity of the cmHsp70.1 mAb was always stronger than that of the isotope-matched control at all time-points, with a maximum at 24 hrs. A summary of the average fluorescence intensities for both groups of treated animals (derived from five animals per time-point) confirmed these results and revealed significantly stronger fluorescence signals over the tumours of mice that received the cmHsp70.1 mAb in comparison to IgG1 isotype-matched control antibody at the time-points 24 (54.33 $\pm$ 3.9 *versus* 16.92 $\pm$ 4.9; $P < 0.001$), 72 (32.97 $\pm$ 4.7 *versus* 24.17 $\pm$ 3.0; $P < 0.05$) and 96 hrs (30.29 $\pm$ 9.1 *versus* 12.01 $\pm$ 1.9; $P < 0.05$) after i.v. injection (Fig. 6D).

Effects of cmHsp70.1 mAb on CT26 tumour cells *in vitro*

Although it is known that IgG1 mouse monoclonal antibodies in general have a low capacity to mediate ADCC, the cmHsp70.1 mAb was tested against Hsp70 membrane-positive CT26 tumour cells.

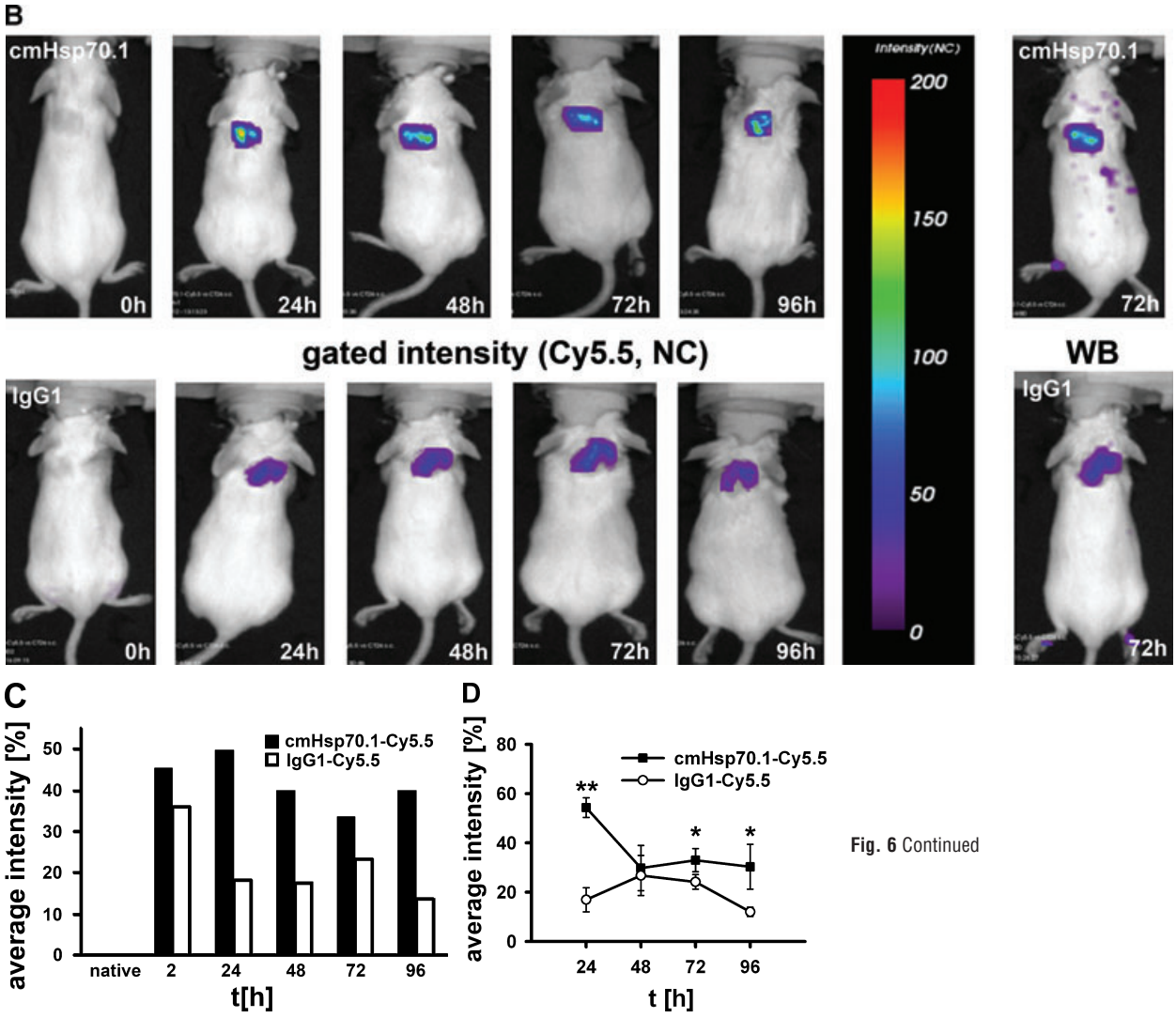

Fig. 6 Continued

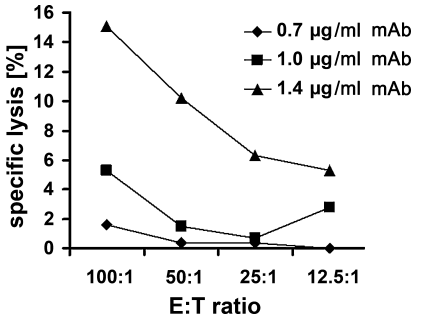

Fig. 7 Capacity of cmHsp70.1 mAb to induce ADCC against CT26 tumour cells *in vitro*. *In vitro* ADCC of CT26 colon (containing 55% Hsp70 membrane-positive cells) carcinoma cells, using 0.7, 1 and 1.4 μg/ml cmHsp70.1 mAb and unstimulated mouse spleen cells at E:T ratios ranging from 100:1 to 12.5:1. The data show one representative experiment out of three independent experiments showing similar results.

As summarized in Figure 7, the cmHsp70.1 induces ADCC in CT26 at the very low concentration of 1.4 μg/ml. In contrast, lower concentrations did not affect the viability of CT26 tumour cells. Presently, experiments are ongoing which test the anti-tumoral effect of cmHsp70.1 mAb in a tumour mouse model.

Discussion

Tumours, but not the corresponding normal tissues, frequently present Hsp70 on their cell surface. Moreover, an Hsp70 membrane-positive phenotype was found to predict a decreased overall survival in tumour patients with an extrahepatic route of metastasis [10], and thus might act as a negative prognostic marker. In contrast, patients whose tumours metastasize into the

liver have shown a better clinical outcome due to the presence of hepatic natural killer cells that may provide an immunological filter for membrane Hsp70 tumour cells [10]. These data indicate the medical need for the development of novel strategies to visualize and target highly aggressive, Hsp70 membrane-positive tumours.

Herein, the role of membrane Hsp70 as a potential tumour-specific target for *in vivo* imaging was evaluated. Our laboratory generated an IgG1 mouse anti-human Hsp70-specific mAb termed cmHsp70.1 which specifically detects the membrane-bound form of Hsp70 on viable human tumour cells with an intact plasma membrane [5, 6]. Human and mouse Hsp70 does not differ within the 8-mer region in the C-terminus, which is recognized by mAb cmHsp70.1 (NLLGRFEL). Therefore, it was assumed that the antibody shows cross-reactivity for Hsp70 in both species. The membrane Hsp70 phenotype was studied in several mouse tumour cell lines derived from different mouse strains. Among others, the mouse colon carcinoma cell line CT26 was found to be strongly membrane Hsp70^{+}. Moreover, a temperature shift from 4°C to 37°C resulted in an internalization of the fluorescence-labelled cmHsp70.1 mAb. This result could be explained by a fast turnover rate of membrane-bound Hsp70 into the cytosol at physiological temperatures. The time-dependent and tumour-specific accumulation of the cmHsp70.1-FITC mAb in early endosomes and lysosomes further supports this hypothesis. In line with these findings it has been shown recently that Hsp70 associates with proteins such as MUC1 and caveolin 1 in lipid rafts of breast cancer cells [24]. These protein aggregates rapidly become endocytosed to re-enter the secretory pathway for recycling to the plasma membrane [25]. Co-staining of Hsp70 with the small GTPases Rab4 and Rab5a, which mark transport routes of proteins from the plasma membrane to early endosomes and back to the plasma membrane, also support this recycling pathway [26]. As expected, part of the intracellular located Hsp70 becomes degraded in lysosomes [26].

Given that the membrane Hsp70 positivity of CT26 tumours derived form mice autopsies was even greater than that of *in vitro* cultured CT26 cells, we addressed the question whether cmHsp70.1 mAb conjugated to different fluorophors also stains mouse tumours *in vivo*. Intraoperative and NIRF imaging techniques revealed a fast and highly specific binding of the Cy5.5-labelled cmHsp70.1 mAb to i.p. and s.c. localized tumours in living animals, as early as 30 min. after i.v. injection into the tail vein which lasts for at least 96 hrs. In contrast, an identically labelled IgG1 isotype-matched control antibody was found to be enriched in the liver at the identical time frame. A detailed macro- and microscopical inspection of tumour-free organs of the mice showed that the cmHsp70.1 mAb did not bind to any normal mouse tissues. A non-specific up-take of antibody-free fluorescence dye into the tumour is unlikely since different cmHsp70.1-fluorophor conjugates produced identical results.

The tumour-specific binding pattern of mAb cmHsp70.1 was further confirmed by NIRF imaging of s.c. located tumours. In the tumour, the fluorescence signals of an identically labelled IgG1 isotype-matched control was significantly lower than that of the cmHsp70.1 mAb. By comparing the 3D flat-panel VCT data to the 2D fluorescence maps [21], generated by NIRF imaging, we successfully matched fluorescence signals from Cy5.5-labelled cmHsp70.1 mAb to pathologic tumour structures. Co-registration of fluorescence signals obtained by Optix to flat-panel VCT data illustrating anatomical sites, as described by Dullin *et al.* [21], might be useful for kinetic measurements of i.p. and orthotopically localized tumours in living animals.

Since it has been shown that radiochemotherapy enhances the cell surface density of Hsp70 selectively in tumours but not in normal tissues [9, 15], the Hsp70-specific antibody might serve as a tool for measuring the therapeutic outcome. Moreover, metastases in general exhibit elevated Hsp70 levels on their cell membranes, compared to primary tumours (unpublished data), and therefore might become detectable earlier by the use of cmHsp70.1 mAb.

Despite the IgG1 isotype of the cmHsp70.1 mAb, its capacity to induce ADCC against membrane Hsp70 tumour cells has been shown. Due to the rapid and tumour-selective uptake of the Hsp70 antibody, which is most likely mediated *via* a high turnover rate of membrane Hsp70 [27–29], it is conceivable that the anti-tumoral activity of cmHsp70.1 mAb can be further enhanced when applied as an antibody-drug or -radionuclide conjugate.

Acknowledgements

This work was supported in part by the multimmune GmbH (Munich, Germany), by grants of the Deutsche Forschungsgemeinschaft (DFG, MU1238 7/2; SFB-824/1), the Bundesministerium für Bildung und Forschung (BMBF-MOBITUM, grant no. 01EZ0826) and the European Union (EU-STEMDIAGNOSTICS, LSHB CT 2007 037703; EU-CARDIORISK, FP7–211403). We thank Prof. Stefan Höning (University of Cologne, Germany) for providing us with the LAMP antibodies for detecting lysosomes.

References

1. **Kampinga HH, Hagemann J, Vos MJ, *et al.*** Guidelines for the nomenclature of the human heat shock proteins. *Cell Stress Chaperones.* 2009; 14: 105–11.
2. **Ferrarini M, Heltai S, Zocchi MR, *et al.*** Unusual expression and localization of heat-shock proteins in human tumor cells. *Int J Cancer.* 1992; 51: 613–9.
3. **Shin BK, Wang H, Yim AM, *et al.*** Global profiling of the cell surface proteome of cancer cells uncovers an abundance of proteins with chaperone function. *J Biol Chem.* 2003; 278: 7607–16.
4. **Multhoff G, Botzler C, Wiesnet M, *et al.*** A stress-inducible 72-kDa heat-shock protein (HSP72) is expressed on the surface of human tumor cells, but not on

normal cells. *Int J Cancer.* 1995; 61: 272–9.

5. **Botzler C, Li G, Issels RD, *et al.*** Definition of extracellular localized epitopes of Hsp70 involved in an NK immune response. *Cell Stress Chaperones.* 1998; 3: 6–11.
6. **Multhoff G, Pfister K, Gehrmann M, *et al.*** A 14-mer Hsp70 peptide stimulates natural killer (NK) cell activity. *Cell Stress Chaperones.* 2001; 6: 337–44.
7. **Hantschel M, Pfister K, Jordan A, *et al.*** Hsp70 plasma membrane expression on primary tumor biopsy material and bone marrow of leukemic patients. *Cell Stress Chaperones.* 2000; 5: 438–42.
8. **Kleinjung T, Arndt O, Feldmann HJ, *et al.*** Heat shock protein 70 (Hsp70) membrane expression on head-and-neck cancer biopsy-a target for natural killer (NK) cells. *Int J Radiat Oncol Biol Phys.* 2003; 57: 820–6.
9. **Farkas B, Hantschel M, Magyarlaki M, *et al.*** Heat shock protein 70 membrane expression and melanoma-associated marker phenotype in primary and metastatic melanoma. *Melanoma Res.* 2003; 13: 147–52.
10. **Pfister K, Radons J, Busch R, *et al.*** Patient survival by Hsp70 membrane phenotype: association with different routes of metastasis. *Cancer.* 2007; 110: 926–35.
11. **Gehrmann M, Radons J, Molls M, *et al.*** The therapeutic implications of clinically applied modifiers of heat shock protein 70 (Hsp70) expression by tumor cells. *Cell Stress Chaperones.* 2008; 13: 1–10.
12. **Gehrmann M, Liebisch G, Schmitz G, *et al.*** Tumor-specific Hsp70 plasma membrane localization is enabled by the glycosphingolipid Gb3. *Plos One.* 2008. DOI: 10.1371/j.0001925.
13. **Falguieres T, Maak M, von Weyhern C, *et al.*** Human colorectal tumors and metastases express Gb3 and can be targeted by an intestinal pathogen-based delivery tool. *Mol Cancer Ther.* 2008; 7: 2498–508.
14. **Schilling D, Gehrmann M, Steinem C, *et al.*** Binding of Hsp70 to extracellular phosphatidylserine promotes killing of normoxic and hypoxic tumor cells. *FASEB J.* 2009; 23: 2467–77.
15. **Vega V, Rodriguez-Silva M, Frey T, *et al.*** Hsp70 translocates into the plasma membrane after stress and is released into the extracellular environment in a membrane-associated form that activates macrophages. *J Immunol.* 2008; 180: 4299–307.
16. **Arispe N, Doh M, Simakova O, *et al.*** Hsc70 and Hsp70 interact with phosphatidylserine on the surface of PC12 cells resulting in a decrease of viability. *FASEB J.* 2004; 18: 1636–45.
17. **Gehrmann M, Marienhagen J, Eichholtz-Wirth H, *et al.*** Dual function of membrane-bound heat shock protein 70 (Hsp70), Bag-4, and Hsp40: protection against radiation-induced effects and target structure for natural killer cells. *Cell Death Differ.* 2005; 12: 38–51.
18. **Dullin C, Zientkowska M, Napp J, *et al.*** Semiautomatic landmark-based two-dimensional-three-dimensional image fusion in living mice: correlation of near-infrared fluorescence imaging of Cy5.5-labelled antibodies with flat-panel volume computed tomography. *Mol Imaging.* 2009; 8: 2–14.
19. **Wang M, Bronte V, Chen PW, *et al.*** Active immunotherapy of cancer with a non-replicating recombinant fowlpox virus encoding a model tumor-associated antigen. *J Immunol.* 1995; 154: 4685–92.
20. **Kim KJ, Kanellopoulos-Langevin C, Merwin RM, *et al.*** Establishment and characterization of BALB/c lymphoma lines with B cell properties. *J Immunol.* 1979; 122: 549–54.
21. **Missbach-Guentner J, Dullin C, Kimmina S, *et al.*** Morphological changes of mammary carcinomas in mice over time as monitored by flat-panel detector volume computed tomography. *Neoplasia.* 2008; 10: 663–73.
22. **Zhang H, Liu R, Huang W.** A 14-mer peptide from HSP70 protein is the critical epitope which enhances NK activity against tumor cells *in vivo*. *Immunol Invest.* 2007; 36: 233–46.
23. **Broquet AH, Thomas G, Masliah J, *et al.*** Expression of the molecular chaperone Hsp70 in detergent resistant microdomains correlates with its membrane expression and release. *J Biol Chem.* 2003; 278: 21601–6.
24. **Staubach S, Razawi H, Hanisch FG.** Proteomics of MUC1-containing lipid rafts from plasma membranes and exosomes of human breast carcinoma cells MCF-7. *Proteomics.* 2009; 9: 2820–35.
25. **Gastpar R, Gehrmann M, Bausero M, *et al.*** Hsp70 surface-positive tumor exosomes stimulate migratory and cytolytic activity of NK cells. *Can Res.* 2005; 65: 5238–47.
26. **Stenmark H**. Rab GTPases as coordinators of vesicle traffic. *Nature Rev Mol Cell Biol.* 2009; 10: 513–25.
27. **Adams GP, Weiner LM.** Monoclonal antibody therapy of cancer. *Nat Biotechnol.* 2005; 23: 1147–57.
28. **Scallon BJ, Snyder LA, Anderson GM, *et al.*** A review of antibody therapeutics and antibody-related technologies for oncology. *J Immunother.* 2006; 29: 351–64.
29. **Bonner JA, Harari PM, Giralt J, *et al.*** Radiotherapy plus cetuximab for squamous-cell carcinoma of the head and neck. *N Engl J Med.* 2006; 354: 567–78.

Targeting membrane heat-shock protein 70 (Hsp70) on tumors by cmHsp70.1 antibody

Stefan Stangl[a,1], Mathias Gehrmann[a,1], Julia Riegger[a], Kristin Kuhs[a], Isabelle Riederer[a], Wolfgang Sievert[a], Kathrin Hube[a], Ralph Mocikat[b], Ralf Dressel[c], Elisabeth Kremmer[b], Alan G. Pockley[d], Lars Friedrich[e], Laszlo Vigh[f], Arne Skerra[e], and Gabriele Multhoff[a,2]

[a]Department of Radiation Oncology, Klinikum rechts der Isar, Technische Universität München, and Clinical Cooperation Group "Innate Immunity in Tumor Biology," [b]Institute of Molecular Immunology, Helmholtz-Zentrum München, Deutsches Forschungszentrum für Gesundheit und Umwelt, 81675 Munich, Germany; [c]Department of Cellular and Molecular Immunology, University of Göttingen, 37073 Göttingen, Germany; [d]Department of Oncology, The Medical School, University of Sheffield, Sheffield S10 2RX, United Kingdom; [e]Lehrstuhl für Biologische Chemie, Technische Universität München, 85354 Freising-Weihenstephan, Germany; and [f]Biological Research Centre, Institute of Biochemistry, Hungarian Academy of Sciences, 6701 Szeged, Hungary

Edited* by Eva Kondorosi, Institute for Plant Genomics, Human Biotechnology and Bioenergy, Szeged, Hungary, and approved December 6, 2010 (received for review October 31, 2010)

Immunization of mice with a 14-mer peptide TKDNNLLGRFELSG, termed "TKD," comprising amino acids 450–461 ($aa_{450–461}$) in the C terminus of inducible Hsp70, resulted in the generation of an IgG1 mouse mAb cmHsp70.1. The epitope recognized by cmHsp70.1 mAb, which has been confirmed to be located in the TKD sequence by SPOT analysis, is frequently detectable on the cell surface of human and mouse tumors, but not on isogenic cells and normal tissues, and membrane Hsp70 might thus serve as a tumor-specific target structure. As shown for human tumors, Hsp70 is associated with cholesterol-rich microdomains in the plasma membrane of mouse tumors. Herein, we show that the cmHsp70.1 mAb can selectively induce antibody-dependent cellular cytotoxicity (ADCC) of membrane Hsp70$^+$ mouse tumor cells by unstimulated mouse spleen cells. Tumor killing could be further enhanced by activating the effector cells with TKD and IL-2. Three consecutive injections of the cmHsp70.1 mAb into mice bearing CT26 tumors significantly inhibited tumor growth and enhanced the overall survival. These effects were associated with infiltrations of NK cells, macrophages, and granulocytes. The Hsp70 specificity of the ADCC response was confirmed by preventing the antitumor response in tumor-bearing mice by coinjecting the cognate TKD peptide with the cmHsp70.1 mAb, and by blocking the binding of cmHsp70.1 mAb to CT26 tumor cells using either TKD peptide or the C-terminal substrate-binding domain of Hsp70.

immunotherapy | syngeneic tumor model | tumor antibody dependent cellular cytotoxicity | epitope mapping | surface antigen

Although the combination of mAbs with standard therapies plays a pivotal role in the treatment of cancer (1–4), the therapeutic success of this strategy is restricted by the availability of tumor-specific antibodies. Global profiling of the surface proteome of human tumors has revealed an abundancy of stress proteins in the plasma membrane (5, 6). Herein, we describe the generation of a mouse mAb directed against a 14-mer peptide TKDNNLLGRFELSG (TKD) of the major stress-inducible heat-shock protein 70 (Hsp70, Hsp70-1, Hsp72, HspA1A #3303), which is present on the cell surface of human tumor cell lines (7). Screening of a large number of primary human tumor biopsies and the corresponding normal tissues has indicated that carcinomas, but none of the tested normal tissues, frequently present Hsp70 on their cell surface (8, 9). Moreover, a membrane Hsp70$^+$ tumor phenotype has been found to be associated with a significantly decreased overall survival in patients with lower rectal and lung carcinomas. The expression of this molecule might therefore serve as a negative prognostic marker (9) in these patient groups. It has been hypothesized that membrane Hsp70 might support the spread of distant metastasis or might confer resistance to standard therapies (10).

The TKD sequence, which is exposed to the extracellular milieu of tumors, resides in the C-terminally localized oligomerization domain of the Hsp70 molecule (11). Furthermore, this TKD peptide in combination with low-dose IL-2 has been found to stimulate the migratory and cytolytic activity of NK cells against membrane Hsp70$^+$ tumor cells (12). In contrast to other commercially available Hsp70 antibodies, the cmHsp70.1 mAb uniquely identifies the membrane form of Hsp70 on viable tumor cells with an intact plasma membrane in vitro.

We have recently shown that the cmHsp70.1 mAb also binds to the CT26 mouse colon tumor cells in vivo (13). Herein, we demonstrate that consecutive injections of the cmHsp70.1 mAb into mice bearing CT26 tumors can significantly reduce the mass of membrane Hsp70$^+$ tumors and increase overall survival during therapy via the induction of antibody-dependent cellular cytotoxicity (ADCC). The in vitro ADCC activity could be further enhanced by using TKD/IL-2–activated NK cells as effector cells instead of unstimulated mouse spleen cells. These findings suggest that membrane Hsp70 could serve as a unique immunotherapeutic target for a broad spectrum of different tumor entities.

Results

Monoclonal Antibody cmHsp70.1 Binds to Membrane Hsp70$^+$ Human and Mouse Tumors. The epitope of the cmHsp70.1 mAb, which was generated by immunizing mice with the 14-mer peptide TKD, was confirmed by SPOT analysis and peptide blocking studies (Fig. S1). Viable human tumor cell lines, such as colon (CX2), breast (MDA436, MCF-7), and lung (A549) carcinomas and malignant melanomas (Malme, Mel Ei, Mel Ho, Parl, A375, Sk Mel29) bind cmHsp70.1 mAb, but not the Hsp70-specific SPA810 mAb (Fig. 1*A*). The cmHsp70.1 mAb also stains immortalized endothelial cells (EA.hy926, HMEC), but not their nontransformed, isogenic counterparts (primary ECs) (Fig. 1*B*, *Upper* two panels). Similar to the human tumor cell lines, single-cell suspensions of primary human gastrointestinal and pancreatic tumor samples (n = 229) also frequently (more than 40% of all tested tumor cases) bind cmHsp70.1 mAb, whereas the corresponding reference tissues are always membrane Hsp70$^-$.

With respect to mouse tumors, the cmHsp70.1 mAb binds to CT26 colon (61%) (Fig. 1 *C* and *D*) and highly malignant B16F10 mouse melanoma cells (74%) (Fig. 1*B*, *Lower Right*), whereas only a minor population of the isogenic, low-malignant counterpart B16F0 (14%) (Fig. 1*B*, *Lower Left*), 1048 pancreatic carci-

Author contributions: G.M. designed research; S.S., M.G., J.R., K.K., I.R., W.S., K.H., R.M., R.D., E.K., A.G.P., and L.F. performed research; E.K., L.V., and A.S. contributed new reagents/analytic tools; S.S., M.G., I.R., W.S., R.D., E.K., A.G.P., L.V., A.S., and G.M. analyzed data; and G.M. wrote the paper.

The authors declare no conflict of interest.

*This Direct Submission article had a prearranged editor.

Freely available online through the PNAS open access option.

[1]S.S. and M.G. contributed equally to this work.

[2]To whom correspondence should be addressed. E-mail: gabriele.multhoff@lrz.tu-muenchen.de.

This article contains supporting information online at www.pnas.org/lookup/suppl/doi:10.1073/pnas.1016065108/-/DCSupplemental.

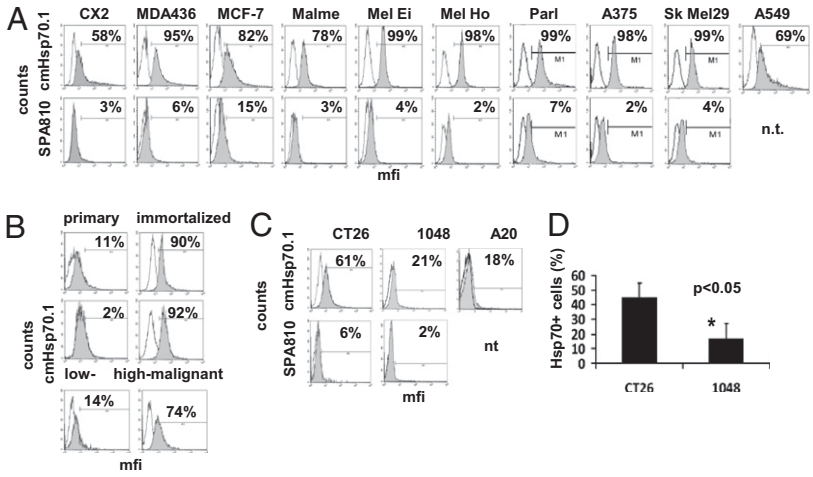

Fig. 1. Representative flow cytometric histograms of membrane Hsp70 expression on human and mouse tumor cell lines. (*A*) Human CX2 (colon), MDA436 (breast), MCF-7 (breast), Malme, Mel Ei, Mel Ho, Parl, A375, Sk Mel29 (all malignant melanomas), A549 (lung) carcinoma, (*B*) primary and immortalized endothelial cells, and (*C*) mouse CT26 (colon), 1048 (pancreas), A20 (B lymphoma), B16F0 (low-malignant melanoma), and (*B*) B16F10 (high-malignant, metastatic melanoma), tumor cell lines were analyzed by flow cytometry using either cmHsp70.1-FITC (*Upper*) or SPA810-FITC (*Lower*) mAb. Results are expressed as log green fluorescence intensity vs. relative cell numbers. The IgG1 isotype-matched control is indicated in white and membrane Hsp70 staining in gray histograms. The whole staining procedure was performed at 4 °C and only viable, 7-AAD$^-$ cells were gated upon and analyzed. (*B*) Comparison of the membrane Hsp70 expression in isogenic human and mouse cells. Human primary endothelial cells (ECs, *Top* and *Middle*) were compared with their corresponding immortalized partner cell lines EA.hy926, a fusion product of human umbilical vein ECs (HUVEC) with A549 lung carcinoma cells, and HMEC, which was derived by a transfection of primary ECs with SV40 large T antigen, were stained with cmHsp70.1 mAb, as described above. Furthermore, the low-malignant mouse melanoma cell line B16F0 (*Left*) was compared with the high-malignant, metastatic tumor cell line B16F10. The IgG1 isotype-matched control is indicated in white and membrane Hsp70 staining using cmHsp70.1 mAb in gray histograms. (*D*) The flow cytometric analysis of CT26 and 1048 tumor cell lines using cmHsp70.1-FITC mAb was repeated six times. The differences in membrane Hsp70 positivity in CT26 and 1048 tumor cell lines was significant (*$P < 0.05$).

noma (21%) (Fig. 1 *C* and *D*), and A20 B-lymphoma cells (18%) (Fig. 1*C*) are membrane Hsp70$^+$. The staining of cytosolic Hsp70 was excluded in all experiments, as only viable, 7-AAD$^-$ tumor cells with intact plasma membranes were gated and analyzed.

Monoclonal Antibody cmHsp70.1 Initiates ADCC in Membrane Hsp70$^+$ Tumors in Vitro. Measurements using fluorescence-conjugated marker beads revealed that ≈10,000 Hsp70 molecules are present on the plasma membrane of CT26 mouse tumor cells (13). Despite this relatively low surface density, 50 μg/mL cmHsp70.1 mAb could induce significant ADCC-mediated killing of CT26 carcinoma cells by unstimulated mouse spleen effector cells at E:T ratios ranging from 50:1 to 6.25:1 (Fig. 2*A*) ($P < 0.05$). The 1048 carcinoma cells that contained only a small proportion of Hsp70$^+$ cells were not sensitive to ADCC (Fig. 2*A*). As a control, the capacity of other mouse IgG1 antibodies (SPA810, Ox7.11) and the cmHsp70.1 Fab fragment to induce ADCC was assessed and compared with that of cmHsp70.1 mAb. As shown in Fig. 2*B*, neither SPA810 mAb nor cmHsp70.1 Fab induced any significant ADCC against membrane Hsp70$^+$ CT26 tumor cells. Similar negative findings were obtained if mouse BW cells (hybrid cross between New Zealand Black and White mice) transfected with theta (56% membrane theta$^+$ cells) were used as target cells for ADCC (Fig. 2*C*). In the same experiment, cmHsp70.1 mAb induces significant ADCC in CT26 colon adenocarcinoma cells (60% membrane Hsp70$^+$ cells) (Fig. 2*C*).

To determine whether preactivating mouse spleen cells with TKD (2 μg/mL) plus IL-2 (100 IU/mL) improves the killing of membrane Hsp70$^+$ CT26 cells in vitro, ADCC experiments were repeated using unstimulated and preactivated effector cells. The stimulation of mouse spleen cells with TKD/IL-2 significantly increased the proportion of CD49b$^+$ NK cells and CD25$^+$ cells (Table 1) ($P < 0.05$) and the lysis of CT26 cells (Fig. 2*D*) ($P < 0.01$). An element of this increase in cytolysis could be explained by a direct killing of membrane Hsp70$^+$ tumor cells by TKD/IL-2–activated NK cells (12), as it was apparent in the absence of the

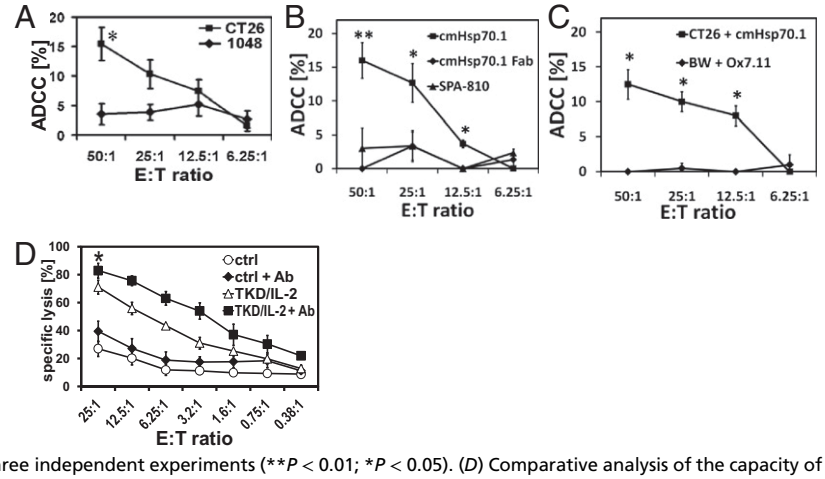

Fig. 2. Comparative analysis of ADCC using different IgG1 mAbs and cmHsp70.1 Fab fragment. (*A*) In vitro ADCC of membrane Hsp70$^+$ mouse CT26 colon (60%, filled squares) and membrane Hsp70$^-$ 1048 pancreatic carcinoma cells (filled diamonds), using 50 μg/mL Hsp70.1 mAb and unstimulated mouse spleen cells at E:T ratios ranging from 50:1 to 6.25:1. (*B*) In comparison with cmHsp70.1 mAb (filled squares), no significant ADCC was induced in mouse CT26 colon carcinoma cells (61% cmHsp70.1$^+$) using the non-binding IgG1 mAb SPA810 (filled circles) or cmHsp70.1 Fab fragment (filled triangles). (*C*) The IgG1 Ox7.11 mAb, which detects the theta antigen on 56% of the BW mouse tumor cells, does not induce ADCC in BW mouse tumor cells (filled triangles). Specific ADCC was measured using 50 μg/mL antibody or Fab fragment, respectively; unstimulated mouse spleen cells at E:T ratios ranging from 50:1 to 6.25:1 were used as effector cells. Specific lysis mediated by the direct cytotoxic effect of NK cells in the absence of cmHsp70.1 mAb was subtracted. The phenotypes of the effector cells are summarized in Table 2. Data are means ± SE of at least three independent experiments (**$P < 0.01$; *$P < 0.05$). (*D*) Comparative analysis of the capacity of unstimulated (ctrl, open circles; ctrl+Ab, filled diamonds) and TKD (2 μg/mL) plus IL-2 (100 IU/mL) preactivated (TKD/IL-2, open triangles; TKD/IL-2+Ab, closed squares) mouse spleen cells to kill CT26 carcinoma cells. The ADCC experiment was performed either in the absence (open symbols) and presence (+Ab; closed symbols) of 50 μg/mL cmHsp70.1 mAb. Lysis is mediated by ADCC in the presence of cmHsp70.1 mAb and by a direct cytotoxic effect of mouse NK cells in the absence of mAb, at E:T ratios ranging from 25:1 to 0.38:1. Data are means ± SE of at least three independent experiments. Lysis of activated effector cells in the absence and presence of cmHsp70.1 mAb was significantly different (*$P < 0.05$, all E:T ratios). ADCC was calculated using the formula: percent of specific lysis = (experimental release − spontaneous release)/(maxiumum release − spontaneous release) × 100.

Table 1. Proportion (%) of marker-positive cells in unstimulated and TKD/IL-2 preactivated mouse spleen cells

Antigen	Proportion of antigen-positive cells (%)	
	Unstimulated	TKD/IL-2–stimulated
CD8 (T cells)	11.2 ± 1.3	13.8 ± 3.4
CD4 (T cells)	21.1 ± 0.9	15.4 ± 5.9
CD205 (granulocytes)	6.4 ± 3.3	12.0 ± 5.4
CD11c (APC)	6.4 ± 3.2	8.4 ± 5.5
Ly6G/Ly6C (Gr-1)	8.7 ± 4.7	7.5 ± 3.0
B220 (B cells)	62.9 ± 5.4	61.0 ± 5.3
CD11b (APC)	14.6 ± 2.9	18.2 ± 4.9
CD49b (NK cells)	12.8 ± 4.7	22.5 ± 4.0*
CD25 (activation marker)	6.9 ± 4.7	9.7 ± 7.1*

*$P < 0.05$, corrected for multiple testing.

cmHsp70.1 mAb (Fig. 2*D*). However, the presence of cmHsp70.1 mAb further enhanced the cytolytic activity of unstimulated and TKD/IL-2–stimulated mouse spleen cells against membrane Hsp70$^+$ CT26 cells. The differences in the killing of CT26 tumor cells by TKD/IL-2–activated mouse spleen cells in the presence and absence of cmHsp70.1 mAb can be viewed in a movie which illustrates two major findings: the targeted migration of effector cells toward membrane Hsp70$^+$ tumor cells, which is enhanced in the presence of the cmHsp70.1 mAb and the concerted attack of tumor cells by effector cells (Movie S1).

ADCC in Tumor-Bearing Mice. An intraperitoneal injection of 2.5×10^4 CT26 mouse colon tumor cells suspended in 100 μL PBS resulted in rapidly growing tumors with a tumor take of 100%. A comparative phenotyping of cultured CT26 and single-cell suspensions derived from CT26 tumor-bearing mice on day 14 revealed the proportion of membrane Hsp70$^+$ cells to be significantly greater in the latter (46.2 ± 9%, $n = 6$ vs. 69.8 ± 14%, $n = 7$; $P < 0.05$).

Based on our observation that the cmHsp70.1 mAb initiates ADCC in membrane Hsp70$^+$ CT26 cells in vitro, the capacity of this antibody to induce tumor killing in CT26 tumor-bearing mice was evaluated. The tumor weights in mice that received two and three consecutive intravenous injections of cmHsp70.1 mAb (20 μg per injection) on days 3, 5, and 7 were significantly lower than those in mice receiving an isotype-matched control antibody (1.7 ± 0.63 g vs. 0.59 ± 0.32 g and 0.44 ± 0.29 g, respectively, $P < 0.05$) (Fig. 3*A*).

Immunohistochemical studies of consecutive CT26 tumor sections following one to three injections of cmHsp70.1 mAb revealed a dramatic increase in F4/80$^+$ macrophages and Ly6G/Ly6C$^+$ granulocytes, and a moderate increase in Ly49b$^+$ CD56$^+$ NK cells within the tumor (Fig. 3*B* and Table 2). CD3$^+$ T cells began to infiltrate tumor tissue from day 21 onwards (Table 2).

Growth curves of CT26 tumors after subcutaneous injection of 1×10^6 cells after one and three intravenous injections of cmHsp70.1 mAb (20 μg per injection) on days 4, 7, and 10 revealed that three repeated injections of cmHsp70.1 mAb resulted in a significant growth delay (Fig. 3*C*) ($P < 0.05$), which correlated with an increased overall survival (Fig. 3*D*) ($P < 0.05$). In line with these findings, overall survival was also greater in mice with intraperitoneal CT26 tumors (Fig. 4*A*, filled squares) ($n = 24$, $P < 0.0001$) than their IgG1 isotype-matched control antibody treated counterparts (Fig. 4*A*, open circles) ($n = 14$). In contrast, an identical treatment regimen had no significant effect ($P = 0.310$) on the survival of mice bearing A20 B-cell lymphomas, which lack membrane Hsp70 expression (Fig. 4*B*). Furthermore, the decrease in tumor weight after three intravenous injections of cmHsp70.1 mAb was associated with a significant increase in serum levels of Hsp70 on day 14 (154 ± 41.7 pg/mL vs. 1,434.5 ± 786 pg/mL, $n = 4$, $P < 0.01$), as measured by ELISA.

TKD Peptide Is the Target for ADCC. Coinjection of cmHsp70.1 mAb (20 μg per injection) with an excess of Hsp70 peptide TKD (50 μg per injection) into CT26 tumor-bearing mice (intraperitoneally) on days 3, 5, and 7 completely reversed the antitumoral effect of the antibody therapy ($P < 0.02$) (Fig. 5*A*). This finding indicated that the TKD peptide, which contains the epitope of the cmHsp70.1 mAb, competes with membrane Hsp70 on the cell surface of mouse tumors for binding in vivo.

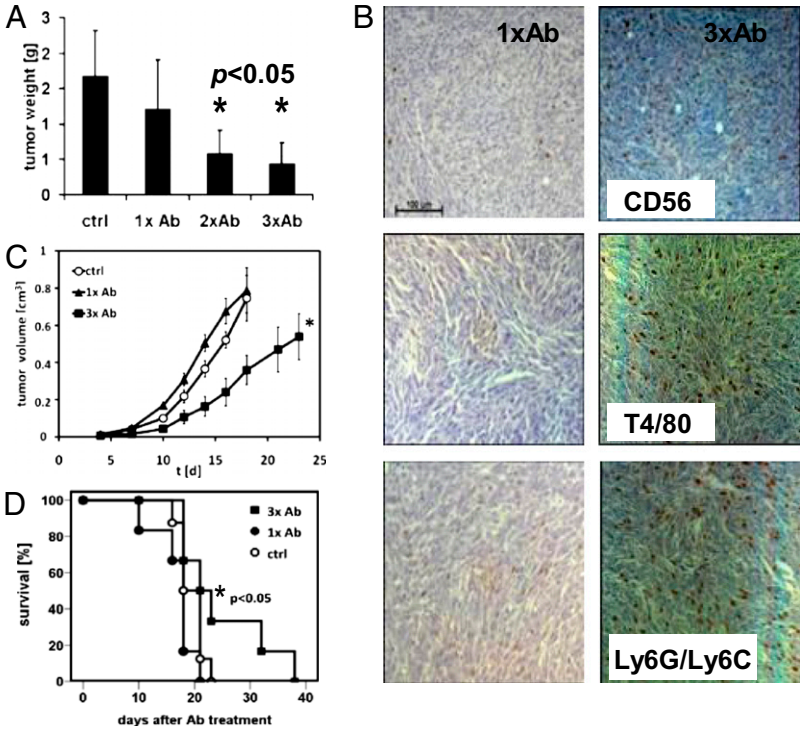

Fig. 3. Reduction in tumor weight and the delay of CT26 tumor growth in BALB/c mice after one to three injections of cmHsp70.1 mAb is associated with an infiltration of immunocompetent effector cells. (*A*) Two and three consecutive injections of cmHsp70.1 mAb (intravenously) result in a significant reduction in tumor weight (*$P < 0.05$). The cmHsp70.1 mAb (20 μg per injection) was injected intravenously on days 3, 5, and 7 following intraperitoneal injection of 2.5×10^4 CT26 tumor cells. Mice were killed on day 14 and tumor weights were determined. Data are means of six to nine animals (*$P < 0.05$). (*B*) Representative photomicrographs of CT26 tumor sections after one (1 × Ab; *Left*) and three consecutive injections of cmHsp70.1 mAb (3 × Ab; *Right*) on days 3, 5, and 7 (20 μg per injection). Infiltration of NK cells (CD56; *Top*), monocytes (T4/80; *Middle*) and granulocytes (Ly6G/Ly6C; *Bottom*) was determined on consecutive sections of CT26 tumors derived from mice on day 14. Semiquantitative data are summarized in Table 2. (Scale bar, 100 μm.) (*C*) Three (filled square) but not one (filled triangle) injections of cmHsp70.1 mAb (i.v.) result in a significant growth delay of subcutaneously injected CT26 tumors (*$P < 0.05$). The cmHsp70.1 mAb (20 μg per injection) was injected intravenously on days 4, 7, and 10 following subcutaneous injection of 1×10^6 CT26 tumor cells. Tumor weight was measured in each mouse every second day after the last antibody injection (*$P < 0.05$ for all time points from day 10 onwards). (*D*) Control mice (open circles) and mice that were injected only once with mAb cmHsp70.1 (filled circles, day 5) became moribund from day 18 onwards, whereas mice that were injected three times (filled squares, day 4, 7, 10) with cmHsp70.1 mAb showed a significant increase in overall survival (*$P < 0.05$). Each datapoint represents measurements of six to nine mice.

Table 2. Semiquantitative analyses of the lymphocytic and granulocytic infiltration of CT26 tumors after one to three injections of the cmHsp70.1 mAb

Marker	Treatment with cmHsp70.1 mAb			
	Ctrl	1×	2×	3×
CD3ε (T cells)	—	—	—	+
Ly49b/CD56 (NK cells)	+	+	++	+++
F4/80 (macrophages)	++	++	++	+++
Ly6G/Ly6C (Gr-1) (granulocytes/macrophages)	+	++	++	+++

BALB/c mice were injected (intraperitoneally) with CT26 tumor cells (2.5×10^4) on day 0 and injected with cmHsp70.1 mAb (20 μg per injection) on days 3, 5, and 7. Mice were killed on day 21 and at least six consecutive tumor sections (5 μm) were examined immunohistochemically using antibodies directed against T cells (CD3ε), NK cells (Ly49b), monocytes (F4/80), and granulocytes (Ly6G/Ly6C). The results indicate the number of infiltrating cells within a defined tumor section of 1 cm^2; —, no infiltration (<10); +, weak infiltration (10–50); ++, intermediate infiltration (50–200); +++, strong infiltration (<200). Representative images of consecutive tumor sections stained with Ly49, CD56, F4/80, and Ly6G/Ly6C antibodies are illustrated in Fig. 3*B*.

The specificity of the interactions was further confirmed by determining whether the binding of cmHsp70.1 mAb to the cell surface of cultured CT26 tumor cells could be blocked by the TKD peptide, which represents the immunogen (Fig. S1), but not by a 14-mer scrambled NGL(NGLTLKNDFSRLEG) peptide consisting of the same amino acid residues in a different order. The proportion of membrane $Hsp70^+$ cells decreased in a concentration-dependent manner from 59% (white graph) to 44% (gray graph; 12.5 μg/mL) and from 60% (white graph) to less than 15% (gray graph; 25 μg/mL) (Fig. 5*B*). In contrast, no inhibition in binding was apparent when the same concentrations of NGL peptide were used for the blocking experiments (Fig. 5*B*, *Right*). As a control, the binding of cmHsp70.1 mAb to CT26 cells was also significantly inhibited using the C-terminal substrate binding domain of Hsp70 ($P < 0.05$) (Fig. 5*C*). All blocking studies were performed at 4 °C because of the rapid internalization of cmHsp70.1 mAb at higher temperatures (13).

Discussion

Hsp70 mediates the stability of tumor cells following environmental stress (14, 15), and it is commonly regarded as an intracellular molecule. However, it is now apparent that a membrane

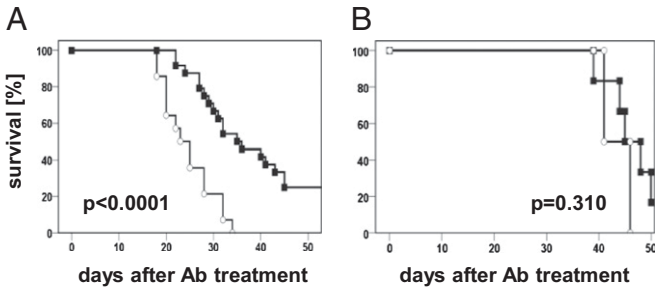

Fig. 4. (*A*) Kaplan-Meyer curves of overall survival of mice treated with an isotype-matched control antibody or cmHsp70.1 mAb on days 3, 5, and 7 after intraperitoneal injection of 2.5×10^4 CT26 tumor cells (20 μg per injection). The overall survival of mice (3 × Ab cmHsp70.1, filled squares; $n = 24$) treated with cmHsp70.1 mAb was significantly higher than that of animals (ctrl, open circles; $n = 14$) that received the IgG1 isotype-matched control antibody ($P < 0.0001$). (*B*) In contrast, the cmHsp70.1-mAb treatment (3 × Ab cmHsp70.1, filled squares) had no significant effect on the survival of mice bearing membrane $Hsp70^-$ A20 lymphomas ($n = 12$) compared with mice receiving the IgG1 isotype-matched control antibody (ctrl, open circles; $n = 4$, $P = 0.310$).

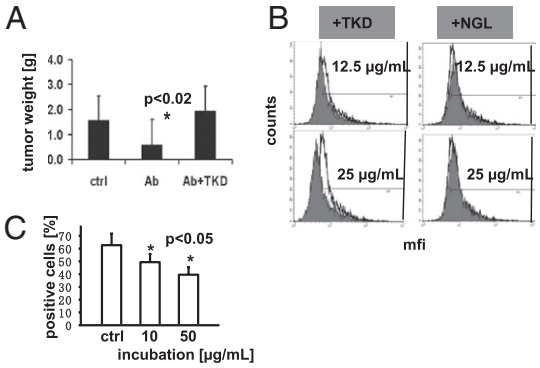

Fig. 5. (*A*) Coinjection of an excess of the Hsp70 peptide TKD with the cmHsp70.1 mAb completely inhibits the significant antitumoral effect of the latter (*$P < 0.02$). The cmHsp70.1 mAb (20 μg per injection) was coinjected intravenously on days 3, 5, and 7 together with 50 μg TKD following intraperitoneal injection of 2.5×10^4 CT26 tumor cells; media, $n = 21$; Ab, $n = 22$; Ab+TKD, $n = 21$. Mice were killed on day 14 and tumor weights were determined. (*B*) Binding of cmHsp70.1-FITC mAb to CT26 tumor cells was inhibited by the coincubation with an excess of TKD peptide. As a control, the scrambled NGL peptide was used. Tumor cells were coincubated either with cmHsp70.1-FITC mAb (5 μg/mL; white histogram) or with cmHsp70.1-FITC mAb (5 μg/mL) plus TKD (gray histogram; *Left*) or NGL peptide (gray histogram; *Right*) at concentrations of 12.5 and 25 μg/mL, respectively. The data illustrate one representative experiment out of three independent experiments, all of which show similar results. (*C*) Binding of cmHsp70.1-FITC to CT26 tumor cells was inhibited significantly (*$P < 0.05$) by the coincubation with the C-terminal substrate-binding domain of Hsp70 in a concentration dependent manner (10 and 50 μg/mL).

form of Hsp70 is frequently expressed on a broad variety of human tumors, but not on the corresponding normal tissues. This membrane expression can be specifically detected using the cmHsp70.1 mAb, which has been generated using the human 14-mer TKD sequence as an immunogen. Because the human and murine TKD sequences only differ in one amino acid (16) (human T**K**DNNLLGRFELSG; mouse T**R**DNNLLGRFELSG), we also screened mouse tumor cell lines for their capacity to express the membrane form of Hsp70. Similar to human tumors (7, 8), the mouse colon tumor cell line CT26 (17) was also membrane $Hsp70^+$. The depletion of cholesterol from the plasma membrane reduced the membrane density of Hsp70 on CT26 mouse colon tumor cells (Fig. S2), whereas changes in the salt concentration or the pH—indicative of receptor-mediated associations—had no effect. These data demonstrate that the membrane form of Hsp70 in mice also appears to be located in cholesterol-rich microdomains (18, 19). Although the cmHsp70.1 mAb can specifically detect membrane Hsp70 expression on viable tumor cells, other commercially available Hsp70-specific antibodies cannot.

We have previously reported that a membrane $Hsp70^+$ phenotype serves as a negative prognostic marker for patients with lower rectal and lung carcinomas (9). Herein, we have demonstrated that immortalized, oncogenic-transformed and highly metastatic tumors, but not their primary counterparts and low-malignant cells, present Hsp70 on their cell surface. The study therefore assessed the capacity of membrane Hsp70 to act as a tumor-specific target for antibody-mediated killing of highly aggressive tumors using a syngeneic CT26 mouse-colon tumor model. Despite the relatively low density of Hsp70 molecules that are presented on the cell surface of CT26 mouse tumor cells (≈10,000 per cell), and that IgG1 has a low capacity to induce ADCC (20) and complement-dependent cytotoxicity (21) in mice, the cmHsp70.1 mAb mediates specific killing in membrane $Hsp70^+$ CT26 tumors. In contrast, other IgG1 control antibodies directed against theta or the Fab fragment of cmHsp70.1 mAb had no such effect. Furthermore, binding of cmHsp70.1 mAb to membrane $Hsp70^+$ tumors did not enhance the intracellular Hsp70 levels

(Fig. S2), and thus a cmHsp70.1 mAb-based therapy is not likely to enhance protection of tumors against Hsp70-mediated apoptosis.

We have previously demonstrated that the incubation of lymphocytes with Hsp70 peptide TKD in the presence of low-dose IL-2 results in an enhanced cytolytic and migratory capacity of NK cells toward membrane Hsp70$^+$ tumor cells in vitro and in vivo (12, 22). The direct cytolytic effects of TKD/IL-2–activated NK cells against membrane Hsp70$^+$ mouse tumors were clearly detectable in the current study, as has previously been described for human tumors (12, 23, 24). In a clinical phase I trial, the tolerability, feasibility and safety of adoptively transferred, autologous TKD/IL-2–activated NK cells has been shown in patients having colorectal and lung carcinomas (23). Here, we show that the in vitro cytotoxic effects of TKD/IL-2–activated NK cells against membrane Hsp70$^+$ tumor cells can be further improved by the addition of cmHsp70.1 mAb. This process is most likely mediated by ADCC. The cmHsp70.1 mAb-induced killing of membrane Hsp70 CT26 tumor cells involves an enhanced migratory capacity of effector cells and a direct cytotoxic attack.

Three intravenous injections of relatively low amounts of unconjugated cmHsp70.1 mAb into tumor-bearing mice induced an infiltration of innate immune cells and significantly reduced the growth of CT26 tumors. The finding that the membrane Hsp70-positivity of CT26 tumors derived from mice autopsies was greater than that of in vitro cultured CT26 cells might explain the cmHsp70.1 mAb-mediated ADCC effect.

We have also previously reported that membrane Hsp70$^+$ tumors actively release Hsp70 surface-positive lipid vesicles (25), which have the biophysical characteristics of exosomes (26, 27) and that these can attract activated, but not resting NK cells. The current study found a significant increase in circulating Hsp70 in those mice in which tumor growth was inhibited. Whether this serum Hsp70 originates from exosomes or from necrotic tumor material has not yet been elucidated. Furthermore, ongoing studies are evaluating whether the administration of low-dose IL-2 into tumor-bearing mice might further improve the antitumoral effect of cmHsp70.1 mAb via the in vivo activation of mouse NK cells.

Remarkably, three consecutive intravenous injections of relatively low amounts of cmHsp70.1 mAb not only delayed the growth of subcutaneous- and intraperitoneal-residing CT26 tumors, but also significantly prolonged the survival of the mice. The Hsp70-specificity of this approach is supported by the finding that cmHsp70.1 mAb had no effect on tumor growth or the survival of mice bearing membrane Hsp70$^-$ A20 B-cell lymphomas. Moreover, coincubating membrane Hsp70$^+$ tumors with an excess of TKD peptide or the C-terminal substrate-binding domain and cmHsp70.1 mAb blocked the antibody binding in vitro, and TKD peptide also completely reversed the antitumoral effect in vivo. These data confirm that the TKD peptide sequence represents the recognition site of cmHsp70.1 mAb (Fig. S1).

As radiochemotherapy has been shown to enhance the cell-surface density of Hsp70 on tumors (10, 28–30), we speculate that a combined approach consisting of an Hsp70 mAb-based immunotherapy, which involves activated NK cells, as has been shown for a Her2-targeted ADCC (31), might provide a previously unexplored strategy to improve the clinical outcome of patients undergoing standard radiochemotherapy or with distant metastases. This proposition is in line with the observation that a metastasis-free survival rate of patients can be associated with an enhanced NK cell activity (32). The clinical relevance of our data are further supported by published observations on the ADCC activity of trastuzumab in metastatic breast cancer patients (33). In this study, the in vitro ADCC activity toward Her2 overexpressing tumor cells, which was quantitatively comparable to that which was seen against Hsp70 membrane-positive tumor cells in the current study, could be correlated to the short-term antitumor responses in trastuzumab-treated breast cancer patients (33).

Materials and Methods

Human Tumor Cell Lines, Mouse Tumor Cell Lines, and Primary Cells. Human tumor cell lines: CX2 (colon), MCF-7, MDA436 (breast), and A549 (lung) carcinoma cell lines (Tumorbank Deutsches Krebsforschungszentrum, Heidelberg, Germany), Malme, Mel Ei, Mel Ho, Parl, A375 and Sk Mel29 malignant melanomas (J. Johnson, Institute of Immunology, Ludwig-Maximilians-Universität Munich, Germany) (34). Mouse tumor cell lines: CT26 (colon, CT26.WT; ADCC CRL-2638, BALB/c) (17), 1048 (pancreatic), A20 (B-cell lymphoma, BALB/c) (35), B16F0 (low malignant, C57BL/6), B16F10 (high malignant, C57BL/6), BW transfected with the theta antigen (E. Kremmer, Helmholtz-Zentrum München, Munich, Germany). Cells were cultured in RPMI 1640 or DMEM supplemented with 10% (vol/vol) heat-inactivated FCS, 2 mM L-glutamine, 1 mM sodium-pyruvate and antibiotics (100 IU/mL penicillin, 100 μg/mL streptomycin) at 37 °C in 5% (vol/vol) CO_2. Single-cell suspensions were derived by short-term (less than 1 min) treatment with 0.25% (wt/vol) Trypsin-0.53 mM EDTA.

Primary macrovascular HUVECs and their isogenic EC counterparts EA.hy.926, which results from a fusion of HUVECs with the epithelial lung-carcinoma cell line A549, and HMEC, which were obtained by a transfection of primary microvascular ECs with the coding region for the simian virus 40A gene product (SV40) large T antigen, were cultured in ECGM medium supplemented with Supplement Mix (Sigma Aldrich). Cell-culture reagents were purchased from Life Technologies and Sigma Aldrich.

Tumor specimens and corresponding normal tissues were obtained from patients at the University Regensburg, Germany between February 2002 and January 2004. Fresh biopsy material was washed in antibiotic (penicillin/streptomycin) containing DMEM and single-cell suspensions were prepared by mincing the tissue and forcing it through a sterile mesh. The corresponding normal tissue was derived from the same patients at a distance of at least 0.2 cm from the tumor. The study was approved by the Institutional Review Board of the Medical Faculty of the University Hospital Regensburg, Germany and all patients included in the study provided signed informed consent.

Flow Cytometry and Blocking of Binding. The membrane Hsp70 phenotype on tumor cells was determined by flow cytometry using either the FITC-conjugated cmHsp70.1 mAb (IgG1; Multimmune GmbH), which is directed against the extracellular exposed sequence of membrane Hsp70 or the SPA810 mAb (IgG1; Stressgen via Assay Designs). Briefly, after incubation of viable cells (0.2×10^6 cells) with the primary antibodies for 30 min at 4 °C and following two washing steps, 7-AAD$^-$ viable cells were analyzed using a FACSCalibur flow cytometer (BD Biosciences). An isotype-matched (IgG1) control antibody was used to determine nonspecific binding to cells. Blocking of the antibody binding was performed by coincubating viable tumor cells (0.2×10^6 cells) using cmHsp70.1-FITC mAb (5 μg/mL) and an excess of TKD or scrambled NGL peptide (12.5 and 25 μg/mL) or the C-terminal substrate binding domain of Hsp70 (aa 383–548, 10 and 50 μg/mL).

The proportion of lymphocyte subpopulations, monocytes, granulocytes, and their expression of the activation marker CD25 (α chain of the IL-2 receptor) was determined using FITC/PE-labeled mAb directed against CD4, CD8, CD205, CD11c, Ly6G/Ly6C (Gr-1), B220, CD11b, CD49b, CD56 and CD25 (BD Biosciences).

Animals. BALB/c mice were obtained from an animal breeding colony (Harlan Winkelmann) and maintained in pathogen-free, individually ventilated cages (Tecniplast). Animals were fed with sterilized, laboratory rodent diet (Meika) and were used for experiments between 6 and 12 wk of age. All animal experiments were approved by the "Regierung von Oberbayern" and were performed in accordance with institutional guidelines of the Klinikum rechts der Isar, Technische Universität München.

Stimulation of Mouse Spleen Cells for ADCC. Freshly isolated BALB/c mouse spleen cells (5×10^6 cells/mL) were cultured in RPMI medium 1640 containing 10% (vol/vol) FCS alone (unstimulated) or medium containing low-dose IL-2 (100 IU/mL) plus TKD peptide (2 μg/mL) (Bachem) at 37 °C for 4 d. TKD is a GMP-grade 14-mer peptide of the C-terminal substrate binding domain of human Hsp70 (TKDNNLLGRFELSG, $aa_{450–463}$), which is known to selectively induce the reactivity of human NK cells against membrane Hsp70$^+$ tumor cells (12). The TKD equivalent region in the mouse (TRDNNLLGRFELSG) exhibits only one conservative amino acid exchange at position 2 (K-R) and this sequence stimulates mouse NK cells, even in the absence of IL-2 (16).

ADCC and Blocking Assays. ADCC was measured using a standard 4 h ^{51}Cr-release assay (36, 37). For blocking, labeled target cells were preincubated with the cmHsp70.1 mAb, the IgG1 isotype-matched control mAbs, SPA810 mAb, the theta-specific Ox7.11 (50 μg/mL, each), or the cmHsp70.1 Fab fragment (50 μg/mL). The degree of ADCC-dependent cytotoxicity was calculated, from which the lysis mediated by NK cells in the absence of cmHsp70.1 mAb/isotype control was subtracted. The spontaneous release for each target cell ranged

between 10 and 15%. Complement-dependent cytotoxicity was performed using identical experimental conditions, but in the absence of effector cells.

Intraperitoneal and Subcutaneous Injection of Tumor Cells. Tumor cells were thawed from a common frozen stock and cultured in vitro for 2 to 3 d before use. Next, 2.5×10^4 CT26 or 8×10^5 A20 cells (35) were injected intraperitoneally. For the growth-delay experiments, 1×10^6 CT26 cells were injected subcutaneously (neck) in BALB/c mice using a 1-mL plastic syringe and a 22-gauge needle. The injection was visually controlled using a 7× Stereomicroscope (Zeiss). The cmHsp70.1 mAb was injected either once on day 4 or on days 4, 7, and 10 after subcutaneous tumor injection and the tumor volume was determined every second day using a caliper and confirmed using ultrasound (GE Healthcare).

Injection of Antibodies and the 14-mer Hsp70 Peptide TKD. For the immunotherapeutic approach, mice were injected with unconjugated cmHsp70.1 mAb (i.v., 20 μg mAb per injection) or an IgG1 isotype-matched control antibody on days 3, 5, and 7 after the injection of CT26 cells (i.p., 2.5×10^4). For the inhibition assays, 20 μg cmHsp70.1 mAb was coinjected with an excess of the TKD peptide (TKDNNLLGRFELSG; 50 μg/mL per injection; purity >97%, EMC Microcollections GmbH) on days 3, 5, and 7 after an intraperitoneal tumor cell injection.

Autopsy. Control mice and cmHsp70.1 mAb treated mice were killed by craniocervical dislocation. The peritoneal cavity was macroscopically inspected for tumor dissemination and the primary tumors were excised in total, and their weights determined.

Immunohistochemistry. After weighing, tumors were cut into 4-mm thick pieces, fixed in Bouin's solution containing 71.5% (vol/vol) picric acid, 23.8% (wt/vol) formaldehyde, 4.7% (vol/vol) acetic acid, and embedded in paraffin. Consecutive section-pairs of the tumors (5 μm) were prepared from the ventral margin of each piece for a distance of 250 μm. The morphology of the excised tumors was visualized using standard H&E and Masson-Goldner staining. Nuclei were costained in 1% (wt/vol) Mayer's Hematoxylin (Dako). For the immunohistochemistry, endogenous peroxidase activity was blocked using freshly prepared 1% (vol/vol) H_2O_2 containing 0.1% (wt/vol) NaN_3. For the detection of effector cells, sections were heated for 30 min at 97 °C and then incubated with anti-NK cell (clone DX5, 1:25, rat–anti-mouse CD49b, IgM; Biozol; clone 12F11, 1:100, rat–anti-mouse CD56; BD Biosciences), anti-T cell (clone 145–2C11, 1:50, hamster–anti-mouse CD3ε, IgG; Biolegend; clone SP7, 1:100, rabbit–anti-goat CD3; Abcam), anti-macrophage (clone BM8, 1:50, rat–anti-mouse F4/80, IgG2a; ACRIS Antibodies GmbH, 1:50), anti-granulocyte/macrophage (clone RB6-8C5, 1:50, rat–anti-mouse Gr-1 Ly6C/Ly6G, IgG2bκ; Biolegend) mAbs or the appropriate isotype-matched control reagent overnight at 4 °C. After washing, sections were incubated for 2 h at room temperature with a rabbit anti-rat or rabbit anti-hamster HRP-conjugated secondary polyclonal antibody preparations as appropriate (Dako) followed, after washing, by diaminobenzidine (Dako) as the chromogen. Sections were counter stained with 1% (wt/vol) Mayer's Hematoxylin (Dako) for 30 s and analyzed on an Axiovert 25 microscope (Zeiss).

Statistical Analysis. Comparative analysis of in vitro data was undertaken using a nonparametric log-rank test (Mann-Whitney). Survival times were estimated from Kaplan-Meyer curves by log-rank test (38).

ACKNOWLEDGMENTS. The authors thank Nicola Dierkes and Anett Lange for excellent technical and editorial assistance, and Integrated BioDiagnostics (Martinsried, Germany) for technical support. This work was supported by the Deutsche Forschungsgemeinschaft (DFG) SFB824/1, DFG-Cluster of Excellence: Munich-Centre of Advanced Photonics, Bundesministerium für Bildung und Forschung (MOBITUM, 01EZ0826; Kompetenzverbund Strahlenforschung, 03NUK007E), the European Union (EU-STEMDIAGNOSTICS, FP7-037703; EU-CARDIORISK, FP7-211403), and Multimmune GmbH.

1. Adams GP, Weiner LM (2005) Monoclonal antibody therapy of cancer. *Nat Biotechnol* 23:1147–1157.
2. Scallon BJ, et al. (2006) A review of antibody therapeutics and antibody-related technologies for oncology. *J Immunother* 29:351–364.
3. Bonner JA, et al. (2006) Radiotherapy plus cetuximab for squamous-cell carcinoma of the head and neck. *N Engl J Med* 354:567–578.
4. Edwards JC, et al. (2004) Efficacy of B-cell-targeted therapy with rituximab in patients with rheumatoid arthritis. *N Engl J Med* 350:2572–2581.
5. Ferrarini M, Heltai S, Zocchi MR, Rugarli C (1992) Unusual expression and localization of heat-shock proteins in human tumor cells. *Int J Cancer* 51:613–619.
6. Shin BK, et al. (2003) Global profiling of the cell surface proteome of cancer cells uncovers an abundance of proteins with chaperone function. *J Biol Chem* 278:7607–7616.
7. Multhoff G, et al. (1995) A stress-inducible 72-kDa heat-shock protein (HSP72) is expressed on the surface of human tumor cells, but not on normal cells. *Int J Cancer* 61:272–279.
8. Hantschel M, et al. (2000) Hsp70 plasma membrane expression on primary tumor biopsy material and bone marrow of leukemic patients. *Cell Stress Chaperones* 5:438–442.
9. Pfister K, et al. (2007) Patient survival by Hsp70 membrane phenotype: Association with different routes of metastasis. *Cancer* 110:926–935.
10. Gehrmann M, et al. (2005) Dual function of membrane-bound heat shock protein 70 (Hsp70), Bag-4, and Hsp40: protection against radiation-induced effects and target structure for natural killer cells. *Cell Death Differ* 12(1):38–51.
11. Fouchaq B, Benaroudj N, Ebel C, Ladjimi MM (1999) Oligomerization of the 17-kDa peptide-binding domain of the molecular chaperone HSC70. *Eur J Biochem* 259:379–384.
12. Multhoff G, et al. (2001) A 14-mer Hsp70 peptide stimulates natural killer (NK) cell activity. *Cell Stress Chaperones* 6:337–344.
13. Stangl S, et al. (2010) In vivo imaging of CT26 mouse tumors by using cmHsp70.1 monoclonal antibody. *J Cell Mol Med*, 10.1111/j.1582-4934.2010.01067.x.
14. Horváth I, Vígh L (2010) Cell biology: Stability in times of stress. *Nature* 463:436–438.
15. Horváth I, Multhoff G, Sonnleitner A, Vígh L (2008) Membrane-associated stress proteins: More than simply chaperones. *Biochim Biophys Acta* 1778:1653–1664.
16. Zhang H, Liu R, Huang W (2007) A 14-mer peptide from HSP70 protein is the critical epitope which enhances NK activity against tumor cells in vivo. *Immunol Invest* 36:233–246.
17. Wang M, et al. (1995) Active immunotherapy of cancer with a nonreplicating recombinant fowlpox virus encoding a model tumor-associated antigen. *J Immunol* 154:4685–4692.
18. Gehrmann M, et al. (2008) Tumor-specific Hsp70 plasma membrane localization is enabled by the glycosphingolipid Gb3. *PLoS One* 3:e1925.
19. Sugawara S, et al. (2009) Binding of *Silurus asotus* lectin to Gb3 on Raji cells causes disappearance of membrane-bound form of HSP70. *Biochim Biophys Acta* 1790(2):101–109.
20. Steplewski Z, Lubeck MD, Koprowski H (1983) Human macrophages armed with murine immunoglobulin G2a antibodies to tumors destroy human cancer cells. *Science* 221:865–867.
21. Houghton AN, et al. (1985) Mouse monoclonal IgG3 antibody detecting GD3 ganglioside: A phase I trial in patients with malignant melanoma. *Proc Natl Acad Sci USA* 82:1242–1246.
22. Stangl S, Wortmann A, Guertler U, Multhoff G (2006) Control of metastasized pancreatic carcinomas in SCID/beige mice with human IL-2/TKD-activated NK cells. *J Immunol* 176:6270–6276.
23. Krause SW, et al. (2004) Treatment of colon and lung cancer patients with ex vivo heat shock protein 70-peptide-activated, autologous natural killer cells: A clinical phase I trial. *Clin Cancer Res* 10:3699–3707.
24. Milani V, et al. (2009) Anti-tumor activity of patient-derived NK cells after cell-based immunotherapy—A case report. *J Transl Med* 7:50.
25. Gastpar R, et al. (2005) Heat shock protein 70 surface-positive tumor exosomes stimulate migratory and cytolytic activity of natural killer cells. *Cancer Res* 65:5238–5247.
26. Bausero MA, Gastpar R, Multhoff G, Asea A (2005) Alternative mechanism by which IFN-gamma enhances tumor recognition: Active release of heat shock protein 72. *J Immunol* 175:2900–2912.
27. Lancaster GI, Febbraio MA (2005) Exosome-dependent trafficking of HSP70: A novel secretory pathway for cellular stress proteins. *J Biol Chem* 280:23349–23355.
28. Gehrmann M, Radons J, Molls M, Multhoff G (2008) The therapeutic implications of clinically applied modifiers of heat shock protein 70 (Hsp70) expression by tumor cells. *Cell Stress Chaperones* 13(1):1–10.
29. Kleinjung T, et al. (2003) Heat shock protein 70 (Hsp70) membrane expression on head-and-neck cancer biopsy-a target for natural killer (NK) cells. *Int J Radiat Oncol Biol Phys* 57:820–826.
30. Farkas B, et al. (2003) Heat shock protein 70 membrane expression and melanoma-associated marker phenotype in primary and metastatic melanoma. *Melanoma Res* 13 (2):147–152.
31. Carson WE, et al. (2001) IL-2 enhances NK cell response to Herceptin-coated Her2/*neu*-positive breast cancer cells. *Eur J Immunol* 31:3016–3025.
32. Kondo E, et al. (2003) Preoperative natural killer cell activity as a prognostic factor for distant metastasis following surgery for colon cancer. *Dig Surg* 20:445–451.
33. Beano A, et al. (2008) Correlation between NK function and response to trastazumab in metastic breast cancer patients. *J Transl Med* 6:25.
34. Dressel R, Johnson JP, Günther E (1998) Heterogeneous patterns of constitutive and heat shock induced expression of HLA-linked HSP70-1 and HSP70-2 heat shock genes in human melanoma cell lines. *Melanoma Res* 8(6):482–492.
35. Kim KJ, Kanellopoulos-Langevin C, Merwin RM, Sachs DH, Asofsky R (1979) Establishment and characterization of BALB/c lymphoma lines with B cell properties. *J Immunol* 122:549–554.
36. Nishioka Y, et al. (1997) Combined therapy of multidrug-resistant human lung cancer with anti-P-glycoprotein antibody and monocyte chemoattractant protein-1 gene transduction: The possibility of immunological overcoming of multidrug resistance. *Int J Cancer* 71(2):170–177.
37. MacDonald HR, Engers HD, Cerottini JC, Brunner KT (1974) Generation of cytotixic T lymphocytes in vitro. *J Exp Med* 140:718–730.
38. Kaplan E, Meyer P (1958) Non-parametric estimation from incomplete observations. *J Am Stat Assoc* 53:457–481.

Radiotherapy and Oncology 99 (2011) 313–316

Contents lists available at ScienceDirect

Radiotherapy and Oncology

journal homepage: www.thegreenjournal.com

Molecular radiobiology

Detection of irradiation-induced, membrane heat shock protein 70 (Hsp70) in mouse tumors using Hsp70 Fab fragment

Stefan Stangl [a], George Themelis [b], Lars Friedrich [c], Vasilis Ntziachristos [b], Athanasios Sarantopoulos [b], Michael Molls [a], Arne Skerra [c], Gabriele Multhoff [a,*]

[a] Dept. of Radiation Oncology, TU München and Helmholtz Zentrum München (HMGU), CCG-Innate Immunity in Tumor Biology, Germany; [b] HMGU, Institute of Biological and Medical Imaging, Munich, Germany; [c] Munich Center for Integrated Protein Science, Technische Universität München, Freising-Weihenstephan, Germany

ARTICLE INFO

Article history:
Received 26 April 2011
Received in revised form 20 May 2011
Accepted 20 May 2011
Available online 23 June 2011

Keywords:
In vivo imaging
Tumor mouse model
Hsp70 Fab fragment
Binding characteristics

ABSTRACT

Background and purpose: The major stress-inducible heat shock protein 70 (Hsp70) is frequently overexpressed in highly aggressive tumors, and elevated intracellular Hsp70 levels mediate protection against apoptosis. Following therapeutic intervention, such as ionizing irradiation, translocation of cytosolic Hsp70 to the plasma membrane is selectively increased in tumor cells and therefore, membrane Hsp70 might serve as a therapy-inducible, tumor-specific target structure.

Materials and methods: Based on the IgG1 mouse monoclonal antibody (mAb) cmHsp70.1, we produced the Hsp70-specific recombinant Fab fragment (Hsp70 Fab), as an imaging tool for the detection of membrane Hsp70 positive tumor cells *in vitro* and *in vivo*.

Results: The binding characteristics of Hsp70 Fab towards mouse colon (CT26) and pancreatic (1048) carcinoma cells at 4 °C were comparable to that of cmHsp70.1 mAb, as determined by flow cytometry. Following a temperature shift to 37 °C, Hsp70 Fab rapidly translocates into subcellular vesicles of mouse tumor cells. Furthermore, in tumor-bearing mice Cy5.5-conjugated Hsp70 Fab, but not unrelated IN-1 control Fab fragment (IN-1 ctrl Fab), gradually accumulates in CT26 tumors between 12 and 55 h after i.v. injection.

Conclusions: In summary, the Hsp70 Fab provides an innovative, low immunogenic tool for imaging of membrane Hsp70 positive tumors, *in vivo*.

 Radiotherapy and Oncology 99 (2011) 313–316

By immunizing mice with the 14-mer peptide TKDNNLLGRFELSG (aa 450–463) derived from the C-terminal region of human Hsp70, the IgG1 mouse monoclonal antibody (mAb) cmHsp70.1 was obtained [1]. This antibody specifically identifies membrane Hsp70 on human and mouse tumors but does not cross-react with healthy human or mouse tissues. Hsp70 (HSPA1A) [2] is frequently present on the membrane of highly aggressive tumors and metastases and therefore, serves as a negative prognostic marker in lower rectal and non-small cell lung carcinomas regardless of their UICC stage [3–5]. Following therapeutic intervention such as radiochemotherapy [6,7], the density of membrane Hsp70 is further enhanced on tumor cells, in particular. Consequently, the Hsp70 specific antibody shows potential for disease prognosis and monitoring therapeutic outcome.

The tumor-specific membrane Hsp70 expression is based on differences in the lipid composition and membrane fluidity between tumor and normal cells. The sphingolipid globoyltriaosylceramide could be identified as a tumor-specific lipid component which enables anchorage of Hsp70 in the plasma membrane of gastrointestinal tumors [8].

Furthermore, we could demonstrate that fluorescence-conjugated mAb cmHsp70.1 was able to specifically detect tumors in mice. Based on these promising *in vivo* imaging results [9] with full size mAb cmHsp70.1 [1], its variable gene regions were cloned and a bacterial expression system was established to generate a chimeric Hsp70 Fab fragment carrying human constant domains [10]. The antigen dissociation constant, as determined by ELISA and Biacore measurements, with K_D values of 5.8 nM and 34.5 nM, respectively, were very similar to the monovalent affinity of the mAb, while human and murine Hsp70 have almost identical amino acid sequences in the relevant epitope region (with one neighboring Lys/K to Arg/R mutation at amino acid position 451). Also the sensitivity of the Hsp70 Fab fragment towards human lines was comparable to that of the mAb [10].

Herein, we describe the binding characteristics of Hsp70 Fab towards mouse tumor cells at 4 °C and 37 °C by flow cytometry and study its capacity to detect tumors in mice by *in vivo* imaging.

* Corresponding author. Address: Klinikum Rechts der Isar, Klinik für Strahlentherapie und Radiologische Onkologie, TU München, Ismaningerstr. 22, 81675 München, Germany.
E-mail address: gabriele.multhoff@lrz.tu-muenchen.de (G. Multhoff).

0167-8140/$ - see front matter © 2011 Elsevier Ireland Ltd. All rights reserved.
doi:10.1016/j.radonc.2011.05.051

Materials and methods

Mouse tumor cell lines

The tumorigenic CT26 mouse colon adenocarcinoma (CT26.WT; ADCC CRL-2638) [11] and the 1048 mouse pancreatic carcinoma cells (kindly provided by Dieter Saur, TU München) which were both derived from BALB/c mouse strains were cultured in RPMI 1640 medium supplemented with 10% v/v heat-inactivted fetal calf serum, 2 mM L-glutamine, 1 mM pyruvate and antibiotics (100 IU/ml penicillin, 100 µg/ml streptomycin) at 37 °C in 5% CO_2 in a humidified atmosphere (95% H_2O). Tumor cells were maintained in their exponential growth phase by regular cell passages twice a week.

Flow cytometry and uptake of Hsp70 Fab fragment

The Hsp70 membrane phenotype was determined by flow cytometry using either the fluorescein-isothiocyanate (FITC)-conjugated full size cmHsp70.1 mAb (multimmune GmbH, Munich, Germany) or the identically labeled recombinant Hsp70 Fab fragment. As controls a correspondingly labeled IgG1 isotype-matched antibody or the recombinant IN-1 Fab fragment (which recognizes the unrelated neuronal antigen Nogo-A) [12] were used. Briefly, after parallel incubation of a suspension of viable tumor cells with the antibodies/Fab fragments for 15 min at 4 °C (5 µg per 100.000 cells), cells were washed in PBS/10% heat-inactivated fetal calf serum (FCS, Gibco BRL). After two washing steps viable, 7-AAD-negative cells were gated and analyzed on a FACSCalibur flow cytometer (Becton Dickinson, Heidelberg, Germany).

The uptake of Hsp70 and control Fab fragments was measured by flow cytometry and immunofluorescence microscopy, by incubating tumor cells with the fluorescence-labeled reagents at 37 °C.

Animals, tumor cell and antibody/Fab injection

Female BALB/c mice (Harlan Winkelmann, Borchern, Germany) between 6 and 12 weeks of age were subcutaneously (s.c.) injected in the neck area with tumor cells (CT26, 2.5×10^4 in 100 µl PBS).

Cy5.5-conjugated Hsp70 Fab, IN-1 control Fab fragment, cmHsp70.1 mAb and IgG1 isotype-matched control antibody (each 100 µg in 100 µl PBS) were injected i.v. into the tail vein of BALB/c mice on day 7 after tumor injection (s.c.). Mice were sacrificed 2, 8, 12, 24, 30 and 48 h after injection of the Fab fragment. The fluorescence imaging measurements were performed either intraoperatively or on isolated organs and tissues using an EM-CCD camera (iXon DV887, Andor, Belfast, Northern Ireland) equipped with a 710/10 nm band pass filter. The laser light was guided through a multimode fiber (200 µm core/0.22 NA) to a collimator and a diffuser (F260SMA-b; ED1-S20, Thorlabs, Newton, NJ) for uniform illumination. White light illumination was achieved under a 250 W halogen lamp (KL-2500 LCD, Edmund Optics). The fluorescence intensity was determined as a ratio comparing the fluorescence in tumor versus adjacent corresponding normal tissue (muscle), liver versus heart and kidney versus heart.

Statistics

Comparative analysis of data was undertaken using the Student's *t*-test ($p < 0.05$).

Results

Kinetics of binding of Hsp70 Fab to mouse tumor cells

Flow cytometric analysis of 1048 and CT26 mouse tumor cells was performed using either FITC-conjugated full size cmHsp70.1 mAb or Hsp70 Fab fragment at 4 °C. As controls an identically labeled IgG1 isotype-matched antibody and the unrelated recombinant IN-1 Fab fragment were used. As illustrated in Supplementary Fig. 1, the binding patterns of cmHsp70.1 mAb and Hsp70 Fab were comparable in non-irradiated and irradiated tumor cells. Mean values of 3 independent experiments revealed a positive staining of 13 ± 5% viable 1048 pancreatic tumor cells for cmHsp70.1 mAb and 8.5 ± 3.4% for Hsp70 Fab. With respect to non-irradiated CT26 colon adenocarcinoma cells, positive staining was detected in 55 ± 6.4% for cmHsp70.1 mAb and 39.4 ± 5.9% for Hsp70 Fab. Following irradiation (2 Gy) the percentage of positively stained CT26 tumor cells increased significantly ($p < 0.05$) up to 80.2 ± 7.7% and 69.1 ± 7.7% using using cmHsp70.1 and Hsp70 Fab, respectively.

Differences in the staining pattern between 1048 (Supplementary Fig. 2a) and CT26 (Supplementary Fig. 2b) tumor cells using Hsp70 Fab at 4 °C (upper panel) versus 37 °C (lower panel) were evident by immunofluorescence microscopy. At 4 °C the binding of Hsp70 Fab to 1048 and CT26 tumor cells revealed a typical ring-shaped, surface staining pattern. A temperature shift to 37 °C for 15 min during the incubation period resulted in the uptake of Hsp70 Fab, but not IN-1 ctrl Fab, into intracellular vesicles. In line with the observation from flow cytometry, 1048 tumor cells showed a lower staining intensity than CT26 tumor cells. A comparison of uptake revealed that approximately 60% of 1048 but 100% of CT26 tumor cells were positively stained for fluorophor-conjugated Hsp70 reagents after 15–20 min. These data indicate that in general tumors with low basal Hsp70 membrane expression can be visualized by Hsp70 specific reagents, however, at lower levels. Similar results were observed with human tumor cell lines that differ in their basal Hsp70 membrane expression pattern (data not shown). A significant increase in the mean fluorescence intensity (mfi) of Hsp70 in CT26 cells after incubation with the FITC-conjugated Hsp70 Fab ($p < 0.05$) and to a lower

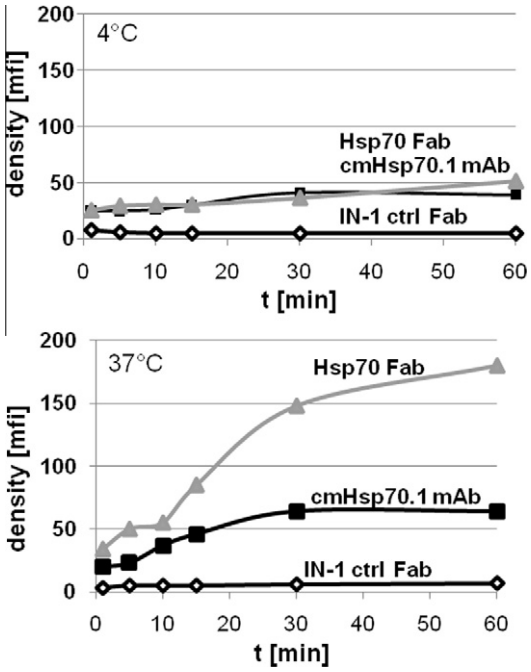

Fig. 1. Representative views of the kinetics of Hsp70 staining density with FITC-labeled Hsp70 Fab, IN-1 ctrl Fab and cmHsp70.1 mAb of CT26 tumor cells at 4 °C (upper panel) and 37 °C (lower panel). CT26 tumor cells were incubated for 2, 5, 10, 15, 30 and 60 min, washed and analyzed on a flow cytometer. The graphs represent the antigen density at the indicated time points at 4 °C and 37 °C expressed as the mean fluorescence intensity (mfi) using flow cytometric analysis.

extent with the cmHsp70.1 mAb at 37 °C between 2 and 15 min incubation (Fig. 1). At 4 °C the density of Hsp70 remained almost unaltered between 2 and 60 min using both Hsp70-specific reagents (Fig. 1).

In vivo imaging of CT26 tumors and organs using Hsp70 Fab fragment

Balb/c mice were injected s.c. into the neck using CT26 mouse colon carcinoma cells. The average tumor size, as determined by calliper measurements on day 7, ranged between 0.2 and 0.5 cm^2 and tumor take was 100%. Cy5.5-labeled Hsp70 Fab (Fig. 2a, upper row) and IN-1 control Fab (Fig. 2a, lower panel) were injected into the tail vein on day 7 and mice were sacrificed at different time points. A strong fluorescence signal of the Cy5.5-labeled Hsp70 Fab within the tumor was found 12 h after injection and further increased up to 55 h (Fig. 2a, upper panel). Quantification of the ratio between fluorescence signals in the tumor versus adjacent tissue confirmed these findings (Fig. 2b, filled symbols). In contrast, no significant increase was observed using the identically labeled IN-1 control Fab (Fig. 2b, open symbols). A comparison of the kinetics of uptake of Hsp70 Fab (Fig. 2b) versus cmHsp70.1 mAb (Fig. 2c) revealed that a maximum in fluorescence intensity was reached with cmHsp70.1 mAb 24 h after injection, whereas in case of Hsp70 Fab progressive accumulation within the tumor was observed between 3 and 55 h.

A comparative analysis of the *in vivo* imaging of different mouse organs including tumor, liver, kidney, skin, gut, heart, fatty tissue, lung and spleen 2, 6, 12, 24 and 48 h after injection of the Hsp70 (Supplementary Fig. 3a) and the IN-1 control Fab (Supplementary Fig. 3b) confirmed positive tumor staining with the latter after 12 h, which gradually increased up to 48 h. Quantification of the ratio of fluorescence between tumor and heart showed similar results (Supplementary Fig. 3c). In contrast, except for a non-specifically increased value at 12 h, the ratio of fluorescence observed for the IN-1 control Fab remained low or gradually decreased between 12 and 55 h (Supplementary Fig. 3c). A comparison of the ratio of the fluorescence intensity between Hsp70 Fab and IN-1 Fab in the liver versus heart revealed a maximum for both reagents at 6 h after injection, which decreased until 48 h (Supplementary Fig. 3d). A gradual decrease in the fluorescence intensity was also observed in the kidney (Supplementary Fig. 3e). Other organs and tissues such as skin, gut, heart, fatty tissue lung and spleen revealed no significant enrichment of the fluorescence labeled Fab fragments at any tested time points (Supplementary Fig. 3a and b).

Discussion

Following stress, such as ionizing irradiation, but also after oxygen deprivation the cell surface density of Hsp70 is enhanced in tumors [13–15] and, hence, might serve as a therapy-inducible, tumor specific marker. Tumor hypoxia limits the therapeutic efficacy of radiation therapy, promotes tumor progression [16–20] and therefore, identification of hypoxic areas in tumors via membrane Hsp70 expression might improve the therapeutic

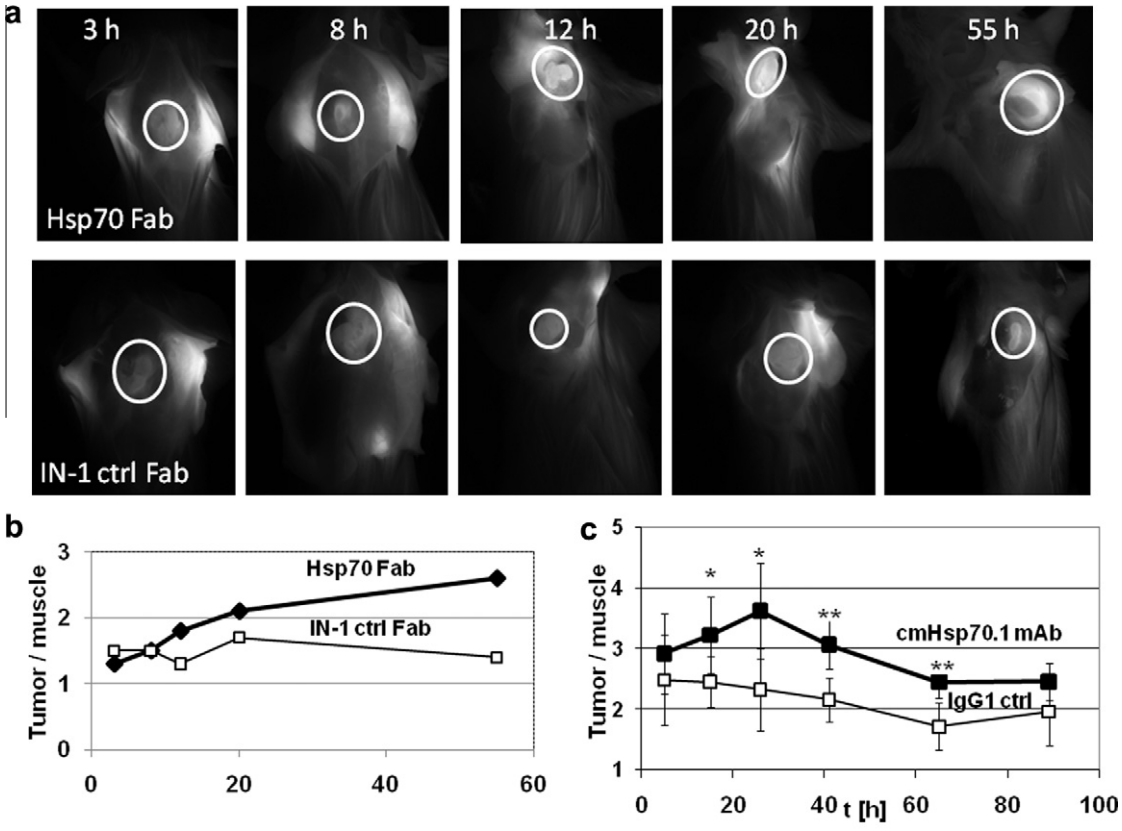

Fig. 2. Intraoperative detection of Cy5.5-labeled Hsp70 Fab (upper panel) and IN-1 ctrl Fab (lower panel) in tumor-bearing (CT26) BALB/c mice. 100 μg of each reagent was injected i.v. into the tail vein on day 7 after tumor injection (s.c.). Representative views of the Cy5.5 fluorescence of the neck part of the mice were taken 3, 8, 12, 20, and 55 h after i.v. injection (a). For each indicated time point 2–3 animals were analyzed. Fluorescence intensity values of Cy5.5-labeled Hsp70 Fab (closed symbols) and IN-1 ctrl Fab (open symbols) in mouse tumors. The graph shows the mean fluorescence data of the mice ($n = 5$) shown in (b). Kinetics of the fluorescence intensity of Cy5.5-labeled cmHsp70.1 mAb (closed symbols) and IgG1 isotype-matched control antibody (open symbols) in the tumor of the mice. $^{*}p < 0.05$; $^{**}p < 0.01$ (c). Each point represents the data derived from at least 4 individual animals.

outcome of radiotherapy an in-homogenous dose distribution [21–25].

Compared to full size antibodies, corresponding Fab fragments are known to have a better tissue distribution and a faster clearance from circulation [26]. Due to the lack of the Fc region, Fab fragments are less immunogenic and thus qualify for repeated imaging and therefore, provide a promising tool to monitor therapeutic intervention and outcome. Fab fragments lack non-specific cross-reactivity with Fc receptors and therefore, provide better signal-to-noise contrast images. Herein, we show that Hsp70 Fab has a similar reactivity pattern towards mouse tumor cells CT26 and 1048 as cmHsp70.1 mAb. *In vitro*, uptake of monovalent Hsp70 Fab at 37 °C into mouse tumor cells was stronger compared to that of the bivalent mAb. Hence, bivalency of the binding agent is not a prerequisite for internalization as it is often observed for other cell surface targets [26,27]. In line with these findings, the kinetics of uptake of Hsp70 Fab in tumor-bearing mice differed from that of cmHsp70.1 mAb. The fluorescence intensity of tumors gradually increased between 3 and 55 h using the Cy5.5-conjugated Hsp70 Fab, whereas, full length Hsp70 mAb reached maximal staining intensity at 24 h after i.v. injection. In contrast, the fluorescence staining of secretion organs, such as liver and kidney versus heart gradually decreased over time. Due to blood flow an enrichment of both reagents, specific and non-specific control Fab, was observed 6 h after i.v. injection in the liver. Since none of the reagents specifically binds to liver the fluorescence intensity decreases thereafter due to degradation. In the kidney both reagents also did not specifically bind but were gradually secreted between 2 and 48 h after i.v. injection. The specificity of the Hsp70 Fab fragment for tumor cells was proven by using the identically labeled IN-1 control Fab fragment, which was unable to bind to tumors in mice [12]. The gradual increase in staining intensity and the tumor-specific accumulation of Hsp70 Fab in tumor cells over time, which was slower than expected for a Fab fragment, could be explained by a fast turnover rate of membrane Hsp70 at 37 °C and possible recycling of the endocytosed Fab fragment to the cell surface [28]. The Hsp70 cycles from early endosomes to the plasma membrane without being degraded in lysosomes, as determined by small marker GTPases for endo-lysosomal pathways [9].

Conclusion

Since ionizing irradiation and hypoxia enhance the membrane density [13,14], as well as the uptake of membrane Hsp70 in tumor cells, we propose that a fluororescence- and/or radionuclide-labeled Hsp70-specific Fab fragment [10] might provide a low immunogenic, useful tool for tumor-specific imaging and for monitoring of therapeutic intervention and outcome.

Conflict of interest statement

Multimmune GmbH has an interested in the Hsp70 Fab fragment for *in vivo* imaging of tumors.

Acknowledgments

The study was supported by multimmune GmbH (Munich, Germany), the Deutsche Forschungsgemeinschaft (SFB-824/1; DFG Cluster of Excellence, Munich Center of Advanced Photonics), the Bundesministerium für Bildung und Forschung (BMBF-MOBITUM, 01EZ0826; Kompetenzverbund Strahlenforschung, 03NUK007E; Spitzencluster m4, 01EX1021C; Innovative Therapies, 01GU0823) and the European Union (EU-CARDIORISK, FP7 211403). The authors want to thank Anett Lange for excellent editorial assistance.

Appendix A. Supplementary material

Supplementary data associated with this article can be found, in the online version, at doi:10.1016/j.radonc.2011.05.051.

References

[1] Stangl S, Gehrmann M, Riegger J, et al. Targeting membrane heat-shock protein 70 (Hsp70) on tumors by cmHsp70.1 antibody. Proc Natl Acad Sci USA 2011;108:733–8.
[2] Kampinga HH, Hageman J, Vos MJ, et al. Guidelines for the nomenclature of the human heat shock proteins. Cell Stress Chaperones 2009;14:105–11.
[3] Pfister K, Radons J, Busch R, et al. Patient survival by Hsp70 membrane phenotype: association with different routes of metastasis. Cancer 2007;110:926–35.
[4] Ciocca DR, Fanelli MA, Cuello-Carrion FD, Castro GN. Heat shock proteins in prostate cancer: from tumorigenesis to the clinic. Int J Hyperthermia 2010;26:737–47.
[5] Calderwood SK, Khaleque MA, Sawyer DB, Ciocca DR. Heat shock proteins in cancer: chaperones of tumorigenesis. Trends Biochem Sci 2006;31:164–72.
[6] Gehrmann M, Schilling D, Molls M, Multhoff G. Radiation induced stress proteins. Int J Clin Pharmacol Ther 2010;48:492–3.
[7] Gehrmann M, Radons J, Molls M, Multhoff G. The therapeutic implications of clinically applied modifiers of heat shock protein 70 (Hsp70) expression by tumor cells. Cell Stress Chaperones 2008;13:1–10.
[8] Gehrmann M, Liebisch G, Schmitz G, et al. Tumor-specific Hsp70 plasma membrane localization is enabled by the glycosphingolipid Gb3. Plos One 2008;3:e1925.
[9] Stangl S, Gehrmann M, Dressel R, et al. In vivo imaging of CT26 mouse tumors by using cmHsp70.1 monoclonal antibody. J Cell Mol Med 2011;15:874–87.
[10] Friedrich L, Stangl S, Hahne H, et al. Bacterial production and functional characterization of the Fab fragment of the murine IgG1/λ monoclonal antibody cmHsp70.1, a reagent for tumour diagnostics. PEDS 2010;23:161–8.
[11] Wang M, Bronte V, Chen PW, et al. Active immunotherapy of cancer with a non-replicating recombinant fowlpox virus encoding a model tumor-associated antigen. J Immunol 1995;154:4685–92.
[12] Bandtlow C, Schiweck W, Tai H-H, Schwab ME, Skerra A. The *Escherichia coli*-derived Fab fragment of the IgM/κ antibody IN-1 recognizes and neutralizes myelin-associated inhibitors of neurite growth. Eur J Biochem 1996;241:468–75.
[13] Gehrmann M, Marienhagen J, Eichholtz-Wirth H, et al. Dual function of membrane-bound heat shock protein 70 (Hsp70), Bag-4, and Hsp40: protection against radiation-induced effects and target structure for natural killer cells. Cell Death Differ 2005;12:38–51.
[14] Schilling D, Gehrmann M, Steinem C, et al. Binding of heat shock protein 70 to extracellular phosphatidylserine (PS) promotes killing of normoxic and hypoxic tumor cells. FASEB J 2009;23:2467–77.
[15] Sorensen BS, Horsman M, Vorum B, et al. Proteins up-regulated by mild and severe hypoxia in squamous cell carcinomas in vitro by proteomics. Radiother Oncol 2009;92:443–9.
[16] Vaupel P. Tumor microenvironmental physiology and its implications for radiation oncology. Semin Radiat Oncol 2004;14:198–206.
[17] Vaupel P, Mayer A, Hockel M. Tumor hypoxia and malignant progression. Methods Enzymol 2004;381:335–54.
[18] Busk M, Toustrup K, Sorensen BS, et al. In vivo identification and specificity assessment of mRNA markers of hypoxia in human and mouse tumors. BMC Cancer 2011;11:63–7.
[19] Yaromina A, Thames H, Zhou X, et al. Radiobiological hypoxia, histological parameters of tumor, microenvironment and local tumor control after fractionated irradiation. Radiother Oncol 2010;96:116–22.
[20] Mujcic H, Rzymski T, Rouschop KMA, et al. Hypoxia activation of the unfolded protein response induces expression of metastasis-associated gene LAMP3. Radiother Oncol 2009;92:450–9.
[21] Mortensen LS, Buus S, Nordsmark M, et al. Identifying hypoxia in human tumors: a correlation study between 18F-FMISO PET and the Eppendorf oxygen-sensitive electrode. Acta Oncol 2010;49:934–40.
[22] Aerts HJ, Lambin P, Ruysscher DD. FDG for dose painting: a rational choice. Radiother Oncol 2010;97:163–4.
[23] Thorwart D, Alber M. Implementation of hypoxia imaging into treatment planning and delivery. Radiother Oncol 2010;97:172–5.
[24] Rodemann HP. Molecular radiation biology: perspectives for radiation oncology. Radiother Oncol 2009;92:293–8.
[25] Muijs CT, Beukema JC, Widder J, et al. (18)F-FLT-PET for detection of rectal cancer. Radiother Oncol 2011;98:357–9.
[26] Yarden Y. Agonistic antibodies stimulate the kinase encoded by the neu protooncogene in living cells but the oncogenic mutant is constitutively active. Proc Natl Acad Sci USA 1990;87:2569–73.
[27] Harari D, Yarden Y. Molecular mechanisms underlying ErbB2/HER2 action in breast cancer. Oncogene 2000;19:6102–14.
[28] Thurber GM, Schmidt MM, Wittrup KD. Antibody tumor penetration: transport opposed by systemic and antigen-mediated clearance. Adv Drug Deliver Rev 2008;60:1421–34.

OPEN ACCESS Freely available online

PLOS ONE

Tumor Imaging and Targeting Potential of an Hsp70-Derived 14-Mer Peptide

Mathias Gehrmann[1☯], Stefan Stangl[1☯], Gemma A. Foulds[2☯], Rupert Oellinger[3], Stephanie Breuninger[1], Roland Rad[3], Alan G. Pockley[2], Gabriele Multhoff[1,4]*

1 Department of Radiation Oncology, Klinikum rechts der Isar, Technische Universität München, Munich, Germany, **2** John van Geest Cancer Research Centre, Nottingham Trent University, Nottingham, United Kingdom, **3** Medical Department II, Translational Gastroenterological Oncology, Klinikum rechts der Isar, Technische Universität München, Munich, Germany, **4** Clinical Cooperation Group (CCG) "Innate Immunity in Tumor Biology", Helmholtz Zentrum München, Deutsches Forschungszentrum für Gesundheit und Umwelt, Munich, Germany

Abstract

Background: We have previously used a unique mouse monoclonal antibody cmHsp70.1 to demonstrate the selective presence of a membrane-bound form of Hsp70 (memHsp70) on a variety of leukemia cells and on single cell suspensions derived from solid tumors of different entities, but not on non-transformed cells or cells from corresponding 'healthy' tissue. This antibody can be used to image tumors *in vivo* and target them for antibody-dependent cellular cytotoxicity. Tumor-specific expression of memHsp70 therefore has the potential to be exploited for theranostic purposes. Given the advantages of peptides as imaging and targeting agents, this study assessed whether a 14-mer tumor penetrating peptide (TPP; TKDNNLLGRFELSG), the sequence of which is derived from the oligomerization domain of Hsp70 which is expressed on the cell surface of tumor cells, can also be used for targeting membrane Hsp70 positive (memHsp70+) tumor cells, *in vitro*.

Methodology/Principal Findings: The specificity of carboxy-fluorescein (CF-) labeled TPP (TPP) to Hsp70 was proven in an Hsp70 knockout mammary tumor cell system. TPP specifically binds to different memHsp70+ mouse and human tumor cell lines and is rapidly taken up via endosomes. Two to four-fold higher levels of CF-labeled TPP were detected in MCF7 (82% memHsp70+) and MDA-MB-231 (75% memHsp70+) cells compared to T47D cells (29% memHsp70+) that exhibit a lower Hsp70 membrane positivity. After 90 min incubation, TPP co-localized with mitochondrial membranes in memHsp70+ tumors. Although there was no evidence that any given vesicle population was specifically localized, fluorophore-labeled cmHsp70.1 antibody and TPP preferentially accumulated in the proximity of the adherent surface of cultured cells. These findings suggest a potential association between membrane Hsp70 expression and cytoskeletal elements that are involved in adherence, the establishment of intercellular synapses and/or membrane reorganization.

Conclusions/Significance: This study demonstrates the specific binding and rapid internalization of TPP by tumor cells with a memHsp70+ phenotype. TPP might therefore have potential for targeting and imaging the large proportion of tumors (~50%) that express memHsp70.

Citation: Gehrmann M, Stangl S, Foulds GA, Oellinger R, Breuninger S, et al. (2014) Tumor Imaging and Targeting Potential of an Hsp70-Derived 14-Mer Peptide. PLoS ONE 9(8): e105344. doi:10.1371/journal.pone.0105344

Editor: Philip C. Trackman, Boston University Goldman School of Dental Medicine, United States of America

Received April 10, 2014; **Accepted** July 21, 2014; **Published** August 28, 2014

Data Availability: The authors confirm that all data underlying the findings are fully available without restriction. All relevant data are within the paper and its Supporting Information files.

Funding: This study was supported by the Deutsche Forschungsgemeinschaft (DFG) SFB824/B4, (DFG) INST95/980-1 FUGG, DFG-Cluster of Excellence: Munich Advanced Photonics (MAP), Bundesministerium für Bildung und Forschung (BMBF) MOBITUM (01EZ0826), m4 Cluster of Excellence (01EX1021C), and Kompetenzverbund Strahlenforschung (03NUK007E). Additional funding was provided to AGP by the John and Lucille van Geest Foundation and the Wellcome Trust (Grant 084399). This study was partly funded by multimmune GmbH. The funders had no role in study design, data collection and analysis, decision to publish, or preparation of the manuscript.

Competing Interests: This study was partly funded by multimmune GmbH. The membrane Hsp70 phenotype on viable tumor and metastatic cells of patients was determined by flow cytometry using an FITC-conjugated cmHsp70.1 monoclonal antibody (mAb, multimmune GmbH, Germany). Gabriele Multhoff declares to have filed a patent relating to the TPP peptide pertinent to this article (Peptide-based compounds and their uses for tumor imaging and targeting). Gabriele Multhoff is a PLOS ONE Editorial Board member. There are no further patents, products in development or marketed products to declare. This does not alter the authors' adherence to all the PLOS ONE policies on sharing data and materials.

* Email: gabriele.multhoff@lrz.tu-muenchen.de

☯ These authors contributed equally to this work.

Introduction

Significant progress in the development of new therapies that can increase overall survival rates for a range of cancer types has been made. However, the heterogeneity within individual tumors and between tumors of the same type in different patients, as well as the different stages and sub-types of tumors, combine to confer a level of resistance to existing treatments in patients, and problems with the application of universal treatment strategies. Although chemotherapy remains one of the primary approaches

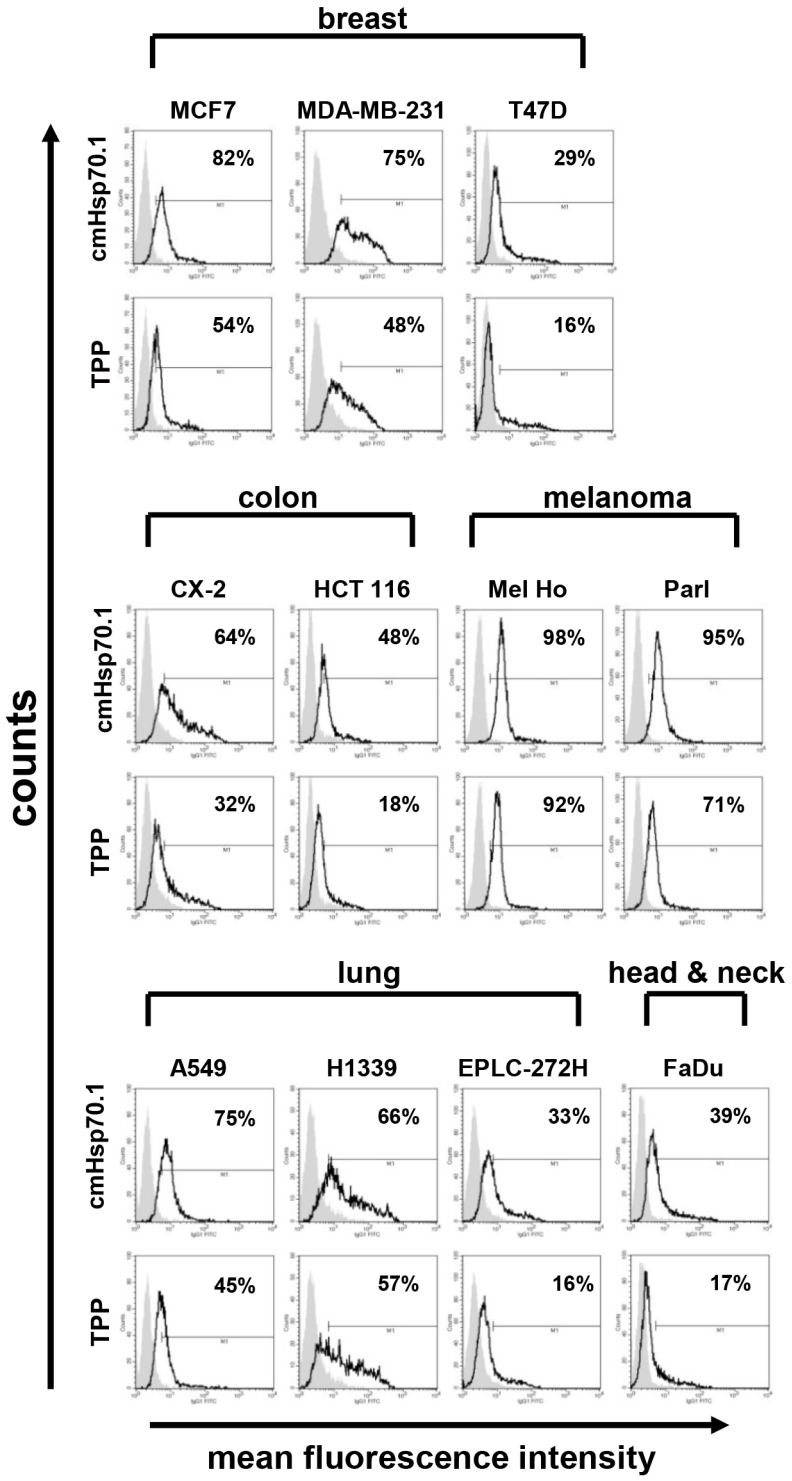

Figure 1. Tumor cell lines expressing memHsp70 are able to bind TPP at 4°C. The memHsp70 status of a panel of human breast, colon, melanoma, lung, head & neck tumor cell lines was assessed using the cmHsp70.1 antibody (top row histograms). Incubation of tumor cells with carboxyfluorescein (CF)-labeled TPP at 4°C (bottom row histograms) results in a similar binding profile to that of cmHsp70.1 antibody in all tumor cell lines; grey, isotype controls, open histograms, Hsp70 specific reagents. The numbers in the histograms show the proportion of Hsp70 membrane-positively stained cells.
doi:10.1371/journal.pone.0105344.g001

for treating cancer, conventional therapy is not specifically targeted to tumor cells and is therefore associated with a high level of side-effects, some of which can be severe. The development of drug resistance and other issues associated with biodistribution and drug clearance also pose significant problems and challenges.

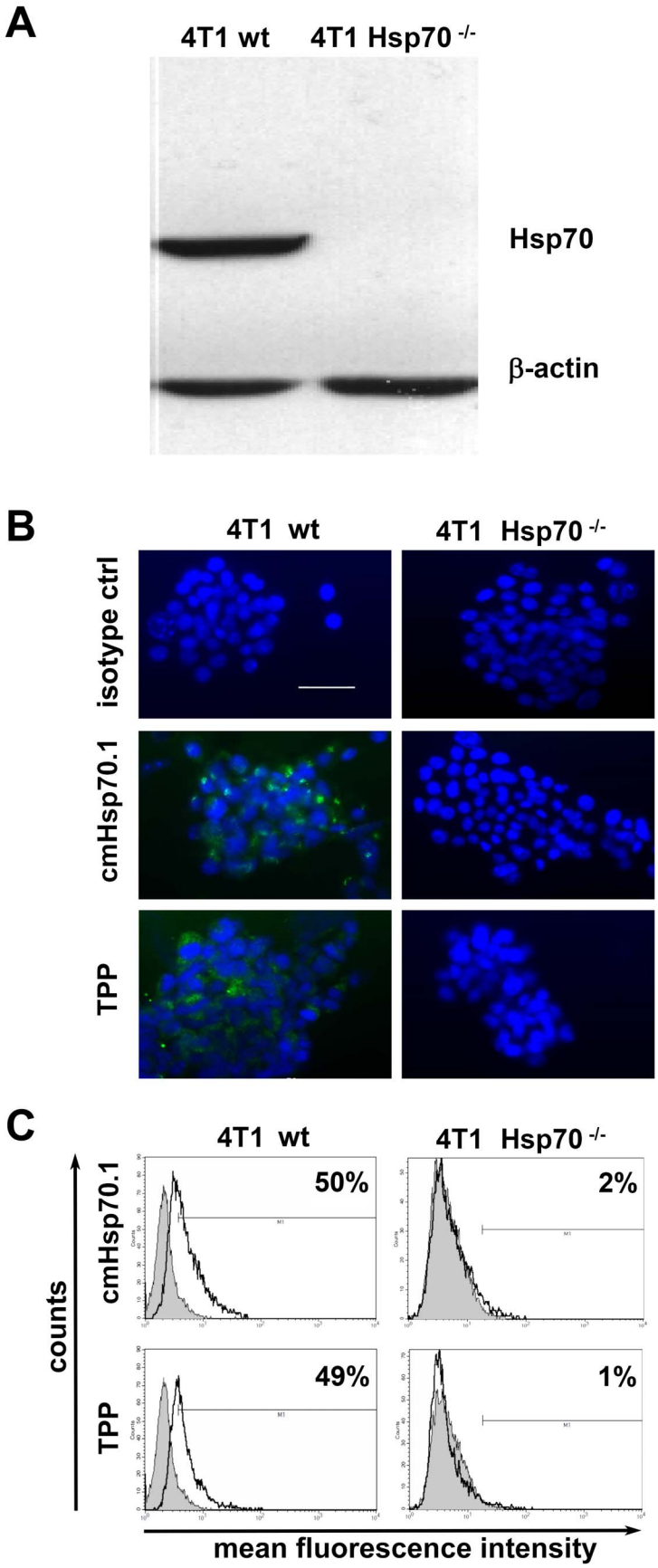
A
4T1 wt
4T1 Hsp70 -/-
Hsp70
β-actin
B
4T1 wt
4T1 Hsp70 -/-
isotype ctrl
cmHsp70.1
TPP
C
4T1 wt
4T1 Hsp70 -/-
cmHsp70.1
TPP
50%
2%
49%
1%
counts
mean fluorescence intensity

Figure 2. TPP specifically binds to Hsp70 *in vitro*. A. Western Blot analysis of whole cell lysates of 4T1 Hsp70 wild type (4T1 wt) and 4T1 knockout (4T1 Hsp70$^{-/-}$) cell lines showed a positive Hsp70 staining in 4T1 wt but not in 4T1 Hsp70$^{-/-}$ cells using the cmHsp70.1 antibody; ß-actin was used as a loading control. **B.** Immunofluorescence staining and **C.** flow cytometric analysis of *in vitro* grown viable 4T1 wt and Hsp70$^{-/-}$ cells proved the Hsp70 specificity of CF-labeled TPP. Binding of TPP to 4T1 wt cells was comparable to that of cmHsp70.1 antibody (left panel, green staining). Neither TPP nor cmHsp70.1 antibody did bind to 4T1 Hsp70$^{-/-}$ cells (right panel). Cells were counter-stained with DAPI (blue staining). **C.** Representative flow cytometric histograms indicate a positive Hsp70 staining of 4T1 wt cells by cmHsp70.1 antibody and TPP. In contrast, 4T1 Hsp70$^{-/-}$ cells were neither stained with cmHsp70.1 antibody nor with TPP; grey, isotype controls, open histograms, Hsp70 specific reagents. The numbers in the histograms show the proportion of Hsp70 membrane-positively stained cells.
doi:10.1371/journal.pone.0105344.g002

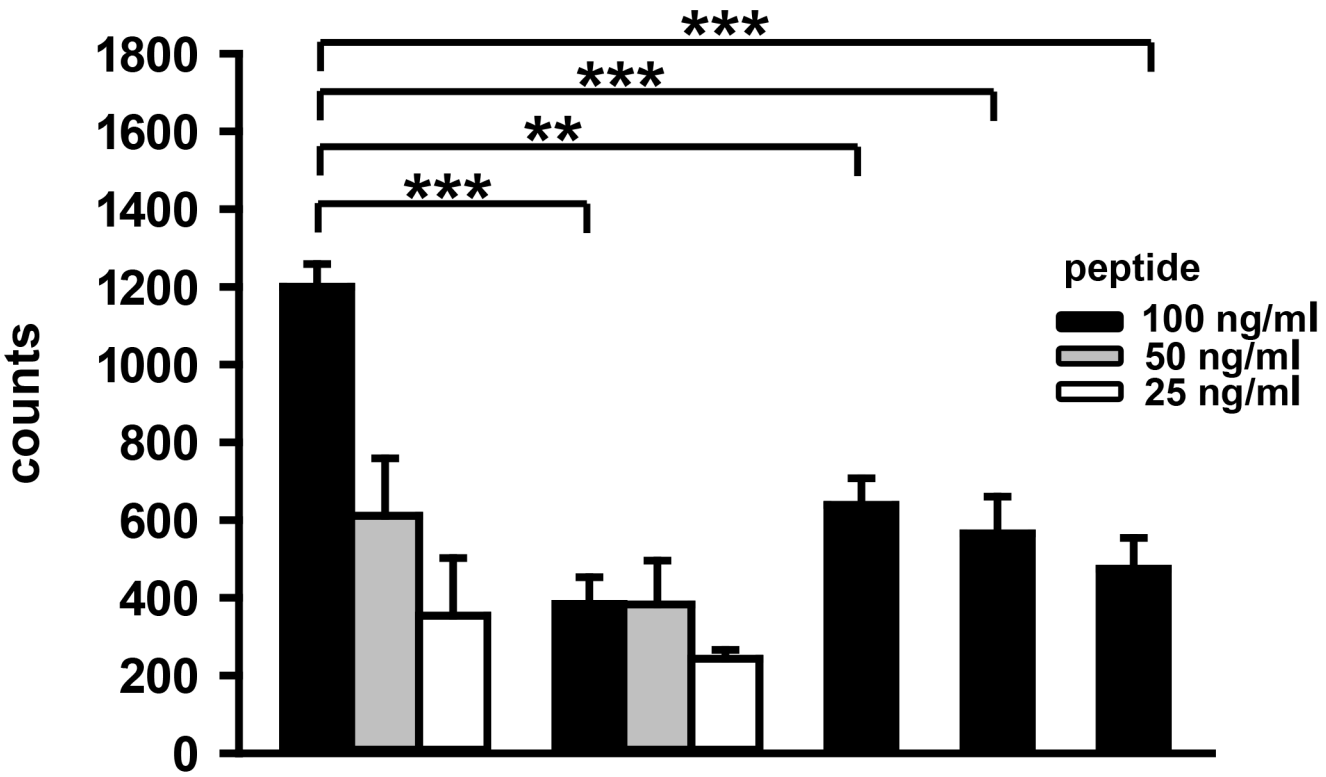

TPP	+	-	+	+	+
scrambled	-	+	-	-	-
Hsp70	+	+	-	-	-
Hsp60	-	-	+	-	-
Grp78	-	-	-	+	-
Hsp27	-	-	-	-	+

Figure 3. TPP specifically binds to Hsp70, but not to other Heat shock proteins (HSPs). A peptide ELISA was performed to determine the *in vitro* binding capacity of peptides to different HSPs. Ninety six well plates that were coated either with Hsp70, Hsp60, Grp78, or Hsp27 were incubated with carboxyfluorescein (CF)-labeled TPP or a scrambled peptide at concentrations ranging from 100 to 25 ng/ml. Fluorescence was measured after 30 min at 27°C using a multiplate reader. Combinations of peptides and proteins are indicated as "+" in the lower panel. Differences in peptide binding (100 ng/ml) were evaluated using the Student's *t*-test (** $p<0.01$; *** $p<0.001$) (n = 3).
doi:10.1371/journal.pone.0105344.g003

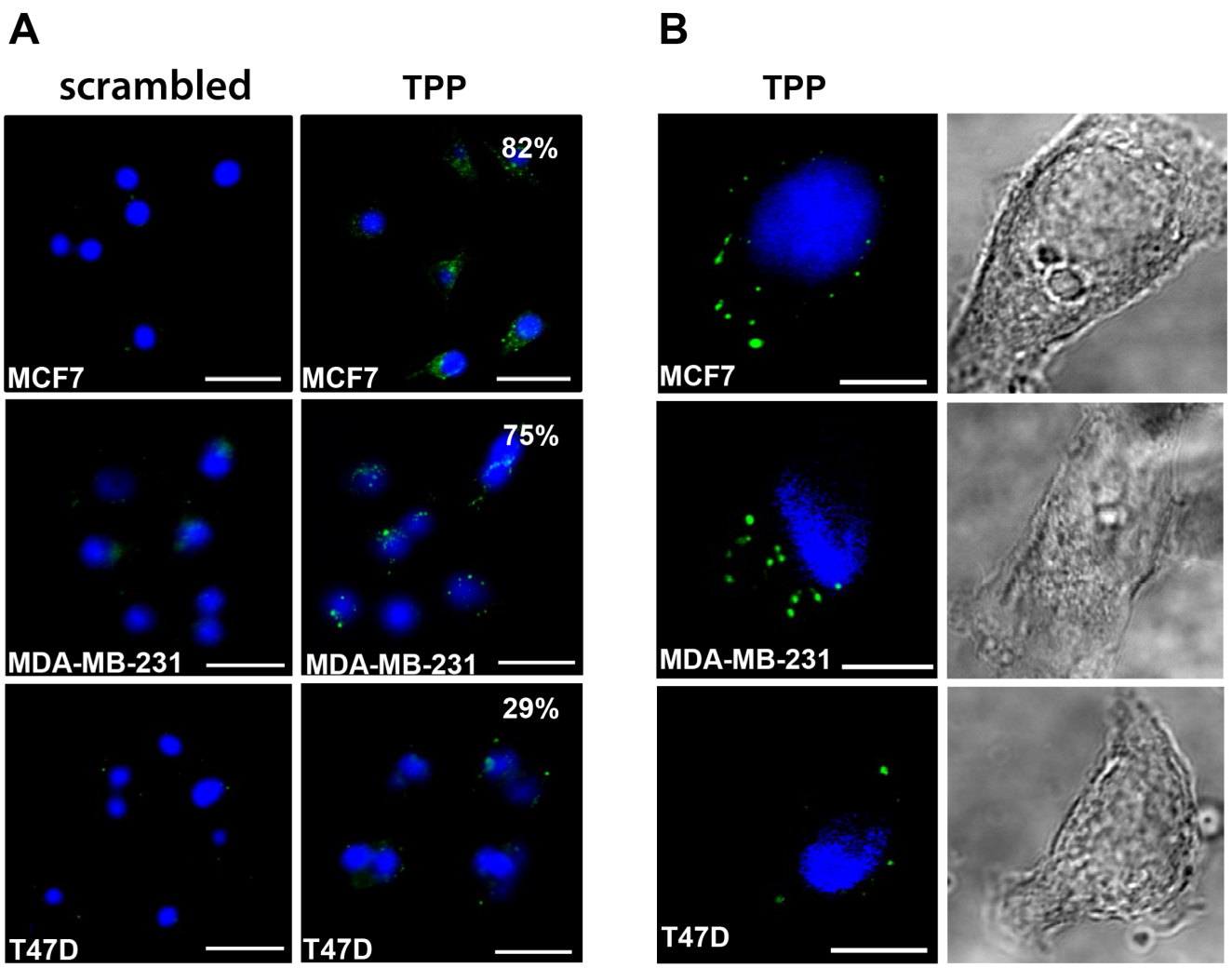

Figure 4. Specific uptake of TPP into tumor cells at 37°C. Human breast cancer cell lines expressing different levels of memHsp70 (MCF7, MDA-MB-231, T47D) were incubated with CF-labeled TPP or a scrambled peptide for 30 min at 37°C and the internalization of peptides imaged using confocal microscopy. **A.** TPP (green, right panel), but not the scrambled peptide (left panel) is internalized into the tumor cell lines. The appearance of the TPP (green, right panel) in well-defined, localized points suggests that the association of the peptide with intracellular vesicles is related to the memHsp70 expression status. The numbers shown as inserts indicate the percentage of memHsp70 positively stained cells. DAPI staining allows visualization of the nucleus (blue). Objective 2×; scale bar 50 μm. **B.** Individual cells were imaged as a z-stack in order to better illustrate the intracellular localization of TPP. Images are representative three-frame composites from approximately mid-way in the stack. Immunofluorescence staining, (left panel); brightfield, (right panel). Objective 63×; scale bar 10 μm.
doi:10.1371/journal.pone.0105344.g004

The difficulties in effectively targeting tumors that result from genetic and phenotypic heterogeneity have prompted the need for more specifically targeted approaches - 'patient stratification' and 'patient-focused medicine'. However, the ability to better treat a patient on the basis of the characteristics of their own tumor requires the identification of key target molecules or features. Although the ability to better identify tumor-associated antigens has led to the development of engineered human monoclonal antibodies for targeting a wide range of common malignancies [1] and the use of radiolabeled antibodies as therapeutics for different kinds of hematological malignancies and solid tumors [2–5], the production and purification of therapeutic antibodies is time-consuming and cost-intensive. Furthermore, antibodies derived from mice are not suitable for therapeutic approaches due to their immunogenicity in humans, and the affinity, avidity, or even the specificity of chimeric humanized antibodies often differ from those of the original murine antibody from which they are derived.

The primary advantage of antibodies is their specificity and ability to target single molecules bearing the epitope. However, this can also be a disadvantage, as antibodies can only target those cancers which express the antigenic determinant. It is also the case that the identification of such targets does not always result in an effective treatment. As an example, only a proportion (~50%) of those patients that bear Her2-positive breast tumors and are therefore theoretically sensitive to trastuzumab (Herceptin), respond to the drug, and many tumors develop resistance to treatment [6].

Attention is now being turned towards the use of small molecules such as peptides for diagnostic imaging and targeted radionuclide therapy, due to the fact that they are easy to produce with a defined and controlled purity in large quantities. Such peptides exhibit a better biodistribution compared to antibodies are generally more stable and their enhanced ability to penetrate tissues makes them better targeting agents. Peptides can be

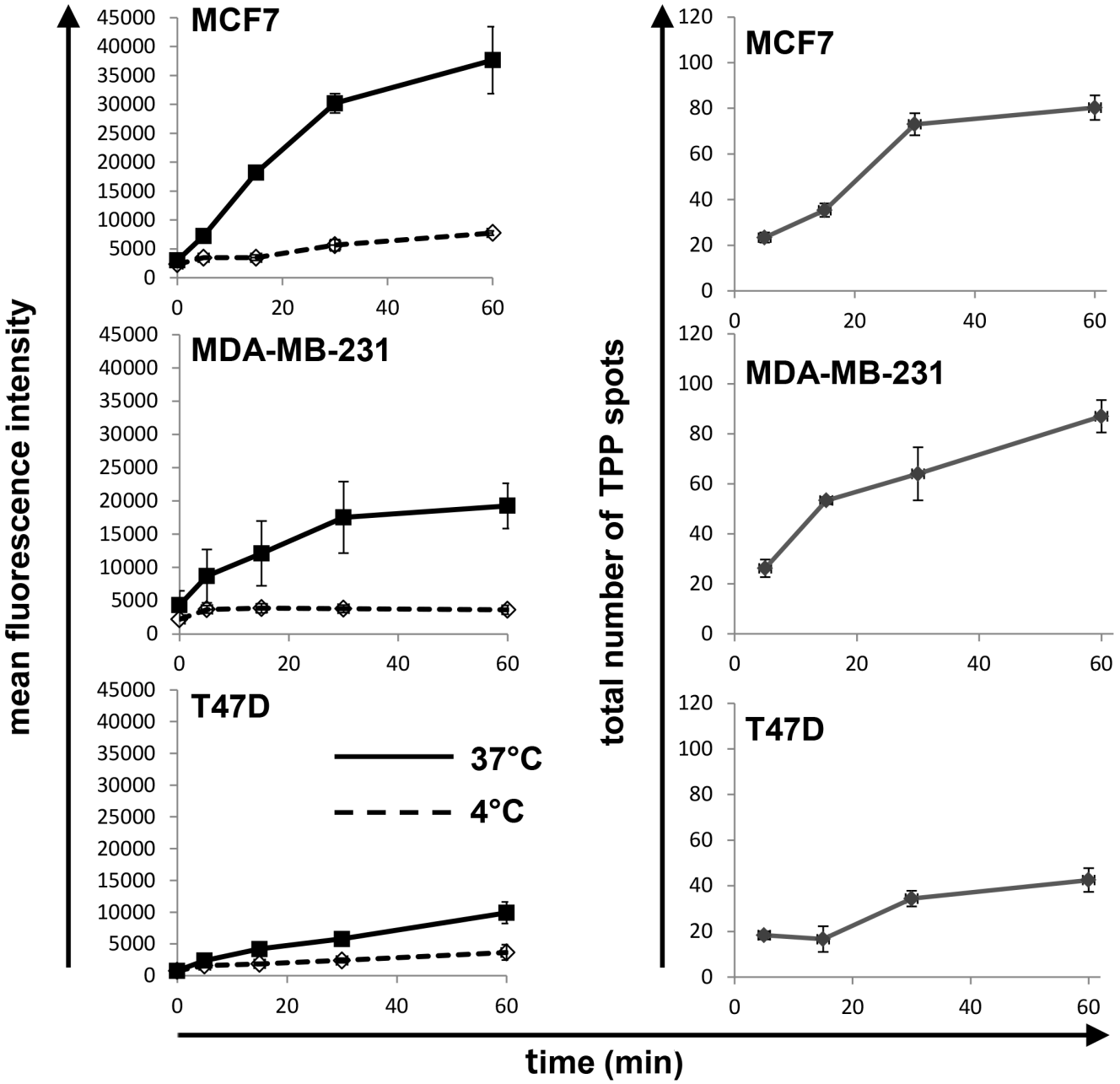

Figure 5. Kinetics of TPP internalization. (Left panel) Flow cytometric analysis of memHsp70 positive human breast cancer lines MCF7, MDA-MB-231, T47D reveals an accumulation of the fluorescence intensity after incubation with CF-labeled TPP at 37°C between 1 and 60 min (solid lines). At 4°C (dashed lines) mean fluorescence intensity remained low within the same time frame. Cell lines with a high percentage of Hsp70 membrane positive cells (MCF7, MDA-MB-231) exhibit a higher and more rapid uptake of TPP, whereas the cell line with low Hsp70 membrane expression (T47D) exhibits only a low uptake of TPP. (Right panel) Confocal microscopy images were analyzed to provide a total count of fluorescent spots per cell after incubation with the TPP at 37°C for 30 min. Although fluorescent spots progressively accumulated in all three cell lines, this was most apparent in the MCF7 and MDA-MB-231 cell lines that express higher levels of memHsp70 than T47D cells.
doi:10.1371/journal.pone.0105344.g005

specifically taken up via specialized receptors [7,8], and therapeutic peptides have been used in the treatment of breast [9] and other types of cancer [10]. Peptides, such as somatostatin, bombesin, cholecystokinin/gastrin, neurotensin and vasoactive intestinal peptide are currently under investigation for their possible clinical applications in nuclear oncology [11]. Despite the potential of these molecules, it remains essential that more universally expressed molecules which can be used as recognition structures for imaging and targeting agents are identified. One recognition structure which has significant potential as a target recognition structure in cancer is a membrane form of the 70 kDa heat shock (stress) protein family of molecules (heat shock protein 70, Hsp70, HSPA1A) [12–16].

Hsp70 is a cytoprotective molecule which is constitutively overexpressed in the cytoplasm of tumor cells [17]. Tumor cells overexpressing Hsp70 are resistant to radiation and cytostatic drugs [18]. In addition to being an intracellular molecule, we have previously reported that Hsp70 can also be selectively expressed

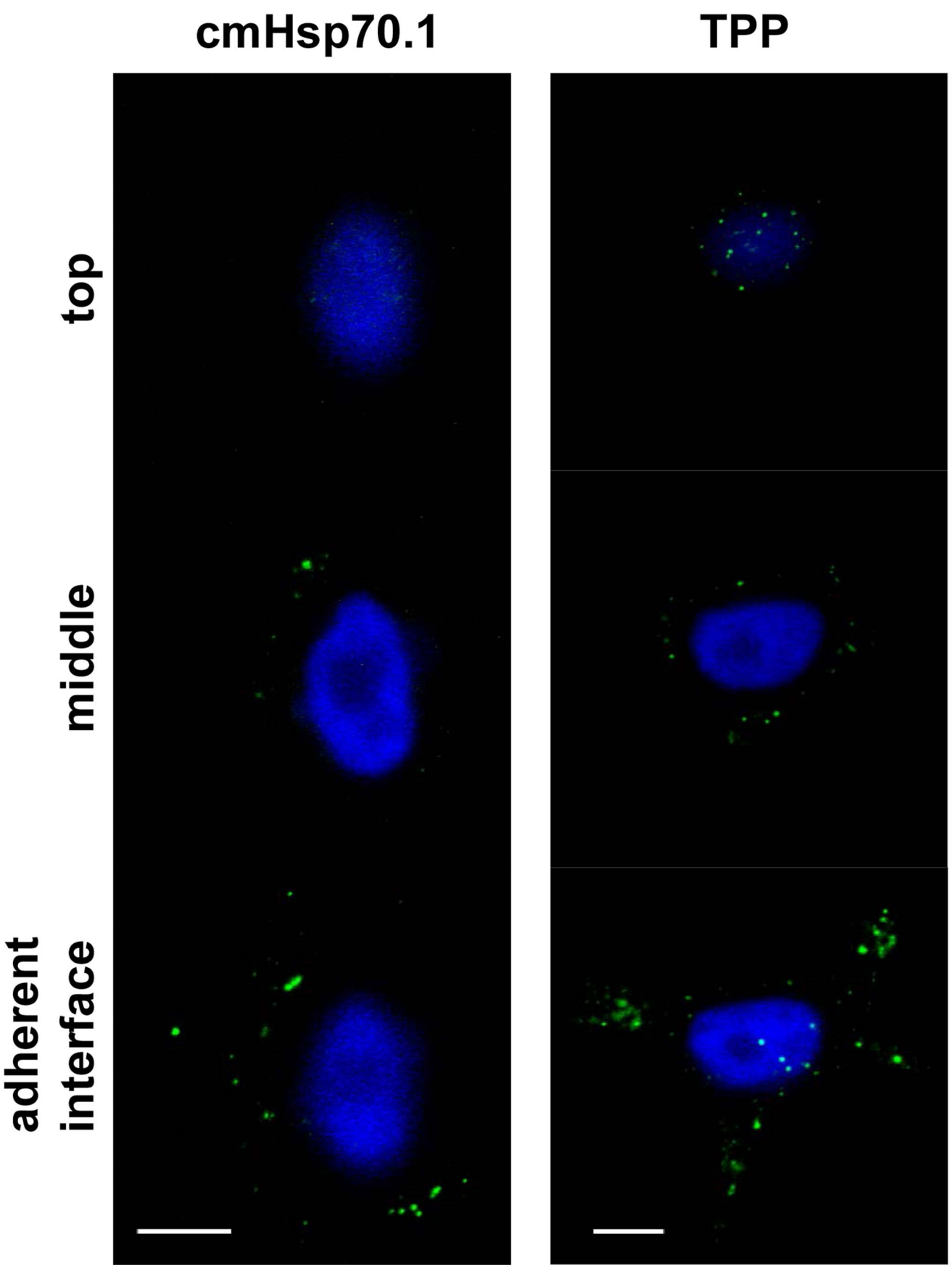
cmHsp70.1
TPP
top
middle
adherent interface

Figure 6. Internalization of TPP and cmHsp70.1 antibody via memHsp70 preferentially occurs at cellular adhesion points. Fluorescent vesicles are more prevalent towards the adherent interface of MCF7 cells after 30 min incubation at 37°C with cmHsp70.1 antibody (left panel) or TPP (right panel). Images are representative three-frame composites from the adherent surface, mid-way up the cell and at the apex. Objective 63×; scale bar 10 μm.
doi:10.1371/journal.pone.0105344.g006

on the plasma membrane of tumor cells using a unique mouse monoclonal antibody (clone cmHsp70.1, multimmune GmbH) which specifically recognizes the membrane form of Hsp70 [12–16,19,20]. The membrane expression of Hsp70 is independent of endoplasmic reticulum (ER) or Golgi apparatus dependent pathways [21], but does appear to be influenced by the lipid composition of the plasma membrane [22].

This membrane form of Hsp70 is widely expressed on cultured cancer cells, including leukemic cells [23,24], lung [12], colorectal [16,25], and breast cancer cells [19]. Furthermore, an ongoing screening program which currently includes the analysis of primary tumors from over 1,000 patients has demonstrated that this membrane form of Hsp70 is also present on approximately 50% of all tumor entities tested, including leukemia [26,27], melanoma [28], gastrointestinal [25] and breast tumors [29]. In contrast, cells from adjacent and other healthy tissues do not express the membrane form of Hsp70 [12–16]. Membrane-Hsp70 therefore appears to offer an ideal target for diagnostic, prognostic, and therapeutic approaches.

Previous experiments have shown that the cmHsp70.1 antibody can be taken up by the memHsp70+ murine colorectal cancer cell line CT26 and that its intracellular transportation occurs via endosomal pathways [30]. Furthermore, the cmHsp70.1 antibody can be used to image memHsp70+ tumors *in vivo* [20] and can induce antibody-dependent cellular cytotoxicity (ADCC) of memHsp70+ mouse tumor cells [19]. MemHsp70 also acts as a target recognition structure for recombinant human granzyme B, which is internalized and induces apoptosis without a requirement for perforin [29–31]. More recently, we observed that an Hsp70-derived 14-mer peptide (TPP) specifically binds to memHsp70+ tumor cells. Preliminary experiments revealed that the binding to Hsp70 is followed by a rapid and quantitative internalization of TPP, whereas scrambled peptides were not internalized. Since TPP is part of the oligomerization domain of Hsp70, we hypothesize that the binding of TPP to Hsp70 involves mechanisms that are related to the oligomerization domain of Hsp70. Furthermore, it appeared that the uptake and intracellular transport of TPP follows similar pathways as those for the cmHsp70.1 antibody.

Given the biodistribution advantages of peptides, this study examined the binding and internalization of the TPP to memHsp70+ cancer cell lines, *in vitro*. The specific binding of the TPP to tumor cells expressing the membrane form of Hsp70 and its uptake into these cells which is demonstrated indicates that this peptide is a promising imaging and therapeutic vehicle for targeting memHsp70+ tumor cells *in vivo*.

Materials and Methods

Cell lines

Human MCF7 (ATCC HTB-22), MDA-MB-231 (ATCC HTB-26), T47D (ATCC HTB-133) breast, CX-2 (TZB 61005), HCT116 (ATCC CCL-247) colon, Mel Ho (DSMZ ACC-62), Parl melanoma (kindly provided by Prof. J. Johnson, Institute of Immunology, Ludwig-Maximilians-Universität München, Munich), A549 (DSMZ MACC-107), H1339 (DSMZ ACC-506), EPLC-272H (DSMZ ACC-383) lung, FaDu (ATCC HTB-43) squamous carcinoma of the head & neck, and mouse 4T1 breast (4T1 wild type, 4T1 $Hsp70^{-/-}$ knock-out) cancer cell lines were grown in appropriate cell culture medium under standard conditions (37°C, 95% v/v humidity, 5% v/v CO_2) and passaged twice a week. Cells were used in exponential phase and their viability (>95%) confirmed prior to use using trypan blue dye exclusion. Cells were routinely tested to ensure the absence of mycoplasma.

Proteins and peptides

Recombinant His-tagged Hsp70 protein, which is equivalent to HSPA1A (P08107), was isolated from transfected Sf9 insect cells (Orbigen, San Diego, CA, U.S.A.), as described elsewhere [32]. Other recombinant HSP proteins including Hsp60 (ADI-NSP-540), Grp78 (ADI-SPP-765), Hsp27 (ADI-SPP-715) were obtained from Assay Designs (Ann Arbor, MI, U.S.A., now Enzo Life Sciences). Carboxyfluorescein (CF-) labeled 14-mer peptides TKDNNLLGRFELSG (TPP) and the scrambled peptide (scrambled) with identical amino acid composition NGLTLKNDFSRLEG were obtained from EMC microcollections (Tuebingen, Germany) at a purity >97%. Lyophilized peptides were reconstituted to a stock concentration of 1 mg/ml using distilled water and stored at 4°C for a period of no more than two weeks.

Antibodies

The expression of the membrane form of Hsp70 was determined using the memHsp70 specific murine monoclonal antibody cmHsp70.1-FITC (IgG1; multimmune GmbH, Germany). Monoclonal antibodies recognizing Rab4, Rab5, Rab7, Rab9 and Rab11 were obtained from Santa Cruz Biotechnology (Santa Cruz, CA, U.S.A.) and antibodies recognizing LAMP1 and LAMP2 were obtained from Sigma-Aldrich (St. Louis, MO, U.S.A.). Appropriate Cy3-conjugated anti-goat and anti-rabbit immunoglobulin secondary antibodies were obtained from Jackson ImmunoResearch (Newmarket, UK).

Peptide and antibody binding - flow cytometry

The expression of memHsp70 on tumor cell lines was determined by flow cytometry using either the FITC-conjugated cmHsp70.1 antibody or the CF-labeled 14-mer peptide TPP, both of which bind to the exposed sequence of memHsp70. Briefly, after incubation of viable cells (2×10^5 cells) with the antibody or peptide for 30 min at 4°C and following two washing steps, viable (propidium iodide negative) cells were analyzed using a FACSCalibur flow cytometer (BD Biosciences, Franklin Lakes, NJ, U.S.A.). An isotype-matched (IgG1) control antibody (BD Biosciences) was used to evaluate non-specific binding to cells.

Hsp70 knockout – CRISPR/Cas9 knockout of the genes Hspa1a and Hspa1b

Knockout of the neighbouring and closely homologous genes Hspa1a (ENSMUSG00000091971) and Hspa1b (ENSMUSG00000090877) in 4T1 tumor cells was achieved by double nicking of closely adjacent sites with CRISPR/Cas9. This DNA damage leads to DNA repair of the NHEJ type and generates small insertions or deletions (indel formation) that often

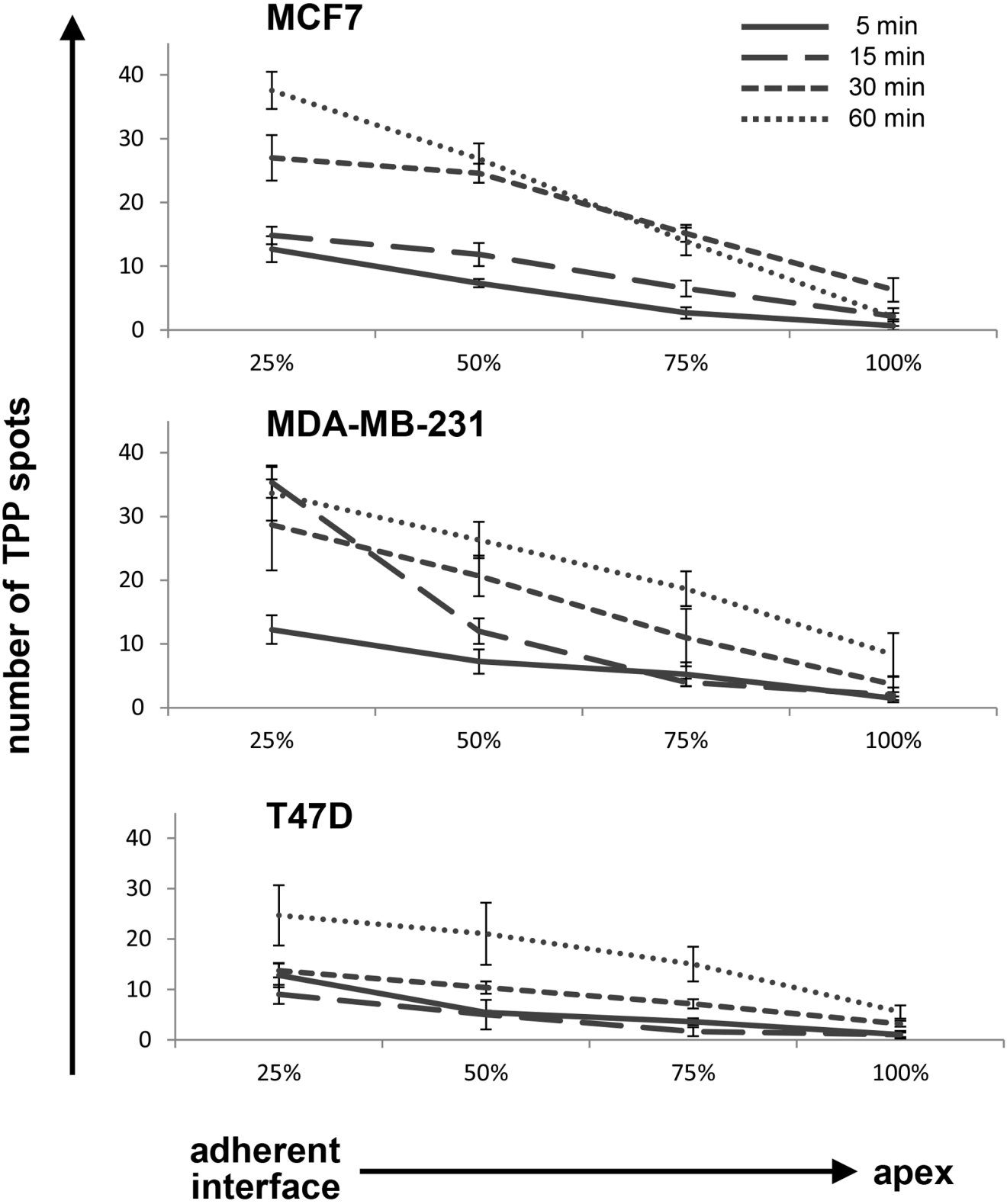

Figure 7. Localization of internalized TPP within cells. Confocal microscopy z-stacks were used to divide cells into quartiles using percentages of cell height from the adherent interface (0%) to the apex of the cells (100%). The number of fluorescent TPP spots in each quartile was counted in order to quantify the peptide distribution. For all time points and all cell lines investigated, TPP spots were found to be more prevalent in the quartile which included the adherent surface. This finding suggests that TPP is preferentially internalized and trafficked via this interface. The data shown are representative composite images of every z-stack frame counted in each quartile. Images were produced using a 63×/1.4 oil immersion lens on an inverted Zeiss 510 confocal microscope.
doi:10.1371/journal.pone.0105344.g007

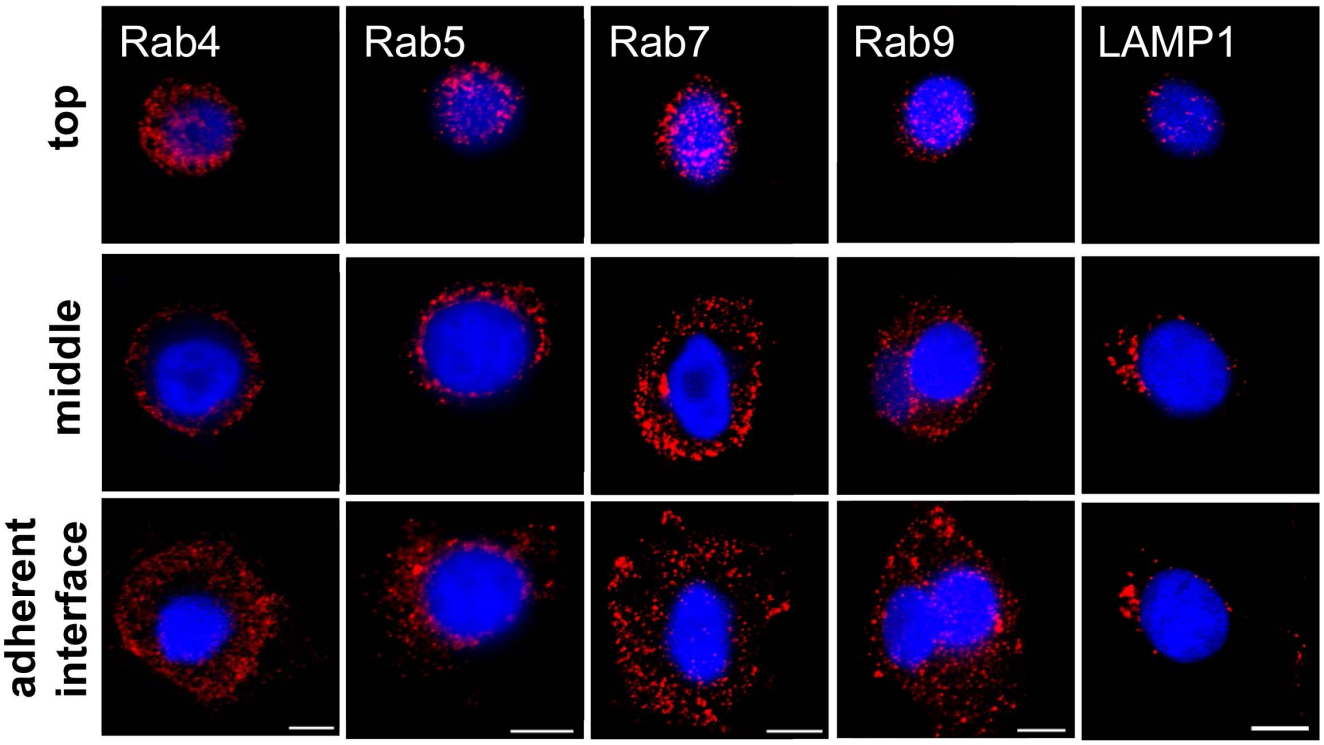

Figure 8. Distribution of intracellular vesicles in MCF7 cells. MCF7 tumor cells grown in glass-bottomed MatTek dishes for 48 h were fixed in paraformaldehyde, permeabilized and stained with primary antibodies specific for early (Rab4, Rab5), late (Rab7, Rab9) and recycling (Rab11) endosomes or lysosomes (LAMP1), followed by an appropriate Cy3-labeled secondary antibody (red). The nucleus was counter-stained with DAPI (blue). Representative three-frame composites from across the z-stack are shown. All of the vesicular markers assessed were found to be homogenously distributed throughout the cells. Objective 63×; scale bar 10 μm.
doi:10.1371/journal.pone.0105344.g008

results in frameshifts within the coding sequence (cds), and therefore knockout of gene expression [33].

To target both genes we selected two guide sequences using the CRISPR design tool [34] (guide-1 GATGCCGATCGCC-GTGTTCT; guide-2 GCACGGCGATCGGCATCGACC) that target the 5' region of the cds of both genes and cloned those into the vector pX462. 4T1 cells were transfected with a mixture of both vectors using Lipofectamine 2000 (Life Technologies, 250 ng each in a 24 well plate) and the transfected cells were put under puromycin selection (2.5 μg/ml) for two days. Single cells clones were generated by limiting dilution assays and tested for knockout of Hspa1a and Hspa1b expression with Western Blot analysis.

Western Blot analysis

Cells were lysed in TBST buffer (1% Triton X-100 in TBS, 1 mM PMSF, protease inhibitor cocktail) and protein content determined using the BCA Protein Assay kit (Pierce). For Western Blot analysis, proteins were detected with monoclonal antibodies directed against Hsp70 (cmHsp70.1, multimmune GmbH) and β-actin (Sigma). Bound antibodies were visualized using horseradish peroxidase-conjugated secondary antibodies (Dako) and a chemiluminescence developing kit (ECL, Amersham Biosciences).

Peptide ELISA

The *in vitro* binding of peptides to heat shock proteins was determined using a peptide ELISA. Briefly, Hsp70, Hsp60, Grp78, and Hsp27 proteins were coated onto 96-well MaxiSorp plates (Thermo Fisher Scientific, Roskilde, Denmark) at a concentration of 1 μg/well/100 μl in carbonate buffer (pH 9.6) at 4°C overnight. After washing, wells were blocked with phosphate buffered saline (PBS) containing 2% w/v bovine serum albumin (BSA) at room temperature for 2 h. Blocking buffer was discarded and wells were incubated with CF-labeled peptides (100, 50, 25 ng/ml) in a total volume of 100 μl at 27°C for 30 min. After another washing step the fluorescence resulting from specifically bound peptides was measured using a Victor X4 Multilabel Plate Reader (PerkinElmer, Waltham, MA, U.S.A.) equipped with appropriate filters.

Peptide uptake – flow cytometry

Cells were grown in T75 flasks for 48 h, at which time they were harvested using trypsin for 1 min at 37°C and counted using trypan blue dye exclusion. Viable cells (1×10^6 cells) were transferred into 1.5 ml microfuge tubes and washed with PBS (300 g, 5 min). CF-labeled TPP (20 μl, 75 μg/ml in PBS) was added to the cells and then the cell/peptide mixture was divided into two microfuge tubes (10 μl in each). One tube was kept on ice and the other put into the 37°C incubator. At the indicated time points (0, 5, 15, 30, 60 min), an aliquot of the cell suspension (2 μl) was transferred into 12×75 mm tubes containing 3 ml of chilled PBS. After washing twice (300 g, 5 min), cells were suspended in 250 μl chilled PBS at 4°C and analyzed on a BD FACSCalibur flow cytometer. Propidium iodide (PI) was added immediately prior to flow cytometric analysis in order to exclude non-viable cells from the analysis. Additionally, after incubation with TPP or scrambled control peptide (7.5, 75, or 750 μg/ml) for 24, 48, or 72 h cell viability was tested with the FITC Active Caspase-3 Apoptosis kit (BD Biosciences) or FlowCellect Cytochrome c kit (EMD Millipore Corporation, Hayward, CA, U.S.A.).

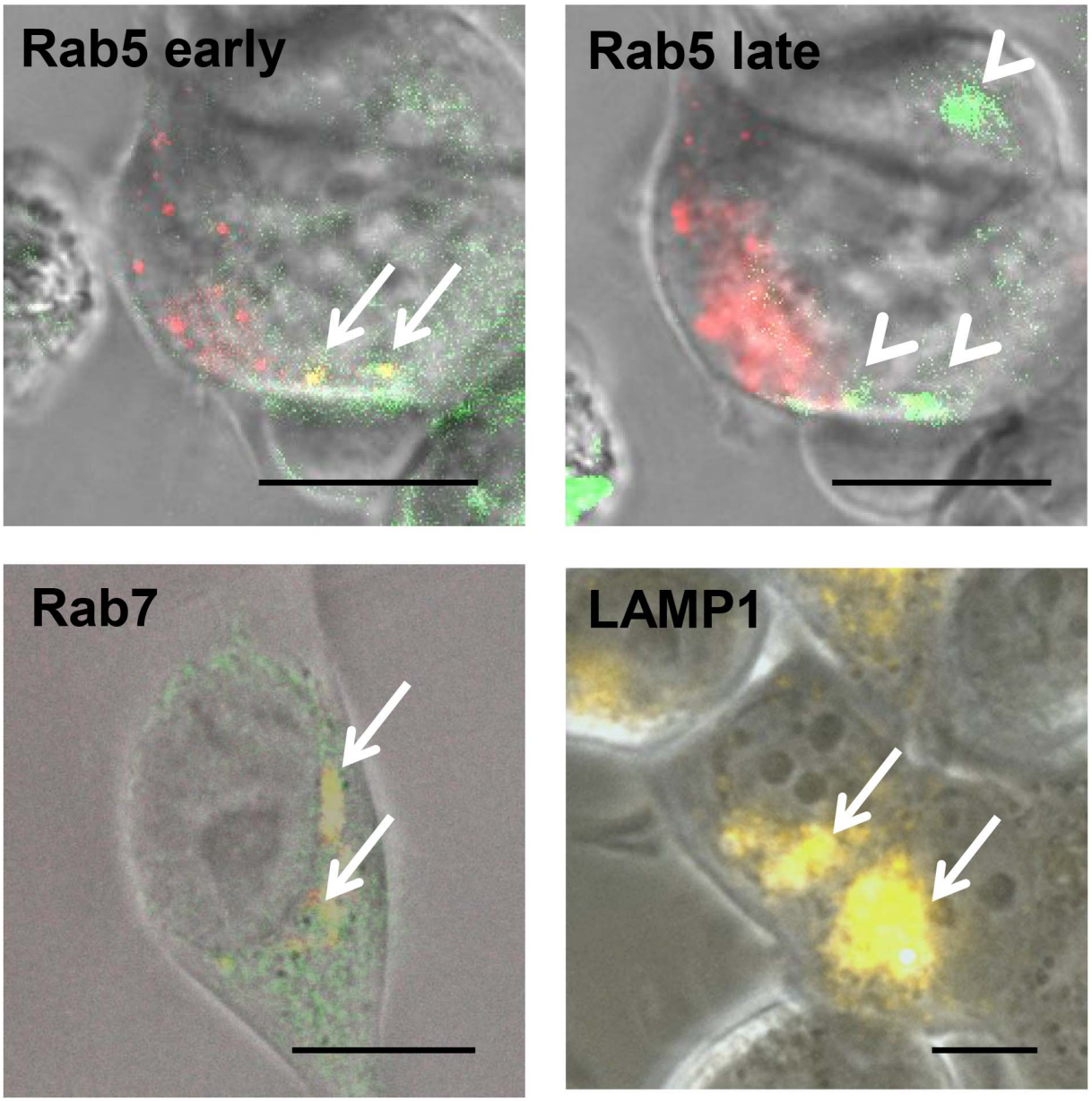

Figure 9. Uptake of TPP between 0 and 60 min follows an endosomal pathway. MCF7 cells take up CF-labeled TPP via an endosomal transport route in a time-dependent manner. Co-localization of TPP (green) with the endosomal marker proteins (Rab5, Rab7, LAMP1; each in red) is visible as a yellow signal. Co-localization of TPP with Rab5 can be seen within early endosomes at early time points (<30 min, arrows, upper left graph), but not at later time points (arrow heads, upper right graph). Between 30 and 60 min, TPP co-localizes with Rab7 vesicles (arrows, lower left graph). After 60 min, TPP co-localizes with LAMP1 positive lysosomes (arrows, lower right graph). Images are representative three-channel composites: brightfield, FITC, RFP. Objective 63×; scale bar 10 µm.
doi:10.1371/journal.pone.0105344.g009

Cells for analysis were identified on the basis of forward and side light scatter characteristics (FSC, SSC respectively) and confirmed as being single cells using the FSC-A(rea) and SSC-H(eight) parameters. Peptide uptake into viable cells was determined on the basis of the fluorescence intensity of the cell population.

Peptide uptake – confocal microscopy

Cells were grown in MatTek (Ashland, MA, U.S.A.) dishes for 48 h. Diluted peptide (100 µl, 75 µg/ml) was added to cells and the dishes were incubated at 37°C for 30 min. Cells were washed in 2 ml PBS at 4°C then fixed with 0.4% w/v paraformaldehyde (Sigma-Aldrich). Coverslips were detached by incubating dishes in 750 µl removal fluid (MatTek) for 20 min. The coverslips were then mounted onto clean microscopy slides using Vectashield Medium containing DAPI (Vector Laboratories, Burlingame, CA, U.S.A.). Coverslips were sealed using clear nail varnish and the slides were kept cool and protected from light until imaging could commence. Cells were imaged on a Zeiss Inverted 510 LSM microscope (Carl Zeiss AG, Oberkochen, Germany). A single frame overview was produced with the pinholes open, from which

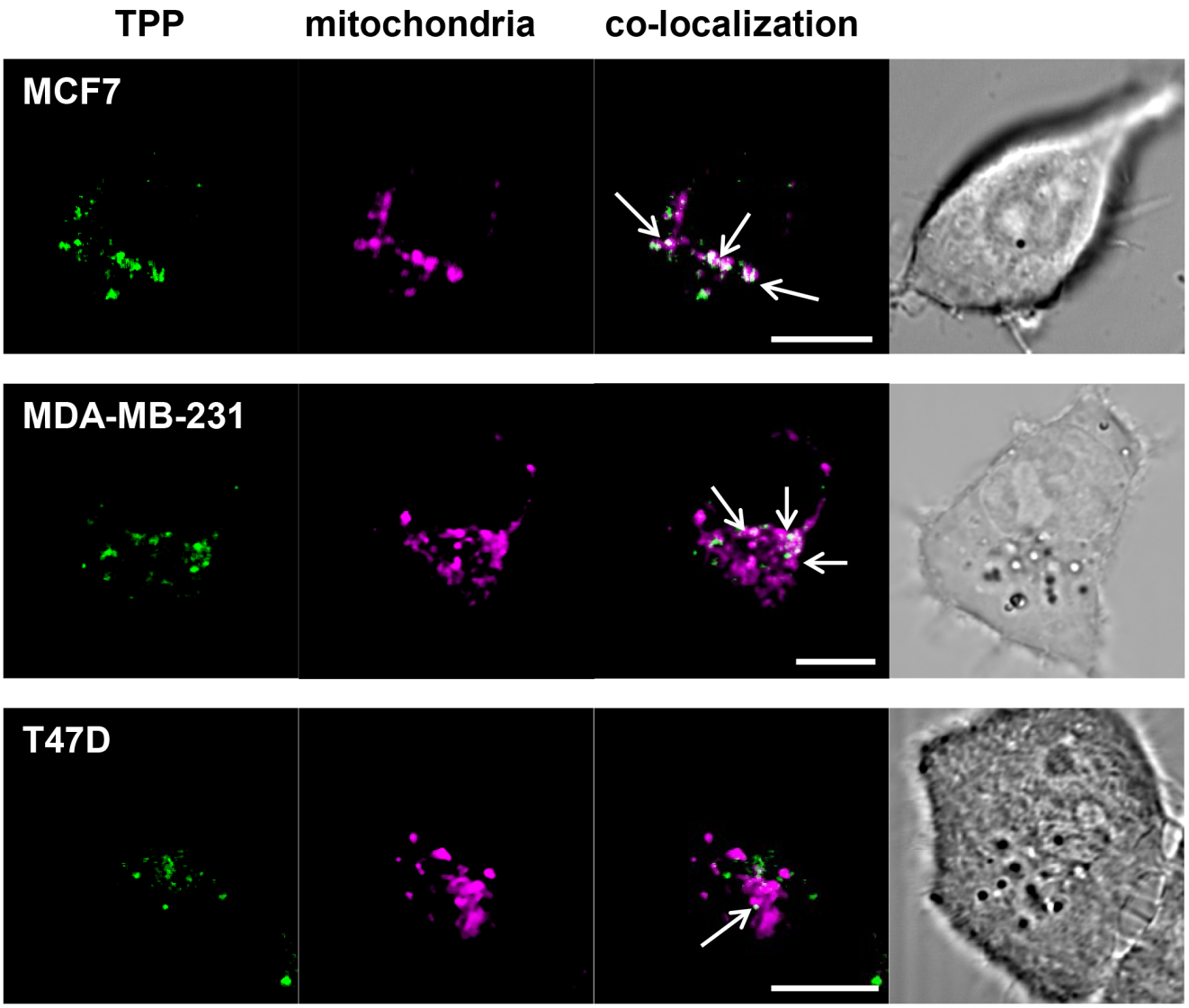

Figure 10. TPP co-localizes with mitochondria after 90 min. MCF7, MDA-MB-231, and T47D cells were incubated with CF-labeled TPP (green) for 90 min, stained with the mitochondrial detection dye Mito-ID (purple) and then imaged using confocal microscopy. A proportion of internalized TPP co-localizes with mitochondria in all three tumor cell lines (Pearson's coefficient: MCF7 r = 0.855, MDA-MB-231 r = 0.585, T47D r = 0.813). The Manders' M1 coefficient was used to estimate the proportion of total TPP that co-localizes with mitochondria (40% in MCF7 cells, M1 = 0.407; 44% in MDA-MB-231 cells, M1 = 0.443). In contrast, 14% of TPP was co-localized to mitochondria in T47D cells (M1 = 0.141). These findings correlate with the differential Hsp70 membrane expression levels of the respective cancer cell lines. Images are representative single frames. Objective 63×; scale bar 10 μm.
doi:10.1371/journal.pone.0105344.g010

individual cells were selected for z-stack imaging. The single frame image was produced using a 20×/0.8 dry objective at 2048×2048 resolution with 16× mean averaging. Z-stack images were obtained using a 63×/1.4 oil immersion objective at 2048×2048 resolution and 8× mean averaging.

Transfection of breast cancer cell lines

Co-localization of CF-labeled peptides with intracellular vesicles was determined using breast cancer cells which had been transfected to express red fluorescent protein (RFP) tagged marker proteins for early endosomes (Rab5), late endosomes (Rab7), or lysosomes (LAMP1) using 'CellLight Reagents *BacMam 2.0*' according the manufacturers' instructions (Molecular Probes, Life Technologies, Carlsbad, CA, U.S.A.). Briefly, cells were grown for 24 h to 50% confluency in MatTek chamber slides (Thermo Scientific, Rochester, NY, U.S.A.). The medium was removed and replaced with fresh medium containing 2 μg/ml transfection reagent with baculovirus containing sequences for the expression of RFP tagged marker proteins for Rab5, Rab7, or LAMP1. RFP could be detected in 70–90% of the cells 24 to 48 h after transfection and the staining was stable for at least 60 h in the cell lines used.

Peptide uptake – fluorescence microscopy

Cells transfected with endosomal or lysosomal markers were grown in chamber slides (Thermo Scientific, Rochester, NY, U.S.A.) for 24 h. Diluted CF-labeled peptide (75 μg/ml, 100 μl) was added to cells and the chamber slides were incubated at 37°C for the indicated time periods. Cells were washed three times with 0.5 ml PBS and imaged on a Zeiss Axio Observer Z1 microscope

(Carl Zeiss AG, Oberkochen, Germany). Z- and t-stack images were measured with a 63× long-distance objectives for different time periods and different settings. Images were taken in brightfield and FITC-, and RFP-channels. Multi-color images were produced by merging.

Imaging and software

Images were taken and processed using AxioVision Software, LSM Image Browser (Carl Zeiss AG, Oberkochen, Germany), or ImageJ (NIH, Bethesda, MD, U.S.A.) [35]. Image processing consisted of brightness and contrast adjustments, as well as running a noise reducing despeckling algorithm. Both Pearson's coefficient and Manders' M1 coefficient co-localization analyses [36] were conducted using the '*Just Another Co-localization Program*' (JACoP) plugin on ImageJ [37]. Further image processing - splitting each image into separate channels and setting fluorescence thresholds - was required prior to undertaking the co-localization analyses.

Statistics

The Student's *t*-test or factorial ANOVA were used, as appropriate, with the significance level set to $p<0.05$. Evaluation of the co-localization of CF-labeled TPP with mitochondria was calculated using Manders' M1 coefficient and Pearson's coefficient.

Miscellaneous

Chemicals or other material were obtained from Sigma Aldrich or Carl Roth GmbH (Karlsruhe, Germany).

Results

Tumor cell lines expressing membrane-Hsp70 (memHsp70) bind TPP

MemHsp70 expression by different human tumor cell lines and the relationship between memHsp70 expression and the ability to bind a 14-mer peptide TPP matching an epitope within the oligomerization domain of the Hsp70 molecule (aa 450–463 TKDNNLLGRFELSG, abbreviation TPP) were determined by flow cytometry at 4°C (**Fig. 1**). MemHsp70 is demonstrated on the basis of the mean fluorescence intensity of cmHsp70.1 antibody staining (open histograms in the top row of each display), with the proportion of cells exhibiting positive staining given in the upper right corner of each histogram (**Fig. 1**). The expression profiles varied between the different cell lines, even cells that have been derived from the same tumor entity. The flow cytometry experiments were all controlled using appropriate isotype-matched reagents (grayed histogram).

The binding profile of carboxyfluorescein (CF)-labeled TPP at 4°C was similar to that of the cmHsp70.1 antibody for all cell lines investigated (**Fig. 1**). No positive cell staining was observed when cells were incubated under identical conditions with a CF-labeled peptide consisting of the same amino acids, but in scrambled order (data not shown).

Specificity of TPP binding to Hsp70

Knockout experiments revealed that Hsp70 was present in whole cell lysates of the 4T1 wild type (4T1 wt) cell line, but not in the Hsp70 knockout cell line 4T1 Hsp70$^{-/-}$, as determined with the Hsp70 specific monoclonal antibody cmHsp70.1 (**Fig. 2A**) and SPA810 antibody (data not shown). Specific binding of CF-labeled TPP to memHsp70 was proven by immunofluorescence staining (**Fig. 2B**) and flow cytometric analysis (**Fig. 2C**). CmHsp70.1-FITC antibody as well as TPP showed specific staining of viable 4T1 wt cells (**Fig. 2B**, left panel), but not of 4T1 Hsp70$^{-/-}$ cells (**Fig. 2B**, right panel). These data were confirmed by flow cytometric analysis. The proportion of Hsp70 positively stained 4T1 wt cells was comparable after incubation with cmHsp70.1-FITC antibody and TPP (**Fig. 2C**, upper panel). In contrast, 4T1 Hsp70$^{-/-}$ cells did not show any staining with both Hsp70 reagents (**Fig. 2C**, lower panel).

The binding capacity of TPP to different heat shock proteins was assessed using a peptide enzyme linked immunoassay (ELISA). For this, Hsp70, Hsp60, Grp78, or Hsp27-coated plates were incubated with CF-labeled TPP or scrambled peptide (27°C for 30 min) at the indicated concentrations (100, 50, 25 ng/ml) and the resultant fluorescence was measured using a multilabel reader. A strong concentration- and time-dependent signal was detectable when TPP was incubated with Hsp70-coated microtiter plates (**Fig. 3** left hand bars; 1,200 ± 154 counts). Peptide binding to Hsp70 was specific, as only a very weak background binding of scrambled peptide was observed (384±119 counts). Furthermore, although there was some interaction between the highest concentration of TPP (100 ng/ml) and Hsp60-, Grp78- or Hsp27-coated microtiter plates (638±154, 566±189, 474±177 counts, respectively, **Fig. 3**, right hand bars), other concentrations of TPP resulted in signals that were similar to those measured following incubation with the scrambled peptide (384±119 counts) (**Fig. 3**, left hand bars).

Internalization of TPP and its relationship with the memHsp70 status

Since the specific binding of TPP to Hsp70 could be shown using the ELISA (**Fig. 3**) and the flow cytometry analysis of tumor cell lines (**Fig. 1**), the dependency of peptide binding is dependent on the Hsp70 membrane expression of cells, the internalization of peptide into tumor cells was assessed using a panel of breast cancer cell lines which exhibit differences in their Hsp70 membrane expression profiles. A lower proportion of T47D cells exhibit memHsp70 expression in culture (~29%), as compared with MDA-MB-231 and MCF7 cells (75% or 82%, respectively) (**Fig. 1**). The internalization of TPP by MCF7, MDA-MB-231 and T47D cells was examined by confocal microscopy using a Zeiss 510 inverted confocal microscope (**Fig. 4**). Initially, tile scans using an open pinhole on the microscope to maximize detected light were produced in order to provide an overview of the internalization (**Fig. 4A**). Incubation with TPP resulted in green fluorescent spots in all of the human breast tumor cell lines (**Fig 4A**, right column), whereas no internalization of the scrambled peptide could be detected (**Fig 4A**, left column). The appearance of the peptide (green) in well-defined areas suggests that it is not randomly distributed within the cytoplasm, but that it is associated with intracellular vesicles. The representative images shown were taken through a 20× objective and subjected to brightness, contrast and noise processing in ImageJ. The internalization of CF-labeled TPP was confirmed by creating z-stacks of individual cells (**Fig. 4B**). MCF7 and MDA-MB-231 cells, which express high amounts of Hsp70 on their plasma membrane, contained a large amount of green fluorescent spots (**Fig. 4B**, left column, top and middle panel), whereas the internalization of TPP by T47D cells was much less pronounced (**Fig. 4B**, left column, bottom panel). Images shown are representative three-frame composites from approximately mid-way up the stack. Brightfield images (**Fig. 4B**, right column) confirmed that imaged cells were morphologically healthy/normal.

Rapid uptake of TPP into memHsp70+ tumor cells

To further quantify the uptake of CF-labeled TPP, the internalization was monitored using flow cytometry. For these experiments, cells were incubated with the peptide for up to 60 min at either 37°C (to allow internalization, solid lines) or 4°C (to allow surface binding only, dashed lines) (**Fig. 5**, left column). The uptake of TPP is seen as an increase of the mean fluorescence intensity (mfi) of the cell population over time. At 4°C there is only surface binding and no progressive increase in the fluorescent intensity, with the mfi of all cell lines being less that 5,000 (**Fig. 5**, left column, dashed line). The cell lines with the highest expression of memHsp70 exhibited the greatest uptake of TPP (MCF7: mfi of 37,637±5,800 after 60 min and MDA-MB-231: mfi of 19,261±3,408 after 60 min; **Fig. 5** left column, top and middle panels). The cell line with the lowest expression of memHsp70 (T47D) exhibited the lowest uptake of TPP (mfi 9,900±1,358 after 60 min; **Fig. 5**, left column, bottom panel). The half-maximum time points are approximately 20 min for all three cell lines (data not shown).

The number of fluorescent spots per cell was also manually counted. The cell lines expressing the highest level of memHsp70 (MCF7, MDA-MB-231) contained around 80 fluorescent TPP spots per cell after 60 min (**Fig. 5**, right column, top panels), whereas the number of spots in the T47D cells was around 50% of this (**Fig. 5**, right column, bottom panel). Again half-maximum time-points for the internalization signal were around 20 min for all three cell lines (data not shown).

Taken together, these data demonstrate a rapid memHsp70 dependent uptake of TPP into breast cancer tumor cells.

Internalization of TPP by memHsp70 expressing cells preferentially occurs at the cell adhesion interface

Across all tumor cell lines and all time points, the greatest number of fluorescent spots was present in the first quartile of the distance between the adherent and non-adherent surfaces of the cell. However, brightfield imaging of the cells (**Fig. 4B**, right column) did not allow accurate measurements of the cell size to be made, and the capacity to definitively interpret the data by normalizing spot number to cross-sectional area is therefore limited. Confocal fluorescence imaging shows that the green spots were visible in MCF7 cells after 30 min incubation with CF-labeled TPP (**Fig. 6**). The number of green spots increases as the focusing plane moves from the top to the bottom (adherent surface) of the cells (**Fig. 6**, from the top down to the bottom panels). Furthermore, there is no obvious difference in staining of FITC-labeled cmHsp70.1 (**Fig. 6**, left column) compared to TPP (**Fig. 6**, right column). Images shown are representative three-frame compositions, from the point of adherence, halfway up the cell and the apex (objective 63, scale bar 10 μm). Similar staining patterns were also observed for MDA-MB-231 and T47D cells (data not shown).

We further evaluated the preferential, intracellular location of internalized CF-labeled TPP by developing an approach to quantify the number of TPP spots throughout the cell. Using confocal microscopy derived z-stacks cells were divided into quartiles from the adherent surface (0%) of the cell to its apex (100%). The number of fluorescent spots in each quartile was counted in order to quantify the localization of TPP within the cells. The maximum number of fluorescent spots (vesicles) at the adherent surface after 60 min was 38±3 in MCF7 cells (**Fig. 7**, top diagram), 34±4 in MDA-MB-231 cells (**Fig. 7**, middle diagram), and 24±6 in T47D cells (**Fig. 7**, bottom diagram). For all time points and all cell lines investigated, the greatest number of fluorescent spots was present in the quartiles adjacent to the adherent surface (MCF7 $p<0.001$, MDA-MB231 $p<0.01$, T47D $p<0.05$, Factorial ANOVA). These findings indicate that TPP is continually internalized via this interface and confirm that there a time-dependent uptake and accumulation of TPP in distinct intracellular vesicles which appears to preferentially occur at the adherent interface.

Endosomal vesicles show distinct patterns in MCF7 cells

As the distinct fluorescent patterning of internalized CF-labeled TPP is suggestive of its association with intracellular vesicles, one possible explanation for the greater accumulation of TPP close to the adherent surface of the cells would be that intracellular vesicles are also preferentially localized to this region of the cell. In order to examine this potential explanation, MCF7 cells were grown in glass-bottomed MatTek dishes for 48 h, at which time they were fixed in paraformaldehyde, permeabilized and stained with primary antibodies that were specific for early endosomes (Rab4, Rab5), late (Rab7, Rab9) endosomes or lysosomes (LAMP1), followed by an appropriate Cy3-labeled secondary antibody (**Fig. 8**). The vesicular marker proteins showed a widespread distribution throughout the cell, and it was not evident that any given vesicle population was highly localized, particularly near the adherent surface (**Fig. 8**).

Uptake of TPP via memHsp70 follows an endosomal pathway

The apparent uniform distribution of endosomal and lysosomal vesicles throughout the cells provides no insight into the final trafficking of CF-labeled TPP. Difficulties were encountered when trying to co-stain cells that had been incubated with TPP with antibodies to endosomal and lysosomal markers (possibly as a result of peptide leakage from permeabilized cells). Therefore, cells were transfected with vectors expressing red fluorescent protein (RFP)-labeled marker proteins in order to identify different vesicles - Rab5 for early endosomes, Rab7 for late endosomes and LAMP1 for lysosomes. Rab5 staining reveals small vesicles near the plasma membrane (**Fig. 9**, upper left graph). Vesicles expressing Rab7 localize between plasma membrane and nucleus (**Fig. 9** lower left graph). LAMP1 staining is detectable in large structures with perinuclear localization (**Fig. 9** lower right graph).

MCF7 cells took up TPP via endosomal transport routes in a time-dependent manner. Co-localization of TPP (green) with early and late endosomal and lysosomal marker proteins (Rab5, Rab7, LAMP1; each in RFP) was visible as a yellow signal. Co-localization of TPP with Rab5 (early endosomes) was detected at time points <30 min (**Fig. 9**, upper left graph). At later time points (<30 min), the yellow signals disappeared, leaving green staining for TPP and red staining for Rab5 (**Fig. 9**, upper right graph). Subsequently (between 30 and 60 min), co-staining of TPP occurs with Rab7 vesicles (**Fig. 9,** lower left graph). TPP is co-localized with LAMP1 vesicles at time points >60 min, indicating transport of TPP into lysosomes (**Fig. 9**, lower right graph).

Internalized TPP co-localizes to the mitochondria after 90 min

In order to measure whether internalized TPP (green) localizes to mitochondria, MCF7, MDA-MB-231 and T47D cells were incubated with TPP and co-stained using the mitochondrial detection dye Mito-ID (magenta) (**Fig. 10**). Cells were imaged using confocal microscopy and subsequent co-localization statistics confirm that TPP localizes to the mitochondria in all three cell lines. The Pearson's r coefficients for MCF7, MDA-MB-231 and T47D cells were 0.855 (**Fig. 10**, top row), 0.585 (**Fig. 10**, middle

row) and 0.813 (**Fig. 10**, bottom row) respectively. An estimation of the proportion of the total TPP that was co-localized with the mitochondria was obtained by calculating the Manders' M1 coefficient. Using this approach, 40–45% of TPP localized to the mitochondria in MCF7 and MDA-MB-231 cells (MCF7, M1 = 0.407, MDA-MB-231, M1 = 0.443), whereas only 14.1% of the TPP co-localized with mitochondria in T47D cells (M1 = 0.141). Again, this correlates with the memHsp70 expression profile of the cells.

Discussion

Breast cancer is the most common tumorigenic malignancy for women in Western countries and is the primary cause of mortality [38,39]. Immunotherapy and targeting mammary-specific targets using antibodies or small molecules coupled with cytotoxic substances offer a good adjunct to standard protocols including surgery, cytotoxic drugs, endocrine therapy and radiation therapy [40]. Although new drugs are in development [41], the heterogeneity of cancer resulting from mutated genes, the differential expression of specific surface molecules, and/or the status of patients with regards to the stage and subtype of disease, makes it difficult to develop molecules and agents with broad specificity across individual patient groups [42]. Interest in the use of peptides as agents for imaging and the specific delivery of therapeutic agents to tumors is therefore growing [11,43–46].

Peptides offer a number of advantages such as better biodistribution profiles and a greater ability to penetrate tissues. The efficacy of peptides for anti-cancer therapies is often dictated by their ease of binding and uptake into tumor cells. As examples, cathelicidin is been a potential therapeutic peptide for gastrointestinal inflammation and cancer [47] and a 15-mer peptide from the follicle-stimulating hormone support the anti-tumor activity of paclitaxel nanoparticles against ovarian cancers [48]. The cancer-specific peptide BR2 penetrates cancer cells, and has been shown to mediate the delivery of a scFv into cancer cells [49]. The therapeutic capabilities of peptides have been demonstrated by a report of a peptide which is able to induce apoptosis in SKOV3 cells by down-regulating Bcl-2 [50]. The kinetics of peptide uptake has been studied in lymphocytes and monocytes [51].

Interestingly, peptides have also been shown to facilitate the delivery of larger molecules. Nanostructured lipid carriers bound to small 5-mer peptides are taken up by EGFR-overexpressing tumors *in vivo* [52] and such peptides might therefore support the targeted delivery of chemotherapeutic agents. Novel peptides are also being used as targeted drug delivery systems for breast cancer therapy and also for tumor imaging strategies [53]. A telomerase-derived peptide has been shown to increase the cytosolic delivery of macromolecules by heat shock mediated cell penetration [54]. Other studies support the use of peptides as lead compounds for anti-cancer therapy. For example a yeast two-hybrid screening has identified peptide aptamers which bind to Hsp70 and specifically inhibit chaperone activity, thereby increasing sensitivity to drug-induced apoptosis [55].

For the first time we have shown that a 14-mer peptide TPP derived from the native Hsp70 protein can specifically recognize and target tumor cells expressing the membrane form of Hsp70. Given the selective, but widespread, expression of memHsp70 on tumor cells, but not their non-malignant counterparts [14,56–58] appropriately formulated TPP could offer a promising new clinically relevant small molecule for imaging and/or specifically targeting tumors. TPP has advantages over other peptides that are currently being evaluated, as the latter are restricted to targeting specific receptors on specific types of tumor cells [7–11]. Another potential advantage of TPP as a therapeutic vehicle is that memHsp70 is expressed on a large proportion of tumors and its expression on tumor cells can be induced/increased using relevant chemotherapeutic agents [59] and radiation therapy [60]. The proportion of patients to which the TPP can be administered can therefore be increased by standard therapies.

Fluorescence microscopy has previously revealed the internalization of Hsp70 and granzyme B (GrB) into the CT26 murine colon cancer cell line involves Rab and LAMP dependent vesicles [30], and we therefore anticipated that the internalization of TPP also involves an endosomal pathway which is associated with Rab proteins inside tumor cells. Endosomes are intracellular vesicles that are responsible for the transport of molecules between different intracellular compartments [61], and they can be described as early endosomes (EE), late endosomes (LE), and recycling endosomes (RE) [62]. The endosomal vesicles are also linked to the endoplasmic reticulum and the trans-Golgi network [62]. Lysosomes are thought to collaborate with endosomal transport routes to generate final vesicles in which molecules are deconstructed or catabolized [63,64]. Monomeric GTPase proteins (Rab) [61] within the membranes of endosomes are responsible for transport, docking, and merging, and these can also serve as targets for imaging. Currently, around 40 different Rab proteins have been described in mammals. As typical marker proteins, Rab5 is described for early endosomes [65], Rab7 for late endosomes [65,66], and Rab11 for recycling endosomes [67,68]. Lysosome associated proteins (LAMP) are integral membrane proteins which stabilize lysosomal membranes [69], with both LAMP1 and LAMP2 being typically used for identifying lysosomes [64].

Gold-nanoparticles coated with pro-apoptotic peptides can damage mitochondria [70] and gold-peptide nano-assemblies targeting mitochondria have been shown to have more pronounced cancer cell killing properties [71]. Alternatively, ionidamine liposomes can be used to enhance the treatment of drug-resistant cancers by acting on mitochondrial signaling pathways [72], or by delivering the redox cycler doxorubicin, as a source of ROS production, to cancer cell mitochondria [73]. Retinoblastoma protein directly induces apoptosis at the mitochondria [74]. Cytotoxic drugs can exert their apoptotic function at the level of the mitochondria, as has been illustrated by the direct influence of Doxorubicin on mitochondria-initiated apoptosis [75]. The mechanisms of action have been elucidated using a number of different approaches, an example of which has been observing the translocation of a peptide through mitochondrial membranes using NMR observing the translocation of a peptide through mitochondrial membranes [76]. Other peptides show anti-tumor activity by directly targeting the mitochondrial membrane and inducing apoptosis [77,78]. With regards to TPP, to date we have been unable to detect a direct apoptotic activity on the basis of cytochrome c release or active caspase-3 staining in breast cancer cell lines at concentrations up to 750 μg/ml and up to 72 h after incubation (data not shown). Targeting the mitochondrial membrane might be useful for the optical imaging of tumors, including breast cancer cells in xenograft mouse models [79]. We are therefore investigating the use of TPP as an imaging and therapeutic agent in murine tumor models (manuscript in preparation).

In summary, this study demonstrates the specific binding and internalization of TPP by different cancer cells expressing the membrane form of Hsp70. TPP might therefore have potential as an agent for targeting and imaging the large proportion of tumors (~50%) which express Hsp70 on their plasma membrane.

Author Contributions

Conceived and designed the experiments: GM. Performed the experiments: MG GAF SB GM SS. Analyzed the data: MG GAF SB GM SS. Contributed reagents/materials/analysis tools: GM RR RO SS. Contributed to the writing of the manuscript: GM MG GAF AGP SS.

References

1. Xin L, Cao J, Cheng H, Zeng F, Hu X, et al. (2013) Human monoclonal antibodies in cancer therapy: a review of recent developments. Front Biosci 18: 765–772.
2. Barbet J, Bardies M, Bourgeois M, Chatal JF, Cherel M, et al. (2012) Radiolabeled antibodies for cancer imaging and therapy. Methods Mol Biol 907: 681–697.
3. Baeuerle PA, Itin C (2012) Clinical experience with gene therapy and bispecific antibodies for T cell-based therapy of cancer. Curr Pharm Biotechnol 13: 1399–1408.
4. Vacchelli E, Eggermont A, Galon J, Sautes-Fridman C, Zitvogel L, et al. (2013) Trial watch: Monoclonal antibodies in cancer therapy. Oncoimmunology 2: e22789.
5. Copeland A, Younes A (2012) Current treatment strategies in Hodgkin lymphomas. Curr Opin Oncol 24: 466–474.
6. Murphy CG, Morris PG (2012) Recent advances in novel targeted therapies for HER2-positive breast cancer. Anticancer Drugs 23: 765–776.
7. Askoxylakis V, Mier W, Zitzmann S, Ehemann V, Zhang J, et al. (2006) Characterization and development of a peptide (p160) with affinity for neuroblastoma cells. J Nucl Med 47: 981–988.
8. Zitzmann S, Kramer S, Mier W, Hebling U, Altmann A, et al. (2007) Identification and evaluation of a new tumor cell-binding peptide, FROP-1. J Nucl Med 48: 965–972.
9. Kaumaya PT, Foy KC (2012) Peptide vaccines and targeting HER and VEGF proteins may offer a potentially new paradigm in cancer immunotherapy. Future Oncol 8: 961-987.
10. Bidwell GL (2012) Peptides for cancer therapy: a drug-development opportunity and a drug-delivery challenge. Ther Deliv 3: 609–621.
11. Okarvi SM (2008) Peptide-based radiopharmaceuticals and cytotoxic conjugates: potential tools against cancer. Cancer Treat Rev 34: 13–26.
12. Botzler C, Issels R, Multhoff G (1996) Heat-shock protein 72 cell-surface expression on human lung carcinoma cells in association with an increased sensitivity to lysis mediated by adherent natural killer cells. Cancer Immunol Immunother 43: 226–230.
13. Botzler C, Schmidt J, Luz A, Jennen L, Issels R, et al. (1998) Differential Hsp70 plasma-membrane expression on primary human tumors and metastases in mice with severe combined immunodeficiency. Int J Cancer 77: 942–948.
14. Multhoff G (2007) Heat shock protein 70 (Hsp70): membrane location, export and immunological relevance. Methods 43: 229–237.
15. Multhoff G, Botzler C, Jennen L, Schmidt J, Ellwart J, et al. (1997) Heat shock protein 72 on tumor cells: a recognition structure for natural killer cells. J Immunol 158: 4341–4350.
16. Multhoff G, Botzler C, Wiesnet M, Muller E, Meier T, et al. (1995) A stress-inducible 72-kDa heat-shock protein (HSP72) is expressed on the surface of human tumor cells, but not on normal cells. Int J Cancer 61: 272–279.
17. Lee SJ, Choi SA, Lee KH, Chung HY, Kim TH, et al. (2001) Role of inducible heat shock protein 70 in radiation-induced cell death. Cell Stress Chaperones 6: 273–281.
18. Gehrmann M, Marienhagen J, Eichholtz-Wirth H, Fritz E, Ellwart J, et al. (2005) Dual function of membrane-bound heat shock protein 70 (Hsp70), Bag-4, and Hsp40: protection against radiation-induced effects and target structure for natural killer cells. Cell Death Differ 12: 38–51.
19. Stangl S, Gehrmann M, Riegger J, Kuhs K, Riederer I, et al. (2011) Targeting membrane heat-shock protein 70 (Hsp70) on tumors by cmHsp70.1 antibody. Proc Natl Acad Sci U S A 108: 733–738.
20. Stangl S, Gehrmann M, Dressel R, Alves F, Dullin C, et al. (2010) *In vivo* imaging of CT26 mouse tumors by using cmHsp70.1 monoclonal antibody. J Cell Mol Med 15: 874–887.
21. Broquet AH, Thomas G, Masliah J, Trugnan G, Bachelet M (2003) Expression of the molecular chaperone Hsp70 in detergent-resistant microdomains correlates with its membrane delivery and release. J Biol Chem 278: 21601–21606.
22. Gehrmann M, Liebisch G, Schmitz G, Anderson R, Steinem C, et al. (2008) Tumor-specific Hsp70 plasma membrane localization is enabled by the glycophospholipid Gb3. PLoS ONE 3: e1925.
23. Hantschel M, Pfister K, Jordan A, Scholz R, Andreesen R, et al. (2000) Hsp70 plasma membrane expression on primary tumor biopsy material and bone marrow of leukemic patients. Cell Stress Chaperones 5: 438–442.
24. Multhoff G (1997) Heat shock protein 72 (HSP72), a hyperthermia-inducible immunogenic determinant on leukemic K562 and Ewing's sarcoma cells. Int J Hyperthermia 13: 39–48.
25. Pfister K, Radons J, Busch R, Tidball JG, Pfeifer M, et al. (2007) Patient survival by Hsp70 membrane phenotype: association with different routes of metastasis. Cancer 110: 926–935.
26. Gehrmann M, Schmetzer H, Eissner G, Haferlach T, Hiddemann W, et al. (2003) Membrane-bound heat shock protein 70 (Hsp70) in acute myeloid leukemia: a tumor specific recognition structure for the cytolytic activity of autologous NK cells. Haematologica 88: 474–476.
27. Steiner K, Graf M, Hecht K, Reif S, Rossbacher L, et al. (2006) High HSP70-membrane expression on leukemic cells from patients with acute myeloid leukemia is associated with a worse prognosis. Leukemia 20: 2076–2079.
28. Farkas B, Hantschel M, Magyarlaki M, Becker B, Scherer K, et al. (2003) Heat shock protein 70 membrane expression and melanoma-associated marker phenotype in primary and metastatic melanoma. Melanoma Res 13: 147–152.
29. Gehrmann M, Doss BT, Wagner M, Zettlitz KA, Kontermann RE, et al. (2011) A novel expression and purification system for the production of enzymatic and biologically active human granzyme B. J Immunol Methods 371: 8–17.
30. Gehrmann M, Stangl S, Kirschner A, Foulds GA, Sievert W, et al. (2012) Immunotherapeutic targeting of membrane-Hsp70 expressing tumors using recombinant human granzyme B. PLoS One 7: e41341.
31. Gross C, Koelch W, DeMaio A, Arispe N, Multhoff G (2003) Cell surface-bound heat shock protein 70 (Hsp70) mediates perforin-independent apoptosis by specific binding and uptake of granzyme B. J Biol Chem 278: 41173–41181.
32. Schilling D, Gehrmann M, Steinem C, De MA, Pockley AG, et al. (2009) Binding of heat shock protein 70 to extracellular phosphatidylserine promotes killing of normoxic and hypoxic tumor cells. FASEB J 23: 2467–2477.
33. Ran FA, Hsu PD, Lin C-Y, Gootenberg JS, Konermann S, et al. (2013) Double nicking by RNA-guided CRISPR Cas9 for enhanced genome editing specificity. Cell 154: 1380–1389.
34. Hsu PD, Scott DA, Weinstein JA, Ran FA, Konermann S, et al. (2013) DNA targeting specificity of RNA-guided Cas9 nucleases. Nat Biotechnol 31: 827–832.
35. Schneider CA, Rasband WS, Eliceiri KW (2012) NIH Image to ImageJ: 25 years of image analysis. Nat Methods 9: 671–675.
36. Manders EMM, Verbeek FJ, Aten JA (1993) Measurement of co-localization of objects in dual-colour confocal images. J Microsc 169: 375–382.
37. Bolte S, Cordelieres FP (2006) A guided tour into subcellular co-localization analysis in light microscopy. J Microsc 224: 213–232.
38. Clarke M, Collins R, Darby S, Davies C, Elphinstone P, et al. (2005) Effects of radiotherapy and of differences in the extent of surgery for early breast cancer on local recurrence and 15-year survival: an overview of the randomised trials. Lancet 366: 2087–2106.
39. Li S, Zhou Y, Fan J, Cao S, Cao T, et al. (2011) Heat shock protein 72 enhances autophagy as a protective mechanism in lipopolysaccharide-induced peritonitis in rats. Am J Pathol 179: 2822–2834.
40. Milanezi F, Leitao D, Ricardo S, Augusto I, Schmitt F (2009) Evaluation of HER2 in breast cancer: reality and expectations. Expert Opin Med Diagn 3: 607–620.
41. McGee SF, O'Connor DP, Gallagher WM (2006) Functional interrogation of breast cancer: from models to drugs. Expert Opin Drug Discov 1: 569–584.
42. Goswami T, Shah M, Isaacs C (2009) Novel molecular prognostic markers in breast cancer. Expert Opin Med Diagn 3: 523–532.
43. Thundimadathil J (2012) Cancer treatment using peptides: current therapies and future prospects. J Amino Acids 2012: 967347.
44. Condeelis J, Weissleder R (2010) In vivo imaging in cancer. Cold Spring Harb Perspect Biol 2: a003848.
45. Fani M, Maecke HR, Okarvi SM (2012) Radiolabeled peptides: valuable tools for the detection and treatment of cancer. Theranostics 2: 481–501.
46. Fass L (2008) Imaging and cancer: a review. Mol Oncol 2: 115–152.
47. Chow JY, Li ZJ, Kei WK, Cho CH (2013) Cathelicidin a potential therapeutic peptide for gastrointestinal inflammation and cancer. World J Gastroenterol 19: 2731–2735.
48. Zhang X, Chen J, Kang Y, Hong S, Zheng Y, et al. (2013) Targeted paclitaxel nanoparticles modified with follicle-stimulating hormone beta 81-95 peptide show effective antitumor activity against ovarian carcinoma. Int J Pharm DOI: 10.1016/j.ijpharm.2013.06.03
49. Lim KJ, Sung BH, Shin JR, Lee YW, Kim da J, et al. (2013) A cancer specific cell-penetrating peptide, BR2, for the efficient delivery of an scFv into cancer cells. PLoS One 8: e66084.
50. Ma C, Yin G, You F, Wei Y, Huang Z, et al. (2013) A specific cell-penetrating peptide induces apoptosis in SKOV3 cells by down-regulation of Bcl-2. Biotechnol Lett DOI: 10.1007/s10529-013-1263-x.
51. Rodrigues M, de la Torre BG, Andreu D, Santos NC (2013) Kinetic uptake profiles of cell penetrating peptides in lymphocytes and monocytes. Biochim Biophys Acta 1830: 4554–4563.
52. Han C, Li Y, Sun M, Liu C, Ma X, et al. (2013) Small peptide-modified nanostructured lipid carriers distribution and targeting to EGFR-overexpressing tumor in vivo. Artif Cells Nanomed Biotechnol DOI: 10.3109/21691401.2013.801848
53. Lu RM, Chen MS, Chang DK, Chiu CY, Lin WC, et al. (2013) Targeted drug delivery systems mediated by a novel peptide in breast cancer therapy and imaging. PLoS One 8: e66128.

54. Lee SA, Kim BR, Kim BK, Kim DW, Shon WJ, et al. (2013) Heat shock protein-mediated cell penetration and cytosolic delivery of macromolecules by a telomerase-derived peptide vaccine. Biomaterials DOI: 10.1016/j.biomaterials.2013.06.015.
55. Rerole AL, Gobbo J, De Thonel A, Schmitt E, Pais de Barros JP, et al. (2011) Peptides and aptamers targeting HSP70: a novel approach for anticancer chemotherapy. Cancer Res 71: 484–495.
56. Kleinjung T, Arndt O, Feldmann HJ, Bockmuhl U, Gehrmann M, et al. (2003) Heat shock protein 70 (Hsp70) membrane expression on head-and-neck cancer biopsy - a target for natural killer (NK) cells. Int J Radiat Oncol Biol Phys 57: 820–826.
57. Multhoff G, Botzler C, Wiesnet M, Muller E, Meier T, et al. (1995) A stress-inducible 72-kDa heat-shock protein (HSP72) is expressed on the surface of human tumor cells, but not on normal cells. Int J Cancer 61: 272–279.
58. Steiner K, Graf M, Hecht K, Reif S, Rossbacher L, et al. (2006) High HSP70-membrane expression on leukemic cells from patients with acute myeloid leukemia is associated with a worse prognosis. Leukemia 20: 2076–2079.
59. Gehrmann M, Radons J, Molls M, Multhoff G (2008) The therapeutic implications of clinically applied modifiers of heat shock protein 70 (Hsp70) expression by tumor cells. Cell Stress Chaperones 13: 1–10.
60. Gehrmann M, Schilling D, Molls M, Multhoff G (2010) Radiation induced stress proteins. Int J Clin Pharmacol Ther 48: 492–493.
61. Mizuno-Yamasaki E, Rivera-Molina F, Novick P (2012) GTPase networks in membrane traffic. Ann Rev Biochem 81: 637–659.
62. Stenmark H (2009) Rab GTPases as coordinators of vesicle traffic. Nat Rev Mol Cell Biol 10: 513–525.
63. Agarraberes FA, Terlecky SR, Dice JF (1997) An intralysosomal hsp70 is required for a selective pathway of lysosomal protein degradation. J Cell Biol 137: 825–834.
64. Eskelinen EL (2006) Roles of LAMP-1 and LAMP-2 in lysosome biogenesis and autophagy. Mol Aspects Med 27: 495–502.
65. Spang A (2009) On the fate of early endosomes. Biol Chem 390: 753–759.
66. Feng Y, Press B, Wandinger-Ness A (1995) Rab 7: an important regulator of late endocytic membrane traffic. J Cell Biol 131: 1435–1452.
67. Chen W, Feng Y, Chen D, Wandinger-Ness A (1998) Rab11 is required for trans-Golgi network-to-plasma membrane transport and a preferential target for GDP dissociation inhibitor. Mol Biol Cell 9: 3241–3257.
68. Nakatsu Y, Ma X, Seki F, Suzuki T, Iwasaki M, et al. (2013) Intracellular transport of the measles virus ribonucleoprotein complex is mediated by Rab11A-positive recycling endosomes and drives virus release from the apical membrane of polarized epithelial cells. J Virol 87: 4683–4693.
69. Gyrd-Hansen M, Nylandsted J, Jaattela M (2004) Heat shock protein 70 promotes cancer cell viability by safeguarding lysosomal integrity. Cell Cycle 3: 1484–1485.
70. Chen WH, Chen JX, Cheng H, Chen CS, Yang J, et al. (2013) A new anti-cancer strategy of damaging mitochondria by pro-apoptotic peptide functionalized gold nanoparticles. Chem Commun (Camb) 49: 6403–6405.
71. Ma X, Wang X, Zhou M, Fei H (2013) A mitochondria-targeting gold-peptide nanoassembly for enhanced cancer-cell killing. Adv Healthc Mater DOI: 10.1002/adhm.201300037
72. Roth A, Drummond DC, Conrad F, Hayes ME, Kirpotin DB, et al. (2007) Anti-CD166 single chain antibody-mediated intracellular delivery of liposomal drugs to prostate cancer cells. Mol Cancer Ther 6: 2737–2746.
73. Malhi SS, Budhiraja A, Arora S, Chaudhari KR, Nepali K, et al. (2012) Intracellular delivery of redox cycler-doxorubicin to the mitochondria of cancer cell by folate receptor targeted mitocancerotropic liposomes. Int J Pharm 432: 63–74.
74. Hilgendorf KI, Leshchiner ES, Nedelcu S, Maynard MA, Calo E, et al. (2013) The retinoblastoma protein induces apoptosis directly at the mitochondria. Genes Dev 27: 1003–1015.
75. Fager RS, Shapiro S, Litman BJ (1977) A large-scale purification of phosphatidylethanolamine, lysophosphatidylethanolamine, and phosphatidylethanolamine, and phosphatidylcholine by high performance liquid chromatography: a partial resolution of molecular species. J Lipid Res 18: 704–709.
76. Yoon TH, Kim IH (2002) Phosphatidylcholine isolation from egg yolk phospholipids by high-performance liquid chromatography. J Chromatogr A 949: 209–216.
77. Moktan S, Raucher D (2012) Anticancer activity of proapoptotic peptides is highly improved by thermal targeting using elastin-like polypeptides. Int J Pept Res Ther 18: 227–237.
78. Shabaik YH, Millard M, Neamati N (2013) Mechanistic evaluation of a novel small molecule targeting mitochondria in pancreatic cancer cells. PLoS One 8: e54346.
79. Yan X, Zhou Y, Liu S (2012) Optical imaging of tumors with copper-labeled rhodamine derivatives by targeting mitochondria. Theranostics 2: 988–998.

Published OnlineFirst October 9, 2014; DOI: 10.1158/0008-5472.CAN-14-0413

Selective *In Vivo* Imaging of Syngeneic, Spontaneous, and Xenograft Tumors Using a Novel Tumor Cell–Specific Hsp70 Peptide-Based Probe

Stefan Stangl[1], Julia Varga[2], Bianca Freysoldt[1], Marija Trajkovic-Arsic[3], Jens T. Siveke[3], Florian R. Greten[2], Vasilis Ntziachristos[4], and Gabriele Multhoff[1]

Abstract

Although *in vivo* targeting of tumors using fluorescently labeled probes has greatly gained in importance over the last few years, most of the clinically applied reagents lack tumor cell specificity. Our novel tumor cell–penetrating peptide-based probe (TPP) recognizes an epitope of Hsp70 that is exclusively present on the cell surface of a broad variety of human and mouse tumors and metastases, but not on normal tissues. Because of the rapid turnover rate of membrane Hsp70, fluorescently labeled TPP is continuously internalized into syngeneic, spontaneous, chemically/genetically induced and xenograft tumors following intravenous administration, thereby enabling site-specific labeling of primary tumors and metastases. In contrast with the commercially available nonpeptide small molecule $\alpha_v\beta_3$-integrin antagonist IntegriSense, TPP exhibits a significantly higher tumor-to-background contrast and stronger tumor-specific signal intensity in all tested tumor models. Moreover, in contrast with IntegriSense, TPP reliably differentiates between tumor cells and cells of the tumor microenvironment, such as tumor-associated macrophages and fibroblasts, which were found to be membrane-Hsp70 negative. Therefore, TPP provides a useful tool for multimodal imaging of tumors and metastases that might help to improve our understanding of tumorigenesis and allow the establishment of improved diagnostic procedures and more accurate therapeutic monitoring. TPP might also be a promising platform for tumor-specific drug delivery and other Hsp70-based targeted therapies. *Cancer Res; 74(23); 6903–12. ©2014 AACR.*

Introduction

Tumor targeting peptides represent a promising new class of prognostic tools due to their advantageous biodistribution with fast body clearance and their capacity to effectively penetrate viable cells (1–3). However, it is essential that such probes exhibit specific binding to tumor cells and exclude normal tissue. The identification of tumor-selective probes is therefore essential.

In addition to its physiologic, stress-induced appearance in the cytoplasm, HSP70 (Hsp70-1, HspA1A, #3303) has been found to be selectively localized on the plasma membrane of a broad variety of different murine and human tumors. Because of its absence in the membranes of normal cells, targeting membrane Hsp70 on tumors offers unique opportunities for the detection, screening, and staging of diseases (4–7), as well as for drug development and treatment evaluation of a wide variety of neoplasms in future theranostic approaches (8–10).

Screening of tumor biopsies and their corresponding normal tissues of well over 1,000 patients has shown that the majority of the primarily diagnosed carcinoma samples, but none of the tested corresponding normal tissues, exhibited an Hsp70-membrane–positive phenotype (5). Furthermore, we have previously shown that Hsp70-membrane positivity is increased in stressed tumor cells that also exhibit elevated cytosolic Hsp70 levels. In the cytosol, Hsp70 acts in an antiapoptotic manner and enhances survival of the tumor cells following therapies such as chemo- and radiotherapy (11). Most importantly, an Hsp70-membrane–positive tumor phenotype has been shown to be associated with a significantly decreased overall survival in cancerous diseases such as leukemia (12), lung, breast (13), lower rectal carcinomas (14), prostate (8), and liver cancer (15). These findings demonstrate that Hsp70 positivity might serve as a useful marker for prediction of clinical outcome. The potential therapeutic value of membrane Hsp70 has been demonstrated in a

[1]Department of Radiation Oncology, Klinikum rechts der Isar, TU München and CCG - "Innate Immunity in Tumor Biology", Helmholtz Zentrum München (HMGU), Munich, Germany. [2]Institute for Tumor Biology and Experimental Therapy, Georg-Speyer-Haus, Frankfurt/Main, Germany. [3]Department of Medicine II, Klinikum rechts der Isar, TU München, Munich, Germany. [4]Institute of Biological and Medical Imaging, Helmholtz Zentrum München (HMGU), Munich, Germany.

Note: Supplementary data for this article are available at Cancer Research Online (http://cancerres.aacrjournals.org/).

Corresponding Author: Gabriele Multhoff, Department of Radiation Oncology, Klinikum rechts der Isar, TU München, Ismaningerstrasse 22, 81675 München, Germany. Phone: 49-89-4140-4514; Fax: 49-89-4140-4299; E-mail: gabriele.multhoff@lrz.tu-muenchen.de

doi: 10.1158/0008-5472.CAN-14-0413

Published OnlineFirst October 9, 2014; DOI: 10.1158/0008-5472.CAN-14-0413

previous study that reported on the generation of an Hsp70-specific antibody termed cmHsp70.1 to specifically induce antibody-dependent cellular cytotoxicity of tumor cells *in vitro* and *in vivo* (16, 17).

Herein, we describe a novel peptide-based probe that binds to membrane Hsp70. Because of its remarkable tumor specificity and capacity for internalization (18), this probe has been termed Hsp70 tumor cell–penetrating peptide (TPP). TPP, which comprises the amino acid sequence $aa_{450–463}$ (TKDNNLLGRFELSG) of the C-terminal oligomerization domain of Hsp70, binds to tumor cells with high affinity *in vivo* as well as *in vitro*. The specificity of TPP toward Hsp70 was shown by ELISA (Supplementary Fig. S1). As recently shown by Mahalka and colleagues (19), the C-terminal and N-terminal domain of Hsp70 are exposed to the extracellular milieu of tumor cells if presented on the plasma membrane. Although *in vitro* TPP exhibits similar binding characteristics toward Hsp70 than the cmHsp70.1 monoclonal antibody (16, 17), TPP exerts a better biodistribution, *in vivo*.

Materials and Methods

Animals

BALB/c, FvB, and SHO-*Prkdc*^{scid}*Hr*^{Hr} (SHO) mice were obtained from an animal breeding colony (Charles River and Harlan Winkelmann) and were maintained in pathogen-free, individually ventilated cages (Tecniplast). All animal experiments were approved by the District Government of Upper Bavaria and performed in accordance with the German Animal Welfare and Ethical Guidelines of the Klinikum rechts der Isar, TUM, Munich, Germany. Tumors were examined after the animals were sacrificed by cervical dislocation.

Syngeneic tumor models

CT26 mouse colon adenocarcinoma cells (5×10^5) or 4T1 mammary carcinoma cells (2.5×10^5; ATCC, authentication not applicable for mouse cell lines) were harvested in the exponential growth phase and injected subcutaneously in the neck or orthotopically into the mammary fad pad of 8-week-old, female BALB/c mice, respectively. Primary tumor growth was followed by ultrasonic measurements (Logiq-5, GE Healthcare). Intraoperative *in vivo* imaging was performed post mortem on exposed tumors when the CT26 tumors reached a size of approximately 0.4 cm^3. 4T1-derived tumors and lung metastases were investigated after 25 to 30 days of tumor growth.

Xenograft tumor models

To test the capacity of TPP to recognize human tumors, 5×10^6 cells from the following human carcinoma cell lines were implanted subcutaneously into the neck area or orthotopically into the mammary fat pad of 8- to 10-week-old, female SHO mice: colon carcinoma cell lines HCT-116 (ATCC) and CX-2 (DKFZ), mammary carcinoma cell lines MCF-7, MDA-MB231 and T-47D (ATCC), pancreas carcinoma cell lines Panc-1, MIA PaCa-2 (provided by J.T. Siveke) and COLO357 (Leibniz-Institute DSMZ, Braunschweig, Germany), small-cell lung cancer H1339, non–small cell lung cancer (NSCLC) A549 (n.t.), head and neck carcinoma FaDu (all ATCC) and Cal-33 (Leibniz-Institute DSMZ), as well as the human cervix carcinoma HeLa (ATCC). Mice were sacrificed and intraoperative *in vivo* imaging was performed on the exposed tumors when tumors had reached a volume of 0.2 to 0.4 cm^3. If not stated otherwise, cell line authentication was performed by short tandem repeat profiles that are generated by simultaneous amplification of multiple short tandem repeat loci by ATCC and DSMZ. Cells were not cultured for longer than 5 months after testing.

Colitis-associated spontaneous tumor model

Spontaneous colonic tumors were induced in 8-week-old female FvB mice (Charles River) using an established approach. Briefly, mice were injected intraperitoneally with a single dose of azoxymethane (AOM; Sigma-Aldrich) at 10 mg/kg body weight. Following AOM treatment, the mice were subjected to three cycles of dextran sulfate sodium salt (MP Biomedicals) administration in their drinking water (20). After 15 to 18 weeks of tumor development, the mice were sacrificed and the colon was resected for experiments. The presence of colorectal tumors was confirmed using standard histologic techniques.

Endogenous pancreatic ductal adenocarcinoma mouse model

The spontaneous pancreatic ductal adenocarcinoma (PDAC) mouse model (*Ptf1a*$^{+/Cre}$;*Kras*$^{+/LSL\text{-}G12D}$;*p53*$^{LoxP/LoxP}$, CKP) has been described previously (21). After sacrificing, the abdominal cavity of tumor-bearing mice, including the pancreas, was exposed for *in vivo* imaging of the tumor area and surrounding normal tissue.

Toxicity testing

Potential toxic effects of TPP were investigated by injecting healthy BALB/c mice intravenously with 500 and 1050 μg of TPP. Concentrations up to 500 μg of TPP per mouse were tested in tumor-bearing mice (s.c. tumors, size 0.4 cm^3). The health status and the general behavior of mice were inspected. Animals were sacrificed on day 5 and the heart, liver, spleen, lung, and kidneys examined for pathologic changes using standard histologic techniques.

Flow cytometry

The membrane-Hsp70 phenotype of tumors grown *in vivo* was determined by flow-cytometric analysis of single cell suspensions that were generated following 30 minutes collagenase/dispase digestion using FITC-conjugated cmHsp70.1 mAb (IgG1, multimmune GmbH) or carboxyfluorescein-conjugated TPP (TPP[CF]). Cell suspensions were incubated with the appropriate reagent for 30 minutes at 4°C, after which they were washed and viable (7-AAD negative) cells were analyzed using a FACSCalibur flow cytometer (Becton Dickinson). Gating was applied to distinguish the $CD45^-/CD140b^-$ tumor cell population from $CD45^-/CD140b^+$ fibroblasts and $CD45^+/F4/80^+$ macrophages.

Published OnlineFirst October 9, 2014; DOI: 10.1158/0008-5472.CAN-14-0413

TPP, control peptide, and IntegriSense 750 in imaging procedures

In *in vivo* imaging experiments, Cy5.5 or DyLight750-conjugated Hsp70-specific 14-mer TPP (OEM manufactured by Thermo Fischer) was compared with the unspecific scrambled control peptide (CP, OEM manufactured by Thermo Fischer) and with IntegriSense 750 (IS750, PerkinElmer; Supplementary Fig. S2). The intraoperative imaging procedure, which captured color and fluorescence images of the exposed tumors and its surrounding normal tissue, was configured to simulate an intraoperative imaging situation. TPP[Cy5.5] or CP[DL750] (100 μg, equal to 45 nmol per animal) or IS750, at the recommended dose of 2 nmol per animal, was injected into the tail vein of tumor-bearing mice. Concentrations above 2 nmol resulted in a higher staining of healthy tissues and thus negatively affected the tumor-to-background ratio (TBR; data not shown). Signal specificity was determined by calculating the ratio of the mean signal intensity in the exposed tumor tissue and that of the surrounding normal tissue (TBR; ref. 22). Kinetic studies were performed 12, 24, 48, and 72 hours after tail vein bolus injection of TPP[Cy5.5] and CP[DL750]. All other experiments were performed 24 hours after intravenous injection of the respective probes.

Fluorescent images were acquired by illuminating the specimens using 670 and 740 nm diode lasers and guiding the emitted fluorescence through appropriate emission filters before capturing it using a back illuminated EM-CCD camera (iXon DU888, Andor), as described previously (16). A more detailed description of the imaging procedures is shown in the Supplementary Section.

Biodistribution studies

For biodistribution, tumor-bearing mice were sacrificed 12, 24, or 48 hours after intravenous injection of TPP[Cy5.5]. Fluorescent signal intensities of 0.25 cm^3 tissue cubes, taken from the tumor, spleen, pancreas, liver, lung, duodenum, kidney, heart, and 0.25 mL of peripheral blood were measured as described above. Agarose-gel cubes with standardized concentrations were used to calculate the probe concentrations in the investigated tissue samples. Detailed information concerning the quantification of TPP[Cy5.5] is provided in Supplementary Fig. S6.

Histology, IHC, and fluorescence microscopy

Paraformaldehyde-fixed and paraffin-embedded tissue sections (2 μm) were stained with hematoxylin and eosin using standard procedures. For IHC on cryosections, unspecific mouse-on-mouse reactions were blocked using a M.O.M. kit (Vector Labs) and stained with cmHsp70.1 mAb following antigen retrieval in citrate buffer. The quantification and volumetric analysis of lung metastases were performed using consecutive tissue sections (100 μm) using Aperio ImageScope software (Leica).

For microscopic *in situ* fluorescence analysis, TPP[CF] (100 μg) and the recommended dose of IntegriSense 750 (IS[750]) were injected intravenously into tumor-bearing mice and allowed to circulate for 24 hours. Tissue was collected and 8 μm cryosections counterstained with DAPI (DAKO) and examined microscopically using a Zeiss Observer Z1 (Carl Zeiss) equipped with standard filters for GFP and Cy7 after 4 minutes of fixation with 1.8% w/v PFA.

Statistical analysis

Statistical analysis was performed using the Student *t* test. Data are mean ± SD. *P* values ≤ 0.05 were considered as being significant different between the compared groups.

Results

The membrane-bound form of Hsp70, but not β3-integrin, is present on a wide variety of human and murine tumors

To examine the presence of the investigated reporter epitopes on cells *in vivo*, a broad variety of murine and human tumors were screened for the presence of membrane Hsp70 and β3-integrin (CD61), the target epitopes for TPP and IntegriSense, respectively. This screening included colon, mammary, pancreatic, lung, head and neck, and cervical carcinomas derived from syngeneic, chemically induced, spontaneous and xenograft mouse models. Flow-cytometric analysis of viable cells derived from the solid tumors demonstrated that all of the cells examined exhibited a comparable membrane Hsp70 staining pattern using the cmHsp70.1 monoclonal antibody or the TPP probe (Fig. 1; Table 1). This finding further emphasizes the fact that targeting membrane Hsp70 could serve as a universal approach for diagnosing a wide variety of tumor entities.

For flow-cytometric analysis, a cell population was defined to be membrane positive if as more than 20% of the cells were stained. The threshold of 20% was defined upon screening of a large panel of healthy human tissues, including human peripheral blood lymphocytes, fibroblast, and healthy tissues surrounding tumor ($n = 86$). CD61 staining revealed $\alpha_v\beta_3$-integrin positivity on mouse colon (CT26) and mammary (4T1) carcinoma, on human mammary (MDA-MB231, T-47D) and head and neck (CAL-33) carcinoma, as well as on human and mouse pancreatic carcinoma (PDAC, Panc-1, MIA PaCa-2, COLO357). However, no β_3-integrin expression could be detected on human colon (HCT-116, CX-2), mammary (MCF-7), lung (H-1339), or cervical (HeLa) carcinoma cells. Cells derived from a murine colitis-associated carcinoma (CAC) model showed a heterogeneous CD61 expression. These data indicate that, in comparison with β_3-integrin, Hsp70 is more frequently expressed on human and murine tumors. However, tumor cell specificity is critical for targeting strategies. Therefore, the presence of membrane Hsp70 and β3-integrin on tumor-residing $CD45^+/F4/80^+$ macrophages and $CD45^-/CD140b^+$ fibroblasts was investigated. TPP only weakly stains (below 10%) tumor-associated fibroblasts and tumor-infiltrating macrophages; in contrast, β3-integrin positivity was found on more than 60% of tumor-associated fibroblasts and tumor-infiltrating macrophages (Fig. 1B). To test Hsp70 positivity on tumors, cryosections were stained with the Hsp70-specific antibody cmHsp70.1. Although tumor cells of the various tumor models were positive, cells of the tumor microenvironment remained negative for Hsp70. A representative staining of a PDAC tumor is shown in Supplementary Fig. S3.

Published OnlineFirst October 9, 2014; DOI: 10.1158/0008-5472.CAN-14-0413

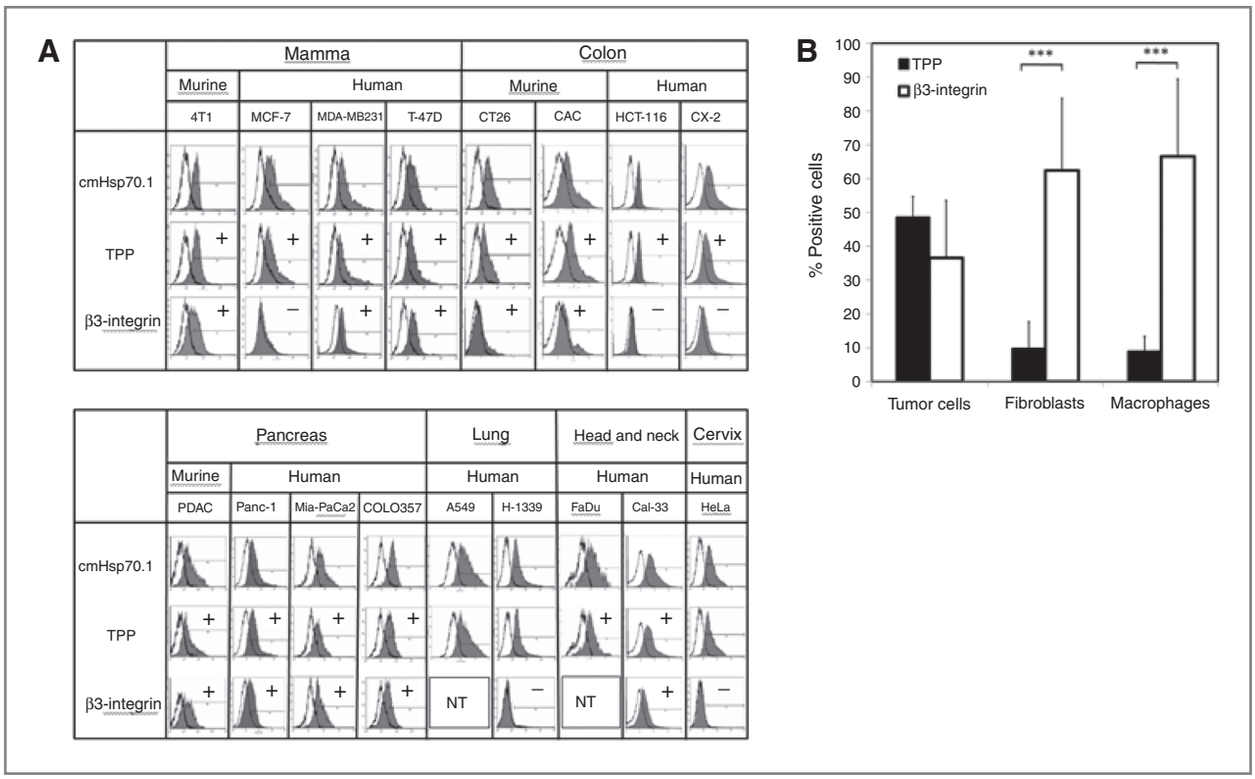

Figure 1. Membrane-Hsp70 and β3-integrin expression on single cell suspensions of human (h) and murine (m) tumors that were grown in mice. A, comparison of the binding capacity of cmHsp70.1 full-length antibody (top), TPP (middle), and β3-integrin antibody (bottom) to mammary (m4T1, hMCF-7, hMDA-MB231, hT-47D), colon (mCT26, mCAC, hHCT-116, hCX-2), pancreas (mPDAC, hPanc-1, hMiaPaCa2, hCOLO357), lung (hA549, hH-1339), head and neck (hFaDu, hCal-33), and cervix (hHeLa) carcinomas. Results are expressed as log fluorescence intensity versus relative cell numbers. The IgG1 isotype-matched control is indicated in white and membrane staining in gray histograms. B, membrane positivity of TPP (black bars) and β3-integrin (white bars) on cells of the tumor microenvironment in comparison with β3-integrin-positive tumors. Membrane staining of TPP remained significantly lower in macrophages ($P = 1.54 \times 10^{-7}$) and fibroblasts ($P = 4.67 \times 10^{-8}$), compared with β3-integrin. Averaged tumor cell positivity revealed no significant difference between TPP and β3-integrin staining.

TPP is not toxic *in vivo*

To examine potential toxic side effects of TPP, healthy and tumor-bearing BALB/c mice were injected intravenously with 500 to 1,050 μg of TPP, which is equivalent to 25 to 50 μg/g of their body weight. Gross monitoring of the mice did not show any toxic reactions such as skin ulcerations or toxic death at any of the tested doses. Nor did any animal exhibit any loss of weight or change in mobility. Histologic examination of the heart, liver, spleen, lung, and kidney on day 5 after injection by a veterinarian, revealed no pathologic changes. An examination of the effects of TPP concentrations up to 500 μg in tumor-bearing mice also did not exert any side effects.

TPP accumulates within the tumor with maximal specificity 24 hours postintravenous injection

To investigate the *in vivo* circulation and tumor-homing properties of TPP, we analyzed its biodistribution in CT26 tumor-bearing mice. The accumulation of TPP in different organs was determined 12, 24, and 48 hours after intravenous injection of 100 μg TPP[Cy5.5] by measuring fluorescent signal intensities in the tumor, spleen, pancreas, liver, lung, duodenum, kidney, heart, and in the peripheral blood (Fig. 2). A strong TPP[Cy5.5] signal could be detected within the tumor (7.6 ± 0.7 μg/cm^3) 12 hours after intravenous injection. This reached a maximum after 24 hours (10.4 ± 2.2 μg/cm^3) and dropped after 48 hours. TPP accumulation was significantly lower at all investigated time points in all other tested organs, except the kidney. The concentration of TPP[Cy5.5] reached its maximum in the kidney after 12 hours at 13.7 ± 0.6 μg/cm^3, and this accumulation was followed by a sharp drop, 24 and 48 hours postinjection. These data further confirm the tumor specificity of TPP and indicate that TPP is cleared from the body by renal excretion.

In further experiments, we investigated the optimal time point for *in vivo* imaging in a CT26 tumor model (subcutaneously) 2 weeks after tumor injection (Supplementary Fig. S5A) and a metastasizing 4T1 mammary carcinoma model (orthotopically) 3 to 4 weeks after tumor injection (Supplementary Figs. S5B and S5C and S7). TPP[Cy5.5] yielded maximal TBR in primary tumors 24 hours after injection of the probe, whereas the peak TBR in metastasized lungs occurred after 48 hours. The scrambled control peptide CP[DL750] did not show any specific accumulation in tumor tissue (Supplementary Fig. S5A–S5C).

Published OnlineFirst October 9, 2014; DOI: 10.1158/0008-5472.CAN-14-0413

Table 1. Binding of TPP to different membrane-Hsp70–positive colon, mammary, pancreas, lung, head and neck, and cervix mouse and human tumors

	Colon				Mammary			
	Murine		Human		Murine	Human		
%	CT26	CAC	HCT-116	CX-2	4T1	MCF-7	MDA-MB231	T-47D
Hsp700	55.5 ± 5.5	51.2 ± 0.8	63.3 ± 9.3	56.6 ± 8.3	56.3 ± 3.5	58.0 ± 3.6	63.3 ± 13.3	48.0 ± 4.2
TPP	42.0 ± 4.3	52.8 ± 7.5	59.0 ± 7.9	45.2 ± 5.2	47.5 ± 2.1	46.0 ± 5.6	62.5 ± 15.6	43.5 ± 2.1
CD61	26.5 ± 7.8	23.0 ± 7.1	15.3 ± 1.5	14.0 ± 5.0	38.3 ± 3.2	13.0 ± 1.7	20.0 ± 5.6	55.5 ± 2.1

	Pancreas				Lung		Head and neck		Cervix
	Murine	Human			Human		Human		Human
%	PDAC	Panc-1	MIAPaCa-2	COLO357	A549	H-1339	FaDu	Cal-33	HeLa
Hsp70	50.0 ± 8.6	46.0 ± 4.2	58.5 ± 7.6	57.8 ± 9.3	76.3 ± 1.5	60.0 ± 7.5	59.0 ± 8.5	68.1 ± 8.5	55.0 ± 18.4
TPP	45.0 ± 1.4	47.0 ± 7.1	42.0 ± 6.6	49.5 ± 4.9	58.3 ± 7.6	67.0 ± 5.7	53.5 ± 0.7	52.0 ± 4.2	63.0 ± 4.2
CD61	50.0 ± 5.7	36.0 ± 2.8	70.0 ± 11.3	20.0 ± 9.9	n.t.	4.0 ± 1.8	n.t.	23.5 ± 3.5	5.0 ± 5.6

NOTE: The proportion of membrane-Hsp70–positive cells was measured with cmHsp70.1 antibody and TPP peptide on single cell suspensions of *in vivo*-grown human and mouse tumors of different entities. The expression of CD61 (β3-integrin) was also determined on these tumor cells. A sample was determined as membrane positive if more than 20% of the cells showed a positive staining.
Abbreviation: n.t., not tested.

The specific accumulation of TPP in syngeneic primary tumors and metastases is superior to that of IntegriSense

To confirm the specificity of TPP[Cy5.5] for primary tumors and metastases *in vivo*, we simultaneously injected 100 μg of TPP[Cy5.5] and the recommended dose of IntegriSense 750 (IS[750]) into CT26 and 4T1 tumor-bearing mice, 24 hours before *in vivo* imaging. Although TPP[Cy5.5] and IS[750] both clearly delineate the tumor, IS[750] signals can also be found in normal tissue surrounding the tumor (Fig. 3A and B, true color images of the region of interest is depicted on the left). TPP[Cy5.5] exhibited a significantly higher TBR than IS[750] ($P = 0.0004$ and 0.003, respectively). To further investigate the specificity of the probes, *ex vivo* imaging of dissected lungs containing metastases was performed. Quantification of metastases can be found in Supplementary Fig. S4. The TBR for IS[750] imaging was also lower than that for TPP[Cy5.5] ($P = 0.04$; Fig. 3C, bottom) in distant lesions. Although the delineation of metastases by TPP[Cy5.5] and IS[750] was comparable, the enrichment of IS[750] in normal lung tissue is marginally higher (Fig. 3C, top). The specificity and colocalization of TPP and IS was further confirmed on cryo-sections of the lesions, which were obtained 24 hours after intravenous injection of TPP[CF] and IS[750] (Fig. 3D). Both probes specifically enriched in the primary tumor and lung metastases, however, a background staining of IS[750] remained in healthy lung tissue. These data demonstrate that, although both compounds specifically stain tumors and metastases, TPP is more effectively washed out of normal tissue and therefore provides a better signal-to-background contrast than IntegriSense.

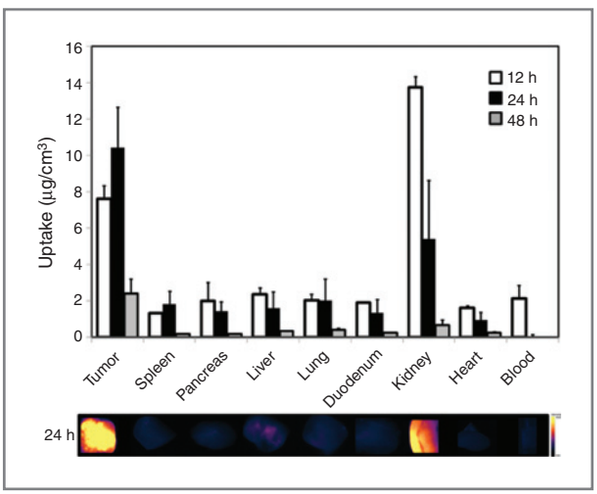

Figure 2. Biodistribution of TPP[Cy5.5] in CT26 tumor-bearing mice, assessed by NIRF quantification. Tumors and organs of CT26 tumor-bearing mice were collected 12, 24, and 48 hours (white, black, and gray bars, respectively) after intravenous injection of TPP[Cy5.5] into the tail vein. The fluorescence signals of the probe were analyzed, *ex vivo*. Two to three mice per time point were assessed; graph bars show mean values ± SD.

The specific tumor-homing capacity of TPP is higher than that of IntegriSense in endogenous tumor models

To more realistically mimic the histologic and molecular features of human tumors in *in vivo* imaging, we took advantage of chemically induced and endogenous mouse models of colorectal (CAC) and pancreatic (PDAC) cancer. Flow-

Published OnlineFirst October 9, 2014; DOI: 10.1158/0008-5472.CAN-14-0413

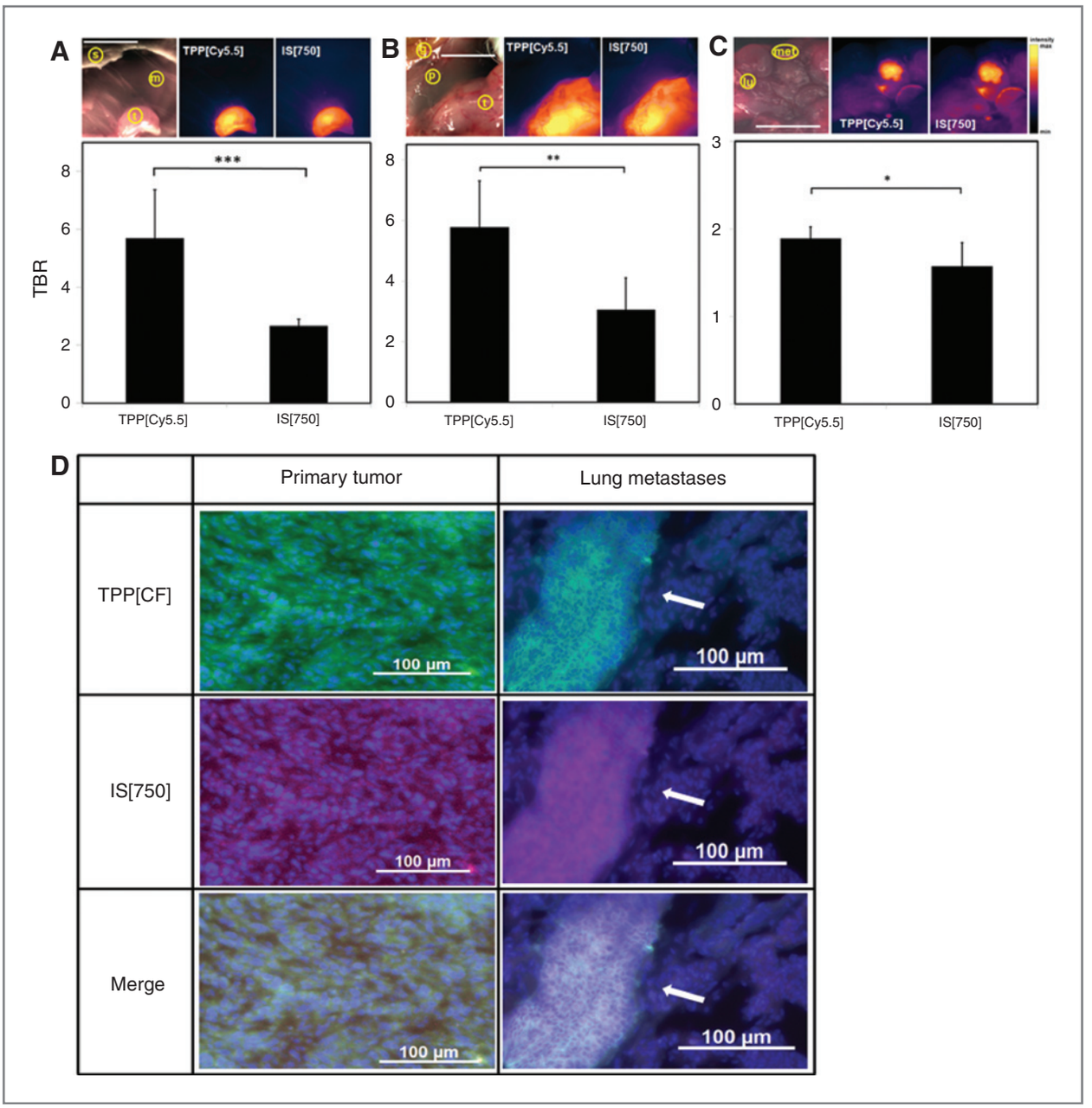

Figure 3. Intraoperative *in vivo* imaging and fluorescence microscopy of syngeneic tumor models after the injection of TPP[Cy5.5] and IS[750]. A, NIRF imaging of CT26 tumors that were injected subcutaneously into the neck area, B and C, 4T1 tumors injected orthotopically (B) and lung metastases (C) derived thereof. Top, true color images of tumor (t) and metastases (met), as well as surrounding normal tissue, including muscle (m), skin (s), gut (g), peritoneum (p), and lung (lu; left, scale bars, 5 mm). Corresponding pseudocolor fluorescence images were taken 24 hours after intravenous injection of TPP[Cy5.5] (middle) and IS[750] (right) into the same animal. Bottom, TBR, 24 hours after intravenous injection of TPP[Cy5.5] and IS[750]. The data are shown as mean ± SD [$n = 4$ (CT26) and 6 (4T1)]; *, $P < 0.05$; **, $P < 0.01$; ***, $P < 0.001$. D, fluorescence microscopy of primary tumor (left) and lung tissue, including metastases, indicated by arrows (right), 24 hours after intravenous injection of TPP[CF] (top) and IS[750] (middle) in the same animal. Bottom, an overlay of both compounds. Scale bars, 100 µm.

cytometric analysis of isolated tumor cells revealed Hsp70 and β3-integrin positivity in both models (Table 1). To investigate the *in vivo* tumor targeting properties in these models, NIR imaging of tumors was performed 24 hours after intravenous injection of TPP[Cy5.5], CP[DL750], and IS[750] (Fig. 4). Although the fluorescence signals of both TPP[Cy5.5] and IS[750] clearly delineated the exposed colon and pancreatic tumors, a clear background staining in the tumor-surrounding normal colon tissue was observed following administration of IS[750]. In the colitis-induced tumors, the TBR of TPP[Cy5.5]

Published OnlineFirst October 9, 2014; DOI: 10.1158/0008-5472.CAN-14-0413

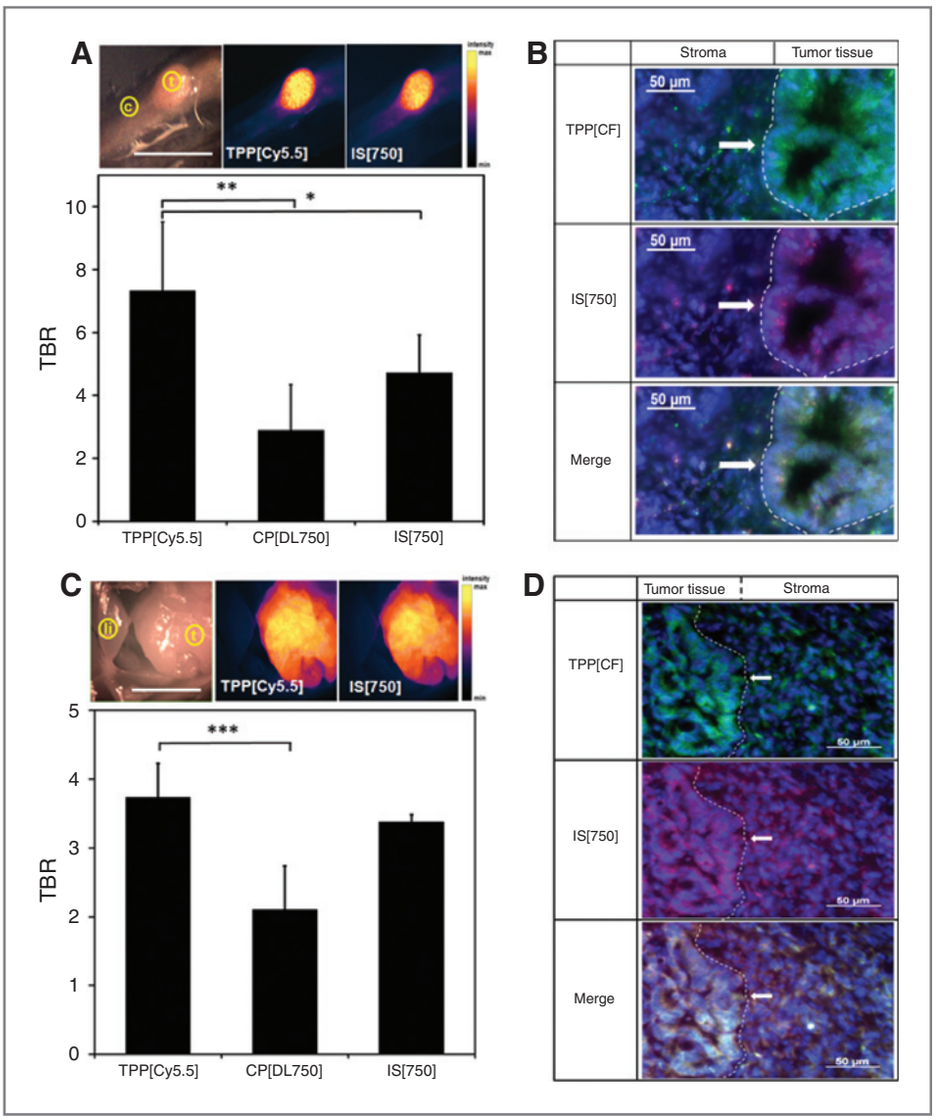

Figure 4. Intraoperative *in vivo* imaging and fluorescence microscopy in spontaneous tumor mouse models 24 hours after injection of TPP[Cy5.5], CP[DL750], and IS[750]. A, NIRF imaging of CAC. Top, true color image of tumor (t) and surrounding colon tissue (c; scale bar, 5 mm), with corresponding pseudocolor fluorescence images 24 hours after intravenous injection of TPP[Cy5.5] (middle) and IS[750] (right). Bottom, TBR, 24 hours after intravenous injection of TPP[Cy5.5], CP[DL750], and IS[750]. The data are shown as mean ± SD, $n = 5$ (TPP[Cy5.5]), 4 (CP[DL750]), and 3 (IS[750]). *, $P < 0.05$; **, $P < 0.01$. B, fluorescence microscopy of identical cryosections of a representative primary tumor (left) and normal tissue (right) 24 hours after intravenous injection of TPP[CF] (top) and IS[750] (middle) into the same animal. Bottom, an overlay of both compounds with enhanced enrichment of TPP[CF] in crypt-like neoplastic tissue (arrows), compared with IS[750]. Normal tissue remained negative for both compounds. Scale bars, 50 µm. C, NIRF imaging of PDAC. Top, true color image of tumor (t) and surrounding normal tissue, including liver (li; left, scale bar, 5 mm), and corresponding pseudocolor fluorescence images, 24 hours after intravenous injection of TPP[Cy5.5] (middle) and IS[750] (right). Bottom, TBR 24 hours after intravenous injection of the compounds. The data are shown as mean ± SD of $n = 7$ (TPP[Cy5.5]), 6 (CP[DL750]), and 2 (IS[750]) animals. ***, $P < 0.001$. D, fluorescence microscopy of identical cryosections of primary tumor tissue (left) including fibrosis of the tumor microenvironment (right) 24 hours after intravenous injection of TPP[CF] (top) and IS[750] (middle). Bottom, an overlay with a comparable enrichment of both compounds in carcinoma tissue and additional IS[750] staining of cells of the tumor microenvironment. Scale bar, 50 µm.

was significantly higher than that of CP[DL750] ($P = 0.005$) and IS[750] ($P = 0.016$; Fig. 4A). The cellular distribution of the compounds at a microscopic level was analyzed using cryosections of the resected tumors that were obtained 24 hours after intravenous injection of TPP[CF] and IS[750]. Although a strong cytosolic signal of TPP[CF] in predominantly crypt-like tumor structures (white arrows) was observed, IS[750] treatment resulted in a weaker and more heterogeneous staining pattern (Fig. 4B). Our recent demonstration that membrane Hsp70 is rapidly endocytosed in tumor cells under physiologic conditions (18) provides an explanation for the cytosolic staining pattern of tumors.

Published OnlineFirst October 9, 2014; DOI: 10.1158/0008-5472.CAN-14-0413

The uptake capacities of TPP and IntegriSense were also investigated using an endogenous pancreatic PDAC model, which has an activating mutation in the *Kras* oncogene concomitant with a deletion of the tumor suppressor *Tp53* (21). Tumor cells of this model exhibited strong membrane positivity of both Hsp70 and β3-integrin (Table 1). Imaging of the pancreatic tumors was performed after opening of the peritoneal cavity; the stomach, liver, and gut were used to calculate the background fluorescence. The TBR for TPP[Cy5.5] was significantly higher than that of the control peptide ($P = 0.0001$) and comparable with that of the integrin $\alpha_v\beta_3$-targeting compound IS[750] (Fig. 4C). Figure 4D shows fluorescence images of a cryo-sliced pancreatic tumors 24 hours after simultaneous injection of TPP[CF] and IS[750]. Although both compounds stained tumor cells equally (left, white arrows), cells of the tumor microenvironment showed a weaker staining with TPP[CF] (right).

TPP has a higher capacity to specifically target human xenograft tumors than IntegriSense

To confirm the tumor homing capacities of TPP[Cy5.5] in human tumors, imaging experiments were performed in 13 different human tumor cell lines derived from six entities (colon, mammary, pancreas, head and neck, cervix, and lung; Fig. 5). The TBRs for TPP[Cy5.5] in the xenograft tumors ranged from 5.6 ± 1.6 (mammary carcinoma cell line, MDA-MB231) to 7.8 ± 1.4 (squamous cell carcinoma cell line of the head and neck, Cal-33), all of which were significantly higher than those of CP[DL750]. This indicates a specific enrichment of TPP[Cy5.5] in all of the investigated xenograft tumors. Because it is known that the majority of human pancreatic carcinomas are positive for β_3-integrin (22), we included three pancreas tumor xenograft models (Panc-1, MiaPaCa-2, COLO357) in our experiment. These models revealed substantial Hsp70 and β_3-integrin positivity (Table 1; Fig. 1). Although IS[750] produced higher TBRs in the pancreatic tumors compared with the other xenograft models that were examined, TPP[Cy5.5] yielded significantly higher ratios in two of these three models [$P = 0.04$ (Panc-1) and $P = 0.03$ (COLO357)].

Other human carcinoma cell lines that were determined as being β3-integrin positive were T-47D, MDA-MB-231 (mammary carcinomas), and Cal-33 (squamous cell carcinoma of the head and neck; see Table 1). The TBRs of IS[750] fluorescence of T-47D and Cal-33 also were significantly lower than the TBRs for TPP[Cy5.5] ($P = 0.04$ and 0.02, respectively). The TBR for IS[750] in all β3-integrin negative tumors remained clearly below the TBRs for TPP[750]. These data indicate that TPP might be a powerful tumor targeting agent for the detection, diagnosis, and targeting of several entities in humans.

Discussion

Interest in the use of peptides as innovative cancer diagnostic and tumor-specific drug delivery tools has increased (1–3). However, one of the most critical issues in cancer detection using tumor-targeting probes is specificity, as most of the recently used markers also bind to tumor-associated stroma and other cells. Despite many reports on tumor markers in oncology, the number of clinically useful, tumor-specific markers with prognostic relevance remains low (23–26). It was shown that membrane Hsp70 is present on nearly all aggressive tumor cells from a wide variety of murine and human tumor entities (4–8, 11–15). Therefore, membrane Hsp70 is of prognostic value and fulfills the criteria for an effective tumor targeting molecule.

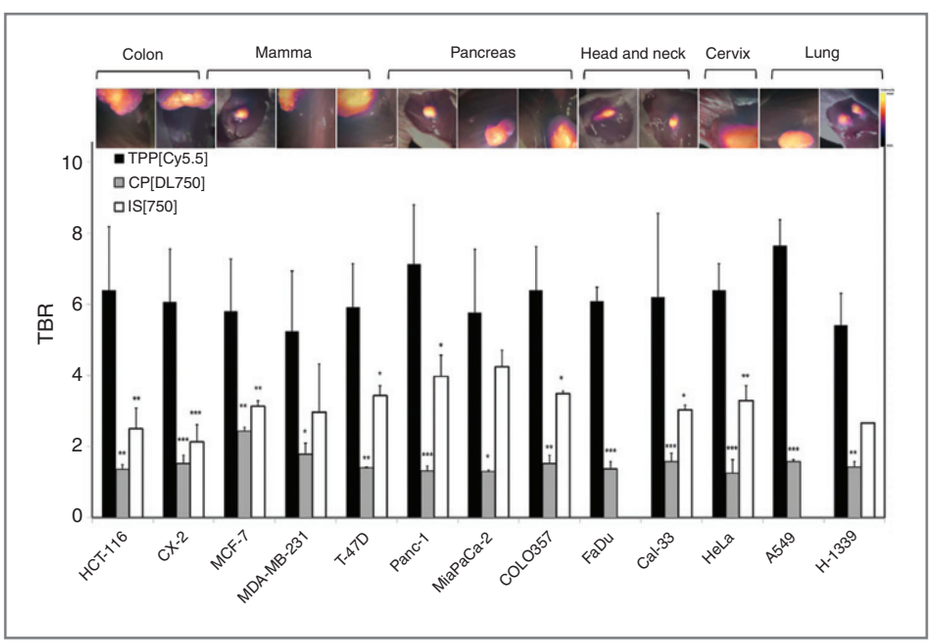

Figure 5. Intraoperative *in vivo* imaging of xenograft tumors 24 hours after intravenous injection of TPP[Cy5.5], CP[DL750], and IS[750]. Top, overlay of intraoperative true color and fluorescence pseudocolor images of subcutaneous tumors and the surrounding normal tissue 24 hours after intravenous injection of TPP[Cy5.5]. Bottom, TBR, 24 hours after intravenous injection of TPP[Cy5.5] (black bars), CP[DL750] (gray bars), and IS[750] (white bars). The data are shown as mean ± SD of two to five mice (H-1339, IS[750]); significance was calculated in comparison with TPP[Cy5.5]; *, $P < 0.05$; **, $P < 0.01$; ***, $P < 0.001$.

Published OnlineFirst October 9, 2014; DOI: 10.1158/0008-5472.CAN-14-0413

Given the widespread expression of membrane Hsp70 in different tumor entities and its prognostic relevance, this study evaluated TPP as a tumor homing peptide probe in a wide range of murine and human tumor models. TPP was shown to be highly specific (18) and is therefore an extremely useful tool for *in vivo* tumor detection and diagnosis. Targeting membrane Hsp70 with TPP is advantageous due to its rapid intracellular uptake, biodistribution, and tumor cell–selective accumulation. Similar to Hsp70, an ectopic and tumor-selective expression of Hsp90 has been utilized for the internalization of optical and radioiodinated tethered Hsp90 inhibitors (27).

The use of a colitis-associated colon carcinoma (20) and an endogenous pancreatic tumor model (21) allowed ample mimicking of the human situation in terms of tumor morphology and microenvironment, whereas the xenograft models of colon, mammary, pancreas, lung, head and neck, and cervix carcinoma were used to screen the performance of TPP in numerous human-derived malignant tumors *in vivo*. TPP was able to specifically detect and penetrate each of the tested tumors at high yields, *in vivo* (Figs. 3–5; Supplementary Fig. S7A and S7B). Furthermore, TPP specifically stains single cell suspensions of solid tumors, *in vitro* (Fig. 1A; Table 1). We also compared the *in vitro* and *in vivo* binding specificity of TPP with the neoplastic cells of various tumor models and nontransformed cells of the tumor stroma with that of a scrambled control peptide and the commercially available marker IntegriSense, which has been shown to stain different tumor entities, including pancreatic cancers, *in vivo* (28–31). The TBRs for TPP were higher than that of a control peptide and IntegriSense for all of the investigated tumors.

Flow-cytometric analysis revealed that the ligand of IntegriSense, β_3-integrin, was absent in five of the 11 human tumor xenografts, whereas all tested human and murine tumors were found to be highly membrane-Hsp70 positive (Fig. 1A; Table 1).

To reflect the more complex *in vivo* situation, we broadened our investigations to non-neoplastic cells of the tumor stroma. We used flow cytometry to analyze the presence of membrane Hsp70 and β_3-integrin on macrophages and fibroblasts in single cell suspensions derived from solid tumors. Both cell types show a low background fluorescence of membrane-Hsp70 but high β_3-integrin positivity (Fig. 1B). Although macrophages internalize IntegriSense and TPP *in vivo*, only a minimal level of TPP staining was detected in tumor-associated fibroblasts. Other studies demonstrated the presence of integrins, including β_3-integrin, on tumor endothelial cells (32, 33), which were negative for membrane Hsp70 (34).

Another recently discovered tumor targeting strategy involves the chemokine receptor CXCR4. Similar to Hsp70, CXCR4 offers the possibility to target different tumor entities. However, some carcinomas, like the NSCLC, do not or only weakly express CXCR4 on their plasma membranes (35, 36). In contrast, Hsp70 is present on all tested NSCLC tumors (xenograft, primary human tumors; ref. 5). Furthermore, potential adverse effects of targeting CXCR4, such as the mobilization of hematopoietic progenitor cells by CXCR4 antagonists (37), remain to be elucidated.

The current study found no evidence that TPP has any toxic side effects, even if it was administered at 10-fold higher doses than those that were used for *in vivo* imaging. *Ex vivo* biodistribution analysis revealed the beneficial tumor-homing capacities of the TPP peptide. Although TPP was effectively washed out of the normal tissue 24 hours after its administration, pronounced levels remained within the tumor tissue at this time point (Fig. 2). The small-molecular weight of TPP ensures that it is cleared via the kidneys and does not accumulate in the liver like high-molecular weight targeting probes such as antibodies. As a consequence, TPP did not result in nonspecific background signals in the liver. Therefore, TPP could be used as an imaging probe for hepatocellular carcinoma and liver metastases (15).

In conclusion, TPP might be a useful peptide-based marker for diagnostic tumor targeting, as well as an efficient tool for drug delivery for a broad variety of human tumors.

Disclosure of Potential Conflicts of Interest

S. Stangl and G. Multhoff have ownership interest in a patent. V. Ntziachristos has ownership interest (including patents) in iThera Medical GmbH and is a consultant/advisory board member for iThera Medical GmbH. No potential conflicts of interest were disclosed by the other authors.

Authors' Contributions

Conception and design: S. Stangl, V. Ntziachristos, G. Multhoff
Development of methodology: S. Stangl
Acquisition of data (provided animals, acquired and managed patients, provided facilities, etc.): S. Stangl, J. Varga, B. Freysoldt, M. Trajkovic-Arsic, J.T. Siveke, G. Multhoff
Analysis and interpretation of data (e.g., statistical analysis, biostatistics, computational analysis): S. Stangl, J. Varga, B. Freysoldt, J.T. Siveke, V. Ntziachristos, G. Multhoff
Writing, review, and/or revision of the manuscript: S. Stangl, J. Varga, J.T. Siveke, V. Ntziachristos, G. Multhoff
Administrative, technical, or material support (i.e., reporting or organizing data, constructing databases): S. Stangl, V. Ntziachristos
Study supervision: F.R. Greten, G. Multhoff

Grant Support

This work was supported by the German Research Foundation (DFG) Collaborative Research Center SFB824/B4—"Imaging for Selection, Monitoring and Individualization of Cancer Therapies."

The costs of publication of this article were defrayed in part by the payment of page charges. This article must therefore be hereby marked *advertisement* in accordance with 18 U.S.C. Section 1734 solely to indicate this fact.

Received February 14, 2014; revised August 11, 2014; accepted August 27, 2014; published OnlineFirst October 9, 2014.

References

1. Snyder EL, Dowdy SF. Cell penetrating peptides in drug delivery. Pharm Res 2004;21:389–93.
2. Kondo E, Saito K, Tashiro Y, Kamide K, Uno S, Furuya T, et al. Tumour lineage-homing cell-penetrating peptides as anticancer molecular delivery systems. Nat Commun 2012;3:951.
3. El-Andaloussi S, Holm T, Langel U. Cell-penetrating peptides: mechanisms and applications. Curr Pharm Des 2005;11:3597–611.
4. Farkas B, Hantschel M, Magyarlaki M, Becker B, Scherer K, Landthaler M, et al. Heat shock protein 70 membrane expression and melanoma-

Published OnlineFirst October 9, 2014; DOI: 10.1158/0008-5472.CAN-14-0413

associated marker phenotype in primary and metastatic melanoma. Melanoma Res 2003;13:147–52.
5. Hantschel M, Pfister K, Jordan A, Scholz R, Andreesen R, Schmitz G, et al. Hsp70 plasma membrane expression on primary tumor biopsy material and bone marrow of leukemic patients. Cell Stress Chaperones 2000;5:438–42.
6. Sakamoto M, Effendi K, Masugi Y. Molecular diagnosis of multistage hepatocarcinogenesis. Japanese J Clin Oncol 2010;40:891–6.
7. Sherman M, Multhoff G. Heat shock proteins in cancer. Ann N Y Acad Sci 2007;1113:192–201.
8. Kurahashi T, Miyake H, Hara I, Fujisawa M. Expression of major heat shock proteins in prostate cancer: correlation with clinicopathological outcomes in patients undergoing radical prostatectomy. J Urol 2007;177:757–61.
9. Multhoff G, Botzler C, Jennen L, Schmidt J, Ellwart J, Issels R. Heat shock protein 72 on tumor cells: a recognition structure for natural killer cells. J Immunol 1997;158:4341–50.
10. Radons J, Multhoff G. Immunostimulatory functions of membrane-bound and exported heat shock protein 70. Exerc Immunol Rev 2005;11:17–33.
11. Nylandsted J, Gyrd-Hansen M, Danielewicz A, Fehrenbacher N, Lademann U, Hoyer-Hansen M, et al. Heat shock protein 70 promotes cell survival by inhibiting lysosomal membrane permeabilization. J Exp Med 2004;200:425–35.
12. Steiner K, Graf M, Hecht K, Reif S, Rossbacher L, Pfister K, et al. High HSP70-membrane expression on leukemic cells from patients with acute myeloid leukemia is associated with a worse prognosis. Leukemia 2006;20:2076–9.
13. Thanner F, Sutterlin MW, Kapp M, Rieger L, Kristen P, Dietl J, et al. Heat-shock protein 70 as a prognostic marker in node-negative breast cancer. Anticancer Res 2003;23:1057–62.
14. Pfister K, Radons J, Busch R, Tidball JG, Pfeifer M, Freitag L, et al. Patient survival by Hsp70 membrane phenotype: association with different routes of metastasis. Cancer 2007;110:926–35.
15. Li H, Sui C, Kong F, Zhang H, Liu J, Dong M. Expression of HSP70 and JNK-related proteins in human liver cancer: potential effects on clinical outcome. Dig Liver Dis 2007;39:663–70.
16. Stangl S, Gehrmann M, Dressel R, Alves F, Dullin C, Themelis G, et al. *In vivo* imaging of CT26 mouse tumours by using cmHsp70.1 monoclonal antibody. J Cell Mol Med 2011;15:874–87.
17. Stangl S, Gehrmann M, Riegger J, Kuhs K, Riederer I, Sievert W, et al. Targeting membrane heat-shock protein 70 (Hsp70) on tumors by cmHsp70.1 antibody. Proc Natl Acad Sci U S A 2011;108:733–8.
18. Gehrmann M, Foulds GA, Breuninger S, Stangl S, Pockley AG, Multhoff G. Tumor imaging and targeting potential of an Hsp70-derived 14-mer peptide. PLoS ONE 2014;28:9e105344.
19. Mahalka AK, Kirkegaard T, Jukolal, Jäättelä M, Kinnunen PHJ. Human heat shock protein 70 (Hsp70) as a peripheral membrane protein. Biochim Biophys Acta 2014;1838:1344–61.
20. Greten FR, Eckmann L, Greten TF, Park JM, Li ZW, Egan LJ, et al. IKKbeta links inflammation and tumorigenesis in a mouse model of colitis-associated cancer. Cell 2004;118:285–96.
21. Ardito CM, Gruner BM, Takeuchi KK, Lubeseder-Martellato C, Teichmann N, Mazur PK, et al. EGF receptor is required for KRAS-induced pancreatic tumorigenesis. Can Cell 2012;22:304–17.
22. Themelis G, Harlaar NJ, Kelder W, Bart J, Sarantopoulos A, van Dam GM, et al. Enhancing surgical vision by using real-time imaging of alphaVbeta3-integrin targeted near-infrared fluorescent agent. Ann Surg Oncol 2011;18:3506–13.
23. Hosotani R, Kawaguchi M, Masui T, Koshiba T, Ida J, Fujimoto K, et al. Expression of integrin alphaVbeta3 in pancreatic carcinoma: relation to MMP-2 activation and lymph node metastasis. Pancreas 2002;25:e30–5.
24. Cardoso F, Saghatchian M, Thompson A, Rutgers ECommittee TCS. Inconsistent criteria used in American Society of Clinical Oncology 2007 update of recommendations for the use of tumor markers in breast cancer. J Clin Oncol 2008;26:2058–9.
25. McShane LM, Altman DG, Sauerbrei W, Taube SE, Gion M, Clark GM, et al. REporting recommendations for tumor MARKer prognostic studies (REMARK). Nat Clin Pract Oncol 2005;2:416–22.
26. Schilsky RL, Taube SE. Tumor markers as clinical cancer tests - are we there yet? Semin Oncol 2002;29:211–2.
27. Barrott JJ, Hughes PF, Osda T, Yang XY, Hartman ZC, Loiselle DR, et al. Optical and radioiodinated tethered Hsp90 inhibitors reveal selective internalization of ectotpic Hsp90 in malignant breast tumor cells. Chem Biol 2013;20:1187–97.
28. He T, Xue Z, Lu K, Valdivia Y, Alvarado M, Wong KK, et al. A minimally invasive multimodality image-guided (MIMG) system for peripheral lung cancer intervention and diagnosis. Comput Med Imaging Graph 2012;36:345–55.
29. Valvidia Y, Alvarado M, Wong K, He TC, Xue Z, Wong ST. Image-guided fiberoptic molecular imaging in a VX2 rabbit lung tumor model. J Vasc Interv Radiol 2011;22:1758–64.
30. Trajkovic-Arsic M, Mohajerani P, Sarantopoulos A, Kalideris E, Steiger K, Esposito I, et al. Multimodal molecular imaging of integrin avβ3 for *in vivo* detection of pancreatic cancer. J Nucl Med 2014;55:446–51.
31. Desgrosellier JS, Cheresh DA. Integrins in cancer: biological implications and therapeutic opportunities. Nat Rev Cancer 2010;10:9–22.
32. Brooks PC, Clark RA, Cheresh DA. Requirement of vascular integrin alphaVbeta3 for angiogenesis. Science 1994;264:569–71.
33. Ruegg C, Yilmaz A, Bieler G, Bamat J, Chaubert P, Lejeune FJ. Evidence for the involvement of endothelial cell integrin alphaVbeta3 in the disruption of the tumor vasculature induced by TNF and IFN-gamma. Nat Med 1998;4:408–14.
34. Gehrmann M, Stangl S, Kirschner A, Foulds GA, Sievert W, Doss BT, et al. Immunotherapeutic targeting of membrane Hsp70-expressing tumors using recombinant human granzyme B. PLoS ONE 2012;7:e41341.
35. Burger M, Glodek A, Hartmann T, Schmitt-Graff A, Silberstein LE, Fujii N, et al. Functional expression of CXCR4 (CD184) on small-cell lung cancer cells mediates migration, integrin activation, and adhesion to stromal cells. Oncogene 2003;22:8093–101.
36. Burger JA, Kipps TJ. CXCR4: a key receptor in the crosstalk between tumor cells and their microenvironment. Blood 2006;107:1761–67.
37. Liles WC, Broxmeyer HE, Rodger E, Wood B, Hubel K, Cooper S, et al. Mobilization of hematopoietic progenitor cells in healthy volunteers by AMD3100, a CXCR4 antagonist. Blood 2003;102:2728–30.